



Libraries and Learning Services

University of Auckland Research Repository, ResearchSpace

Copyright Statement

The digital copy of this thesis is protected by the Copyright Act 1994 (New Zealand).

This thesis may be consulted by you, provided you comply with the provisions of the Act and the following conditions of use:

- Any use you make of these documents or images must be for research or private study purposes only, and you may not make them available to any other person.
- Authors control the copyright of their thesis. You will recognize the author's right to be identified as the author of this thesis, and due acknowledgement will be made to the author where appropriate.
- You will obtain the author's permission before publishing any material from their thesis.

General copyright and disclaimer

In addition to the above conditions, authors give their consent for the digital copy of their work to be used subject to the conditions specified on the [Library Thesis Consent Form](#) and [Deposit Licence](#).

**Poor Nutrition Leading to Potential Clinically
Relevant Pathologies: The Role of Epigenetics and
Myostatin Signalling**

Aida Zarfeshani

A thesis submitted in fulfilment of the requirements for the
degree of Doctor of Philosophy in Molecular Medicine,
The University of Auckland, 2016

Outputs arising from this thesis

Published papers

Zarfeshani A, Ngo S, Sheppard A M: Leucine alters hepatic glucose/lipid homeostasis via the myostatin-AMP-activated protein kinase pathway-potential implications for nonalcoholic fatty liver disease. *Clinical Epigenetics*. 2014;6:27.

Zarfeshani A, Ngo S, Murphy R, Sheppard, A. Micro RNAs as Biomarkers of Bariatric Surgery Outcome and Putative Regulators of Hepatokines Selectively after Gastric Bypass, but not Sleeve Gastrectomy. *Obesity and Bariatrics*. 2016;3(1): 12.

Zarfeshani A, Ngo S, Sheppard A M. MicroRNA expression relating to the dietary induced liver diseases NAFLD and NASH. *Clinical Medicine*. 2016;4:1938-1950.

Conferences

Oral presentation

Zarfeshani A, Ngo S, Murphy R, Sheppard A M: Micro RNAs as biomarkers of bariatric surgery outcome and putative regulators of hepatokines selectively after gastric bypass, but not sleeve gastrectomy.

The Annual Scientific Meeting of Australian & New Zealand Obesity Society, Melbourne, 15th - 18th October, 2015.

Poster presentation

Zarfeshani A, Ngo S, Sheppard A M: Leucine alters hepatic glucose/lipid homeostasis via the myostatin-AMP-activated protein kinase pathway-potential implications for nonalcoholic fatty liver disease. Queenstown Research week, 25th- 27th August, 2014.

Abstract

The increasingly prevalent “Western style” diet is typified by an excessive intake of high caloric foods with little or poor nutritional value. Notably, the branched-chain amino acids (BCAAs) and free fatty acids (FFAs) micronutrients have been linked with diet induced progression of metabolic syndrome. Branched-chain amino acids concentrations are increased in the plasma of obese and type 2 diabetes mellitus (T2DM) patients and may be potential inducers of initial hyperglycemia and insulin resistance (IR). Specifically, the BCAA leucine (leu) has been highlighted as potentially significant for stimulating the secretion of insulin and promoting IR as a consequence. However, seemingly contradictory evidence suggests that leu may also be protective against the development of IR and T2DM. By examining the molecular mechanism underpinning the effects of leu on hepatic glucose metabolism (the central physiological mediator of systemic glucose homeostasis) I have arrived at a potentially parsimonious explanation allowing for a reconciliation of the many disparate observations about leu that exist in this literature. Specifically, leu supplementation is initially linked with a beneficial hepatic sequestration of ‘circulating’ glucose. However, this results in a consequential hepatic accumulation of triglycerides (TGs), through the activation of the glucose transporter solute carrier family 2 (SLC2A2), its transcriptional factor forkhead box A2 (FOXA2) and downstream genes. Thus, as a consequence of persistent dietary intake, the resulting metabolic ‘trade-off’ in which enhanced glucose uptake in the shorter term leads to elevated TGs in the longer term, could account for the pathological appearance of intra-hepatic fat droplets and progression of fatty liver disease that is often associated with IR and metabolic syndrome.

Notably, my studies link leu supplementation with intracellular signalling

through the key metabolic regulator myostatin (MSTN) and the associated AMP-kinase (AMPK). There is a growing body of evidence that MSTN activity enhances systemic insulin sensitivity and prevents obesity. Further, I have identified a strong epigenetic component to this regulation and specifically, identify miR-143, miR-92b* and miR-335 as instrumental to the leu-dependent induction of hepatic MSTN, SLC2A2 and FOXA2.

I have also explored the molecular basis of hepatic metabolic shifts resulting from free fatty acid (palmitate) supplementation. Multiple clinical studies identify palmitate as likely the primary FFA contributing to obesity driven by dietary excess. Again MSTN dependent signalling is found to be central to these responses, as are specific miRNA species, and in particular miR-335. A key terminal effector in this signalling cascade is the hepatokine fetuin A (FetA), which is linked pathologically with clinical obesity and promotes peripheral IR by reducing insulin sensitivity. My *in vitro* work establishes a mechanistic link between FFA supplementation and hepatokine induction, a central element of which is the epigenetic regulation of MSTN.

To further test the validity of these latter observations and in an attempt to translate these lab bench observations to the clinical setting, I have also explored these pathways in the context of pre and post bariatric surgery. Currently the clinical intervention of last resort for morbid obesity, bariatric surgery encompasses a range of surgical procedures designed to lower dietary intake. Whilst each surgical approach results in similar levels of initial weight loss, the longer term outcomes would seem to vary particularly with regard to the remission of metabolic syndrome and associated complications. The current consensus from prospective studies of post surgery T2DM remission suggest that gastric bypass (GBP) is superior to other modalities such as

sleeve gastrectomy (SG), However, relatively little is known about the mechanistic basis of the metabolic shifts resulting from these types of surgery, although FetA hepatokine expression has been described as a possible biomarker of efficacy.

I have defined a specific set of circulating miRNAs for which post-surgery expression is strongly correlated with both decreased body mass index (BMI) and glycated hemoglobin (HbA1c) level, but only following GBP and not SG. Of these, miRNA-355 is one of the principal regulators of MSTN that I had identified *in vitro* in the context of MSTN dependent FetA expression following palmitate supplementation, suggesting that epigenetically regulated hepatokine expression may indeed be of clinical significance to the physiological changes initiated by GBP surgery at least. It remains to be seen why similar changes are not observed with SG, but clearly implies mechanistic differences in the biological responses initiated by the different surgical approaches.

Collectively, the work presented herein illustrates the centrality of epigenetic regulation and of the MSTN-dependent signalling axis in underpinning pivotal metabolic shifts invoked by two distinct micronutrient stimuli (BCAA and FFA), each of which is linked with deleterious consequences of dietary excess. Further, the relevance of these findings to understanding the observed features of metabolic syndrome is encouraged by the first steps that have been taken to recapitulate the initial *in vitro* observations in the context of clinical patients.

*To my mom Fahimeh and brother
Kaveh who believed in my abilities and
supported me in my intention to make
some of my dreams come true*

Acknowledgments

It gives me great pleasure to acknowledge the following people whose advice and effort has made this dissertation possible.

First of all, I would like to express my gratitude to my supervisor Dr. Allan Sheppard for the honour of accepting me as his student and without whom I could not have completed and written this dissertation. Allan was more than a supervisor to me; he taught me how to believe in myself, my ideas and abilities and showed me how to free my mind, think and not to be scared to share my opinions and how to turn them into reality.

Thanks to Dr. Sherry Ngo for providing guidance and advice that has made my interdisciplinary project a success.

I really appreciate Assoc. Prof Mhoyra Fraser for her kind support and advice throughout my journey at Liggins.

This dissertation is part of the research carried out in Dr. Allan Sheppard's lab; I am deeply indebted to many people throughout my PhD studies. Hence, I extend my thanks to our former and current Developmental Epigenetics lab members Phillip Shepherd, Jing Rong, Chandrakanth Bhoothpur and Xiaoling Li, as well as Zengxiang Pan for his guidance and patience in helping me with bioinformatics analysis.

My sincere thanks to our PhD students Dr. Jinbi Zhang and Kui Xie for their comments, assistance and company as desk-mates over these years.

My deepest thanks go to my beloved mum Fahimeh and brother Kaveh for their unconditional and overwhelming love that they have showered upon me and also for their constant support which made this wonderful journey possible.

To all of you, thank you.

TABLE OF CONTENTS

CHAPTER 1: LITERATURE EVIEW	1
1.1 Nutrition in human health and diseases	1
1.1.1 Leucine metabolism in human health	3
1.1.1.1 Leucine and glucose homeostasis	7
1.1.1.2 Leucine and energy metabolism	8
1.1.2 Fatty acid metabolism in liver	11
1.2 Definition of non-alcoholic fatty liver and associated disorders	11
1.2.1 Hepatic dyslipidaemia	12
1.2.2 Risk factors of non-alcoholic fatty liver	13
1.2.3 Diagnosis, laboratory abnormalities and treatment of non-alcoholic fatty liver	16
1.3 Hepatokines and human health	17
1.3.1 Role of fetuin-A in insulin signalling and inflammation	19
1.3.2 Role of fetuin-A in obesity, diabetes and non-alcoholic fatty liver disease	20
1.3.3 Metabolic regulation of fetuin-A concentration	21
1.4 Myostatin regulatory roles in body metabolism	24
1.4.1 Myostatin and hepatic glucose metabolism	26
1.4.2 Myostatin and obesity	26
1.4.3 Myostatin and diabetes	28
1.4.4 Myostatin and fatty liver	28
1.5 Expression of epigenetic modulators	29
1.5.1 DNA methylation	31
1.5.2 Histone modification	31
1.5.3 MicroRNAs biogenesis and function	32
1.5.3.1 MicroRNAs in obesity	34
1.5.3.2 MicroRNAs and glucose homeostasis	35
1.5.3.3 MicroRNAs and lipid homeostasis	35
1.5.3.4 MicroRNAs in non-alcoholic fatty liver	36
1.6 Scope of study	37
1.6.1 Aims	38
1.6.2 Hypothesis	38
CHAPTER 2: METHODS	39
2.1 Cell culture of HepG2 hepatocytes	39
2.2 Maintenance and differentiation of murine C2C12 myoblast	39
2.3 Maintenance and differentiation of PANC-1 pancreatic cells	39

2.4 Human subjects	40
2.5 Bichinonic assay to determine cellular protein concentrations	41
2.6 Western blotting or immunoblotting	41
2.7 Purification of total RNA including miRNA	42
2.8 cDNA synthesis	43
2.9 Real-time quantitative PCR assay	44
2.10 MicroRNA isolation from human plasma	44
2.11 cDNA synthesis assay for microRNAs	45
2.12 Real-time quantitative PCR assay for microRNAs	45
2.13 MicroRNA array	46
2.14 Reverse transfection	46
2.15 DNA extraction	46
2.16 DNA methylation	47
2.17 MTT cell proliferation assay	51
2.18 Glucose uptake assay	51
2.19 Glucose output assay	52
2.20 Triglyceride content assay	53
2.21 Glycogen content assay	53
2.22 Insulin concentration assay	54
2.23 Statistical analysis	55
CHAPTER 3: LEUCINE ALTERS HEPATIC GLUCOSE/LIPID HOMEOSTASIS VIA THE MYOSTATIN-AMP-ACTIVATED PROTEIN KINASE PATHWAY- POTENTIAL IMPLICATIONS FOR NON-ALCOHOLIC FATTY LIVER DISEASE	56
3.1 Preface	56
3.2 Abstract	57
3.3 Introduction	58
3.4 Results	59
3.4.1 Leucine changes hepatic glucose and triglyceride homeostasis	59
3.4.2 Leucine changes hepatic expression of glucose/lipid sensing genes	60
3.4.3 Myostatin is involved in the regulation of leucine modified genes	63
3.4.4 MiRNA array validation using quantitative real-time PCR	67
3.5 Discussion	69
3.6 Conclusions	74
3.7 Methods	75
3.7.1 Chemicals and antibodies	75
3.7.2 Cell culture and treatment	75

3.7.3 Glucose uptake assay	76
3.7.4 Glucose output assay	76
3.7.5 Triglyceride Measurement	76
3.7.6 Glycogen measurement	76
3.7.7 Real-time PCR	77
3.7.8 Western blotting	77
3.7.9 Reverse transfection	78
3.7.10 MiRNA microarray	78
3.7.11 Validation of miRNA expression/ gene targets	79
3.7.12 Statistical analysis	80
3.8 Competing interests	80
3.9 Authors' contributions	80
3.10 Acknowledgements	81
3.11 Supplementary data	82
3.11.1 Determining the appropriate dose of leucine	82
3.11.1.1 General conclusion	82
3.11.2 Determining the type of branched-chain amino acid	84
3.11.2.1 General conclusion	86
3.11.3 Effect of leucine on DNA methylation in HepG2 cells	87
3.11.3.1 General conclusion	88
3.12 Supplementary data 2	90
3.12.1 Insulin production in pancreatic cells exposed to conditioned medium from leucine-treated hepatocytes	90
3.12.1.1 General conclusion	91
3.12.2 Glucose uptake in myotubes exposed to conditioned medium from leucine-treated hepatocytes	93
3.12.2.1 General conclusion	95
CHAPTER 4: MIRNAS AS BARIATRIC SURGERY OUTCOME BIOMARKERS AND HEPATOKINE REGULATORS AFTER GBP BUT NOT SG	96
4.1 Preface	96
4.2 Abstract	97
4.3 Introduction	98
4.4 Material and methods	100
4.4.1 Chemicals and antibodies	100
4.4.2 Human clinical study	100

4.4.3 Cell culture and treatment	102
4.4.4 MiRNA microarray	102
4.4.5 RNA isolation and quantitative real-time PCR	103
4.4.6 Western blotting	105
4.4.7 Reverse transfection	105
4.4.8 Statistical analysis	105
4.5 Results	106
4.5.1 Clinical characteristics	106
4.5.2 MicroRNA expression profile between pre- and post-bariatric surgery	108
4.5.3 Fatty acids induced hepatokine expression in HepG2 cells	110
4.5.4 MSTN mediates the effects of FFA on hepatokine FetA	112
4.5.5 MiRNAs may play a role in the regulation of MSTN in the presence of palmitate	116
4.5.6 BMI and HbA1c was correlated with miRNAs expression	118
4.6 Discussion	120
4.7 Acknowledgements	123
4.8 Conflict of interests	123
4.9 Abstract for oral presentation based on this study	124
CHAPTER 5: GENERAL DISCUSSION AND CONCLUSION	125
5.1 Future Directions	130
5.1.1 Does MSTN levels serve as a biomarker for the beginning of the NAFLD	130
5.1.2 Does MSTN/MSTN regulatory miRNAs drug targeting combat NAFLD	130
5.1.3 MiRNAs as diagnostic biomarkers for the efficiency of different types of bariatric surgery	130
5.1.4 Exosomes as leading biomarkers in miRNA studies	131
5.1.5 Histone modification	131
Appendix I	132
Appendix II	138
Appendix III	139
Appendix IV	140
Appendix V	146
LIST OF REFERENCES	157

LIST OF FIGURES

Figure 1.1 L-leucine chemical structure	4
Figure 1.2 Branched-chain amino acids metabolism	6
Figure 1.3 Role of leucine in the mTOR signalling pathway regulation	10
Figure 1.4 Development of non-alcoholic fatty liver	14
Figure 1.5 Metabolic consequences of increased production of fetuin-A	23
Figure 1.6 The MSTN signalling pathway	25
Figure 1.7 Epigenetic modifications	29
Figure 1.8 MiRNA biogenesis	33
Figure 2.1 Designed amplicons for DNA methylation	50
Figure 3.1 Effect of leucine supplementation on glucose and lipid metabolism in HepG2 cells	60
Figure 3.2 Expression of the genes involved in glucose and lipid sensing after leucine supplementation of HepG2 cells	62
Figure 3.3 AMP-activated protein kinase (AMPK) but not mammalian target of rapamycin complex 1/ Ribosomal protein S6 kinase beta-1 (mTOR/ S6K1) activity was regulated by leucine in HepG2 cells	64
Figure 3.4 Effects of myostatin (MSTN) on AMP-activated protein kinase (AMPK) activity and glucose /lipid sensing in leucine- treated HepG2 cells	66
Figure 3.5 Discovery and validation of miRNA expression after leucine supplementation	68
Figure 3.6 Schematic summaries of findings	71
Figure 3.7 MTT assay	83
Figure 3.8 Effect of branched chain amino acids treatment for various durations	85
Figure 3.9 DNA methylation ratio in HepG2 cells	89
Figure 3.10 Morphological changes of PANC-1 cells	92
Figure 3.11 Insulin secretion in Panc-1 cells	92
Figure 3.12 Morphological changes of C2C12 cells	94
Figure 3.13 Glucose uptake in C2C12 cells	94
Figure 4.1 Hierarchical clustering heat map	109
Figure 4.2 Fatty acids (FA) induction, regulated expression of lipogenesis enzymes and hepatokines	111

Figure 4.3 Myostatin (MSTN) regulated fatty acids-overexpressed genes	113
Figure 4.4 Mechanisms of fetuin-A (FetA) regulation by palmitate	115
Figure 4.5 miRNA regulatory role on fatty acids (FA)-induced HepG2 cells	117

LIST OF TABLES

Table 3.1 Real-time PCR (qPCR) validation of differentially expressed microRNAs in leucine-treated HepG2 cells compared with control	67
Table 3.2 Primer sequences used in real-time PCR (qPCR)	78
Table 3.3 Primer sequences used in DNA methylation	88
Table 4.1 Selection criteria for bariatric surgery	101
Table 4.2 List of primers sequences used in real-time PCR (qPCR)	104
Table 4.3 Clinical characteristics of study subjects	107
Table 4.4 Correlation analysis between certain miRNA expression and BMI/HbA1c	119

LIST OF ABBREVIATIONS

2-DG/2-DOG	2- Deoxy glucose
AA(s)	Amino acid(s)
ACC1	Acetyl CoA carboxylase
ActRII/ ActRIIb	Activin receptor II/ IIb
AFLD	Alcoholic fatty liver diseases
AKT	Protein kinase B
ALT	Alanine aminotransferase
AMP/ATP	Adenosine monophosphate/ Adenosine triphosphate
AMPK	Adenosine monophosphate kinase
AST	Aspartate aminotransferase
BCAA	Branched-chain amino acids
BCKAs	Branched-chain α -keto acids
BMI	Body mass index
BSA	Bovine serum albumin
CpG	Cytosine Guanine nucleotides
CRP	C-reactive protein
CT	Computed tomography
DMEM	Dulbecco's Modified Eagle Medium
DNMs/DNMT1	DNA methyltransferases/ DNA methyltransferase 1
dNTP	Deoxynucleotide
DTT	Dithiothreitol
ECL	Enhanced chemiluminescence
EDTA	Ethylenediaminetetraacetic acid
ELISA	Enzyme-linked immunosorbent assay
FBS	Fetal bovine serum

FetA (AHSG)	Fetuin-A (α 2-HS-glycoprotein)
FFA(s)	Free fatty acid(s)
FGF-21	Fibroblast growth factor 21
FOXA2	Forkhead box A2
FOXO1	Forkhead Box Protein O 1
g	G-force
G6Pase	Glucose 6-phosphatase
GBP	Gastric bypass surgery
GDF-8	Growth differentiation factor-8
GK	Glucokinase
GLUT2/4	Glucose transporter 2/4
GPAT1	Glycerol-3-phosphate acyltransferase
H	Histone
HAT	Histone Acetyl Transferases
HbA1c	Hemoglobin A1c
HDAC	Histone deacetylase
HDL	High-density lipoprotein
HFD	High fat diet
HOMA-IR	Homeostasis model assessment-Insulin resistance
IGF(s)	Insulin-like growth factor(s)
IGFBP(s)	Insulin-like growth factor binding protein(s)
IL-6	Interleukin-6
IR	Insulin resistant
IRS/IRS-1/2	Insulin receptor substrate/ Insulin receptor substrate-1/2
ITS-G	Insulin-Transferrin-Selenium
JNK	c-Jun NH2-terminal kinases

K	Lysine
KIC	α -ketoisocaproate
KIV	α -ketoisovalerate
KRP	Krebs-Ringer phosphate buffer
LDL	Low-density lipoprotein
LECT2	Leukocyte cell-derived chemotaxin 2
Leu	Leucine
miRNA	MicroRNA
miRNP	MicroRNA containing ribonucleoprotein
MRI	Magnetic resonance imaging
MSTN	Myostatin
mTORC 1/2	Mammalian target of rapamycin Complex 1/2
MTP	Microsomal triglyceride transfer protein
NAFLD	Non-alcoholic fatty liver
NASH	Non-alcoholic steatohepatitis
NF κ B	Nuclear factor kappa B
NS	Non-significant
p53	Tumor protein p53
PBS	Phosphate-buffered saline
PC	Pyruvate carboxylase
PCK1	Phosphoenolpyruvate carboxykinase (PEPCK)
PCR	Polymerase chain reaction
Pdx1	Pancreatic and duodenal homeobox 1
PEPCK	Phosphoenolpyruvate Carboxykinase
PGC1- α /PPARGC1A	Proliferator-activated receptor gamma coactivator 1-alpha
PI3K	Phosphoinositide 3-kinase

PKB (AKT)	Protein kinase B
PPAR α/γ	Peroxisome proliferator-activated receptor
PPIA	Peptidyl-prolyl isomerase A
PVDF	Polyvinylidene difluoride
qPCR	Real-time quantitative PCR
RMA	Robust multi-array average
RPM	Revolution per minutes
S6K1/p70S6K1	70KDa ribosomal protein S6 kinase 1
SAM	S-adenosylmethionine
SDHA	Succinate dehydrogenase complex
SDS-PAGE	Sodium dodecyl sulfate polyacrylamide gel electrophoresis
SG	Sleeve gastrectomy
SHBG	Sex hormone-binding globulin
SIRT	Sirtuin enzymes
SLC2A2	Solute carrier family member2
SMAD	Small mothers against decapentaplegic
SREBP-1c	Sterol regulatory element binding protein-1c
T2DM	Type 2 diabetes mellitus
TAE	Tris-acetate-EDTA
TCA cycle	Tricarboxylic acid cycle
TG	Triglyceride
TGF- β	Transforming growth factor- β
TLR4	Toll-like receptor 4
TNF- α	Tumor necrosis factor- α
TRBP	Transactivator RNA-binding protein
TSC2	Tuberous sclerosis complex 2

VLDL Very low-density lipoprotein

Vol Volume

Co-Authorship Form

This form is to accompany the submission of any PhD that contains research reported in published or unpublished co-authored work. **Please include one copy of this form for each co-authored work.** Completed forms should be included in all copies of your thesis submitted for examination and library deposit (including digital deposit), following your thesis Acknowledgements.

Please indicate the chapter/section/pages of this thesis that are extracted from a co-authored work and give the title and publication details or details of submission of the co-authored work.

Chapter 3. Leucine alters hepatic glucose/lipid homeostasis via the myostatin-AMP-activated protein kinase pathway-potential implications for nonalcoholic fatty liver disease. *Journal of Clinical Epigenetics* 2014;6:27. Pages 61-85.

Nature of contribution by PhD candidate	Project conception, Experimental design & planning, Execution, Data analysis & interpretation, Drafting /reviewing/editing of manuscript.
Extent of contribution by PhD candidate (%)	80%

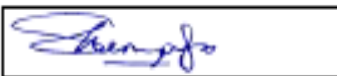

CO-AUTHORS

Name	Nature of Contribution
Sherry Ngo	Conceived the study, reviewed & edited the manuscript
Allan M Sheppard	Conceived the study, reviewed & edited the manuscript

Certification by Co-Authors

The undersigned hereby certify that:

- ❖ the above statement correctly reflects the nature and extent of the PhD candidate's contribution to this work, and the nature of the contribution of each of the co-authors; and
- ❖ in cases where the PhD candidate was the lead author of the work that the candidate wrote the text.

Name	Signature	Date
Sherry Ngo		23/09/2015
Allan M Sheppard		23/09/2015
		Click here
		Click here
		Click here
		Click here

Co-Authorship Form

This form is to accompany the submission of any PhD that contains research reported in published or unpublished co-authored work. Please include one copy of this form for each co-authored work. Completed forms should be included in all copies of your thesis submitted for examination and library deposit (including digital deposit), following your thesis Acknowledgements.

Please indicate the chapter/section/pages of this thesis that are extracted from a co-authored work and give the title and publication details or details of submission of the co-authored work.

Chapter 4. Zarfeshani A, Ngo S, Murphy R, Sheppard A M: Micro RNAs as Biomarkers of Bariatric Surgery Outcome and Putative Regulators of Hepatokines Selectively after Gastric Bypass, but not Sleeve Gastrectomy. Obesity and Bariatrics. 2016;3(1): 12. Pages 101-129.

Nature of contribution by PhD candidate	Project conception, Experimental design & planning, Execution, Data analysis & Interpretation, Drafting /reviewing/editing of manuscript.
Extent of contribution by PhD candidate (%)	70%




CO-AUTHORS

Name	Nature of Contribution
Sherry Ngo	Conceived the study, reviewed & edited the manuscript
Rinki Murphy	Providing plasma samples, reviewed & edited the manuscript
Allan M Sheppard	Conceived the study, reviewed & edited the manuscript

Certification by Co-Authors

The undersigned hereby certify that:

- ❖ the above statement correctly reflects the nature and extent of the PhD candidate's contribution to this work, and the nature of the contribution of each of the co-authors; and
- ❖ in cases where the PhD candidate was the lead author of the work that the candidate wrote the text.

Name	Signature	Date
Sherry Ngo		23/09/2015
Rinki Murphy		23/09/2015
Allan M Sheppard		23/09/2015
		Click here
		Click here
		Click here

Co-Authorship Form

This form is to accompany the submission of any PhD that contains research reported in published or unpublished co-authored work. Please include one copy of this form for each co-authored work. Completed forms should be included in all copies of your thesis submitted for examination and library deposit (including digital deposit), following your thesis Acknowledgements.

Please indicate the chapter/section/pages of this thesis that are extracted from a co-authored work and give the title and publication details or details of submission of the co-authored work.

Appendix V. MicroRNA expression relating to the dietary induced liver diseases NAFLD and NASH. Clinical Medicine, 4, 1938-1950; doi:10.3390/jcm4111938. Pages 146-156.

Nature of contribution by PhD candidate	Conceived the review, Drafting /reviewing/editing of manuscript.
Extent of contribution by PhD candidate (%)	90%



CO-AUTHORS

Name	Nature of Contribution
Sherry Ngo	Conceived the review, reviewed & edited the manuscript
Allan M Sheppard	Conceived the review, reviewed & edited the manuscript

Certification by Co-Authors

The undersigned hereby certify that:

- the above statement correctly reflects the nature and extent of the PhD candidate's contribution to this work, and the nature of the contribution of each of the co-authors; and
- in cases where the PhD candidate was the lead author of the work that the candidate wrote the text.

Name	Signature	Date
Sherry Ngo		23/09/2015
Allan M Sheppard		23/09/2015
		Click here
		Click here
		Click here
		Click here

1 LITERATURE REVIEW

1.1 Nutrition in human health and diseases

Nutrition is one of the most significant environmental exposures that affects health; poor nutrition caused by an insufficient, excessive or poorly balanced diet has been linked with (1) common human chronic diseases and their complications, such as type 2 diabetes mellitus (T2DM), insulin resistance (IR), metabolic syndrome, non-alcoholic fatty liver (NAFLD), and (2) many cancers, cardiovascular and neurological diseases. Epidemiological studies suggest that environmental factors before birth (and shortly afterwards) affect long-term consequential risks of metabolic diseases, by determining the levels of intracellular expression of various genes. The developing embryo is particularly susceptible to nutrient-induced adaptations in gene expression, often referred to as metabolic programming, which can persist into adulthood. Although, metabolic programming is believed to enable short term *in utero* survival in a suboptimal nutritional environment, in the longer term the individual may be more susceptible to metabolic and other diseases in adulthood (2).

Conversely, this inherent plasticity to nutritional inputs suggests that focused interventions, particularly when anticipating or early in disease etiology, may help ameliorate long-term risks. The extent to which a ‘window of opportunity’ for intervention exists is however still a key question for research to address. Obesity is an obvious disease target for such manipulation as it generally develops when energy intake surpasses energy expenditure over a protracted period of time (3). The identification of dietary components responsible for the growing prevalence of obesity has received much attention and has led to the proposition that it is the overall composition of the diet that influences body weight, perhaps even independently of total calorie intake (4, 5). For example, the effect of dietary fat on body weight and obesity is likely increased through utilization of energy-dense foods resulting in storage as body fat (6, 7). Therefore, it was initially presumed that reducing dietary fat intake would result in a spontaneous reduction of body weight (8). Although decreasing dietary inputs of saturated fat did indeed promote weight loss in the absence of other energy intake

compensation (9), focussed intervention studies have shown that reducing dietary fat alone is not a particularly effective way to lose weight when other non-fat dietary component calories are consumed (10, 11). The excessive dietary intake of carbohydrates for example, can similarly stimulate weight gain via elevating insulin levels, and thus promoting anabolic pathways (12). Furthermore, obese individuals very often have increased levels of plasma branched chain amino acids (BCAA), linked to impaired insulin activity (13), and leading to excessive pancreatic β -cells stimulation (14) and hepatic TG accumulation (15). Yet despite obesity being associated with excess levels of multiple dietary components, obese individuals very often suffer from micronutrient deficiencies (16) such as vitamin D (in 57%), iron (in 6-16%), vitamin B₁₂ (in 3-18%), folic acid, zinc and selenium (17, 18). Further, the gut microbiota has recently been suggested as an important ‘confounding’ environmental factor that interacts with dietary input to influence iposity and obesity (19), such that the number of bacteroidetes is reduced in obesity (20, 21), while weight loss would seem to enhance the amount of bacteroidetes (20, 22) in a manner highly dependent on overall caloric intake (20).

Given the evident complexity of the interacting signals generated by, and varying with dietary composition, it will be necessary to identify the pivotal underpinning mechanisms that interpret and integrate these various inputs in order to specify appropriate physiological responses. Without such an understanding, the formulation of targeted and effective interventions for diseases such as obesity would seem only a distant possibility. All organisms have acquired the ability to adapt to their nutrient environment by modulating protein activity in order to control signalling of biochemical pathways at a post-translational level (1). Micronutrients and bioactive food components can also regulate epigenetic processes to alter gene expression at the transcriptional level (23), in some cases leading to persistently altered mammalian phenotypes (24) that may be heritable (25) (more details about epigenetics can be found in section 1.5). These fundamental processes are likely key to orchestrating metabolic shifts during programming and during disease etiology, and may offer opportunities for effective preventive/therapeutic regimes.

1.1.1 Leucine metabolism and human health

Manipulating the dietary composition of micronutrients deserves deep consideration as they not only provide the building blocks of polypeptide and protein synthesis, but some may also function as signaling molecules to affect energy balance (26). There is growing evidence that IR and T2DM are conditions of a broad dysregulation of metabolic physiology involving significant changes in both fat and amino acid metabolism, in addition to glucose (27). The BCAA leucine (leu; Figure 1.1), isoleucine and valine are the most abundant essential amino acids in human diet and have been shown to act as regulators of hormonal signaling, in addition to serving as classic nutrients (28). Among BCAAs, leu is the major component of dietary protein. Beyond its role as structural building block, leu can also function as a signaling molecule, stimulating protein synthesis in muscle, leptin secretion in adipocytes and insulin release in pancreas. Thus leu can impact the regulation of body metabolism in multiple ways (29).

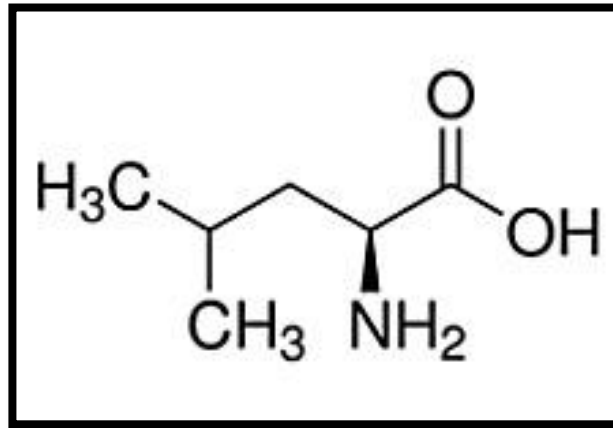


Figure 1.1 L-leucine chemical structure

Leu is a BCAA with the chemical formula $\text{HO}_2\text{CCH}(\text{NH}_2)\text{CH}_2\text{CH}(\text{CH}_3)_2$. It is encoded by UUA, UUG, CUU, CUC, CUA, and CUG codons and is classified as an essential AA therefore must be taken through diet.

Abbreviation: AA: amino acid, BCAA: branched-chain amino acid, leu: leucine.

The first step in the metabolism of the BCAAs is a reversible transamination reaction to their branched-chain α -keto acids (BCKAs), catalyzed by the enzyme BCAA aminotransferase. Therefore, BCAAs may be either transformed into their keto acids or synthesized from them. The transamination reaction requires α -ketoglutarate/ glutamate. When the direction is toward the formation of the BCKAs, α -ketoglutarate receives the amino group of the BCAAs and glutamate is produced. As a result, α -ketoisocaproate (KIC), α -keto-b-methylglutarate (KIM), and α -ketoisovalerate (KIV) are produced from L-leu, L-isoleucine and L-valine, respectively. Conversely, when the transamination reaction occurs in the opposite direction, the amino group of glutamate is added to BCKAs to generate BCAAs and α -ketoglutarate. The second phase in BCAAs catabolism is the oxidative decarboxylation of the BCKAs by the branched chain keto acid dehydrogenase complex, which is an inner mitochondrial membrane enzyme. This irreversible enzymatic step commits the BCKAs to oxidation, producing eventually NADH, CO₂, and other end-products depending on the particular BCKAs being oxidized. The end product arising from leu is acetoacetate and acetyl-CoA, while isoleucine renders propionyl-CoA and acetyl-CoA and valine yields propionyl-CoA (30). In summary, the catabolism of BCAAs leu, isoleucine and valine generates three α -keto acids which are further oxidized by a general branched-chain α -keto acid dehydrogenase thus yielding three CoA derivatives. Consequently, the metabolic pathway diverges, leading to production of tricarboxylic acid cycle (TCA) cycle intermediates (Figure 1.2) (31).

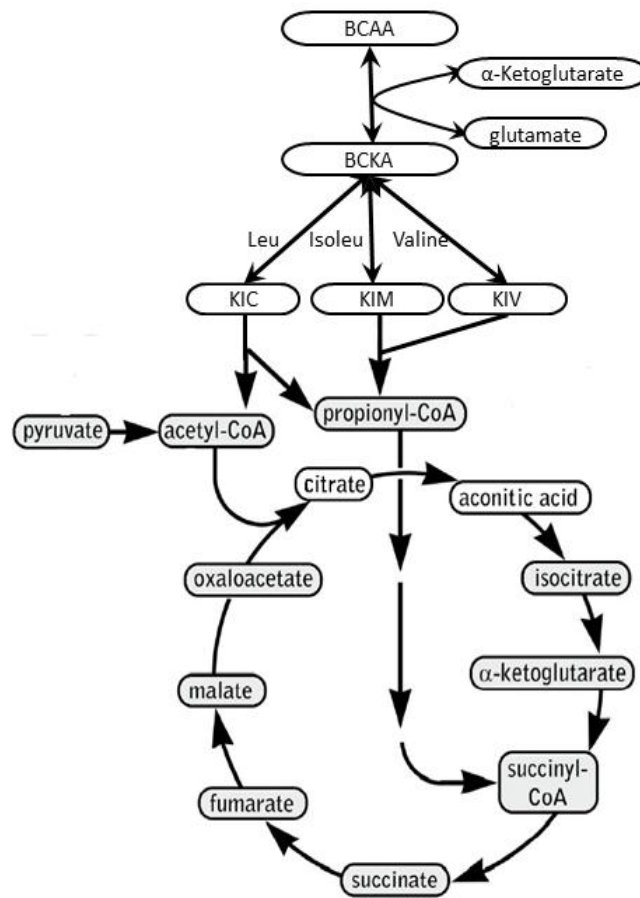


Figure 1.2 Branched-chain amino acids metabolism

BCAAs undergo transamination and release their amino group and convert to their particular keto acids. As a result of an irreversible enzymatic step, oxidized keto acids produce acetyl-CoA and propionyl-CoA which generate the TCA cycle intermediates.

Abbreviation: BCAA: branched-chain amino acid, BCKA: branched-chain α -keto acids, Isoleu: isoleucine, KIC: α -ketoisocaproate, KIM: α -keto-b-methylglutarate, KIV: α -ketoisovalerate, Leu: leucine.

Modified from (30, 32).

1.1.1.1 Leucine and glucose homeostasis

The potential effects of leu on metabolic roles are proportional to its dietary intake. When the requirements for protein synthesis are met, leu can be used as a signal to activate metabolic pathways; therefore these functions are dependent on intracellular concentrations of leu (33-35). Leucine can impact directly on the maintenance of glucose homeostasis by enhancing recycling of glucose through the glucose–alanine cycle in muscles, a process dependent upon enhanced degradation of the BCAA (33). During hypoglycemia when dietary glucose is limited and protein is plentiful, leu supplementation serves to stimulate gluconeogenesis and thus supporting blood glucose levels. Leucine donates its amino group to pyruvate, converting it to alanine, which then circulates to the liver where it serves as a substrate for endogenous glucose production. Leucine is not only the source of substrate in this case, but also inhibits pyruvate oxidation from participating in the glucose–alanine cycle.

The primary glucose transporter in the liver is glucose transporter (GLUT2), which facilitates glucose uptake into hepatocytes so that glucokinase (GK) in the cytoplasm can convert it by phosphorylation to generate G6P. The enzyme glucose 6-phosphatase (G6Pase) catalyzes the final step in both glycogenolytic and gluconeogenic pathways and is reversed by the glycolytic enzyme glucokinase. Therefore, these metabolic cycles regulate the rate and direction of glucose flux based on its concentration (36). Two enzymes specific for gluconeogenesis, G-6-Pase and phosphoenolpyruvate carboxykinase (PEPCK) are opposed by the glycolytic enzymes (37). In the presence of excess calories from glucose, acetyl-CoA enters the TCA cycle where it is converted to citrate, which departs the mitochondria to be used for FA synthesis via acetyl CoA carboxylase (ACC1). Acyl-CoAs then are used to esterify glycerol-3-phosphate acyltransferase 1 (GPAT1) which further produces TG. Liver TG can be stored in the form of lipid droplets or transported to very low-density lipoprotein (VLDL) by the mitochondrial TG transport protein (38). After BCAA induction, the expression of GLUT2 and GK is accelerated, and G6Pase expression is suppressed without affecting glycogen or serum glucose concentration. However, as yet the specific effect of leu on hepatic glucose metabolism has not been fully considered in human cells (36).

1.1.1.2 Leucine and energy metabolism

Animal models indicate that leu can influence the development of metabolic syndrome disorders and T2DM. A target component for leu in the regulation of food intake and energy homeostasis is mammalian target of rapamycin complex 1 (mTORC1) catalytic activity which is also affected by the phosphatidylinositol 3-kinase (PI3K) /protein kinase B (AKT) pathway (39). MTOR exists and functions in two distinct multiprotein complexes, mTORC1 and mTOR complex 2 (mTORC2). The former is sensitive to rapamycin and controls whole body energy homeostasis (40-42). On the other hand, activation of mTORC1/ribosomal protein S6 kinase 1 (S6K1) pathway by BCAAs has been shown to phosphorylate the serine (Ser-1101) of insulin receptor substrate 1 (IRS-1) and represses tyrosine phosphorylation and activity of PI3K, a critical kinase involved in the mechanism of insulin action on glucose transport and metabolism (43-46). Therefore, BCAA excess may inhibit the first steps of insulin signaling and reduce glucose utilization in skeletal muscle, thus promoting IR (46-48). Elevation of BCAAs including leu, contributes to the development of IR in rats fed HFD (49). Furthermore, rats supplemented with 4.5% leu in their dietary protein, also showed significantly increased perimuscular fat mass with reduced whole-body glucose tolerance. Therefore, extra leu may have been used as energetic substrate, utilized and stored as TG by adipose cells, and thus increasing adiposity (50).

The effects of insulin on mTOR signaling are largely due to upstream control of mTOR through the (tuberous sclerosis complex 1-2 (TSC1-TSC2) protein complex, which is largely mediated by activation of protein kinase B (PKB or Akt) through a PI3K-dependent pathway. Signal transduction from TSC2 to mTOR is mediated by a G protein called Ras homolog enriched in brain (Rheb). In its active status, Rheb is bound to GTP while TSC2 has GTPase-activating protein toward Rheb and converts Rheb to its inactive Rheb-GDP form (51). On the other hand, several proteins including the 4E-BP1 and the S6 kinases involved in the translational machinery that phosphorylate multiple sites in the C-terminus of the 40 S ribosomal protein S6 are regulated by mTORC1 (51). Rapamycin-sensitive mTORC1 phosphorylates and activates the cell growth regulators S6K 1 (52) which phosphorylates

and inactivates the translational repressors eukaryotic translation initiation factor 4E-binding protein 1 (4E-BP1) (53). The mTORC1 inhibitor rapamycin, dephosphorylates S6K1 and 4E-BP1, resulting in G1 growth arrest and suppresses ribosome biosynthesis and autophagy (54, 55) (Figure 1.3).

Leucine activates mTORC1 in skeletal muscle and adipose tissues more potently than other amino acids (56) mainly through regulating TSC2 complex *in vitro* and *in vivo* (57). mTORC1 activity also appears to be influenced by intracellular adenosine triphosphate (ATP) levels (58). Depletion of ATP activates adenosine monophosphate kinase (AMPK) which in turn phosphorylates and activates TSC2, resulting in mTORC1 inhibition (59). Therefore, mTORC1 activation by AKT could be through both direct phosphorylation of TSC2 and by keeping a high level of ATP, with a simultaneous decrease in the adenosine monophosphate (AMP):ATP ratio and thus inactivation of AMPK.

Metabolic disorders have been interpreted in terms of mitochondrial loss or dysfunction (60, 61). Leucine plays critical roles in both adipocytes and skeletal muscle energy metabolism (62) by regulating lipid metabolism in adipocytes to provide the energy substrate for protein synthesis in skeletal muscles. Leucine, specifically elevates mitochondrial mass and relevant modulatory gene expression in both myocytes and adipocytes (63), further evidence that leu may influence energy utilization. In addition, leu metabolism can provide different anaplerotic substrates for the TCA cycle, such as α -ketoisocaproate, which can be further metabolized to ACC and acetoacetate (64). Therefore, leu induction induces mitochondrial energy production which is critical for insulin release from β -cells (65). Moreover, as outlined above leu increases insulin secretion by β -cells through activation of PI3K/mTORC1/S6K1 signaling pathway and (66) and inhibition of the mTOR signaling pathway via rapamycin, impairs glucose-induced insulin secretion in the pancreatic β -cells (67).

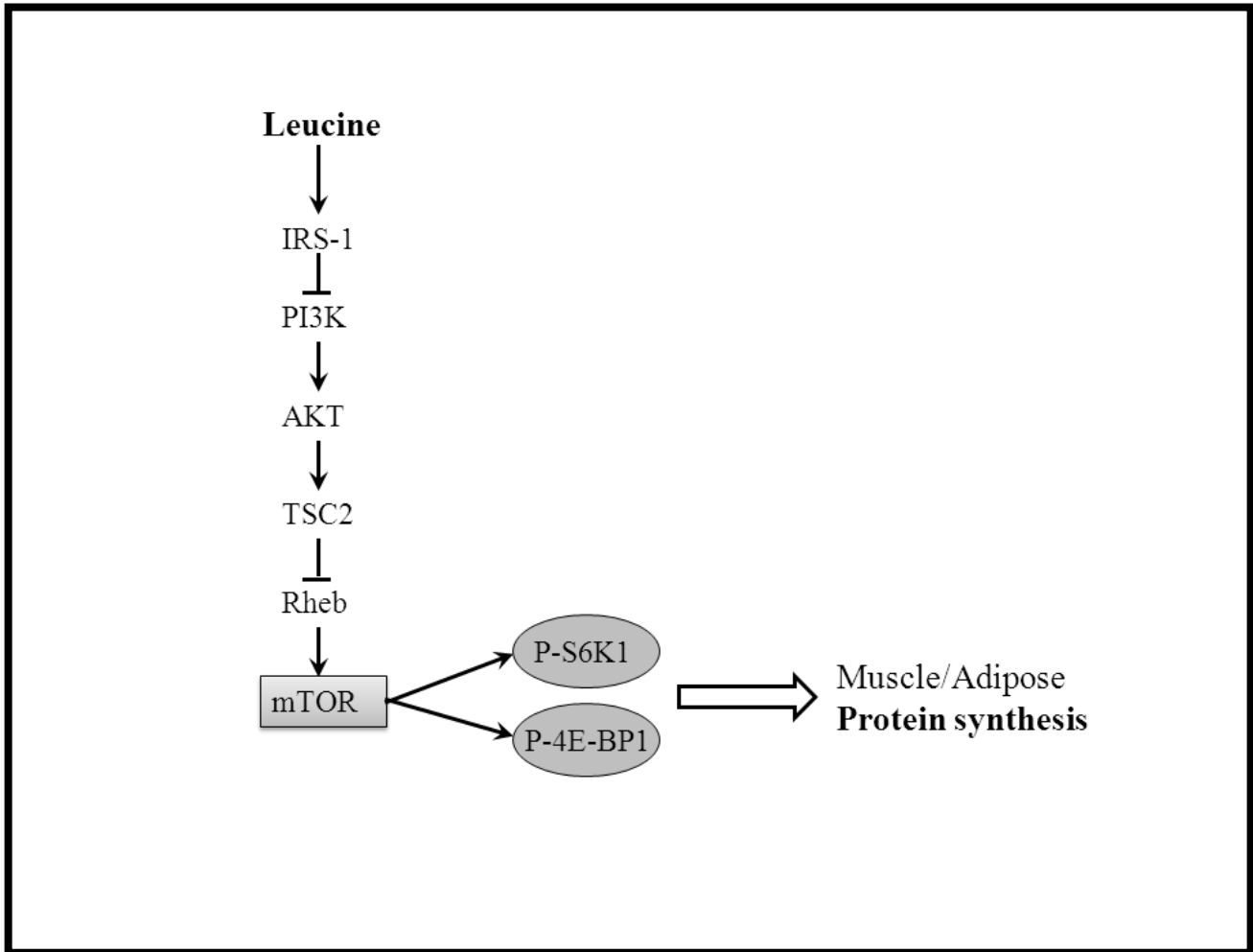


Figure 1.3 Role of leucine in the mTOR signalling pathway regulation

Leucine regulates mTOR signalling pathway in skeletal muscle and adipose tissues thus phosphorylation of both S6K1 and 4E-BP1. Activation of PI3K/AKT by leucine leads to inactivating phosphorylation of TSC2 and decreases its GAP activity toward Rheb which in turn activates the mTOR pathway. mTOR directly phosphorylates S6K1 and 4E-BP1 leading to enhanced protein translation. Abbreviations: 4E-BP1: eukaryotic initiation factor 4E binding protein 1; AKT: protein kinase B, IRS-1, insulin receptor substrate 1; mTOR: mammalian target of rapamycin; PI3K, phosphatidylinositol 3-kinase; Rheb: Ras homolog enriched in brain; S6K1: ribosomal protein S6 kinase 1; TSC2: tuberous sclerosis complex 2.

Modified from (68).

1.1.2 Fatty acid metabolism in liver

The liver is central to whole body energy homeostasis because of its ability to co-ordinate the metabolism of both glucose and fatty acids. Under fasting conditions where glucose and insulin are limited, hepatic glycogen stores and fatty acid production are reduced. This leads to hydrolysis of stored TG in the adipose tissue to generate FFAs which are then mobilized into the blood to reach the liver mitochondria where they undergo oxidation to generate energy and converted to ketone bodies to be used as an energy source by extrahepatic tissues (69, 70). Conversely, under conditions of excess energy intake, mammals preferentially utilise carbohydrates to generate ATP. The liver is also able to store considerable quantities of lipids; under conditions of replenished glycogen storages and prolonged availability of excess energy or abnormal FA metabolism which leads to hepatic fat accumulation. FFAs can also be reesterified to TG and thereby stored in the form of lipid droplets or combined with apolipoproteins to be secreted as VLDL from the liver (71).

1.2 Definition of non-alcoholic fatty liver and associated disorders

The obese hepatic environment induces hepatic IR, leading to increased lipogenesis in hepatocytes. Fatty liver diseases are clinically categorized into alcoholic fatty liver diseases (AFLD) and NAFLD (72). NAFLD is the most common liver disease worldwide and comprise a spectrum of diseases ranging from relatively benign simple steatosis, to non-alcoholic steatohepatitis (NASH), NAFLD-associated cirrhosis and end-stage liver disease. The NAFLD syndrome is increasingly recognized as an important risk factor for primary liver cancer and future need for liver transplantation (73, 74). Currently, the only clinical feature distinguishing individuals with NASH is that they drink little (less than 20 g/day ethanol for women and less than 30 g/day ethanol for men) or no alcohol (72, 75). Definitive diagnosis is further complicated by that lack of clear histological features in the early stages of alcoholic steatohepatitis (ASH) and NASH (72). The intracytoplasmic accumulation of TG in hepatocytes presents initially as liposomes around the nucleus. In more advanced stages, the vesicles size increase such that the nucleus is distorted and displaced to the periphery of the hepatocytes, a condition that is known as *macrovesicular steatosis* (76). In contrast, non-pathological accumulation of

small intracytoplasmic *microvesicular* fat droplets in hepatocytes does not lead to displacement of the centrally located nucleus (72). In AFLD and chronic NAFLD, hepatic steatosis is predominantly macrovascular, but in some cases exhibits an increase in microvascular droplets as well (75, 77, 78).

1.2.1 Hepatic dyslipidaemia

Insulin is a powerful regulator of lipid metabolism in liver and impaired insulin signalling contributes greatly to the body dyslipidaemia (79). Impaired insulin signalling in the liver and adipose tissue leads to increased endogenous glucose production which results in hyperglycaemia; the latter can lead to glucotoxicity and thus, the pathogenesis of T2DM and coronary vascular diseases (80-82). Furthermore, hyperglycaemia in T2DM patients (whose blood glucose levels are not controlled appropriately) enhances *de novo* hepatic lipogenesis, stimulates the development of hepatic IR and NAFLD, and its progression to cirrhosis and severe liver diseases like hepatocellular carcinoma (71). Recent studies suggests a strong association between fatty liver disease and IR in obesity (83, 84). Kotronen *et al.* (85) have reported that intrahepatocellular rather than intramyocellular fat is correlated with hyperinsulinemia in nondiabetic men. Also, Fabbrini *et al.* (86) have shown that intrahepatic triglyceride (TG), but not visceral adipose tissues, is a better marker of multiorgan obesity associated IR. D'Adamo *et al.* (87) have shown that obese adolescents with high hepatic fat content show less body-insulin sensitivity independent of intramyocellular lipid content and visceral fat. Although these studies indicate a strong correlation between fatty liver and IR in humans, whether fatty liver disease can directly cause IR in obese subjects has yet to be studied.

The accumulated hepatic TG is derived from dietary excess, *de novo* lipogenesis and adipose tissues lipolysis. Dietary fats absorbed through the intestine are packaged into chylomicrons which are delivered to the blood circulation and thus liver (88). Almost 25% of liver TG is derived from enhanced *de novo* lipogenesis, where under IR conditions the inhibitory effects of insulin on peripheral lipolysis is reduced, thus increasing the availability of FFAs for liver (72). This FA accumulation could be triggered by increased levels of insulin that stimulates the transcription factor sterol regulatory element

binding protein-1c (SREBP-1c) and leads to the up-regulation of lipogenic enzymes, such as GPAT1 and ACC1 (89, 90), under the transcriptional regulation of peroxisome proliferator-activated receptor γ (PPAR γ) (91-93). Increased activities of hepatic lipase and cholesteryl ester transfer in hepatic IR state, results in the conversion of VLDL particles into small and dense low-density lipoprotein (LDL). Further, elevated levels of VLDL alters high-density lipoprotein (HDL) composition and ultimately enhances HDL catabolism (79).

1.2.2 Risk factors of non-alcoholic fatty liver

The etiology of NAFLD and its progression is complicated and remains incompletely understood. Although animal studies has revealed several molecular pathways that present major features of NASH, no animal model has recapitulated the entire spectrum of NAFLD in humans (94). Environmental factors, especially in genetically susceptible populations, are likely key to the etiology of NAFLD. Among these, nutrient abundance is considered a primary cause, especially presented as the typical Western-style diet which is rich in simple carbohydrates and saturated fat. When coupled with a sedentary lifestyle, severe caloric imbalance can occur and lead to increased weight gain in most individuals. In both adult and paediatric populations, an increasing prevalence of overweight/obesity phenotypes is associated with the increased prevalence of NAFLD (94) (Figure 1.4).

The dysregulation of lipid metabolism, as well as immune responses, have been identified as pertinent to progression along the NAFLD spectrum (95). Molecular mechanisms underpinning NAFLD appear to share similarities with those linked to the development of obesity and metabolic syndrome disorders. The first recognized stage of NAFLD, benign steatosis, arises when the fat storage capacity of adipose tissue, and of visceral adipose in particular, has been exceeded (95). Hepatic and visceral fat levels in the body are highly correlated (96, 97), although only hepatic fat (and not visceral fat) is associated with insulin resistance. Obese individuals with elevated visceral fat have increased whole-body lipolysis compared to lean subjects (98, 99) and patients with NAFLD have preferential

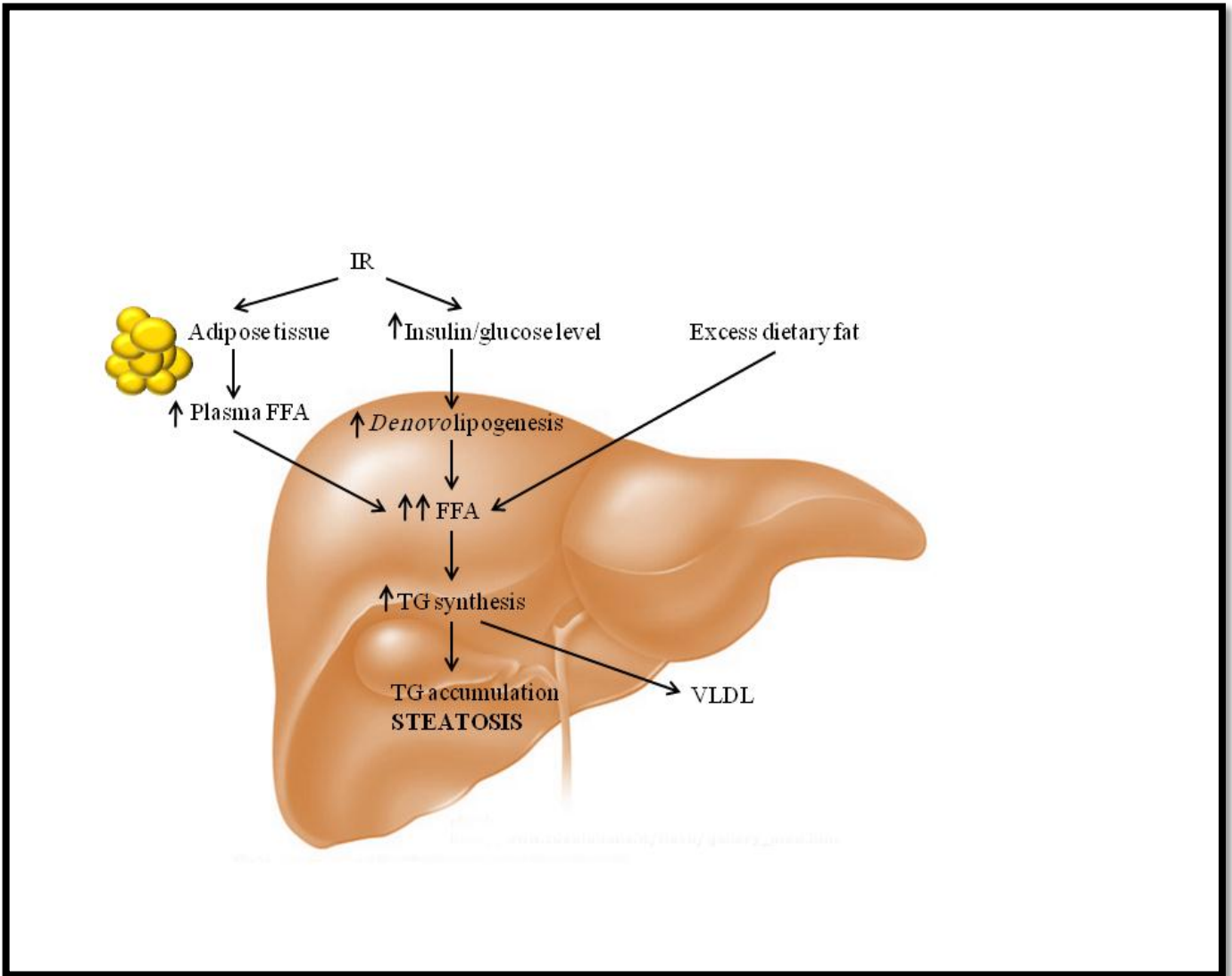


Figure 1.4 Development of non-alcoholic fatty liver

Under IR condition, insulin is unable to induce its inhibitory effect on lipase leading to increased TG lipolysis. The produced circulating FFAs are then taken up by liver. Dietary FAs released to plasma and enter the liver. Hyperinsulinemia induces *de novo* synthesis of FAs in hepatocytes leading to hepatic TG synthesis which exports through VLDL.

Abbreviations: FFA: free fatty acids, IR: insulin resistance, TG: triglyceride, VLDL: very-low density lipoproteins.

accumulation of abdominal fat. In upper body obesity, portal FFA concentrations, arising from lipolysis of both systemic and visceral fat, is significantly greater than arterial FFA concentrations, thus exposing the liver to even greater amounts of FFA (100, 101). In the obese state, hepatocytes present selective IR, where insulin is unable to prevent gluconeogenesis, but still able to promote *de novo* hepatic lipogenesis leading to both hyperglycemia and hyperlipidemia (102, 103).

Despite the high circulating levels of insulin in NAFLD subjects, they have reduced hepatic insulin sensitivity, elevated FFA and TG concentrations, and postprandial glucose clearance (96, 104, 105). Therefore, in conditions of IR increased lipolysis (especially from visceral fat) enforces an overload of glycerol and FFA in the liver. This leads to increased hepatic TG synthesis and favours lipid droplet formation to form intracellular storage reservoirs. Lipids are collected within the phospholipid bilayer of the endoplasmic reticulum membrane and finally bud off from terminal regions of the membrane to form the monolayer phospholipid that eventually binds to lipid droplets (106). It is therefore unsurprising that increased formation of hepatic lipid droplets is clearly associated with NAFLD, AFLD, metabolic syndrome and T2DM. This hepatic fat accumulation can result in hepatic IR by translocating protein kinase C from the cytosol to the membrane and thus interrupting insulin signalling via the IRS/PI3K pathway (107). Although obesity would seem likely as a risk factor for the development of NAFLD, there is as yet no direct evidence of a causal link. Notably, there are a few studies of NAFLD in non-obese patients who display IR, systematic inflammatory responses (108) or dietary components (109) as independent inducers of NAFLD.

Increased inflammatory markers, including interleukin-6 (IL-6) and nuclear factor kappa B (NF κ B), correlate with *de novo* hepatic lipogenesis and thus steatosis (110). Fatty acids, and potentially several metabolites arising from FA metabolism (eg acyl-CoAs and diacylglycerol) serve as signaling molecules that stimulate and activate immune related protein kinases such as c-Jun NH₂-terminal kinases (JNK) and the inhibitor of NF κ B (111). These kinases can also interfere with insulin signaling by increasing the inhibitory serine phosphorylation of IRS, the main mediator of insulin receptor

signaling (112). Furthermore, the liver contains a large amount of resident macrophages or Kupffer cells (113) which are highly activated in NAFLD-induced inflammation (114) and their activity is associated with hepatic IR (113, 115). However, despite these observations there is not yet compelling evidence to support the idea that inflammation is a primary cause of NAFLD. Given that chronic inflammatory responses are a feature of diverse pathologies, including several distinct types of cancers (116-118) and heart disease (119, 120), it is perhaps more likely that in NAFLD inflammation is simply a correlate of disturbed metabolism.

1.2.3 Diagnosis, laboratory abnormalities and treatment of non-alcoholic fatty liver

The prevalence of NAFLD is nearly 50% in people with diabetes, 76% in those with obesity, and 100% in those morbidly obese with diabetes (75). Steatosis is diagnosed when lipid content in the liver exceeds 5–10% by weight (77, 121). The main diagnostic indicator of fatty liver disease is elevated levels of serum aspartate aminotransferase (AST) and alanine aminotransferase (ALT). However, levels of these aminotransferases are seldom higher than 3 or 4 times the upper limit measured in a normal liver. Generally ALT levels are higher than those for AST levels, although this trend is reversed in the presence of cirrhosis, with an ALT/AST ratio of greater than 1 predicting the presence of more advanced fibrosis (122). However, many individuals across the entire histological range of NAFLD have normal ALT values (123). Ultrasonography is the most commonly used imaging technique in the diagnosis of NAFLD, and although remarkably sensitive, it cannot accurately quantify the degree of steatosis. Conversely, computed tomography (CT) imaging can accurately detect and quantify the amount of steatosis in patients but cannot differentiate simple steatosis from more advanced steatohepatitis. Magnetic resonance imaging (MRI) is currently the most accurate technology for diagnosis and quantification of hepatic steatosis, but is limited in use because of cost, inability to use in patients with implantable devices, claustrophobia or excess iron levels (123, 124). In any event, imaging is often a prequel to confirmation by biopsy, which remains the gold standard tool for diagnosis of NAFLD and the estimation of histological features to determine the risk of progression to more advanced liver disease. Liver biopsies are only undertaken with strong clinical indications, given

the cost and invasive nature of the procedure with its likely risk of bleeding and associated possibility of death. The value of biopsy is further questioned given the current absence of effective treatments for NAFLD, with lifestyle modification being the primary strategy for slowing NAFLD regardless of the stage of the disease (125). This includes weight loss by decreased caloric intake, informed choice of diet, such as low fat/high carbohydrate versus high fat/low carbohydrate, as well as increased physical activity. In some cases, NAFLD benefits from bariatric surgery when it is associated with morbid obesity (126).

Classically, the pathogenesis of NAFLD and obesity is considered to be due to excess caloric intake in association with reduced energy expenditure (127). However, the relationship of specific dietary habits to the development of NAFLD is yet to be fully explored and although excess adiposity is a major risk factor for NAFLD, it is not clear whether specific dietary patterns add to NAFLD independently of excessive adiposity. These observations suggest that the hepatic steatosis seen in NAFLD may begin as a simple 'overstorage' of unmetabolized energy in the hepatocytes of individuals who do not utilize their excess energy intake (128).

1.3 Hepatokines and human health

Fat accumulation in the abdominal cavity, predominantly in the liver, is commonly accompanied by inflammation and is thought to be more important in the pathogenesis of IR than is an overall increase in body fat mass (86, 129). NAFLD has become a global health threat in parallel with the obesity epidemic (130). This has focussed attention on the role of hepatokines, secretory proteins which act as cytokines and can affect body glucose and lipid metabolism (131, 132). Hepatokines are strongly linked to the development of IR and subclinical inflammation (133, 134).

Major hepatokines in the context of metabolic syndrome are angiopoietin-related protein 6 (Angptl6), fibroblast growth factor 21 (FGF-21), leukocyte cell derived chemotaxin 2 (LECT2) and alpha-2-HS-glycoprotein (AHSG, fetuin-A). Genetic knock-out of Angptl6 in mice is associated with

lipid accumulation in liver and skeletal muscle, IR, decreased energy expenditure and obesity (135). In agreement with this, targeted activation of *Angptl6* by adenoviral transduction in HFD-induced mice was associated with weight loss, increased insulin sensitivity, increased energy expenditure, and resistance to HFD-induced obesity, IR and hepatic steatosis. Hepatic overexpression of *Angptl6* was also associated with an approximately 2.5 fold increase in serum levels of this protein (135). So far, the precise physiological role of *Angptl6* is not known and it is not clear whether the effects observed in murine models translate to humans, although preliminary reports suggest *Angptl6* levels is elevated in patients with T2DM and positively correlated with fasting serum glucose levels (136).

Fibroblast growth factor-21 may be another important hepatokine, predominantly produced and secreted by the liver but also expressed to a lesser extent in white adipose tissue, pancreas, testis and duodenum in mice (137). Administration of FGF-21 reduces plasma TG, hepatic TG and glucose levels in obese and diabetic male mice (138) and was related to weight reduction in response to an increase in energy expenditure (138). Fibroblast growth factor-21 specifically down regulates the level of the hepatic transcription factor *Srebp-1*, resulting in increased lipogenesis and enhanced expression of the metabolic regulator proliferator-activated receptor gamma coactivator 1-alpha (*PGC-1 α*), in both the liver and white adipose tissue of mice. It also improved the insulin sensitivity of liver and peripheral tissues, in both lean and obese mice independently of adiposity and reduced body weight (139). In addition, FGF-21 might have a role in the maintenance of β -cell function in diabetic mice. However, these diverse and intriguing findings in rodents have yet to be translated to humans. Fibroblast growth factor-21 levels are consistently enhanced in patients with obesity, IR, NAFLD or T2DM and an increase in hepatic FGF-21 is associated with enhanced hepatic glucose and lipid synthesis (140).

Leukocyte cell derived chemotaxin 2 is expressed specifically by human fetal and adult hepatocytes and released into the bloodstream (141, 142). *Lect2*-deficient mice exhibit abnormal numbers of natural killer T cells (143). While the role of *LECT2* in the development of obesity and IR has yet to be defined, elevated levels of *LECT2* are positively and strongly correlated with those of

hemoglobin A1c (HbA1c), AST, C-reactive protein (CRP), LDL cholesterol, clinical markers of HOMA-IR, T2DM and dyslipidemia in patients (144). Recently, it has been suggested that liver may contribute to muscle IR in obese mice by secreting Lect2 (145).

Currently clinical findings suggest that AHSG, also known as fetuin-A (FetA), is perhaps the most important hepatokine regulating human metabolism (146). During embryogenesis, human FetA is expressed in several developing tissues and organs such as the liver, kidney, brain, bone and cardiovascular and respiratory system (147). After birth, FetA is predominantly synthesized in the liver and released into the bloodstream (148). An inhibitory role of FetA on the insulin receptor tyrosine kinase in the hepatocytes and skeletal muscles resulting in IR has been established (149). In targeted FetA gene knockout experiments in mice, insulin sensitivity was improved and the mice resistant to weight gain (150). The mRNA expression of FetA is increased in mice with fatty liver (151, 152). In humans, higher circulating levels of FetA is strongly associated with NAFLD (152, 153) and metabolic syndrome (154) independent of adiposity. Further, modifications in lifestyle such as exercise and weight loss, reduce serum FetA concentration while limiting NAFLD (155). Increased FFA levels can induce FetA overexpression through increased NF κ B activity (156). High circulating levels of FetA are a strong predictor of the future development of T2DM (154). In adipocytes, FetA also strongly stimulates inflammatory cytokine expression in adipocytes (156, 157). This collective data set has led to the suggestion that FetA may be a key to integrating many of the features seen in metabolic syndrome.

1.3.1 Role of fetuin-A in insulin signalling and inflammation

Auberger *et al.*, initially isolated FetA as a 63-kD secreted glycoprotein from adult liver and showed that a purified and phosphorylated murine form of FetA suppressed insulin receptor protein tyrosine kinase activity in both rats and FaO cells (149). Similarly, purified FetA from human serum also repressed tyrosine phosphorylation of the insulin-stimulated insulin receptor and its substrate 1 (158), leading to IR (159). However, the exact site of FetA interaction with the insulin receptor has not yet been defined (159). The secretion of FetA from hepatocytes is likely to initiate

systemic changes in metabolism. Notably, human adipocytes from fat biopsies treated with FetA exhibit reduced expression of adiponectin (157). Furthermore, FetA actively taken up by adipocytes (in a calcium-dependent manner) following intraperitoneal injection of mice leads to altered expression of multiple cytokines and adipokines and in particular, the overexpression of proinflammatory IL-6 and TNF- α (160). This data suggests a key role for FetA in the induction of IR and associated inflammatory responses.

1.3.2 Role of fetuin-A in obesity, diabetes and non-alcoholic fatty liver disease

The importance of FetA in metabolic disorders was further highlighted by transcriptomic analysis of rats fed either high- or low-fat diets (161). FetA mRNA was also up-regulated in hepatocytes of high-fat-induced mice with pathologically defined fatty liver (162), and in *db/db* mice used as a model for T2DM (160). Also, FetA/AHSG knockout mice exhibit increased glucose clearance and insulin-stimulated phosphorylation of the insulin receptor and AKT, and are resistance to high-fat-induced obesity (150). Taken altogether, these findings suggest that high-fat-induced obesity may lead to the accumulation of hepatic fat and the increased hepatic expression and secretion of FetA.

In humans, pregnant women with gestational diabetes had significantly higher levels of FetA than healthy pregnant or non-pregnant women (157). During a normal pregnancy, development of IR is common, and maternal FetA levels are elevated during the second and third trimesters (157). More generally, serum FetA levels are negatively correlated with insulin sensitivity, measured by euglycemic-hyperinsulinemic clamp in normal subjects, and positively associated with IR in nondiabetic patients (163) (151). In a recent study, FetA levels have been measured in participants classified on their response to a 75-g oral glucose tolerance test and found to be higher in subjects with impaired fasting glucose, impaired glucose tolerance or explicit T2DM (164). Moreover, in patients with coronary artery diseases, FetA concentration was also positively associated with metabolic syndrome, higher TG and LDL, and lower HDL concentrations (165).

These studies indicate that FetA levels are clearly elevated in prediabetic pathologies conditions.

A positive correlation between FetA expression and hepatic fat accumulation in human liver has been shown by proton magnetic resonance spectroscopy (151) and higher serum FetA levels reported in patients confirmed to have NAFLD by liver biopsy (151). In obese children with NAFLD, the general absence of many confounding effects driven by coronary diseases, alcohol consumption, smoking and medication intake means that they present with less complicated metabolic factors than adults. FetA levels are still significantly higher in comparison to those who are lean or without signs of NAFLD (155). Furthermore, in patients (aged 40 ± 10) with morbid obesity (body mass index (BMI) $> 45 \text{ kg/m}^2$) FetA levels were almost thrice as high as healthy, non-obese individuals (166). More recent prospective studies, suggest that the relationship between FetA levels and diabetes risk may be of considerable prognostic value. Higher basal levels of FetA are associated with increased visceral adipose tissue after 5 years (167) and a higher chance of diabetes development within 6 years, in older subjects (aged 70-79 years) (168) and could predict T2DM after 7 years of follow-up, after adjustment for age, gender and BMI (169). Collectively, these results suggest FetA as an independent risk factor for T2DM.

1.3.3 Metabolic regulation of fetuin-A concentration

Fetuin-A regulation is not well understood. Altered lifestyle factors such as weight loss, aerobic exercise and weight loss are known to reduce FetA levels, accompanied by decreased fat accumulation in hepatocytes in adults (151) and among obese children during a one year lifestyle intervention (155). In morbid obesity, dramatic weight loss after Roux-en-Y gastric bypass surgery leads to reduced FetA levels (166). Also, FetA levels are inversely associated with maximal oxygen uptake in men with chronic physical activity, and its plasma concentration higher in more sedentary subjects (170). These findings suggest FetA levels could be modulated by lifestyle interventions, but the extent and persistence of change clearly depends on the intensity, duration, and length of physical training and associated weight loss. Indeed, even 3-months aerobic exercise

failed to reduce FetA levels if body weight remained unchanged (171). Pharmacological interventions are also possible and early indications are that these may be more efficacious than modulation by exercise. The drug pioglitazone, an insulin sensitizer, blunts FetA levels in T2DM patients (171) as it is able to decrease the hepatic fat content (80, 172), and thus may improve IR through down-regulating FetA. Additionally, an extended-release treatment with niacin over 6 weeks reduced FetA levels are positively correlated with total TG and C-reactive protein concentrations in subjects with metabolic syndrome (173).

It has been shown that saturated FAs induce obesity-related inflammation in a TLR4-dependent manner, and that FetA is the adaptor protein that directly links saturated fatty acids to activation of TLR4 and the resulting impaired insulin sensitivity (174, 175). Saturated FAs reduce membrane fluidity, resulting in the accumulation of TLR4 receptors in lipid rafts, specific domains within the cell membrane. Free fatty acids bind to FetA and then complex with the concentrated TLR4, driving activity of transcription factors such as NF κ B, promoting expression of inflammatory cytokine and thus IR in adipocytes (Figure 1.5). Under these conditions, the activity of AMPK which normally inhibits NF κ B transcription, is itself suppressed by FFA (palmitate) signalling (176). While FetA is clearly linked with the induction of IR and T2DM (and thus an obvious target for intervention) little is known about its synthesis in hepatocytes (177), although FFA and palmitate in particular stimulates FetA overexpression in hepatocytes leading to TG accumulation (178).

In summary, FetA is a focus for the work which is described herein because of its potential role in the development of fatty liver, its potential as a prognostic marker of T2DM and coronary vascular disease risk and as a drug target for therapy of NAFLD-associated disease.

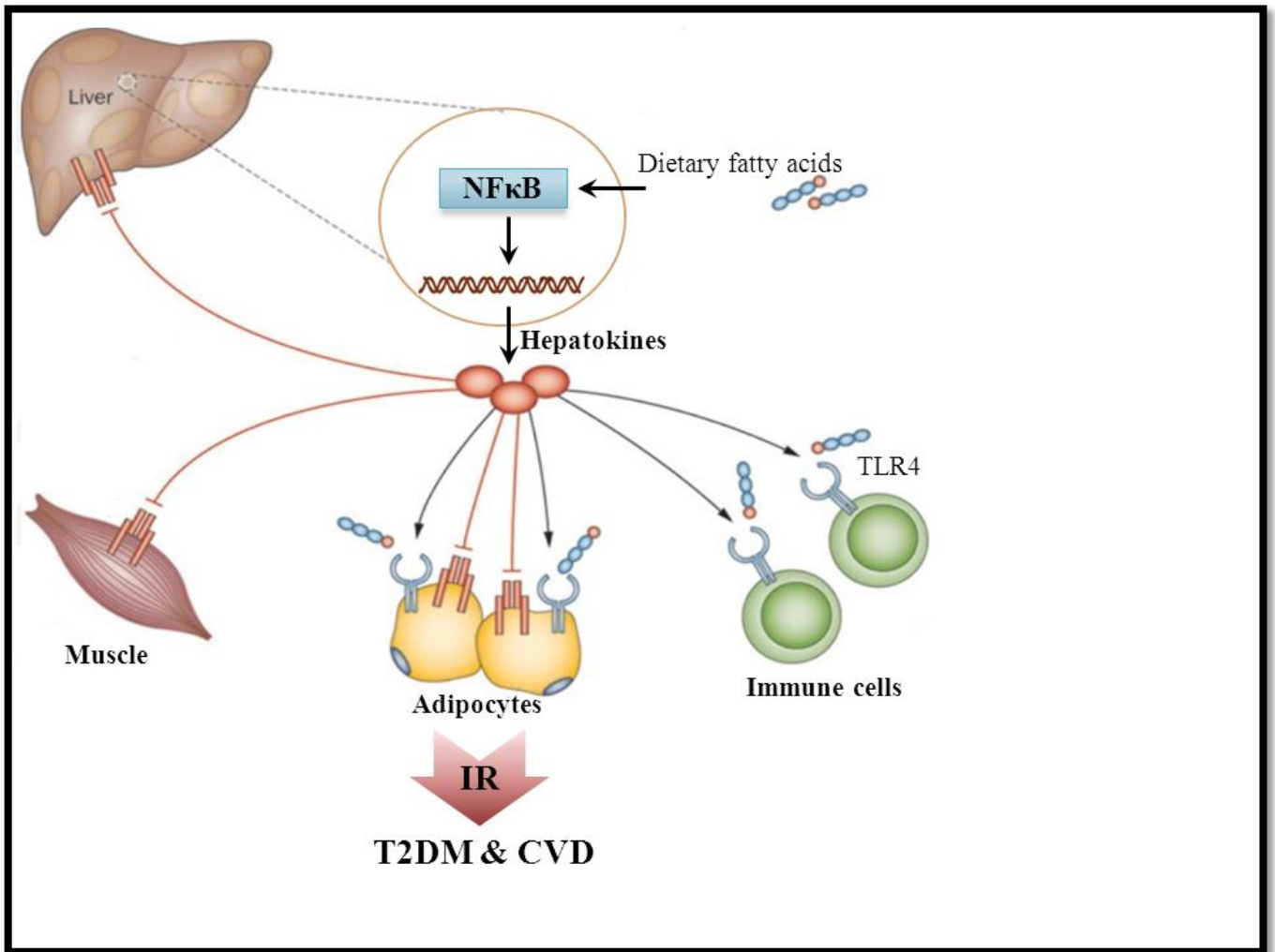


Figure 1.5 Metabolic consequences of increased production of fetuin-A

Liver secretion of hepatokines can be induced by external factors such as high levels of saturated FAs. FetA released into the blood stream and inhibits insulin signalling via binding to the insulin receptor thus stimulating IR in muscles and adipocytes. FetA also plays an adaptor role for saturated FAs resulting in TLR4 activation thus inducing inflammatory cytokines expression and IR in monocytes and adipocytes. Insulin resistance is known as a major risk factor for T2DM and CVD.

Abbreviations: CVD: cardiovascular diseases; FA: fatty acid, FetA: fetuin-A, IR: insulin resistance, T2DM: type 2 diabetes mellitus; TLR4: Toll like receptor4.

Modified from (146).

1.4 Myostatin regulatory roles in body metabolism

Myostatin (MSTN) or growth and differentiation factor-8 (GDF-8) is a secreted protein of the transforming growth factor- β (TGF- β) superfamily (179). Myostatin is a potent anti-anabolic regulator of muscle growth that may also play a role in energy metabolism (180).

Within the cell MSTN is proteolytically cleaved in the endoplasmic reticulum, generating an amino terminal and a carboxy terminal, and the latter being the active domain (181). In its secreted form, MSTN is held inactive within a multi-protein complex consisting of carboxy terminal dimers bound to inhibitory proteins. The active dimer is freed from the inhibitory protein complex by interaction with the tolloid and tolloid-like extracellular proteases (182) and then binds to the cell surface activin receptor type II or IIb (ActRII, ActRIIb), leading to phosphorylation and activation of the 'small mothers against decapentaplegic' (SMAD) family of signalling molecules (183). Mammalian SMAD proteins are divided into 3 subfamilies based on their functions; receptor-regulated SMADs (R-SMADs), inhibitory Smads (I-SMADs) and common-partner SMADs (Co-SMADs) (184, 185). Receptor-regulated SMADs are phosphorylated and thus activated through serine kinase activity of the type I receptors, and include SMAD1, SMAD2, SMAD3, SMAD5 and SMAD8. While SMAD2 and SMAD3 are involved in TGF- β signaling pathways (186, 187), SMAD4 positively regulates R-SMADs as a co-SMAD (185). MSTN activation of SMAD2 and SMAD3 triggers the subsequent formation of heterooligomers with SMAD4 and the consequential translocation of the entire complex into the nucleus, where it then regulates transcription of different downstream genes (Figure 1.6) (188, 189). It is well established that MSTN signalling through MSTN driven cross talk through ActRIIb mediated JNK signaling determines muscle myoblast proliferation and differentiation (190), although cross talk with MSTN triggered non-SMAD dependent MAPK pathway signalling also contributes to the balance of muscle myoblast proliferation (180, 191).

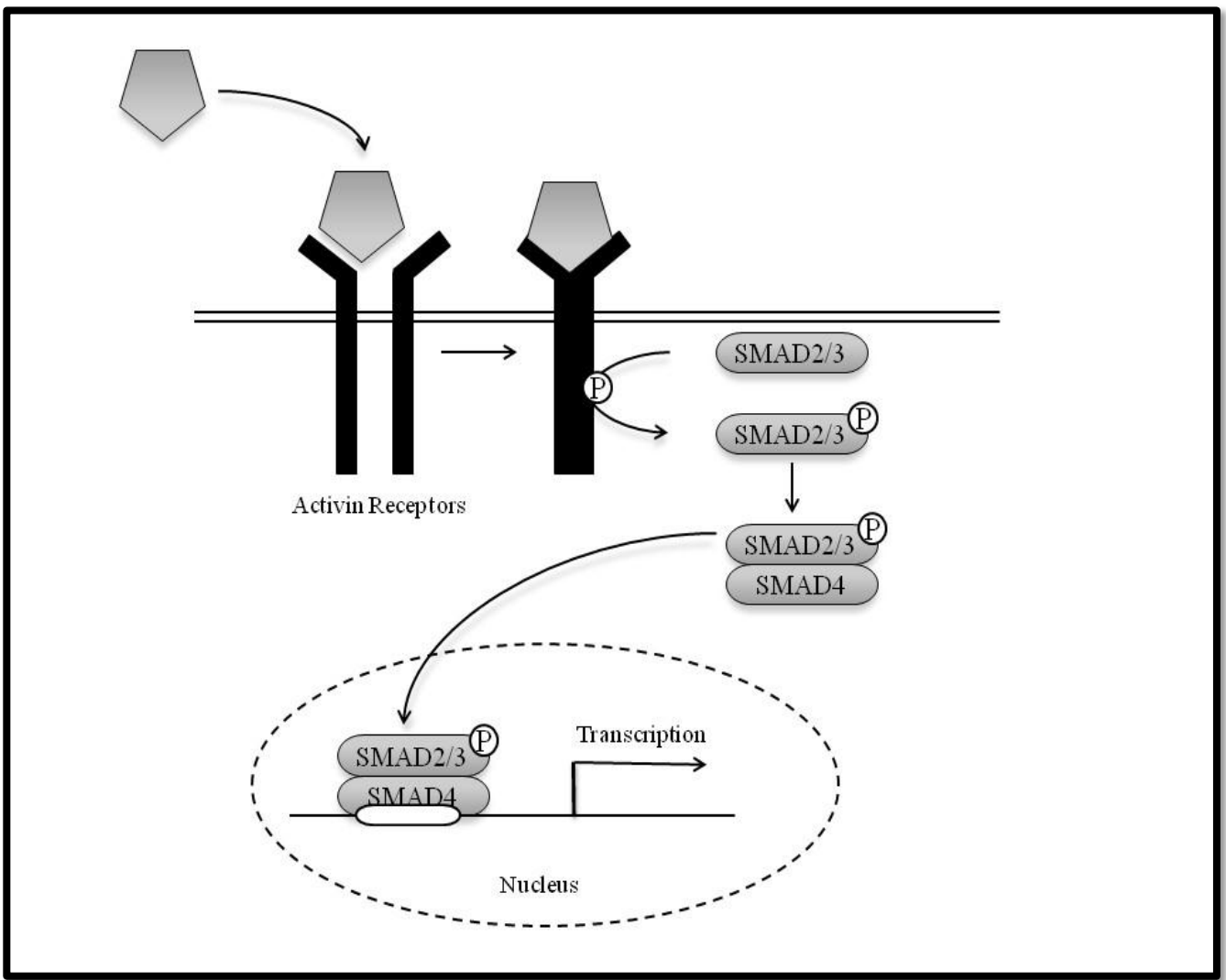


Figure 1.6 The MSTN signalling pathway

Synthesized MSTN interacts with ActRII on the cells surface thus recruiting ActRI which is then phosphorylates SMAD2 or SMAD3. These phosphorylated SMADs are recognised by mediator co-SMAD4 and translocate into the nucleus to interact with the promoter of target genes to regulate expression of MSTN-downstream target genes such as p38 MAPK.

Abbreviation: ActRI/II: activin receptor I/II, MSTN: myostatin, p38 MAPK: p38 mitogen-activated protein kinase, SMAD: small mothers against decapentaplegic.

Modified from (192).

1.4.1 Myostatin and hepatic glucose metabolism

Only more recently has the potential impact of for MSTN signaling beyond skeletal muscle become apparent. Specifically, it has been proposed that MSTN function may impact on metabolism in liver and adipose tissues, independently of its role in determining muscle mass (181). MSTN phosphorylation and activation of SMAD signaling also occurs in liver. In HepG2 cells, a human hepatocarcinoma cell line, ActRIIb receptors are expressed and MSTN enhances phosphorylation of SMAD2 and increases transactivation of a promoter holding SMAD-binding element (193). Therefore, it has been suggested that MSTN inhibition may lead to a decrease in hepatic SMAD signaling and subsequently enhanced hepatic insulin sensitivity. However, the relationship between MSTN activity and liver glucose metabolism is not yet clearly established.

1.4.2 Myostatin and obesity

Myostatin mRNA expression is increased in the skeletal muscles of obese women with IR resulting in enhanced circulating MSTN levels (194) compared to non-obese women (181). MSTN mRNA levels are also elevated in both skeletal muscle and adipose of genetically obese, wild type mice fed a HFD for one month and leptin-deficient ob/ob mice (195). Conversely, MSTN mRNA levels are reduced following weight loss in muscle and adipose tissues of ob/ob mice (195), as well as in muscle from obese human patients (196) or following gastric bypass surgery (197). Manipulation of MSTN expression or signalling can significantly influence obesity progression with several studies reporting that MSTN inactivation can reduce the development of obesity in mice. MSTN-null obese ob/ob mice exhibit a reduction in adipose mass, hyperlipidemia, hyperglycemia and hyperinsulinemia (198). Moreover, MSTN-inhibited postnatal transgenic mice also shown enhanced muscle growth and attenuated the effects of HFD on the promoting adipose mass and increased glucose and insulin levels (199, 200). Notably, the injection of soluble ActRIIb receptor decreases fat mass, while enhancing muscle mass in mice fed either HFD or standard chow (201). Therefore, it seems

likely that adipocytes may respond directly to MSTN signalling. The elevation of ActRIIb mRNA expression in ob/ob mice is consistent with increased MSTN signalling in the adipocytes under an obese state (195). Although MSTN inhibition is thought to prevent the development of obesity, several studies have now shown that MSTN treatment can affect adipocytes differentiation in both *in vitro* and *in vivo*. Specifically, adipogenic differentiation in 3T3-L1 was found to be inhibited by MSTN (183, 202) resulting in smaller and more immature adipocytes (203). Similarly, in adipose-specific transgenic mice over-expressing MSTN, dexamethasone-induced MSTN leads to reduced adipocyte size, although body composition remains unchanged (203).

Collectively, these findings suggest while that adipocyte precursors treated with exogenous MSTN are less 'differentiated', impact of this on the pathological progression of obesity remains unclear. Adipose and muscle-specific promoter-mice have also been used to stimulate the expression of a dominant negative form of the ActRIIb gene, to explore how prevention of MSTN signalling might impact on the development of obesity. As expected, mice with inhibited MSTN exhibit more muscle mass, and reduced adipose depot weights and smaller adipocytes compared to wild type mice. They also gained less weight and had lower fasting TG, blood glucose and insulin (204). However, the mice with inhibited MSTN in adipocytes did not show any difference fat or lean mass, nor circulating glucose and insulin levels, when fed either a standard or HFD (204). These results clearly suggest that the beneficial effects of MSTN blockade on obesity are clearly tissue dependent. Ob/ob mice injected with a neutralizing antibody to MSTN, showed the expected increase in muscle mass, but no change in adipose mass despite increased energy expenditure, and reduced serum glucose and FA levels (205). Similarly, both *in vitro* and *in vivo* studies show supplementation with recombinant MSTN has no effect on fat mass or adipocyte function (lipid release) in mice (206). Thus, the beneficial effects of MSTN modulation on limiting the negative consequences of obesity would appear to be an indirect result of the loss of MSTN in other tissues. In this regard, the role of hepatic MSTN signalling needs to be elucidated more fully.

1.4.3 Myostatin and diabetes

Recently, a possible role for MSTN in the progression of diabetes (in addition to or independent of its role in obesity) has been suggested. Skeletal muscle biopsies, from either T2DM or non-obese but hyperinsulinemic patients, revealed elevated MSTN mRNA levels (207). Moreover, in insulin-resistant middle-aged men undergoing aerobic exercise training, muscle and plasma MSTN protein levels are decreased and strongly correlated with insulin sensitivity, while their BMI and fat mass remained unchanged (208). Furthermore, injection of a neutralizing antibody to MSTN or a recombinant form of MSTN reduced insulin sensitivity, and both fasting and post-prandial blood glucose levels, (without any change in both adipose and muscle mass) in male mice or mice on a HFD (205, 208, 209). Together, these studies have suggested that enhanced MSTN expression is adversely associated with insulin sensitivity, independent of obesity. Interestingly, MSTN supplementation promotes glucose uptake in human placental tissue (210), and increase glycolysis and suppresses glycogen synthesis, via AMPK signaling, in cultured skeletal muscle cells (211). MSTN may thus be significant in the etiology of peripheral IR.

It has also been suggested that MSTN plays a role in liver metabolism, the pivotal organ in regulating systemic glucose homeostasis. Mice injected with a recombinant soluble ActRIIb receptor exhibit enhanced hepatic insulin sensitivity (201) and mice with MSTN loss-of-function mutations fed a HFD have decreased hepatic steatosis and lower insulin-dependent suppression of hepatic glucose production (209). Modulation of MSTN signaling leads to greater hepatic steatosis and hypertension in mice (212). The potential for activating mediated MSTN signaling has been reported in the liver of mice, as well as both human and mouse hepatic cell lines (213, 214). There is still much work to be done before the role of MSTN in hepatic metabolism will be fully elucidated..

1.4.4 Myostatin and fatty liver

The total mass of liver is notably attenuated in obese MSTN-deficient mice compared with that of mice with normal MSTN expression, even when liver histology has indicated that steatosis is not

sever in the MSTN-deficient mice (215). MSTN gene mutation also reduces HFD-induced hepatic steatosis (209), while MSTN knockout decreases decreased lipid accumulation in skeletal muscle (215). However, the reasons for reduced accumulation of fat in both the liver and muscle after MSTN modulation remain unclear.

1.5 Expression of epigenetic modulators

A growing number of epidemiological studies suggest that environmental factors and exposures during gestation and soon after birth can significantly alter the long-term consequent risks of metabolic diseases. The environmental stimuli are presumed to influence the level of expression of various genes and the stability of the gene products. These effects are variable across the population and modifiable within the generation, although they influence the phenotype outcome over the the life-course of the individual, and likely mediated through “epigenetic” mechanisms. Epigenetics allows the organism to adapt to exogenous influences and to pass information about the environmental cues between generations without the need for permanent alterations in the base structure of their DNA, such as occur with mutations (216).

The primary epigenetic modifications currently recognized include DNA methylation, chromatin structure modifications, histone modifications (acetylation, methylation, phosphorylation and ubiquitination) and differential expression of small non-coding RNAs (Figure 1.7).

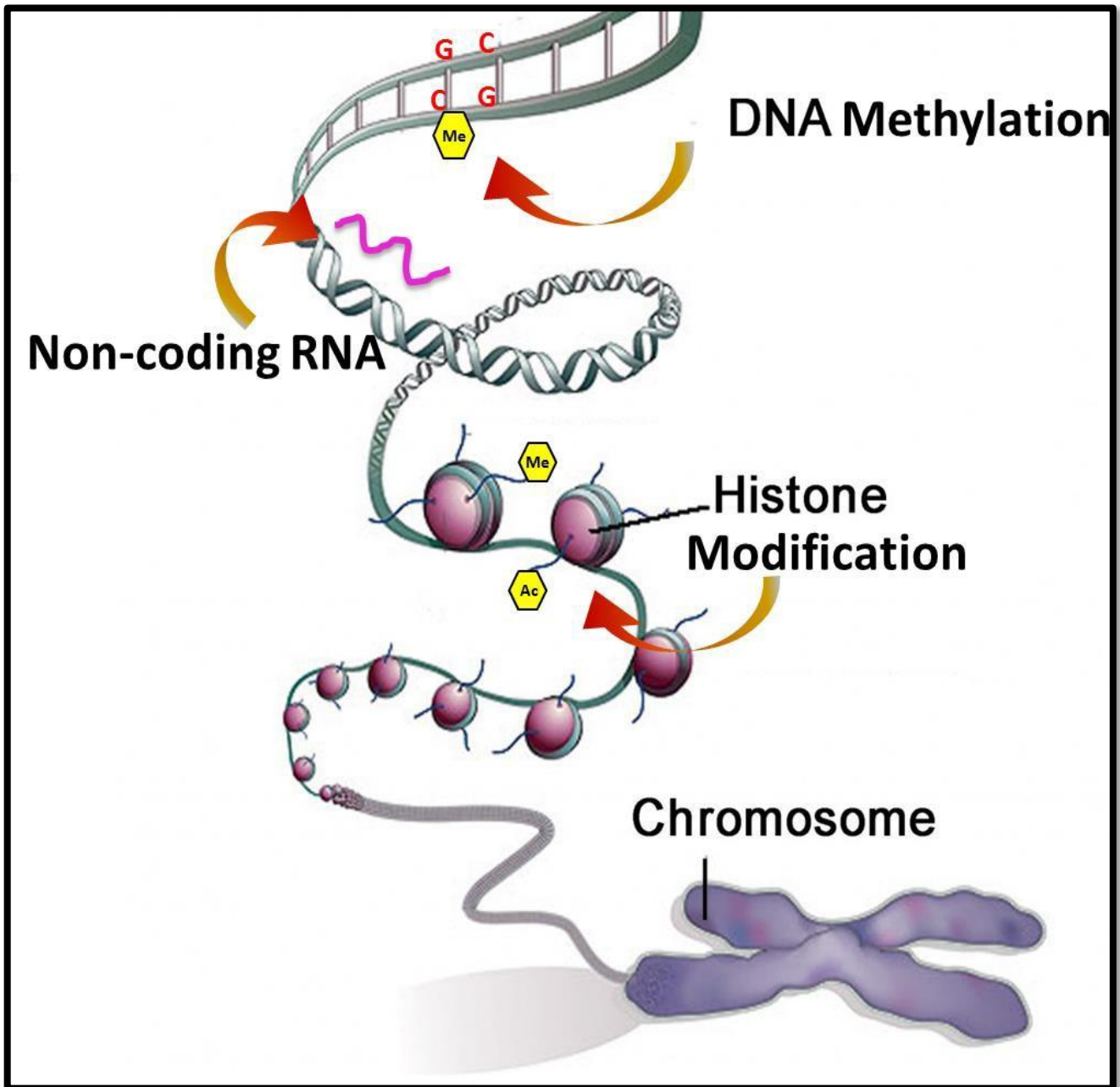


Figure 1.7 Epigenetic modifications

In the nucleus of each cell, the DNA molecule is packaged into structures called chromosomes. Chromosomes of organisms consist of protein, DNA and RNA. In DNA methylation, methyl groups are added to CpG dinucleotides thus inhibit gene transcription via limiting DNA accessibility for transcriptional factors. Non-coding RNAs including microRNAs repress gene expression at both mRNA and translational levels. Histone tails are the target of certain molecules that alter the activity of wrapped DNA around the histone.

Modified from (217).

1.5.1 DNA methylation

The regulation of gene transcription is not only dependent of DNA-binding transcriptional factors but also involves processes affecting the ability of transcription factors to access and bind their target DNA (218). DNA methylation is a reversible physiological process which is catalysed by DNA methyltransferases (DNMs) (219) and involves the donation of a methyl group from S-adenosylmethionine (SAM) to the 5'-position of a linked cytosine nucleotide to a guanine nucleotide (CpG dinucleotide) through a phosphodiester bond. Regions with a high CpG content form CpG islands that reside in the regulatory regions of many genes including promoters and enhancers (220). Methylation modifications determine DNA interaction with histones (see below), leading to states which either facilitate (hypomethylation) or suppress (hypermethylation) gene expression (221). When DNA methylation occurs in a gene promoter, it acts to repress gene transcription via limiting transcription factors access to the promoter. In normal mammalian cells, over 85% of CpG dinucleotides are methylated and these are used for maintenance of the chromatin structure and for transcriptional regulation (222). CpG islands in the genes promoter are usually unmethylated. Epigenetic information is heritable between cell generations via recognition and methylation of CpG dinucleotides by DNA methyltransferase 1 (DNMT1) on the newly synthesized strand (223). The link between nutritional exposures and later risk of diseases such as IR and obesity could be regulated by DNA methylation. It has been suggested that DNA methylation has an important role in the regulation of glycolytic genes in liver (224) and in HFD-induced obesity (225).

1.5.2 Histone modification

Histones are proteins that interact directly with DNA and play an important role in regulating gene expression. The nucleosome, the fundamental repeating unit of chromatin, is composed of an octamer of four core histones (H2A, H2B, H3 and H4 histones) surrounded by 147 DNA base pairs (233). Post-translational modifications on N-terminal tails of each histone alter the chromatin structural properties (234) and include methylation of arginine or lysine, phosphorylation of threonine and serine, acetylation and ubiquitination of lysine and adenosine diphosphate (ADP)-ribosylation (235). Histone

methyltransferase catalyses histone methylation via transferring one to three methyl groups from SAM to Arg or lysine residues of histone. Gene expression can be also affected by histone acetylation (236). Histone acetyl transferases (HAT) catalyse acetylation of lysine residues at the N terminus of histones (237) and neutralizes the positive charge on histone and decreases the interaction of the N termini of histones with the negatively charged DNA phosphate group thus promoting transcription (238). In addition, histone phosphorylation of H3 may also be significant, and have been shown to be necessary for cytokine-induced gene expression (239).

1.5.3 MicroRNAs biogenesis and function

MicroRNAs (miRNAs) are a class of short, non-protein coding, single-stranded gene products and typically 20–22 nucleotides in length. They are coded for in the genomes of eukaryotic organisms and known to modulate the expression of target genes post-transcriptionally, via interactions with specific mRNA products arising from regular transcription processes (226, 227).

Both the nucleus and cytoplasm of mammalian cells engage in the biogenesis of mature, and thus functional, miRNA from the corresponding miRNA gene. A multistep process of biogenesis begins within the nucleus where the enzyme RNase III Drosha binds specifically to a genomic motif known as the ‘DiGeorge syndrome chromosomal region 8’ (DGCR8), thus cleaving ‘pri-miRNA’ species into pre-miRNA precursors consisting of ~70 nucleotides. These stem-looped pre-miRNAs are then exported into the cytoplasm via Exportin 5, where they are further cleaved by Dicer (another RNase III enzyme) and the transactivator RNA-binding protein (TRBP) partner into smaller incomplete miRNA: the final miRNA double-stranded RNA duplex of 22 nucleotides contains the mature miRNA strand and its complementary strand (228, 229) (Figure 1.8).

The duplex is then untwisted to yield functional single-stranded miRNA (~22 nucleotides) and complexed as a ribonucleoprotein (miRNP). This mature miRNA is inserted into an RNA-induced silencing complex and by binding to the 3'-untranslated region of a target mRNA results in latter's

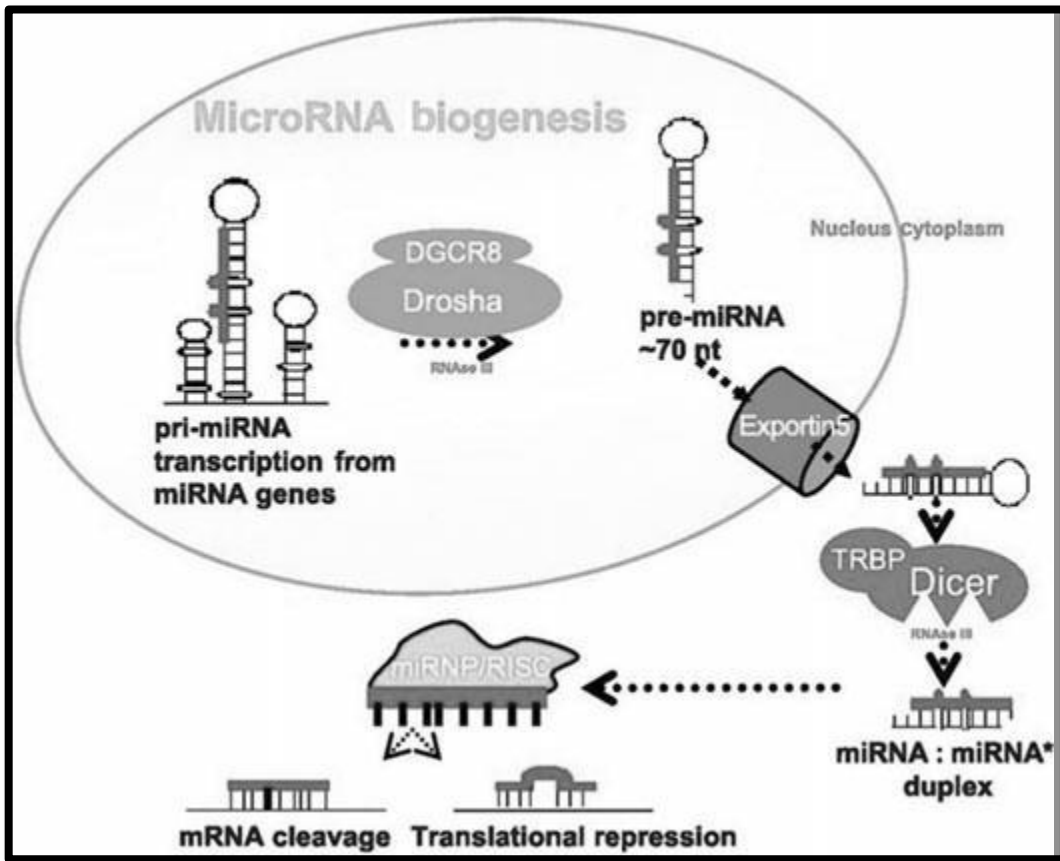


Figure 1.8 MiRNA biogenesis

The miRNA biogenesis begins in the nucleus where miRNA gene is transcribed to pri-miRNA and cleaves by Drosha and its binding partner DGCR8 to form pre-miRNA. The pre-miRNA is then exported to the cytoplasm by Exportin 5. In the cytoplasm, the precursors are cleaved by Dicer and TRBP into dsRNA duplex which subsequently incorporated into the RNA-induced silencing complex (RISC) and miRNP complexes. MiRNAs regulate expression of genes through cleavage of mRNAs and repression of protein translation.

Abbreviation: DGCR8: DiGeorge syndrome chromosomal region 8, TRBP: Transactivator RNA-binding protein, dsRNA: double-stranded RNA, RISC: RNA-induced silencing complex, miRNP: microribonucleoprotein.

Modified from (229).

degradation by deadenylation, leading to the targeted suppression of ‘translation initiation’ by the inhibition of 80S ribosome complex assembly, and the suppression of ‘translation elongation’ by the premature termination of ‘ribosome drop-off’ (230). miRNAs nearly always lead to the decreased protein synthesis of both activators or inhibitors of metabolic pathways.. However, in contrast with the general assumption of a linear one-way process of miRNA-mediated gene downregulation, it has recently been shown that this process is potentially reversible (231). MiRNAs can also function to up-regulate expression of their target mRNA products (232), likely through both enhancing mRNA stability and/or the activation of translation, either by direct activation or indirect repression (233).

The absence or mutation of miRNAs (identified by genetic analysis) has been associated with different diseases, and offers opportunities for diagnostic marker development. Commonly used methods for detecting and measuring the expression of miRNA include polymerase chain reaction (PCR), microarray panels and Northern blot (234).

1.5.3.1 MiRNAs in obesity

Candidate species have already been linked with obesity. Notably miR-335 is upregulated in the adipose tissue of three different murine obesity models, including the leptin-receptor-deficient db/db mice, leptin-deficient ob/ob mice and KKAY44 mice, although the experimental validation of mRNA targets has yet to be done (235). A further forty hepatocyte specific miRNAs are downregulated after the induction of obesity, but only in obesity-resistant mice, suggesting that miRNA regulation may be influenced by the genetic background of the organism (236-238). In humans, fat depots from overweight and obese individuals, with either normal glucose tolerance or recently diagnosed with T2DM, have been used to identify miRNAs associated with key diabetic metabolic indicators, such as fasting plasma glucose, circulating adiponectin, leptin and IL-6 expression (239).

Esau et al., (240) have described the role of miRNAs in the general biology of human adipocyte by comparing the miRNA signatures in preadipocytes and differentiated adipocytes, and suggest that miR-143 in particular is key to differentiation. Following inhibition of -miR-143,

adipocytes not only exhibit impaired morphological differentiation, but also reduced TG accumulation and decreased expression of the glucose transporter 4 (GLUT4) and PPAR γ . In addition, ectopic expression of miR-143 in preadipocytes stimulated adipogenesis and induced TG accumulation, as well as the expression of adipogenic markers (240). Several miRNAs have since been shown to target PPAR γ mRNA expression and thus influence lipid homeostasis (241, 242). Further, miR-519d targets the related PPAR α and regulates lipid accumulation during adipogenic differentiation (243).

1.5.3.2 MiRNAs and glucose homeostasis

The effect of miRNAs on metabolism was initially explored in the insulin responsive tissues (adipose, liver and muscle), of healthy and Goto-Kakizaki rats, a model of T2DM (244). Notably, miRNAs appear to influence blood glucose metabolism by changing the insulin sensitivity or resistance of target tissues (245, 246). More recently, a number of miRNAs have been linked with the development of pancreatic islets, the differentiation of β -cell specifically and with insulin secretion and signalling (247). Altered plasma glucose concentrations appear to influence miRNA expression. For example, the exposure of pancreatic β -cells to high-glucose concentrations significantly upregulates the expression of miR-124a, miR-107 and miR-30d, while miR-296, miR-484 and miR-690 are downregulated (248). Of these, overexpression of miR-30d under high-glucose concentrations has been shown to negatively correlate with insulin gene expression, although not with insulin secretion (248). Other species are also involved in both in the lineage development of pancreatic cells and subsequent insulin secretion (249). Additional miRNAs also induce IR in adipocytes, by targeting genes involved in AKT, PI3K and p38MAPK subunit regulation (250, 251). Taken together, miRNAs could target different genes involved in glucose homeostasis therefore affect multiple levels in signaling pathways.

1.5.3.3 MiRNAs and lipid homeostasis

The first miRNA to be linked with metabolism, miR-122, is expressed primarily in the liver, but influences hepatic lipid and cholesterol metabolism during hepatocyte differentiation. Antisense

targeting of miR-122 in high-fat induced mice, led to 30% decrease in circulating cholesterol levels (252), decreased hepatic cholesterol and fatty acids biosynthesis and an elevated fatty acid β -oxidation associated with a reduction in TG and hepatosteatosis (252), suggesting the possibility of miR-122 antisense oligonucleotides as novel treatment approach to lower circulating cholesterol.

The alpha subunit of AMPK α 1 is the target of regulation by both miR-33a and miR-33b. As mentioned earlier, in response to low cellular energy level AMPK decreases energy consuming processes, such as FA biogenesis, to promote ATP synthesis. Notably, AMPK inhibits SREBPs (a family of key transcriptional regulator of lipid genes), and miR-33 dependent suppression of AMPK leads to stimulation of SREBPs (and their target genes) leading to increased intracellular levels of TG, cholesterol and FAs. Interestingly, IRS-2 is also regulated by miR-33 (253, 254), influencing the activity of downstream effectors, such as PI3K and AKT. It is reported that in a NAFLD mouse model, reduced hepatic level of IRS-2 results in increased IRS-1 levels, and in turn, the induction of SREBP-1c (255). Taking together, miR-33 antisense targeting could lead to reversal of the hepatic IRS-1 and IRS-2 suppression reduce the elevated SREBP-1c levels associated with hepatosteatosis.

1.5.3.4 MiRNAs in non-alcoholic fatty liver

A number of miRNAs are dysregulated in both rodent models of NAFLD, obesity and T2DM, and in clinical patients with obesity-induced NAFLD and NASH. Among these, miR-34a in particular is highly overexpressed in both NAFLD and NASH patients, as well as T2DM subjects (256-258). MiR-34a targets Sirtuin1 (SIRT1), a key metabolic regulator (281), which responds to intracellular NAD⁺ levels by deacetylating both histone and non-histone targets, including PPARs, PGC-1 α , forkhead Box Protein O 1 (FOXO1), tumor protein p53 (p53) and SREBPs. Thus, miR-34a mediation of SIRT1 impacts on both lipid and cholesterol synthesis, and energy homeostasis (259-262). Indeed, high levels of miR-34a and low levels of hepatic SIRT1 are strongly associated with fatty liver diseases (263). Serum samples of patients with NAFLD and NASH also exhibit differential overexpression of additional miRNAs with as yet poorly defined impacts (256, 264-266).

Moreover, expression of a subset of these miRNAs also correlates with the severity of NAFLD, with miR-34a showing the strongest correlation (266, 267). Taken together, miRNAs clearly act as circulating epigenetic regulators that potentiate features of metabolic syndrome and associate with the severity of disease.

1.6 Scope of this study

Poor dietary habits can lead to weight gain and subsequently, obesity-related comorbidities such as NAFLD. While it has been suggested that diet composition may influence body weight, independent of total calories intake, identification of specific dietary components contributing to an increased propensity for obesity has been controversial. Obese individuals exhibit notably increased levels of plasma BCAAs and elevated FFAs, both presumed to result from excessive dietary intake in the context of Western style diets. The primary focus of the current work is to explore the molecular effects of BCAA and FFA supplementation on hepatic biology and in particular, to define the importance of epigenetic mechanisms in these effects. Finally, I attempt to translate aspects of these laboratory findings to a clinically relevant setting by considering the molecular consequences of bariatric surgery intervention in obese individuals.

1.6.1 Aims

1. Identify the signalling mechanisms driven by BCAA and FFA-mediated regulation of hepatic metabolism.
2. Investigate the novel epigenetic regulators (miRNA) associated with these metabolic shifts.
3. Identify novel miRNAs likely to originate in liver and that are expressed differentially in obesity.

1.6.2 General Hypothesis

Epigenetics mechanisms (miRNA) contribute to the response of the liver to nutrient imbalance in the context of metabolic syndrome.

2 METHODS

The methods section explains the basic protocols performed for this thesis.

2.1 Cell culture of HepG2 hepatocytes

Human HepG2 (Appendix I, Table 1) hepatoma cells were grown and maintained in monolayer culture in low-glucose Dulbecco's Modified Eagle Medium (DMEM) supplemented with 10% volume/volume (vol/vol) fetal bovine serum (FBS) (Appendix I, Table 2) in an atmosphere of 5% CO₂ at 37 °C. For experiments, adherent cells were passaged and medium was renewed when 70%-80% confluence (almost 72 hours) in 1:3 splitting ratio. 0.25% (w/vol) trypsin- Ethylenediaminetetraacetic acid (EDTA) solution (containing 0.53 mM EDTA) was used to detach cells. Cells were used for experiments at the third passage after reviving and seeded at 10⁴ to 10⁵ cells /cm². This cell line was used throughout the thesis when experiments were performed on hepatocytes.

2.2 Maintenance and differentiation of murine C2C12 myoblast

C2C12 (Appendix I, Table 1) myoblasts at passage four were cultured when no more than 80% confluence (almost 48 hours) in proliferation medium containing high-glucose DMEM, 10% FBS and 1% L-glutamine (Appendix I, Table 2). Media was renewed daily. C2C12 myoblasts were in an atmosphere of 5% CO₂ at 37 °C. Seeded cells were confluent after almost 5 days. Confluent myoblasts were washed with warm phosphate-buffered saline (PBS) before differentiation by substituting 10% FBS with 2% horse serum for 4 days. Differentiation medium was also renewed every day. Myotubes were used for experiments 4 days after initiation of differentiation. Cells were seeded at 3x10³ cells/ cm². This cell line was used to perform glucose uptake assay using conditioned medium from HepG2 cells.

2.3 Maintenance and differentiation of PANC-1 pancreatic cells

PANC-1 (Appendix I, Table 1) cells were cultured in proliferation medium containing high-glucose DMEM, 10% FBS and 1% L-glutamine (Appendix I, Table 2) and was renewed every other

day until reach 80% confluence was reached (almost 4 days). PANC-1 cells were cultured in an atmosphere of 5% CO₂ at 37 °C. Confluent cells were washed with serum-free DMEM/F-12 medium twice before harvesting with 0.05% trypsin. Cells were seeded in DMEM/F-12 (containing 17.5 mM glucose), 1% bovine serum albumin (BSA) and insulin-transferrin-selenium (ITS- G) for 4 days to be differentiated. The BSA was sterile filtered with 0.22µm pore filters. The medium was changed every other day using gravity to permit clusters sedimentation whereby single cells and debris were removed in the suspension. Cells were seeded at 7x10⁴ cells/ cm². This cell line was used to perform insulin concentration assay using conditioned medium from HepG2 cells.

2.4 Human subjects

Nine obese subjects with T2DM participated in a prospective randomised bariatric surgery whereby 4 received GBP and 5 received SG. All patients with at least 6 months of T2DM that referred for bariatric surgery were invited to participate in first surgical assessment. After attending an initial information evening, potential participants were assessed by a bariatric surgeon for suitability for surgery and whether the relevant inclusion and exclusion criteria were fulfilled. Baseline blood samples and physiological measurements were taken at this and all subsequent clinical encounters. All subjects, immediately pre-operation were on a very low calorie diet to achieve pre-operative weight loss and reduce liver fat to make laparoscopic surgery safer. The inclusion and exclusion criteria are shown in Table 4.1. The baseline characteristics with respect to age, BMI, ethnicity and duration of diabetes are shown in Table 4.2. Following fasting for at least 10 hours, blood samples were obtained 3 days before operation and 1 year after either GBP or SG surgeries. Bloods were collected into EDTA tubes and centrifuged following routine procedures to yield plasma samples which were stored at -80 °C until analysis. All patients provided written informed consent and the experiments conformed to the principles set out in the WMA Declaration of Helsinki and the Department of Health and Human Services Belmont Report. All experimental protocols were registered with the Australian New Zealand Clinical Trial Registry (NCT01486680) and approved by the Northern X Regional Ethics Committee, New Zealand (NZ93405).

2.5 Bichinonic assay to determine cellular protein concentrations

The Pierce kit (Appendix I, Table 3) was used to measure cellular protein content according to manufacturer's instruction as follow. Triplicates for BSA standards and duplicates for samples were performed in 96-well microplates. 50 μ l of diluted BSA standards (0.02, 0.04, 0.06, 0.08, 0.1 and 0.2 mg/ml), Milli-Q water as blank and 50 times- diluted samples in Milli-Q water was pipetted into each well. Then, 200 μ l of bichinonic assay reagents was added to the appropriate wells followed by 45 minutes incubation at 70°C while protected from light. The absorbance was measured at 595 nm using enzyme- linked immunosorbent assay (ELISA) plate reader (BioTek, Synergy 2, USA) using Gen5 software version 1.4.5.0 (BioTek, USA). The absorbance of BSA standards was measured to generate a standard curve with which the unknown sample proteins were compared.

2.6 Western blotting or immunoblotting

To generate whole cell lysates, cells were harvested into lysis buffer (50 mM HEPES, 150 mM NaCl, 10 mM EDTA.Na₂ (pH 8.0) and 1% triton X-100 (diluted in water); pH adjusted to 7.4 with 10 M NaOH) in the presence of phosphatase inhibitor cocktail (2 mM Na₃VO₄, 30 mM NaF, 1 mM Na₄P₂O₇ and 1X Protease Inhibitor Cocktail). Equal amount of protein for each sample was used for immunoblotting. 5X sample loading dye (1 M Tris-HCl pH 6.8, 10% SDS, 50% Glycerol, 0.0025% Bromophenol blue and 500 mM DTT) were added to 20 μ g proteins from whole cell lysates to a 1X final concentration of loading dye. Similar amount of dye was added into diluted samples with MilliQ-water in 1:4 ratio. A molecular-weight size marker was used as protein standards (Precision Plus Protein Dual Xtra Standards). All samples were loaded on the same gel and all experiments were done in triplicate. Appropriate loading control (β -actin) with same protein level across the gel was used to normalize the level of detected proteins. The mixed protein samples were heated at 98°C for 5-10 minutes to denature proteins and were resolved by electrophoresis on 10% sodium dodecyl sulfate polyacrylamide gel electrophoresis (SDS- PAGE) in a Tris-glycine gel running buffer (SDS, TRIS base and glycine) before transferring onto polyvinylidene difluoride (PVDF) membrane using standard semi-dry Western transfer method. Briefly, 100% methanol was used to activate PVDF

membrane followed by incubation with transfer buffer. The pre-wet gels, membranes and filter papers in transfer buffer (SDS, TRIS base, glycine, and methanol) were then assembled to make a sandwich and were exposed to a constant current of 180 mA on 25 V for 1.5 hour. After transferring, gels were visualised by coomassie-stained (acetic acid and Coomassie brilliant blue) to determine the equal loading of proteins and transfer efficiency and membranes were blocked with blocking solution followed by incubation with primary antibodies over night at 4°C (Appendix I, Table 5). Incubation with secondary antibodies at the appropriate dilutions (Appendix I, Table 5) was carried out for 45 minutes at room temperature. Membranes were washed with PBST (PBS and Tween 20) for at least 3 times (5 minutes each) on constant agitation after incubation with either primary or secondary antibodies. To visualise immunoblots, enhanced chemiluminescence (ECL) detection were used according to manufacturer's instruction. The intensity of bands was quantified using Image J software, version 1.4.3.67 (Wright Cell Imaging Facility, NIH, USA). HRP activity was detected using Western Lighting™ Chemiluminescence Reagent Plus. Films were exposed to the membranes and the developed films were analyzed using Quantity One imaging software (Bio-Rad, USA).

2.7 Purification of total RNA including miRNA

Total RNA from cells was isolated using TRIzol reagent (Appendix I, Table 3) with the PureLink RNA mini kit (Appendix I, Table 3) according to manufacturer's protocol as follow. After addition of TRIzol and passing the cell lysate several times, the lysate was incubated for 5 minutes at room temperature to allow complete nucleoproteins dissociation. After addition of chloroform to denature protein and make it soluble in organic phase, the lysate was shaken by hand for 15 seconds before centrifuge at 12000 G-force (xg) for 15 minutes at 4°C to remove protein from the sample. Upper phase was transferred to a new tube and mixed with equal amounts of 70% ethanol to precipitate RNA and transferred to the spin Cartridge and centrifuged at 12000 x g for 15 seconds at room temperature. 700 µl of Wash buffer I (provided in the kit) was added to the spin cartridge followed by another centrifuge at 12000 x g for 15 seconds at room temperature. 500 µl of Wash buffer II also added and centrifuged at 12000 x g for 15 seconds at room temperature. This step was repeated twice with increased centrifugation duration to 1 minute to ensure the membrane is dried. 50 µl of RNase-free

water was added to the center of the spin Cartridge and after 5 minutes incubation at room temperature, centrifuged in new tubes for 2 minutes at full speed at room temperature to collect RNA samples. RNA samples were quantified by NanoDrop spectrophotometer (ND-1000; NanoDrop Technologies Inc., DE, USA) whereby the ratio of absorbance at 260 nm and 280 nm (260/280) was used to assess the purity of RNA. A ratio of 2 ± 0.2 was accepted as pure for RNA. The 260/230 ratio out of 2.0-2.2 may indicate the presence of contamination which absorbs at 230 nm. The samples were stored at -80°C prior to use.

2.8 cDNA synthesis

A total of 2 μg of RNA was used for cDNA synthesis using Roche transcriptor first strand cDNA synthesis kit (Appendix I, Table 3) according to the manufacturer's instructions. RNA samples were mixed with 10X incubation buffer and DNase I in a 20 μl reaction to remove DNA contamination which affects the gene expression values. The reaction mixture was incubated for 20 minutes at 37°C , followed by addition of EDTA to stop the DNase activity to protect synthesized cDNA and heating for 10 minutes at 75°C to denature RNA secondary structure. To synthesize cDNA, 5X reaction buffer, protector RNase inhibitor, deoxynucleotide (dNTP) mix, transcriptor RT (contains RNase H activity to remove RNA template after cDNA synthesis) and random hexamers were added to DNase I-treated samples in a 40 μl reaction and incubated at 10 minutes at 25°C and 50 minutes at 50°C to synthesize the cDNA based on the pairing of RNA base pair and then 5 minutes at 85°C to inactive transcriptor RT at 55°C . Synthesized cDNA was then stored at -20°C prior to use.

2.9 Real-time quantitative PCR assay

The cDNA (50 ng) was further added to the mixture of forward and reverse primers, SYBR (fluorescent DNA binding dye) Master Mix (contains MgCl₂) topped up with polymerase chain reaction (PCR)-grade water to 10 µl per reaction. Quantitative real time PCR was carried out in triplicates under thermocycling conditions as follows: 95°C for 10 minutes for initial activation of Taq polymerase, followed by 45 cycles of 95°C for 10 seconds to melt double stranded DNA into single stranded fragments, 57°C-60°C for 20 seconds for annealing to form hydrogen bonds between primers and template DNA and 72°C for 15 seconds to elongation of new synthesized DNA strand. Following the amplification process, a melting curve analysis was performed by heating the plate at 95°C for 5 seconds, incubating at 60°C for 1 minute, followed by cooling to 37°C for 10 seconds. Real-time quantitative PCR (qPCR) was performed and analysed on a LightCycler-480 II (Roche, Switzerland). Gene expression was analysed as fold change whereby normalised to internal controls expression. The relative amount of target gene and a reference gene is determined for each sample and is then divided by the target/reference ratio of the calibrator. To create standard curve, the reactions were carried out with various concentrations of DNA template. Primers optimum temperature was checked by gel electrophoresis. Total 50 ng of cDNA samples mixed with 6X DNA loading dye and separated on 1% agarose gel with SYBR DNA gel using 1X Tris-acetate-EDTA (TAE) buffer for 30 minutes on gradient PCR using a range of annealing temperatures. The gel was quantified using Image Quant (GE Healthcare, USA).

2.10 MicroRNA isolation from human plasma

To perform microarray, frozen human plasma sample (See section 2.4 for more details on samples), were thawed on ice at room temperature before centrifuging at 10000 xg for 5 minutes at 4°C to remove possible debris and blood cells. Qiagen miRNeasy plasma kit (Appendix IV, Table 3) was used for RNA purification. 200 µl of the centrifuged supernatant was transferred to a new tube and 5 vol QIAzol was added and after vortex mixing was incubated for 5 minutes at room temperature to dissolve cell components. Lyophilized *C. elegans* miR-39 miRNA mimic was added to control samples

as a Spike-In control to check miRNA purification efficiency. Chloroform was then added at equal volume to the starting sample volume and after vortex mixing left for 2-3 minutes at room temperature before centrifuge at 12000 x g for 15 minutes at 4°C to participate proteins at organic phase. Upper aqueous phase transferred to a new tube and mixed with 1.5 vol of 100% ethanol and pipetted several times. The mixture was pipet into a spin Cartridge and centrifuged at 8000 x g for 15 seconds at room temperature. 700 µl of Buffer RWT was added to the spin Cartridge and spin at 8000 xg for 15 seconds followed by addition of 500 µl of 80% ethanol onto the spin Cartridge and centrifuged under similar conditions for 2 minutes. To dry membrane, spin Cartridge was centrifuged at full speed with open lid for 5 minutes. 15 µl of RNase-free water was directly added to the centre of the Cartridge and after incubation for 5 minutes at room temperature, was centrifuged at full speed for 1 minute using a new tube. Collected RNA samples then stored at -80°C.

2.11 cDNA synthesis assay for microRNAs

The cDNA synthesis was performed with 2 µg total RNA using a Qiagen miScript II RT Kit (Appendix I, Table 3) according to the manufacturer's instructions. The RNA samples were further added to the mixture of 5X miScript HiSpec buffer to facilitate conversion of mature miRNA, 10X miScript Nucleics mix that contains dNTPs and oligo-dT primers, RNase-free water and miScript Reverse Transcriptase Mix (an optimized blend of poly (A) polymerase and reverse transcriptase) in a 20 µl reaction. The reaction mixture was incubated for 60 minutes at 37°C to allow cDNA synthesis followed by 5 minutes at 95°C to inactivate miScript Reverse transcriptase and placed on ice. To proceed with qPCR immediately, cDNAs were vortex and mixed gently.

2.12 Real-time quantitative PCR assay for microRNAs

The expression of miRNAs with at least ± 2 fold-change in micro array and potential/validated target genes in the context of metabolic syndrome, were validated using qPCR. The synthesized cDNA (100 ng) was diluted 1 in 5 with PCR-grade water and was further added to the mixture of 2X

SYBR Green, 10X miScript Universal Primer (reverse primer), RNase-free water (Appendix I, Table 3) and miScript primer (forward primer). Quantitative real-time PCR was carried out in triplicates under thermocycling conditions as follows: Initial activation step at 95°C for 15 minutes, 45 cycles at 94°C for 15 seconds for denaturation, 55°C for 30 seconds for annealing and 70°C for 30 seconds for elongation and incubation at 60°C for 1 minute. QPCR was performed and analysed on a LightCycler-480 II (Roche, Switzerland). Gene expression was analysed as fold change and data was normalised to RNU6-2 snRNA and snoRNA SNORD72 expressions as endogenous reference RNAs whose expression level did not change under the experimental condition.

2.13 MicroRNA array

Reverse transcription was carried out using 155 ng (for plasma samples) and 500 ng (for lysed cells) total RNA. Samples were sent to Adelaide Microarray Centre to conduct the array and the preliminary data analysis using Affymetrix GeneChip miRNA version 4.0. cDNA was further labelled with Biotin using Affymetrix Flash Tag Biotin HSR RNA Labeling kit and washed to remove any unbound RNA before hybridization by fluorescent staining (GeneChip Hybridization, Wash and Stain kit) and scanning with a GeneChip Scanner 3000 system (Affymetrix). The raw intensity values were background corrected (subtracting the average signal intensity of the area between spots), log₂ transformed (to make variations similar across the samples and closer to normal distribution) and then quantile normalized (to make identical distribution between arrays). Then a linear model was fit to normalized data to obtain an expression measure for each probe set on the array by robust multi-array average (RMA).

2.14 Reverse transfection

I used reverse transfection as the method of choice for high-throughput transfection in HepG2 cells. The transfection reagents (Appendix I, Table 4) were prepared inside the wells and the cells were added to the top of the reagents. SiRNA/Block-iT or control oligonucleotides were diluted in Opti-MEM serum-free medium and then lipofectamin RNAiMAX was added in 3:47 ratio. The

complex was incubated for 20 minutes at room temperature followed by addition of cells on top of them. Cell density for transfection was no more than 10^5 cells per ml and the final siRNA concentration was 10 nM. Transfected cells were incubated at 37°C in a 5% CO₂ incubator for 24 hours prior to experiments. After incubating lipofectamin for 20 minutes at room temperature, it was diluted in 3:47 ratio with Opti-MEM serum-free medium. The siRNA was also diluted in 1:49 ratio with Opti-MEM serum-free medium. The Block-iT was also diluted in Opti-MEM to the 10 nM and 30 nM final concentrations to assess the quality of transfection using fluorescence microscopy.

2.15 DNA extraction

DNA was extracted from the cells using King Fisher cell and tissue DNA kit (Appendix I, Table 3) according to the manufacturer's instruction. 200 µl of lysis buffer and 25 µl proteinase K premixture was added into each well of cultured cells plates and pipetted several times till cells were lysed then transferred into tubes. Samples were vortex and incubated at 70°C for 15 minutes. After 5 minutes of incubation, RNase was added to the final concentration of 0.22 mg/ml to remove possible RNA contamination before vortex and incubation for another 10 minutes at room temperature. To remove debris, samples were centrifuged at 6000 xg for 5 minutes and washing buffers I, II and III were added to appropriate rows of King Fisher deep well plate. After resuspending of King Fisher magnetic beads, a premixture of 25 µl beads and 360 µl of binding buffer were added to each well of a specific row before addition of 225 µl of lysed samples to each well. After running the program using King Fisher Duo (ThermoScientific, Finland), DNA was collected in 50 µl DNase/RNase-free distilled water and stored at -20°C.

2.16 DNA methylation

Bisulfite conversion is used to deaminate unmethylated cytosine to produce uracil in DNA-methylated cytosines that are protected from the conversion to uracil. Bisulfite conversion was carried out using Zymo DNA Methylation kit (Appendix I, Table 3). 1 µg DNA sample and

methylated/unmethylated controls were mixed with 5 µl of M-Dilution buffer and Milli-Q water to reach 50 µl and incubated at 37°C for 15 minutes to denature DNA to increase cytosine availability for bisulfite reagents. Then 100 µl of prepared CT conversion reagent (mixed with M-Dilution buffer and water) was added to each sample and mixed before putting in the thermocycler under following conditions: 95°C for 30 seconds and 16 cycles under 50°C for 60 minutes and cooled down and hold at 4°C for 10 minutes. Samples were added to the spin Cartridge that already loaded with 400 µl M-Binding Buffer and mixed by inverting the tubes before centrifuge at 16000 xg for 30 seconds at room temperature. After washing with washing buffer, 200 µl of M-Desulphonation buffer was added to the column and let stand for 20 minutes at room temperature followed by centrifuge at 16000 xg for 30 seconds. After 2 washing steps with 200 µl of washing buffer, 40 µl of DNase/RNase-free distilled water was directly added to the columns and centrifuged at 16000 xg for 30 seconds to elute the DNA. The DNA was stored at -80°C for later use.

Amplification was performed using HotStar Taq DNA Polymerase kit. A reaction premixture was prepared using 0.5 µl 10X PCR buffer, 0.04 µl dNTP mix, 0.04 µl DNA polymerase, 2 µl primers and 0.42 µl PCR-grade water and dispensed into each well of PCR plate in 3 µl vol followed by addition of 2 µl DNA bisulfite sample. PCR was performed under following conditions: 94°C for 15 minutes followed by 45 cycles of 94°C for 20 seconds, 55°C-62°C for 30 seconds, 72°C for 1 minute and a single step of 72°C for 3 minutes. Samples were stored at 4°C overnight or -20°C for longer storage. A shrimp alkaline phosphatase (SAP) step was performed to dephosphorylate all of the remaining dNTPs from PCR by addition of 0.3 µl SAP and 1.7 µl RNase-free water into each well. Samples were incubated at 37°C for 20 minutes then 85°C for 5 minutes. The efficiency of PCR was checked by running 1% Agarose gel (Agarose, TAE buffer and SYBR DNA gel stain). The base-specific cleavage generates products that can be analysed quantitatively by mass spectrometry. T-cleavage leading to fragments with differing masses. Cleavage was carried out using restriction enzymes. 2 µl of PCR products were added to 5 µl of Mass CLEAVE T reagent kit cocktail (RNase A) and incubated at 37°C for 3 hours followed by

conditioning the samples via adding resin powder to de-salt the samples followed by centrifuge at 3200 xg for 10 minutes at room temperature. 20 nl of samples were dispensed (SEQUENOM, SAMSUNG, Korea) to each well of a SpectroCHIP which was subjected to the SEQUENOM mass spectrometry (SEQUENOM, CA, USA) for quantitative analysis of methylation.

For primer design, a sequence starting 500-2000 base pair upstream from the transcriptional start site of the genes was used in the UCSC browser (<http://genome.ucsc.edu/cgi-bin/hgGateway>) to search for the appropriate regions. The considered criterias to find the proper primer position were transcription start site, conserved regions, CpG islands and histone modifications. Furthermore, the amplicons quality and coverage were checked by http://blast.ncbi.nlm.nih.gov/Blast.cgi?PROGRAM=blastn&PAGE_TYPE=BlastSearch&LINK_LOC=blasthome), (<http://sg.idtdna.com/unafold>) and (<http://www.epidesigner.com/>) in regard to melting temperature, product length, E-value, close proximity with annotated transcription start, coverage, risk of secondary products, etc. (Figure 2.1 A-D).

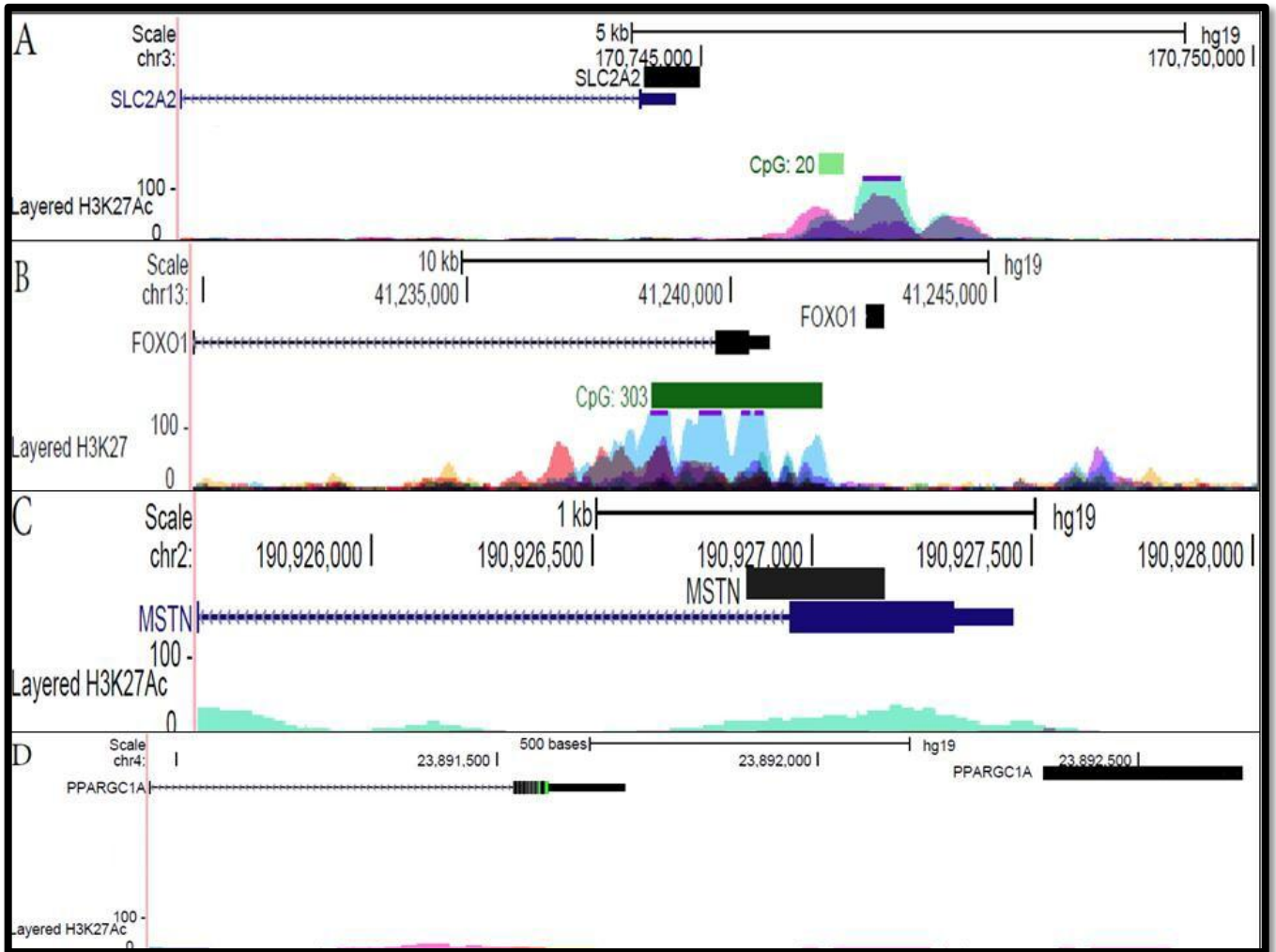


Figure 2.1 Designed amplicons for DNA methylation

Extracted DNA from HepG2 cells treated with leu (or not) at 0.1 mM and 2.5 mM concentration for 48 hours was used to assess DNA methylation for A) SLC2A2, B) FOXO1, C) MSTN and D) MSTN genes. Amplicons were designed to be close or overlapped with the annotated transcription start site.

2.17 MTT cell proliferation assay

To determine cell number and viability, Vybrant MTT (3-(4,5-dimethylthazol-2-yl)-2,5-diphenyltetrazolium bromide) Cell Proliferation Assay Kit (Appendix I, Table 3) was used in accordance with the manufacturer's instruction. Cells were cultured in a 96-well microplate and on the day of MTT assay, the medium was replaced with 100 μ l of fresh phenol-free medium (to avoid optical interfering) and 10 μ l of 12 mM MTT stock solution was added to each well followed by incubation at 37°C for 4 hours. The yellow MTT is reduced by metabolically active cells via dehydrogenase enzymes therefore producing intracellular purple formazan. Then 75 μ l of medium was removed from wells (25 μ l remained) and 50 μ l of DMSO was added to solubilize formazan and mixed thoroughly before incubation at 37°C for 10 minutes. Samples and controls were mixed prior to reading the absorbance at 540 nm using ELISA plate reader (BioTek, Synergy 2, USA) using Gen5 software version 1.4.5.0 (BioTek, USA).

2.18 Glucose uptake assay

HepG2 and C2C12 cells were seeded and cultured to 80% confluence in 24-well plates. Prior to the assay, cells were incubated in Krebs-Ringer's Phosphate Buffer (KRP)/BSA (Buffer K: 136 mM NaCl, 4.5 mM KCl, 1.25 mM CaCl₂, 1.25 mM MgSO₄; Buffer P: 0.6 mM Na₂HPO₄, 0.4 mM NaH₂PO₄; Mix buffers K and P in 1:1 ratio with 10% 1M HEPES and 0.2% BSA) for 1.5 hours at 37°C and a mixture of un-labelled and tritiated 2-deoxy glucose (2-DG, Appendix I, Table 3) were prepared as a 20X stock mix (50 μ M 2-DG, 1 μ Ci/ml HOTDG and KRP-0.2% BSA) in Krebs-Ringer's Phosphate Buffer (KRP)/0.2% BSA pH 7.4 (HOT-DG). The assay was performed in a vol of 500 μ l per well. Insulin was added to the appropriate wells in a final concentration of 1 nM at 37°C, 10 minutes before initiation of glucose uptake assay. In addition, to correct for non-specific glucose uptake, Cytochalasin B was added to a final concentration of 30 μ M in some wells and incubated for 2 min prior to the initiation of glucose transport. Glucose transport was introduced to the cells with addition of 25 μ l of 20X HOT-DG per well to yield a final concentration of 50 μ M of un-labelled 2-DG and 1 μ Ci/ml tritiated 2-DG. Glucose uptake into the cells was measured over 10 minutes (for HepG2 cells) or

15 minutes (for C2C12) at 37°C. Glucose uptake was terminated by chilling the plates on ice and cells were immediately washed with ice-cold PBS four times and harvested using 120 µl per well of 1% Triton X-100 diluted in Milli-Q water. 100 µl of samples was pipetted into 1 ml of Ultima Gold scintillant and incubated at room temperature overnight while protected from light before being β-counted on a Tri-Carb 2900 TR liquid scintillation analyzer (Perkin Elmer Biosciences, Waltham, MA, USA). 0 µl, 1 µl and 2 µl of the 20X HOT-DG was β-counted as control. Glucose uptake activity was corrected for non-specific uptake and normalised to total intracellular protein content.

2.19 Glucose output assay

The amount of secreted glucose into the medium was measured using Amplex Red Glucose Kit (Appendix I, Table 3) according to manufacturer's instruction with slight modifications on standard curve concentrations which was set from 0 µM to 50 µM instead of 200 µM. Prior to glucose output assay, cells were washed with prewarmed PBS twice and incubated in glucose and phenol red-free DMEM that was treated with 2 mM sodium pyruvate and 20 mM sodium lactate for 1.5 hours at 37°C. 1 nM insulin was also added to the appropriate cells 10 minutes prior to the end of incubation. A premixture of a working solution for each reaction was prepared as follow: 0.5 µl of 10 mM Amplex Red reagent, 1 µl of 10 U/ml HRP stock solution and 1 µl of 100 U/ml glucose oxidase stock and 47.5 µl of 1x Reaction buffer. 50 µl of samples, standard samples and controls was pipetted to each well of a black 96-well microplate and 50 µl of prepared working solution premixture was added per well. The plate was then incubated at room temperature for 30 minutes while protected from light. The absorbance was measured at 560 nm excitation and fluorescence emission detection at 590 nm using ELISA plate reader (BioTek, Synergy 2, USA) using Gen5 software version 1.4.5.0 (BioTek, USA). The absorbance of standards was measured to generate a standard curve with which the unknown sample glucose was compared and data was normalised to total intracellular protein content.

2.20 Triglyceride content assay

Intracellular TG content was measured using Triglyceride Quantification kit (Appendix I, Table 3) in accordance with the manufacturer's instructions with slight modification on samples volume as follow to fit the range suggested by the manufacturer. Prior to the assay, a premixture of 47.6 μ l of TG assay buffer, 0.4 μ l of TG probes and 2 μ l of TG enzyme mix was prepared. Cells were homogenised in 5% Tergitol Type NP-40 (diluted in water) while agitating at room temperature for 5 minutes then heated at 100°C for another 5 minutes until Tergitol Type NP-40 became cloudy and cooled down by placing on ice and the heating step was repeated once again to solubilise all TGs. After centrifuging at 12000 xg for 2 minutes, 30 μ l of samples was added to each well of a black 96-well microplate and the vol was adjusted to 50 μ l with TG assay buffer. 2 μ l of lipase was then added to each sample, standard and control samples and after mixing was incubated at room temperature for 20 minutes to convert TGs to glycerol and fatty acids. A total 50 μ l of reaction premixture was pipetted to all wells and after mixing was incubated at room temperature for 1 hour while protecting from light. Absorbance was measured at 535 nm excitation and fluorescence emission detection at 590 nm using ELISA plate reader (BioTek, Synergy 2, USA) using Gen5 software version 1.4.5.0 (BioTek, USA). The absorbance of standards was measured to generate a standard curve with which the unknown sample TG was compared and data was normalised to total intracellular protein content.

2.21 Glycogen content assay

Glycogen content was measured using Glycogen Fluorometric Assay Kit (Appendix I, Table 3) in accordance with manufacturer's instruction. Cold Milli-Q water was used to homogenise cells on ice followed by heating them at 100°C for 5 minutes to inactive enzymes. Boiled samples were centrifuged at 13000 revolutions per minute (RPM) for 5 minutes and supernatant was used for the assay. 5 μ l of sample was diluted with 45 μ l of hydrolysis buffer and added to each well of a black 96-well microplate. Then, 50 μ l of hydrolysis enzyme mix (contained 46 μ l of development buffer, 2 μ l of development enzyme mix and 2 μ l of OxiRed probe) was also added to sample, standards and control

wells before incubating at room temperature for 30 minutes while protecting from light. Absorbance was measured at 535 nm excitation and fluorescence emission detection at 590 nm using ELISA plate reader (BioTek, Synergy 2, USA) using Gen5 software version 1.4.5.0 (BioTek, USA). The absorbance of standards was measured to generate a standard curve with which the unknown sample glycogen was compared and data was normalised against total intracellular protein content.

2.22 Insulin concentration assay

On the day of assay, medium was collected from the cells and centrifuged at 1000 RPM for 5 minutes at 4°C. To measure level of secreted insulin to the medium, Insulin Human ELISA Kit (Appendix I, Table 3) was used according to manufacturer's instruction with slight modifications on samples concentration to fit the standard curve. Samples were diluted 1 in 4 with diluent B buffer and 100 µl of prepared standards and samples were pipetted to each well of the provided 96-well microplate and incubated for 2.5 hours at room temperature at gentle shaking while covered to be protected from light. Solution was discarded and wells were washed with 1X Wash buffer for 4 times. Then, 100 µl of 1X Biotinylated Insulin Detection Antibody was added and incubated for 1 hour at room temperature with gentle shaking. After washing step, 100 µl of 1X HRP- Streptavidin solution was pipetted to the wells and incubated for 45 minutes under same condition. After final washing step, 100 µl of TMB One-Step substrate was added to the wells following 30 minutes incubation as above. 50 µl of Stop Solution was pipetted and absorbance was measured at 450 nm immediately using ELISA plate reader (BioTek, Synergy 2, USA) using Gen5 software version 1.4.5.0 (BioTek, USA). The absorbance of standards was measured to generate a standard curve with which the unknown sample insulin was compared and data was normalised against total intracellular protein content.

2.23 Statistical analysis

All analyses were performed using the international business machines statistical package for the social science (IBM SPSS) statistical program (version 21, NY, USA). All results are presented as mean \pm SEM from at least three independent experiments done in triplicate. A one-way ANOVA with a Tukey post-hoc test was used to assess differences between groups. Pearson correlation analysis with a two-tailed test of significance was performed. The Shapiro-Wilk test was performed to check the normality of distributed data and the Kolmogorov-Smirnov statistical test was carried out to determine the difference in frequency distribution between valuables when relevant. $P \leq 0.05$ was considered statistically significant.

3 LEUCINE ALTERS HEPATIC GLUCOSE/LIPID HOMEOSTASIS VIA THE MYOSTATIN-AMP-ACTIVATED PROTEIN KINASE PATHWAY - POTENTIAL IMPLICATIONS FOR NON-ALCOHOLIC FATTY LIVER DISEASE

3.1 Preface

The following chapter contains the published original research article “*Leucine alters hepatic glucose/lipid homeostasis via the myostatin-AMP-activated protein kinase pathway- potential implications for non-alcoholic fatty liver disease*”, doi:10.1186/1868-7083-6-27. The article was published in the Journal of Clinical Epigenetics in 2014. The Journal of Clinical Epigenetics is an open access, peer-reviewed journal that encompasses all aspects of epigenetic principles and mechanisms in relation to human disease, diagnosis and therapy.

The screenshot shows the journal's homepage with a navigation bar including 'Home', 'Articles', 'Authors', 'Reviewers', 'About this journal', and 'My Clinical Epigenetics'. A search bar is present with 'Clinical Epigenetics' entered. The main content area features a 'Research' section with an 'Open Access' badge. The article title is 'Leucine alters hepatic glucose/lipid homeostasis via the myostatin-AMP-activated protein kinase pathway - potential implications for nonalcoholic fatty liver disease' by Aida Zarfeshani, Sherry Ngo, and Allan M Sheppard. Below the title, it says 'For all author emails, please log on.' and 'Author Affiliations'. The journal information is 'Clinical Epigenetics 2014, 6:27' with doi:10.1186/1868-7083-6-27, published on 18 November 2014. A sidebar on the left promotes '1,000,000 antibodies ELISA kits proteins and more' with a '5% off' discount.

The Western dietary pattern is characterised by relative nutrient abundance. This diet contains multiple combinations of nutrients that may interact in a complimentary or act independently toward chronic development of disorders such as metabolic syndrome including non-alcoholic fatty liver diseases (NAFLD), type 2 diabetes mellitus (T2DM), visceral obesity and insulin resistance (IR). Considering the extensive portion of branched-chain amino acids (BCAAs) (15%-25%) in total protein of Western diets and their levels in the plasma of obese and T2DM patients, BCAAs have been proposed as markers in association with metabolic syndrome and its co-morbidities as well as predictive indicators of future T2DM. However, some studies

(268, 269) suggest that leucine (leu) is a BCAA propose a degree of inhibition against T2DM and IR through increasing the muscle mass thus the enhanced capacity for glucose uptake from blood and elevating the energy expenditure in thermogenic tissues such as brown adipose tissue. To address this issue, understanding of shifts in liver metabolism, as the main regulatory organ for glucose homeostasis after leu supplementation and the underpinning mechanisms was necessary.

My observations suggest leu may help to reduce blood glucose level via promoting glucose sequestration but as a consequence of driving lipid accumulation in the liver. Further, I provide evidence that myostatin (MSTN) regulation of AMP-activated protein kinase (AMPK) is a key pathway in the hepatic glucose stimulated by excess leu. I also reported associated changes in miRNA expression previously linked to obesity etiology.

3.2 Abstract

Elevated plasma levels of the BCAA leu are associated with obesity and IR, and thus the propensity for T2DM development. However, other clinical studies suggest the contradictory view that leu may in fact offer a degree of protection against metabolic syndrome. Aiming to resolve this apparent paradox, we assessed the effect of leu supplementation on the metabolism of human hepatic HepG2 cells. We demonstrate that pathophysiological leu appears to be antagonistic to insulin, promotes glucose uptake (and not glycogen synthesis), but results in hepatic cell TG accumulation. Further, we provide evidence that MSTN regulation of AMPK is a key pathway in the metabolic effects elicited by excess leu. Finally, we report associated changes in miRNA expression (some species previously linked to metabolic disease etiology), suggesting that epigenetic processes may contribute to these effects. Collectively, our observations suggest leu may be both ‘friend’ and ‘foe’ in the context of metabolic syndrome, promoting glucose sequestration and driving lipid accumulation in liver cells. These observations provide insight into the clinical consequences of excess plasma leu, particularly for hyperglycemia, IR and non-alcoholic fatty liver disease (NAFLD).

3.3 Introduction

The relative nutrient abundance that is associated with modern Western dietary patterns causes a rapid increase in postprandial plasma glucose and insulin levels and is associated with a propensity toward the development of metabolic syndrome characterized by visceral obesity, IR and T2DM. The branched-chain amino acids account for 15% to 25% of the total protein intake in the Western diet (270), and increased plasma levels are clinically associated with an obese phenotype (49) and progression to T2DM (31, 271). Indeed, the levels of BCAAs are more strongly associated with IR than are many of the common circulating lipid species (49) and may even be predictive indicators of future T2DM risk (31). However, whether elevated BCAAs directly promote progression of metabolic syndrome remains unclear, some studies even suggesting that the BCAA leucine offers a level of protection against IR, either by increasing muscle glucose utilization (269) or by energy expenditure in thermogenic tissues (268).

To address this somewhat contradictory clinical picture, we explored the phenotypic and molecular changes induced in hepatic cells following leucine supplementation. As previously reported for an *in vivo* study (272), we also report enhanced glucose uptake *in vitro*, a presumed benefit for limiting the onset of IR. However, we also find increased *de novo* hepatic lipogenesis and TG deposition. Human and animal studies link high glycemic diets with increases in hepatic fat storage, steatosis and nonalcoholic fatty liver disease (NAFLD) (273) and the Western lifestyle of nutrient abundance and physical activity (94). Thus, leu is perhaps both ‘friend and foe’ in the context of metabolic syndrome. We also report central roles for myostatin (*MSTN*)-dependent AMP-activated protein kinase (AMPK) signaling and miRNA-dependent epigenetic processes in these metabolic effects.

3.4 Results

3.4.1 Leucine changes hepatic glucose and triglyceride homeostasis

To examine the effect of increased leucine on hepatic glucose utilization, we first assessed uptake by HepG2 cells. Compared to untreated controls, basal 2-deoxy-D-[1,2-³H] glucose (2-DOG) uptake was significantly increased (25% and 33%) with 0.1 mM and 2.5 mM leu, respectively ($P \leq 0.05$; Figure 3.1A). Interestingly, insulin-stimulated 2-DOG uptake was further enhanced (50% and 71%) in the presence of leu ($P \leq 0.05$), indicating that leu may augment glucose utilization independent of insulin. As we found no evidence that leu stimulated glucose secretion (Figure 3.1B), we suggest that its primary effect on hepatocyte glucose homeostasis is to enhance sequestration.

We questioned whether this increase in glucose uptake resulted in enhanced conversion to lipids by measuring total intracellular TG, which increased significantly (16% and 21%) at 0.1 mM and 2.5 mM of leu respectively compared to the untreated control ($P \leq 0.05$; Figure 3.1C). Moreover, cellular glycogen was unchanged after leu supplementation (Figure 3.1D).

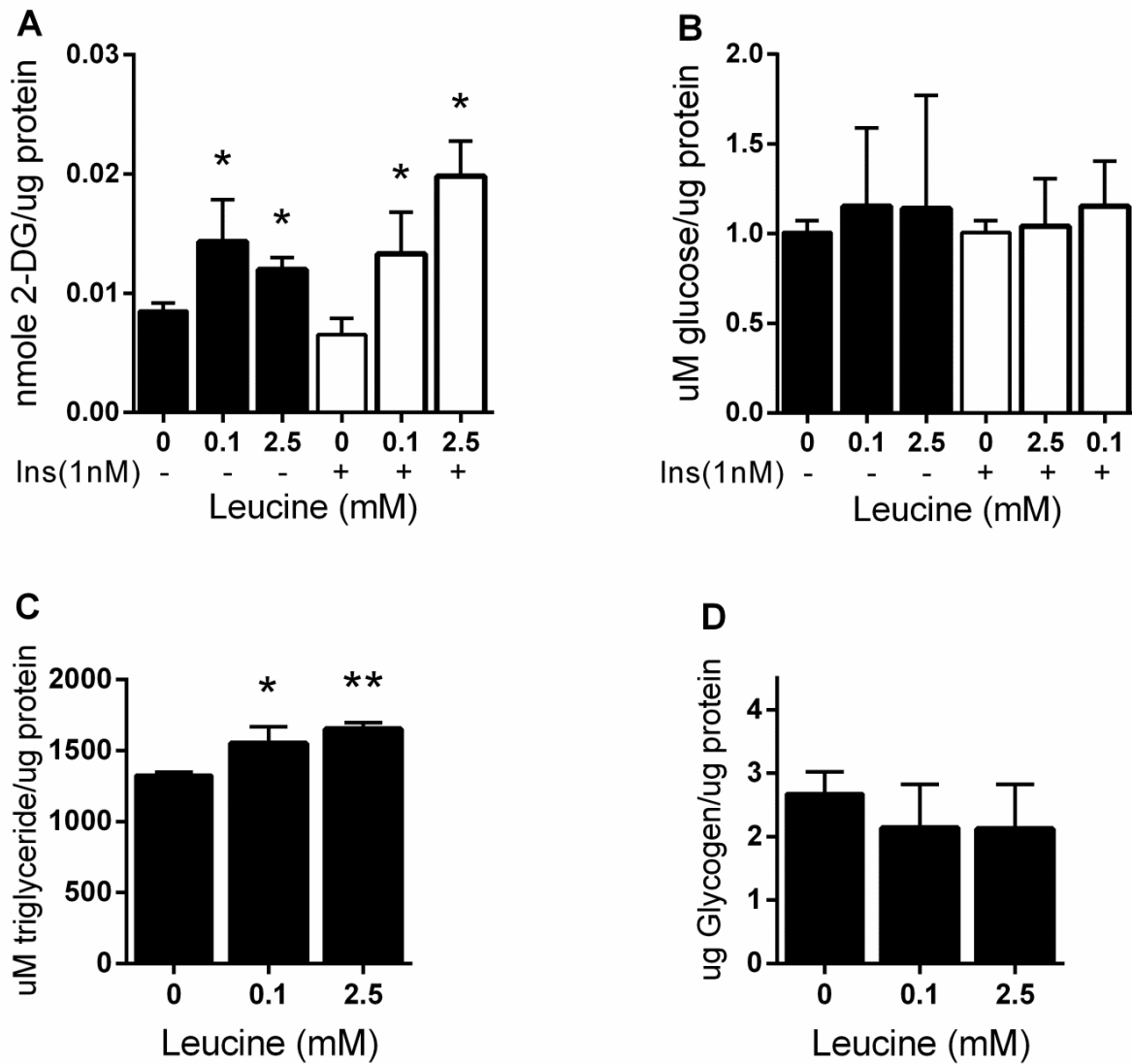


Figure 3.1 Effect of leucine supplementation on glucose and lipid metabolism in HepG2 cells
(A) 2-deoxy-D-[1,2-³H] glucose (2-DOG) consumption with or without the addition of insulin (1nM). Total intracellular glucose uptake was normalized to total protein content. **(B)** Levels of glucose secreted into the media with or without addition of insulin (1nM). **(C)** Total intracellular amount of triglyceride (TG), normalized to total protein content. **(D)** Glycogen content of homogenized samples treated with glucoamylase to hydrolyze glycogen into glucose. Glycogen amount was normalized to total protein content. Values are presented as mean \pm SEM. Statistical significance relative to untreated control, * $P < 0.05$, ** $P < 0.01$ (n=3).

3.4.2 Leucine changes hepatic expression of glucose/lipid sensing genes

Excessive hepatic glucose uptake is likely to contribute to the development of obesity-related dyslipidemia. To provide molecular evidence for the role of leu in perturbing hepatic metabolism, mRNA expression levels of several key genes involved in lipid and glucose sensing were measured. The expression of pyruvate carboxylase (*PC*), a ligase that catalyzes the carboxylation of pyruvate to oxaloacetate (37); phosphoenolpyruvate carboxykinase (*PCK1*; *PEPCK*), which decarboxylates and phosphorylates oxaloacetate into phosphoenol pyruvate (37); and glucose 6-phosphatase (*G6Pase*), which catalyzes the final steps of gluconeogenesis, resulting in production of glucose (274), were measured. Although *PC* and *PCK1* expression remained unchanged, G6-Pase increased by 61% ($P \leq 0.05$) at 2.5 mM leu compared to the control (Figure 3.2A). In addition, the mRNA level of solute carrier family member2 (*SLC2A2*) was increased ($P \leq 0.05$) by 34% at 0.1 mM and 46% at 2.5 mM of leucine. Moreover, peroxisome proliferative activated receptor- γ co-activator 1 (*PPAR γ*) expression, a stimulator of endogenous *SLC2A2* mRNA transcription and key regulator of the genes associated with steatosis liver (275), was enhanced by about 40% after the leu treatment ($P \leq 0.05$; Figure 3.2A). Furthermore, expression of forkhead box protein A2 (*FOXA2*), which synergistically increases the promoter activity of the *SLC2A2* gene (276), was also increased by 33% ($P \leq 0.05$; Figure 3.2A). We also found a significant increase in glucokinase (*GK*), 33.3% at 2.5 mM ($P \leq 0.05$; Figure 3.2A).

Glycerol-3-phosphate acyltransferase (*GPAT1*) catalyzes glycerol synthesis and thus TG biosynthesis (277). *GPAT1* expression was increased by 33% at 2.5 mM leucine ($P \leq 0.05$; Figure 3.2A). Acetyl-CoA carboxylase (*ACCI*) catalyses long-chain fatty acid biosynthesis (278) and was increased by 26% at 2.5 mM leu ($P \leq 0.05$; Figure 3.2A). Collectively, our data indicate that leu supplementation promotes hepatic lipid synthesis; however, they do not demonstrate that overexpression of *SLC2A2* and *GPAT1* alone mediate the effect of leu on glucose uptake and TG biosynthesis.

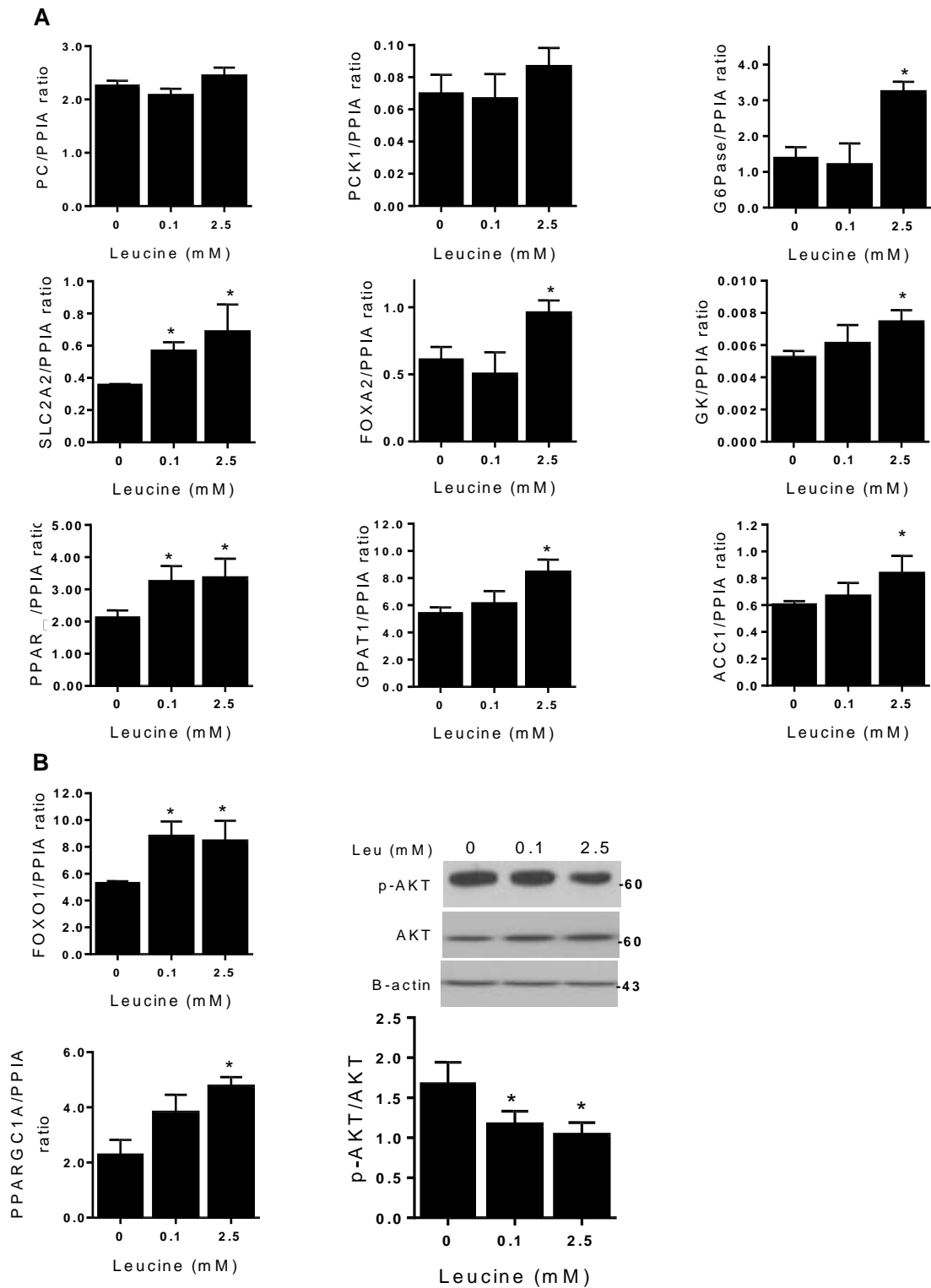


Figure 3.2 Expression of the genes involved in glucose and lipid sensing after leucine supplementation of HepG2 cells

(A) Real-time PCR (qPCR) and immunoblotting analysis of expression levels of genes involved in gluconeogenesis, glucose uptake and lipogenesis. (B) qPCR and immunoblotting analysis of specific upstream genes involved in glucose/lipid sensing. Western blotting was performed using cell lysates supplemented with leucine for 48 h. Values are presented as mean \pm SEM. Statistical significance relative to untreated control, $*p \leq 0.05$ ($n=3$).

PPARGCIA and forkhead transcription factor (*FOXO1*) play important roles in glucose metabolism (279), and nuclear accumulation of the latter also stimulates TG synthesis (280). Expression of both increased by 54% ($P \leq 0.05$) and 37%, respectively (Figure 3.2B). Activated protein kinase B (AKT) phosphorylates *FOXO1* (281) to prevent nuclear translocation, yet we found that (Ser⁴⁷³)-AKT phosphorylation was reduced by about 30% at both 0.1 mM and 2.5 mM leu, suggesting that *FOXO1* was not only upregulated but functionally activated by leu.

Mammalian target of rapamycin complex 1, a nutrient and hormonal sensor (282), regulates gene translation through phosphorylation and activation of ribosomal protein S6 kinase beta-1 (S6K1) (46). We found either mTORC1 activity or S6K1 phosphorylation remained unchanged (Figure 3.3A). In addition to mTOR, AKT activity not only stimulates (Ser²⁴⁴⁸)-mTORC1 phosphorylation but also negatively regulates p(Thr¹⁷²)-AMPK- α [357]. Leucine enhanced phosphorylation of (Thr¹⁷²)-AMPK- α by 40% ($P \leq 0.05$) and 50% ($P \leq 0.01$) at 0.1 mM and 2.5 mM, respectively (Figure 3.3B).

Clinical obesity is associated with increased *MSTN* expression (194), and *MSTN* mRNA levels are increased in both adipose and skeletal muscle of obese mice (195). We detected a fourfold increase in *MSTN* expression at 2.5 mM leu ($P \leq 0.05$) (Figure 3.3C).

3.4.3 Myostatin is involved in the regulation of leucine modified genes

To determine the effect of *MSTN* on the cellular glucose uptake, we measured 2-DOG uptake in *MSTN* inhibited cells followed by leu supplementation (Figure 3.4A). In the basal state, siRNA-mediated knockdown of *MSTN* led to a 40% ($P \leq 0.05$) decrease in glucose uptake whereas in the presence of leu, *MSTN* suppression led to 40 to 60% ($P \leq 0.05$) reduction in glucose uptake across the various leu doses, suggesting an *MSTN*-dependent effect of leu on promoting glucose uptake. Next, we hypothesized that *MSTN* promoted leu-mediated glucose uptake via AMPK activation and indeed found that *MSTN* knockdown decreased p(Thr¹⁷²)-AMPK approximately 50% in the presence of both

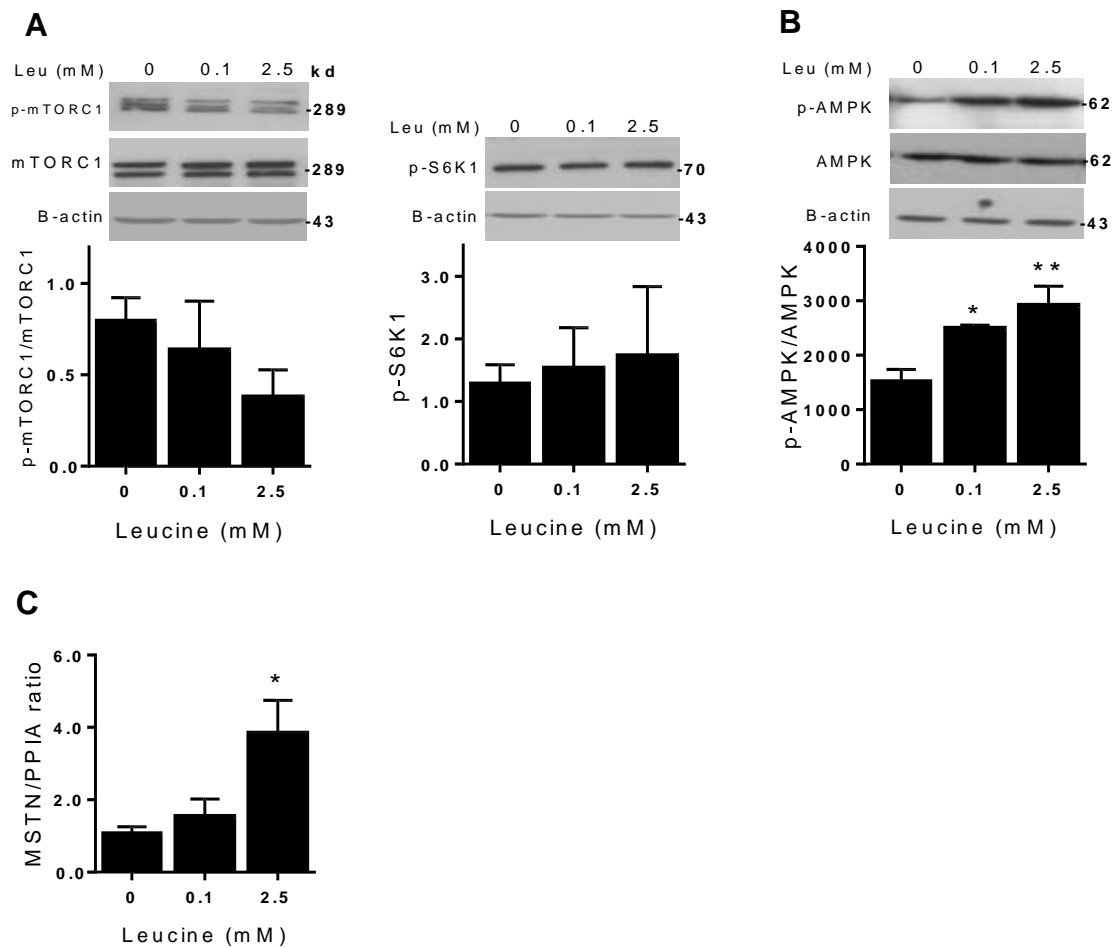


Figure 3.3 AMP-activated protein kinase (AMPK) but not mammalian target of rapamycin complex 1/ Ribosomal protein S6 kinase beta-1 (mTOR/ S6K1) activity was regulated by leucine in HepG2 cells

(A) Western blots and densitometry analysis of leucine-supplemented HepG2 cells stained for p-mTOR and p-S6K1 and (B) p-AMPK. (C) Effect of leucine supplementation on myostatin (MSTN) mRNA level. Values are the presented as mean \pm SEM. Statistical significance relative to untreated control, * P <0.05, (n=3).

0.1 mM and 2.5 mM leu ($P \leq 0.05$), while p(Thr¹⁷²)-AMPK levels remained unchanged (with and without *MSTN*-knockdown) in the absence of leu (Figure 3.4B). These results suggest that leu-induced AMPK phosphorylation is mediated by *MSTN* signaling.

To identify which of the leu-responsive genes were regulated by *MSTN*, we measured candidate mRNA expression following *MSTN* inhibition. As shown in Figure 3.4C, expression of most of them was markedly reduced (37% to 75%; $P \leq 0.01$). *ACCI* and *PPAR γ* were notable exceptions.

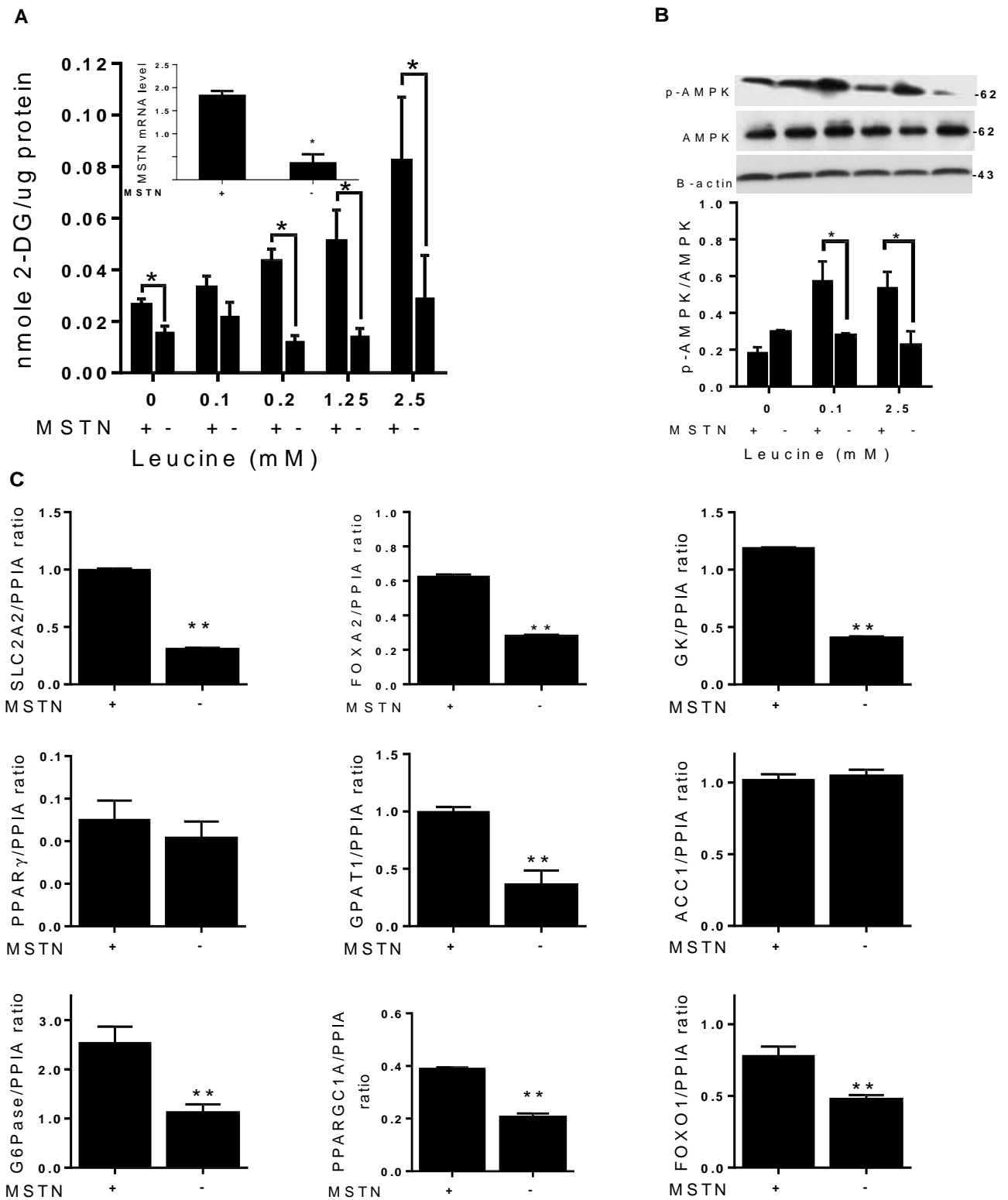


Figure 3.4 Effects of myostatin (MSTN) on AMP-activated protein kinase (AMPK) activity and glucose /lipid sensing in leucine- treated HepG2 cells

(A) Glucose uptake is inhibited in MSTN-suppressed cells. MSTN knock-down efficiency using siRNA (B) The leucine- induced AMPK signaling pathway was suppressed following MSTN suppression. (C) mRNA levels of leucine-sensitive genes in the presence and absence of MSTN. Values are presented as the mean \pm SEM. Statistical significance relative to untreated control, * P <0.05, ** P <0.01 (n=3).

3.4.4 MiRNA array validation using quantitative real-time PCR

Criteria for candidate miRNA selection for qPCR validation were: (1) at least a ranked ± 2 fold change in differential expression from the microarray analysis, (2) their putative function in the context of obesity and diabetes based on the existing literature, (3) *in silico* identification of predicted or validated miRNA targets using miRBase (<http://microrna.sanger.ac.uk/>) and miRWalk (<http://www.umm.uni-heidelberg.de/apps/zmf/mirwalk/>) databases. We identified 35 and 5 human miRNAs to be significantly up- or downregulated, respectively by 2.5 mM leu compared to untreated controls (Figure 3.5A). We validated the expression of leu-dependent microRNAs in HepG2 cells, including miR-143, miR-92b*, miR-335, miR-181d, miR-3185 and miR-4763 by real-time PCR (qPCR) (Table 3.1). As expected, the expression of miRNA-143 was reduced 1.5-fold ($P \leq 0.05$), while that of miRNA-92b* and miR-335 was up-regulated 1.8- and 1.5-fold ($P \leq 0.05$) at 2.5 mM of leu, respectively (Figure 3.5B). However, there was no significant difference in the expression of miR-181d, miR-3185 and miR-4763 (See Appendix II for the full list of the miRNAs and their fold change in the array).

Table 3.1 Real-time PCR (qPCR) validation of differentially expressed microRNAs in leucine-treated HepG2 cells compared with control

<i>Probe set ID</i>	<i>Fold- Change</i>
hsa-miR-143	-1.52
hsa-miR-92b*	1.83
hsa-miR-335	1.51
hsa-miR-181d	-1.05
hsa-miR-3185	-1.04
hsa-miR-4763	1.22

To confirm whether up/downregulated miRNAs can modulate leu's effects on glucose and lipid metabolism, we measured the expression of leu-dependent genes of interest in suppressed (or not) miRNAs. Following miR-143 suppression, leu supplementation induced a significant increase in *PPAR γ* expression by 6- and 8.6-fold at 0.1 mM and 2.5 mM leu, respectively, compared to cells without miR-143 suppression (Figure 3.5C). This is in contrast to our earlier observation that leu

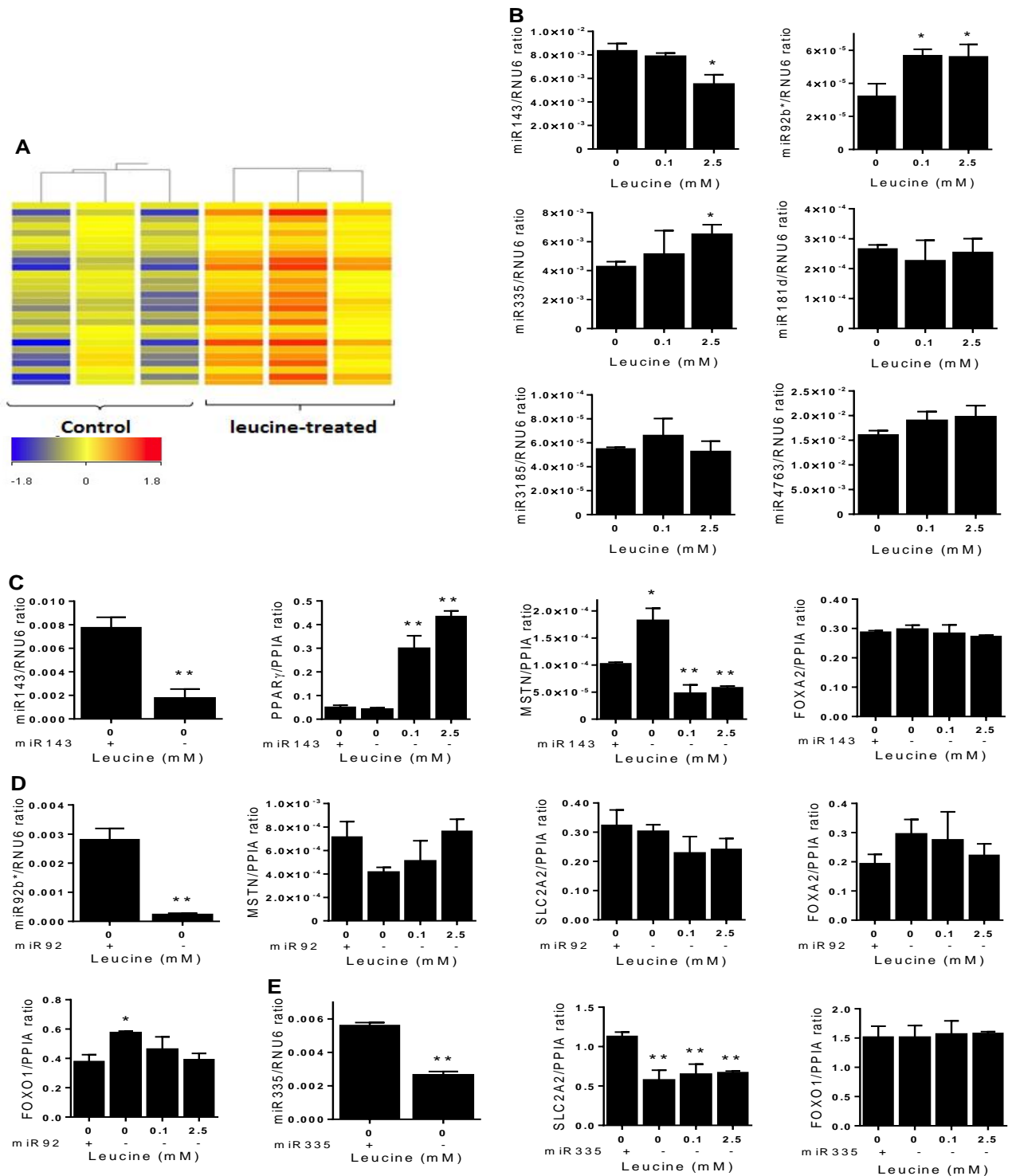


Figure 3.5 Discovery and validation of miRNA expression after leucine supplementation in HepG2 cells

(A) Cluster analysis of miRNAs available on Affymetrix miRNA chips. The red color shows relatively abundant expression of the same miRNA when compared to controls, whereas the blue color indicates a low expression relative to other samples. Cluster analysis was performed with Gene Spring GX. (B) Validation of specific miRNA species exhibiting significant difference from the control group, using real-time PCR (qPCR). Finally, differential expression of specific target genes measured after (C) inhibition of miR-143, (D) miR-92b* and (E) miR-335 using selective siRNAs. Values are presented as the mean \pm SEM. Statistical significance relative to untreated control, * $P \leq 0.01$. All experiments were performed 3 times in triplicate.

induced a modest 1.6-fold increase in HepG2 cells (without miR-143 suppression; Figure 3.5C), suggesting an inhibitory effect of miR-143 on *PPAR γ* via leu.

Also, we found increased *MSTN* level (1.8-fold; $P \leq 0.05$) in the absence of leu (Figure 3.5C). On the contrary, miRNA-143 suppression led to a reduced *MSTN* expression by 50% ($P \leq 0.01$) in the presence of leu, suggesting that *MSTN* is also regulated in a miR-143 dependent manner. Notably, leu supplementation did not promote *FOXA2* expression (Figure 3.5C). Suppression of miR-92b* tended to reduce gene expression of *MSTN* in the absence of leu but increased the *MSTN* level with the 2.5 mM leu treatment, despite being statistically not significant (Figure 3.5D). Although not statistically significant, there was also a decrease in both *SLC2A2* and *FOXA2* expression, but only in the presence of leu (Figure 3.5D). Also, *FOXO1* expression was increased by 1.5-fold ($P \leq 0.05$) in the absence of leucine (Figure 3.5D). Therefore, miR-92b* suppression, decreased the leu-dependent overexpression of these genes. Finally, following miR-335 suppression, *SLC2A2* expression was reduced by 50% ($P \leq 0.01$) in the presence and absence of leucine, but *FOXO1* expression was unchanged (Figure 3.5E). Collectively, these data indicate miRNAs influence key metabolic genes, either directly or in response to leu.

3.5 Discussion

The intake of dietary protein (BCAAs) influences glucose metabolism and insulin sensitivity. Both IR and T2DM associated with metabolic syndrome often correlate with considerable changes in amino acid metabolism (27). We show that elevated leu increases glucose uptake by HepG2 cells and activates the GK gene, the apical sensor of intracellular glucose levels. Further, we suggest this enhanced glucose uptake may be a consequence of increased *SLC2A2* gene transcription, resulting from increased expression of *FOXA2* a critical downstream effector of metabolic processes and transcription factor known to promote *SLC2A2* transcription (276). Meanwhile, we do not see evidence for glucose secretion or for any change in the *PEPCK* and *PC* gene transcription, implying that leu does not promote gluconeogenesis. However, we did note increased *G6Pase*

transcription (Figure 3.6). Although often linked to gluconeogenesis, the key cellular role of *G6Pase* in buffering G6P concentrations is also dependent on the processes of glycolysis and glycogenolysis (274). Further, we did not observe any increase in glycogen content, rather a tendency towards decreasing glycogen.

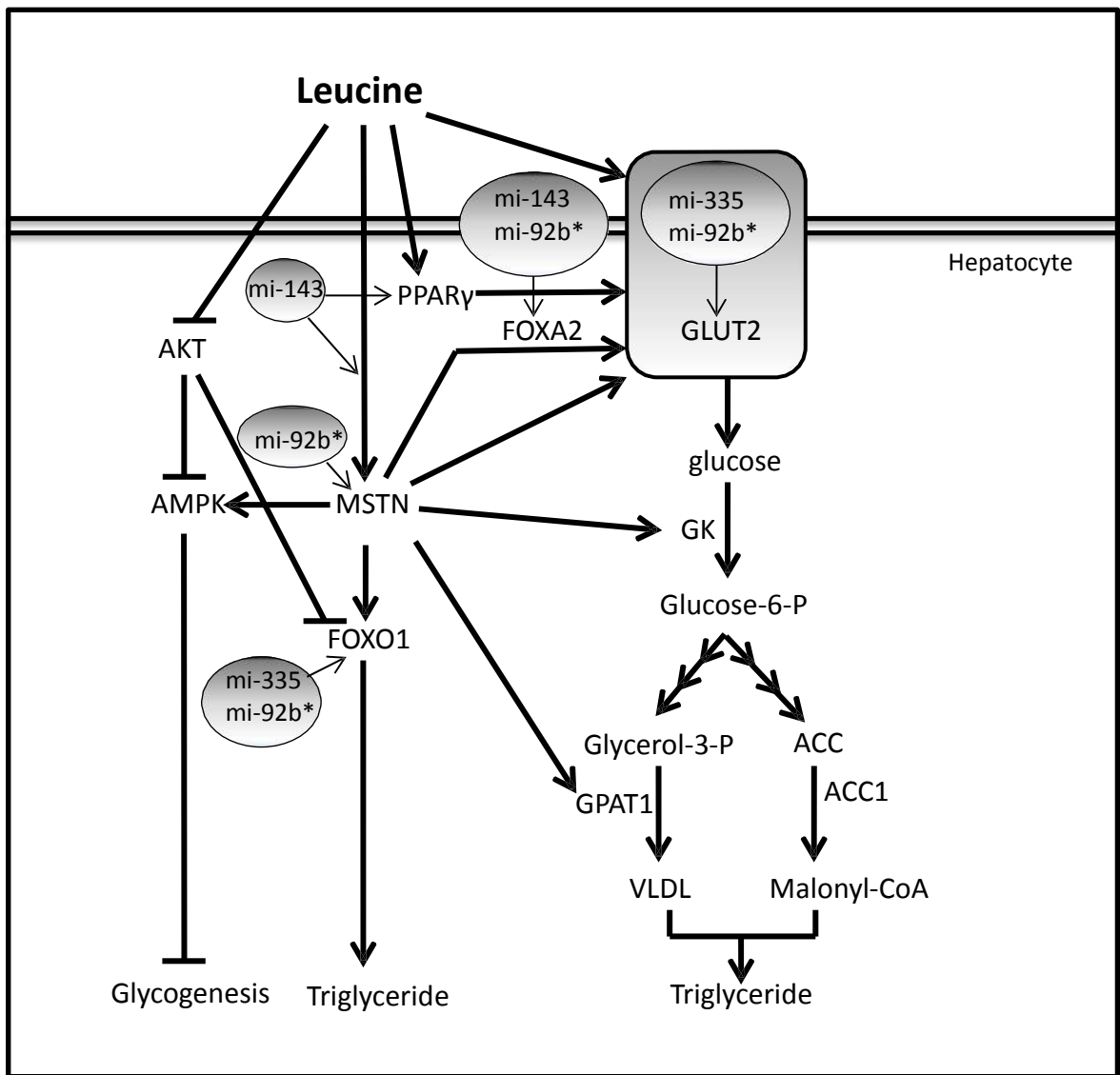


Figure 3.6 Schematic summaries of findings

Leucine supplementation promotes hepatic cell glucose uptake by upregulating solute carrier family Member 2 (*SLC2A2*) expression via myostatin (*MSTN*). *MSTN* activity leads to the activation of AMP-activated protein kinase (AMPK) and inhibition of glycogen synthesis. Furthermore, activation of *MSTN* leads to overexpression of genes involved in glucose uptake, which is further responsible for triglyceride synthesis. Moreover, leucine supplementation alters the expression of several small RNA species including miR-143, miR-335 and miR-92b*, which target main gene regulators of these effects.

The primary regulation of systemic glucose levels by insulin is triggered when hepatic receptors recruit the IRS, leading to activation (phosphorylation) of PI3K/AKT and in turn phosphorylation of FOXO1, which blocks its nuclear translocation and inhibits mRNA expression of gluconeogenic genes (notably *PEPCK* and *PC*) to reduce net cellular glucose output (281). However, under our culture conditions of basal insulin and supplemented leu, phosphorylation of AKT was markedly decreased, suggesting that leu is antagonistic to insulin, at least with respect to the regulation of AKT activity. When activated, AKT also suppresses the phosphorylation and activity of the serine/threonine kinase AMPK (283), an intracellular energy regulator influencing both glucose and lipid metabolism. Thus, with leu supplementation the suppression of AKT would have been predicted to promote an AMPK-dependent increase in the terminal pathway effector mTORC1 (282). However, we observed both a decrease in mTORC1 phosphorylation (leading to activation) and unchanged levels of mTORC1-dependent S6K1 phosphorylation. Collectively, then, our data suggest that leu could affect this glucose sensing seminal pathway.

Recently, AMPK regulation of the TGF β family member *MSTN* has been linked to acute increases in glucose transport and IR (284, 285). *MSTN* mRNA levels are elevated in peripheral tissues from obese, leptin-deficient *ob/ob* mice and high fat-fed wild-type mice (195) and promote glucose uptake *in vitro* by C2C12 myotubes (211). Meanwhile, *MSTN* knock out enhances systemic insulin sensitivity and prevents obesity (200, 209). Clinically, plasma levels of *MSTN* protein are elevated in obese patients (194, 196) and a comparison of muscle cells isolated from obese and non-obese women revealed increased *MSTN* secretion (194). Conversely, *MSTN* mRNA levels are reduced in peripheral tissues following weight loss in mice and human patients (181, 197). Our observations are parsimonious with these collective observations, providing perhaps the first empirical data supporting increased hepatic glucose uptake in the presence of excess extracellular leuc and suggesting that it occurs through *MSTN*-dependent AMPK modulation of glucose transporter expression.

While AMPK activates glucose transport and glycolysis in skeletal muscles, it also suppresses glycogenolysis (286), and we reported a mild reduction of glycogen in hepatic cells, but also an accumulation of TG. Under normal conditions, the excess glucose is converted into lipids carried as very-low-density lipoprotein (VLDL) and ultimately stored as TG. However, under chronic conditions of glucose uptake, pathologic levels of TG accumulation can occur and a fatty liver phenotype may develop. As described above we show leucine-dependent accumulation of *FOXO1*, which promotes transcription of microsomal TG transfer protein (MTP) and VLDL production and leading to hepatic hypertriglyceridemia (280). With leucine supplementation we see elevated transcription of several genes involved in fatty acid synthesis, including *GPAT1*, *ACCI* and *PPAR γ* . *GPAT1* is a key enzyme in the regulation of hepatic TG biosynthesis, such that an acute reduction of mitochondrial *GPAT1* in the liver of ob/ob mice reduces TG synthesis and obesity (277). Expressed at high levels in lipogenic tissues, *ACCI* controls the regulation of long-chain fatty acids biosynthesis, and its inhibition has been proposed as a potential strategy for the treatment of obesity and related disorders (278). In addition, *PPAR γ* binds to the promoters of *SLC2A2* and *GK* (287) activating transcription, and when overexpressed leads to lipid accumulation in hepatocytes (288). We observe analogous *in vitro* transcriptional changes, consistent with the stimulation of hepatic lipogenesis after leu supplementation and again, these effects appear to require *MSTN*-dependent AMPK signalling. *GPAT1* expression in particular, was significantly altered by *MSTN* suppression in our experiments. This data suggests a regulatory role for *MSTN* in hepatic TG synthesis.

In *MSTN*-null mice, insulin sensitivity of skeletal muscle is improved and body fat reduced (198, 289). Further, a constitutive *MSTN* loss-of-function mutation also attenuates fat accumulation in muscle tissue and hepatic steatosis in mice fed a high-fat diet (215). The most common cause of abnormal liver function is NAFLD (290), in which increased TG synthesis contributes to hepatic steatosis and is frequently a sequela observed with advancement of metabolic syndrome. NAFLD may even cause pancreatic β -cells to attempt compensation by increasing insulin production, leading to hyperinsulinemia and in turn, further stimulating hepatic *de novo* lipogenesis (reviewed by

(291)).

Emerging data from both human and animal studies support a causal role of intracellular hepatic TG accumulation in the pathogenesis of hepatic IR and human NAFLD subjects often exhibit peripheral IR as well (292).

We have also investigated a role for miRNA-mediated epigenetic effects in the manifestation of the hepatic responses to leucine exposure. MicroRNAs have now been linked to a variety of biological phenomena, and specifically to insulin secretion (248, 293), reduced viability and numbers of pancreatic β -cells (249), glucose metabolism (294) and pathological development of obesity (229). In particular, expression of miR-143, miR-17-92b and miR-335 are significantly altered in diet-induced obese mice (295), during 3 T3-L1 adipocyte differentiation (296), and in human adipose tissues inflammation (297). We found that suppression of miR-143 led to a strong increase in the hepatic expression of *PPAR γ* and blocked the ability of leu to induce both *MSTN* and *FOXA2* expression. Meanwhile, it has been reported that the miR-17-92 cluster, which yields six mature miRNAs including miR-92, is upregulated and promotes adipogenesis by inhibiting the key cell cycle regulator and tumor suppressor gene *Rb2/p130* (296). We found suppression of miR-92b* reduced the leu-dependent upregulation of *MSTN*, *FOXO1*, *SLC2A2* and *FOXA2*. Further, miR-335 upregulation combines with increased expression of interleukin-6 and tumor necrosis factor- α during inflammation of human visceral adipose tissue in obesity-related IR (297), and occurs in parallel with that of *PPAR γ* after the induction of 3T3-L1 adipocyte differentiation (248). Notably, we found that miR-335 suppression inhibited leu-dependent increases in *FOXO1* and *SLC2A2* gene expression. This data suggests the regulatory role of miRNAs in leu-induced glucose metabolism in liver.

3.6 Conclusions

In summary, we suggest that leu may be both ‘friend’, stimulating hepatic cell uptake of extracellular glucose, and ‘foe’, with progression toward NAFLD-like phenotypes being perhaps the

unavoidable and obligatory consequence of the enhanced glucose sequestration promoted by extracellular leu when in pathophysiological excess. We also extend the potential functional importance of the metabolic axis of AMPK-*MSTN* signaling and miRNA mediated mechanisms in the context of metabolic syndrome and NAFLD in particular. We also will look to extend these encouraging findings to primary cultures of hepatocytes in future studies as the cell lines may not represent what is occurring *in-vivo*. While our findings may offer an intriguing resolution to the apparent paradox associated with the reported pathophysiological consequences of BCAA exposures, further investigation in cultures of primary hepatocytes from clinical patients is warranted to substantiate them.

3.7 Methods

3.7.1 Chemicals and antibodies

DMEM and FBS were from Invitrogen (CA, USA). The 2-DOG was from PerkinElmer (Boston, USA). All other chemicals were from Sigma (St. Louis, MO, USA) unless otherwise stated. Antibodies for mTORC1, p(Ser²⁴⁴⁸)-mTORC1, p(Thr³⁸⁹)-p70-S6K1, AMPK α , p(Thr¹⁷²)-AMPK α , AKT and p(Ser⁴⁷³)-AKT were from Cell Signaling Technology (Boston, MA, USA) and B-actin antibody was from Santa Cruz Biotechnology (Santa Cruz, CA, USA). The predesigned miRNA primers and siRNAs were from Qiagen (Hilden, Germany).

3.7.2 Cell culture and treatment

The HepG2 cell line was purchased from American Type Culture Collection (Manassas, VA, USA) and were passaged in low glucose DMEM supplemented with 10% FBS at 37°C with 5% CO₂. Cells were seeded at 10⁴ to 10⁵ cells/cm² and after 24 h treated (or not) with 0.1 mM or 2.5 mM leucine for 48 h before being harvested for various assays. The survival of the cells was measured by an MTT assay after 48 h of exposure to leu (See section 2.1 for more details).

3.7.3 Glucose uptake assay

HepG2 cells treated (or not) with leucine were washed with pre-warmed PBS twice and incubated in a glucose-free Krebs-Ringer phosphate buffer (KRP) buffer containing 1% BSA for 1.5 h at 37°C. Glucose uptake assay was then performed as described previously (298). Results were normalized against the total intracellular protein content, which was determined by BCA assay (Thermoscientific, IL, USA) (See section 2.18 for more details).

3.7.4 Glucose output assay

Glucose secreted into the medium was measured using Amplex Red Glucose Kit (Invitrogen, Carlsbad, NM, USA) according to manufacturer's instructions. Following leucine treatment (or not), cells were washed twice with pre-warmed PBS and incubated for 1.5 h in glucose production assay medium (glucose and phenol red-free DMEM containing 2 mM sodium pyruvate and 20 mM sodium lactate). Next, 1 nM insulin was added 10 min before the end of the incubation period as appropriate. Media was collected for analysis. Data were normalized against total intracellular protein (See section 2.19 for more details).

3.7.5 Triglyceride measurement

Total intracellular TG content was measured using a fluorometric method kit (BioVision, CA, USA) in accordance with the manufacturer's instructions. Data were normalized against total intracellular protein (See section 2.20 for more details).

3.7.6 Glycogen measurement

The assay was performed using a Glycogen Assay Kit (BioVision, CA, USA) according to the manufacturer's instructions. Glycogen content was normalized against the total intracellular protein (See section 2.21 for more details).

3.7.7 Real-time PCR

Total RNA was isolated from leucine-treated (or not) HepG2 cells using PureLink RNA Mini Kit (Invitrogen, CA, USA) and cDNA was synthesized from 2 µg of total RNA using Transcriptor First Strand Synthesis kit (Roche, Mannheim, Germany). QPCR analysis was carried out on a LightCycler-480 II (Roche, Switzerland) in 10 µl volumes containing Light Cycler 480 SYBR Green, 0.5 mM of reverse or forward PCR primers (Table 3.2) and 1 µl of first-strand cDNA. The endogenous control peptidyl-prolyl isomerase A (*PPIA*) gene expression was chosen as the housekeeping gene as its threshold was constant across different conditions. The mRNA expression levels were normalized against *PPIA* by subtracting its average cycle threshold from the average threshold for each cDNA sample yielding a level of mRNA expression for the target molecule relative to the endogenous RNA reference gene (See section 2.9 for more details).

3.7.8 Western blotting

HepG2 cells (treated or not) were washed twice with ice-cold PBS. Ice-cold TK lysis buffer was added containing protease and phosphatase inhibitors. A total of 20 µg protein from whole cell lysates was resolved using 10% SDS-PAGE followed by transfer onto Immobilon-P PVDF membrane (Millipore, MA, USA). Primary and secondary antibodies were diluted in 2% skim-milk/PBS-0.1% Tween 20 (See section 2.6 for more details).

Table 3.2 Primer sequences used in real-time PCR (qPCR)

Gene name	Primers	Primer sequences	Accession number
Solute carrier family member2 (<i>SLC2A2</i>)	Sense	5'- CATTCCAATTAGAAAGAGAGAACGTC-3'	NM_001278658.1
Glucose 6-phosphatase (<i>G6Pase</i>)	Antisense	5'-AGCAAACCTGTTTATGCAACC-3'	NM_001270397.1
	Sense	5'-TACGTCCTCTCCCATCTG-3'	
Phosphoenolpyruvate carboxykinase 1 (<i>PCK1</i>)	Antisense	5'-CCTGGTCCAGTCTCACAGGT-3'	NM_002591.3
	Sense	5'-GGTCCCAGGGTGCATGAAA-3'	
Pyruvate carboxylase (<i>PC</i>)	Antisense	5'-CACGTAGGGTGAATCCGTCAG-3'	NM_001040716.1
	Sense	5'-TTGCCCACTTCAAGGACTTC-3'	
Forkhead box O1 (<i>FOXO1</i>)	Antisense	5'-CTTTGATGTGCAGCGTCTTG-3'	NM_002015.3
	Sense	5'-GCTGCATCCATGGACAACAACA-3'	
Peroxisome proliferator-activated receptor gamma, coactivator 1 alpha (<i>PPARGCIA</i>)	Antisense	5'-TGTGCAACTCTCTGGAAGT-3'	NM_013261.3
	Sense	5'-TGAGGACTTGCTGAGTGGTG-3'	
Myostatin (<i>MSTN</i>)	Antisense	5'-GAAATCAGACTCTGTAGGCATGGT-3'	NM_005259.2
	Sense	5'-CGTCTGGAAACAGCTCCTAACA-3'	
Glycerol-3-phosphate acyltransferase (<i>GPAT1</i>)	Antisense	5'-AACCCAGTATCCCGTCTTT-3'	NM_001244949.1
	Sense	5'-CAGTCACATTGGTGGCAAAC-3'	
Forkhead box A2 (<i>FOXA2</i>)	Antisense	5-TGTTTCATGCCGTTTCATCCC-3	NM_021784.4
	Sense	5-GGAGCGGTGAAGATGGAAG-3	
Glucokinase (<i>GK</i>)	Antisense	5'-GATGCACTCAGAGATGTAGTCG-3'	NM_000162.3
	Sense	5'-TGAAGGTGGGAGAAGGTGAG-3'	
Acetyl-CoA carboxylase (<i>ACCI</i>)	Antisense	5'-ATCCCG TACCTTCTTCTACTG-3'	NM_198836.2
	Sense	5'-CCCAAACATAAGCCTTCACTG-3'	
Peroxisome proliferator-activated receptor gamma (<i>PPARγ</i>)	Antisense	5'-CCACTATGGAGTTCATGCTTGTGAAGG-3'	NM_138711.3
	Sense	5'-TGCAGCGGGGTGATGTGTTTGAAGT-3'	
Peptidylprolyl isomerase A (<i>PPIA</i>)	Antisense	5'-TCTTGAGGGAAGCATATTGG-3'	NM_001300981.1
	Sense	5'-CAGGGAGACTGACTGTAGCAC-3'	

3.7.9 Reverse transfection

MSTN siRNA (4392420-s5679, Invitrogen, CA, USA) or control oligonucleotides (4390843, Invitrogen, CA, USA) were reverse transfected into HepG2 cells in a 24-well plate using Lipofectamine RNAiMAX (Invitrogen, CA, USA). Briefly, Lipofectamine and diluted siRNA were added to Opti-MEM I Medium (Invitrogen, NY, USA) and incubated in wells for 20 min. Cells were then added at a density of 10^5 cells/well and 24 h later treated with leucine for a further 48 h before being harvested (See section 2.14 for more details).

3.7.10 MiRNA microarray

A PureLink RNA Mini Kit was used to extract total RNA (Invitrogen, CA, USA). The RNA was initially evaluated by 260/280 ratio using a NanoDrop ND-1000 Spectrophotometer (NanoDrop Technologies, DE, USA) and was further assessed on Agilent 2100 Bioanalyzer (Agilent Technologies, CA, USA) after preparation with an Agilent RNA 6000 Nano kit. All samples showed values of 260/280 above 1.8 and RIN scores of at least 8.0. Reverse transcription was carried out using 500 ng total RNA. Then, cRNA was labeled with Biotin using Affymetrix Flash Tag Biotin HSR RNA Labeling kit. The fragmented-Biotin-labeled cRNA was then added to the array (Affymetrix GeneChip miRNA 3.0), and after washing to remove any unbound RNA, hybridization was assessed by fluorescent staining (GeneChip Hybridization, Wash and Stain kit) and scanning with a GeneChip Scanner 3000 system. Robust multi-array average (RMA) background correction and quartile normalization were used to adjust signal intensity data (See section 2.13 for more details).

3.7.11 Validation of miRNA expression/ gene targets

Candidate targets for validation by qPCR were determined according to both fold-change (Appendix II) and significance at $P \leq 0.05$. Also, miRBase (<http://microrna.sanger.ac.uk/>) and miRWalk (<http://www.umm.uni-heidelberg.de/apps/zmf/mirwalk/index.html>) databases were used to identify

potential and validated gene targets. The cDNA synthesis was carried out with 2 µg total RNA using a miScript II RT Kit (Qiagen, Hilden, Germany) , and expression of the miR-143, miR-92b*, miR-335, miR-181d, miR-3185 and miR-4763 was assayed with a miScript SYBR Green PCR kit (Qiagen, Hilden, Germany). Data was normalized to RNU6-2 snRNA expression. Commercially available siRNAs were used to inhibit differentially expressed miRNAs (Qiagen, Hilden, Germany) following qPCR to assess target gene effects (See section 2.12 for more details).

3.7.12 Statistical analysis

All analyses were performed using the IBM SPSS statistical program (version 21, NY, USA). All results are presented as mean ± SEM from at least three independent experiments done in triplicates. A one-way ANOVA with a Tukey post-hoc test was used to assess differences between groups. $P \leq 0.05$ was considered statistically significant.

3.8 Competing interests

The authors declare that they have no competing interests.

3.9 Authors' contributions

AZ conceived the study, undertook the molecular biology and data analysis, wrote the first draft of the manuscript, reviewed the manuscript, and edited the manuscript. SN conceived the study and reviewed and edited the manuscript. AS conceived the study and reviewed and edited the manuscript. AZ is the guarantor of this work and, as such, takes full responsibility for the work as a whole, including the study design, access to data, and the decision to submit and publish the manuscript. All authors read and approved the final manuscript.

3.10 Acknowledgements

AZ is supported by a Univ. of Auckland Doctoral Scholarship, and we acknowledge Dr. Zengxiang Pan (Liggins Institute) for assistance with statistical analysis. The funders played no role in the conception or design of this study, data collection and analysis, decision to publish, or preparation of this manuscript. There are no potential conflicts of interest relevant to this article.

3.11 Supplementary data 1

In this section, I take a look at validation of my *in vitro* leu-supplemented HepG2 cells model and its effect on DNA methylation of certain genes as another epigenetic regulatory mechanism.

3.11.1 Determining the appropriate dose of leucine

The MTT assay is a colourimetric assay to determine cell number thus viability and metabolic activity. The appropriate dose of leu was determined to avoid cell toxicity and death after supplementation.

To assess the appropriate doses of leu in our *in vitro* model using HepG2 cells, we determined the effect of various doses of leu (from 0 mM to 100 mM) on cell cytotoxicity and viability.

As shown in Figure 3.7, at 5 mM of leu and above, cell viability was reduced significantly ($p \leq 0.05$) from 1.4 fold to 0 while doses less than 5 mM slightly affected cells viability (1.1 fold reduction). Therefore, the doses 2.5 mM of leu and less were assumed as safe doses to perform the experiments.

3.11.1.1 General conclusion

Taken together, we chose 2.5 mM of leu as the highest dose of treatment which did not affect cells viability as well as 0.1 mM dosage which is considered as the physiological concentration of leu in human plasma.

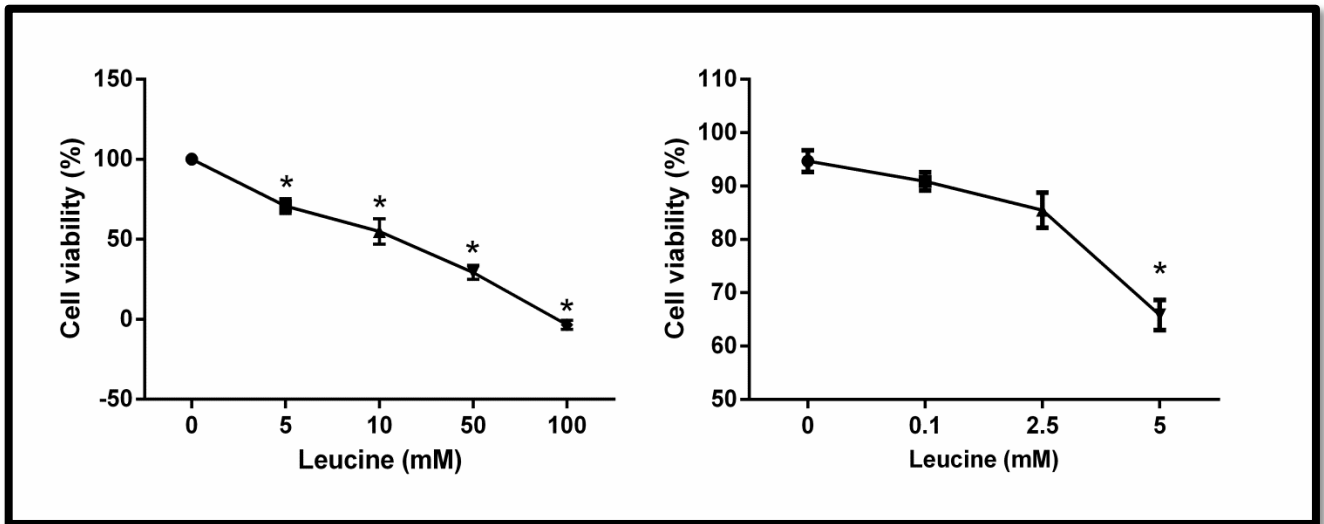


Figure 3.7 MTT assay

The relationship between the cells viability and various doses of leucine. HepG2 cells were treated (or not) with leucine for 48 hours. Values are presented as the mean \pm SEM. Statistical significance relative to untreated control, * $P \leq 0.01$ (n=3).

3.11.2 Determining the type of branched-chain amino acid

The association of BCAAs with features of metabolic syndrome has been addressed (68); however some studies have concentrated on the characteristic role of leu (33, 299).

To examine the stated distinctive role of leu among other BCAAs in our *in vitro* model, we measured the expression of certain genes treated or not with leu involved in hepatic glucose and lipid metabolism in the presence of either leu or a combination of BCAAs before running further experiments. In addition, to set the appropriate duration of treatment, we assessed the expression of these genes over various timecourses in HepG2 cells; this cell line represent most of the normal human hepatocytes features specially TG synthesis pathways.

We measured mRNA expression of *SLC2A2*, *PPARGC1A* and *FOXO1* after 2 hours, 24 hours and 48 hours of different doses of leu and a combination of BCAAs treatment (See sections 2.7, 2.8 and 2.9 for methods). Although there was a slight increase ($p \leq 0.05$) in *SLC2A2* expression after 2 hours exposure to 0.1 mM leu, *SLC2A2* mRNA was upregulated by 1.57 fold after 48 hours of treatment with either leu or BCAAs combination ($p \leq 0.05$; Figure 3.8). Besides, *PPARGC1A* was overexpressed by 0.1 leu after 2 hours (1.5 fold, $p \leq 0.05$; Figure 3.8), by 2.5 mM leu and 2.5 mM BCAAs mixture after 24 hours (2.28 fold, $p \leq 0.05$; Figure 3.8) and by both doses of leu and BCAAs mixture up to 2.5 fold after 48 hours ($p \leq 0.05$; Figure 3.8). The expression of *FOXO1* mRNA was also increased after 2.5 mM of either leu or BCAAs combination in 24 hours and increased up to 1.66 fold in all treatment conditions after 48 hours ($p \leq 0.05$; Figure 3.8). Furthermore, only leu was able to phosphorylate thus activate the AMPK while the combination of leu with other BCAAs could not induce any change in AMPK activity (See sections 2.5 and 2.6 for methods). This data suggest the unique role of leu compare to the other BCAAs as the level of mRNAs expression remained almost similar in leu treated cells compared to when a combination of leu, isoleucine and valine was used and the level of phosphorylated AMPK remained unchanged when the combination of BCAAs was applied. Also, 48 hours was used as the proper time point for leu exposure as the mRNA expressions reached their highest

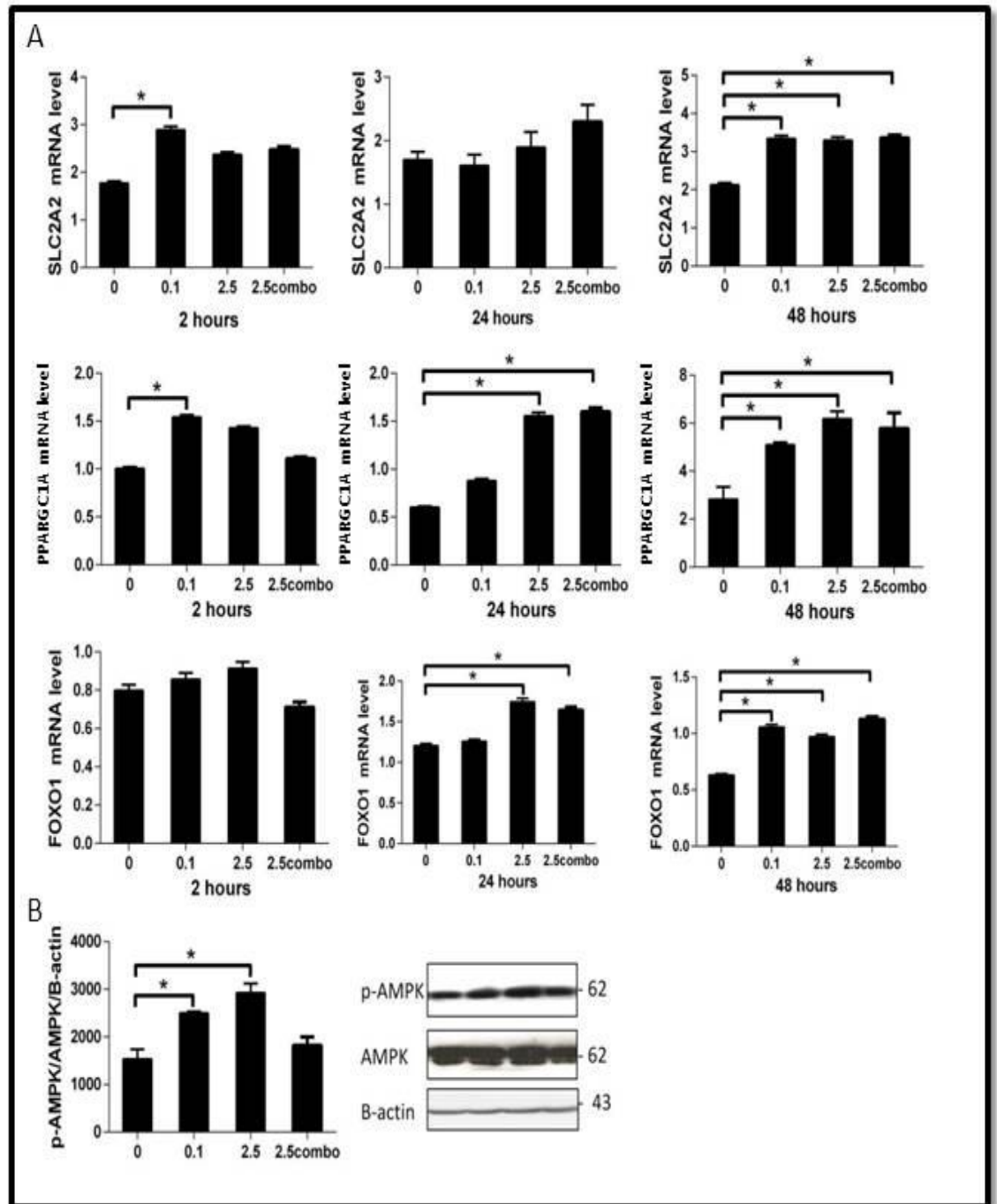


Figure 3.8 Effect of branched chain amino acids treatment for various durations

A) HepG2 cells were treated (or not) with either 0.1 mM and 2.5 mM of leu or 2.5 mM of BCAAs combination for 2 hours, 24 hours and 48 hours and the expression of *SLC2A2*, *PPARGC1A* and *FOXO1* genes was compared at these time points. B) HepG2 cells were treated (or not) with either 0.1 mM and 2.5 mM of leu or 2.5 mM of BCAAs combination for 48 hours and the phosphorylation of AMPK α at Thr172 residue was compared. Values are presented as the mean \pm SEM. Statistical significance relative to untreated control, * $P \leq 0.05$ (n=3).

level in this time frame.

3.11.2.1 General conclusion

Taken together, there was no augment in the expression of genes when combination of BCAAs was used compared to leu alone. In addition, the greatest change in the mRNA level of genes occurred 48 hours after exposure to leu whereby 2.5 mM of leu showed the highest influence on the expression of the target genes evaluated. These results suggest the potential role of leu on cells metabolism within 48 hours. Therefore, we established leu treatment for 48 hours in our experiments.

3.11.3 Effect of leucine on DNA methylation in HepG2 cells

DNA methylation at the genes promoters appears to play critical role in gene silencing (220) and thus may be a mediator of epigenetic inheritance. DNA methylation is implicated in gene regulation, differentiation, chromatin structure and complex diseases (300).

It has been shown that methylation levels of PPARGC1A promoter inversely correlates with abundance of its mRNA in the liver biopsies obtained from NAFLD patients (301). Therefore, to evaluate whether liver DNA methylation status of leu-responsive genes is associated with their mRNA expression, we measured methylation ratio of *SLC2A2*, *FOXO1*, *PPARGC1A* and *MSTN* involved in glucose and lipid metabolism with influenced mRNA expression after leu induction.

I examined DNA methylation status on the promoter regions of the *SLC2A2*, *FOXO1*, *MSTN* and *PPARGC1A* genes in HepG2 cells treated or not with leu (primers are listed in Table 3.3). I analyzed the methylation levels of four to six adjacent CpG sites at the same time in each gene. The average methylation level from each CpG site was used as a representative DNA methylation level for each group. *SLC2A2* showed moderate levels of DNA methylation while we found high to quite low levels of DNA methylation in the *FOXO1* promoter. Both *MSTN* and *PPARGC1A* showed moderate to very low levels of DNA methylation however, there was no significant change between DNA methylation of HepG2 cells treated with leu compared to the control group. Taken together, these data suggest that DNA methylation was not involved in the regulation of these genes (Figure. 3.9) (See sections 2.15 and 2.16 for methods).

Table 3.3 Primer sequences used in DNA methylation

Gene name	Primers	Primer sequences
<i>SLC2A2</i>	Sense	TTGTGTGAGTGTGGTATATGTATTTG
	Antisense	ATAACCATTCAAATCAACAATAATCTCC
<i>FOXO1</i>	Sense	TTTTAAAGATTTTAAGGATTTGGGG
	Antisense	AACAATCTAAACCTCCTCTAACAACC
<i>PPARGCIA</i>	Sense	GAAGAGTTGTTGTAGTTTTTTTTGTTTT
	Antisense	AATATTTTTCCCTCAATTCACAAAC
<i>MSTN</i>	Sense	TAGTTTGTTTAAAAGAGTTTGAAAATAGA
	Antisense	AAAAACCATTTAAAATACAAATCCTCAA

3.11.3.1 General conclusion

Methylation of DNA occurs mostly at the promoter region of eukaryotic cells and inhibits transcriptional factors binding thus gene transcription (218). CpG islands are located more frequently at promoters (302) and account for most of the nonmethylated CG dinucleotides (218). It is indicated that DNA methylation and histone modification can be dependent on one another whereby histone methylation can directly induce DNA methylation therefore gene silencing (303). This data suggests that leu has no potential in regulating genes expression through methylation of DNA within 48 hours in HepG2 cells which could be due to the short duration of treatment with leu as most of the DNA methylation experiments have been applied *in vivo* or for longer periods (7 days and more) *in vitro* using different cell lines (304). Although the short duration of leu exposure could lead to this result, another *in vivo* study also showed no change in DNA methylation of liver from rats with high fat sucrose diet for 2 months; they have suggested that diet-induced obesity may determine gene expression independent of DNA methylation status (305).

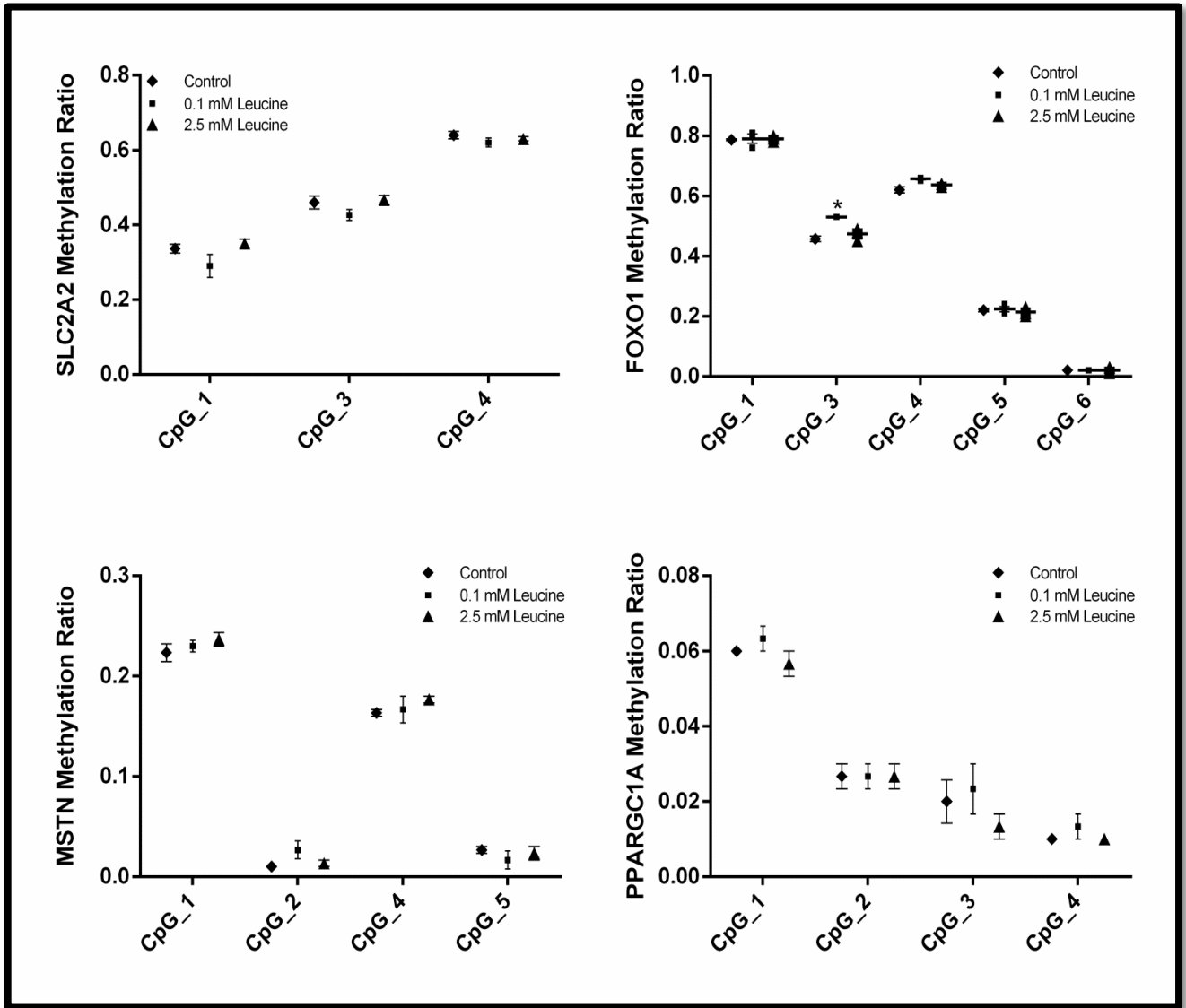


Figure 3.9 DNA methylation ratio in HepG2 cells

Each set of symbols corresponds to the DNA methylation ratio in a specific CpG site in promoters of SLC2A2, FOXO1, MSTN and PPARGC1- α genes. HepG2 cells were treated (or not) with 0.1 mM and 2.5 mM leucine for 48 hours. Values are presented as the mean \pm SEM. Statistical significance relative to untreated control, * $P \leq 0.05$ (n=3).

3.12 Supplementary data 2

Recent studies have reported an association between fatty liver disease and systemic IR. While the causal relationship between these features remains unclear, an evident possibility is that an increased release of heptokines and miRNA from ‘diseased’ liver might contribute to muscle IR and/or elevated insulin release from pancreas.

In this section, I begin to explore this notion by testing the effect of conditioned medium, collected from HepG2 cells treated with leu for 48 hours, on cell lines representative of peripheral tissue, namely PANC-1 pancreas and C2C12 muscle. Specifically, I have asked whether hepatic factors in the conditioned media can subsequently stimulate insulin secretion from the pancreatic cells and/or the uptake of glucose by muscle cells.

3.12.1 Insulin production in pancreatic cells exposed to conditioned medium from leucine-treated hepatocytes

The impact of leu supplementation on liver metabolism has been described above (See chapter 3). Extending these observations, I have measured insulin levels in either differentiated (able to produce insulin) or undifferentiated (unable to produce insulin) pancreatic cells in the presence of leu-induced hepatic conditioned media as described elsewhere (See sections 2.3 and 2.22 for methods). Surprisingly, in neither undifferentiated PANC-1, nor cells having undergone five days of a differentiation protocol (Figure 3.10), did I see any evidence of any further elevation of insulin secretion after 48 hours in response to conditioned media from HepG2 cells, treated initially with either low (0.1mM) or high (2.5mM) doses of leu (Figure 3.11 A and B). As expected, control differentiated PANC-1 cells were clearly responsive to stimulation with the addition of glucose, indicating the clear capacity for a response to appropriate humoral factors.

3.12.1.1 General conclusion

These exploratory data were disappointing in that they failed to illicit a core response from the pancreatic cells, despite the demonstrated capacity for insulin induction in this *in vitro* model system. Given this preliminary result with the pancreatic cells, I did not pursue further examination of this paradigm. However, it might be worth exploring further 1) whether the initial period of leu supplementation of the hepatic cells was insufficient to generate effective concentrations of the necessary secreted factors, despite the use of both low and high doses of BCAA in these experiments, and 2) whether any effects that were elicited on the PANC-1 cells may have been transient and dissipated by the time of the 48 hour measurement of insulin secretion time that is reported here.

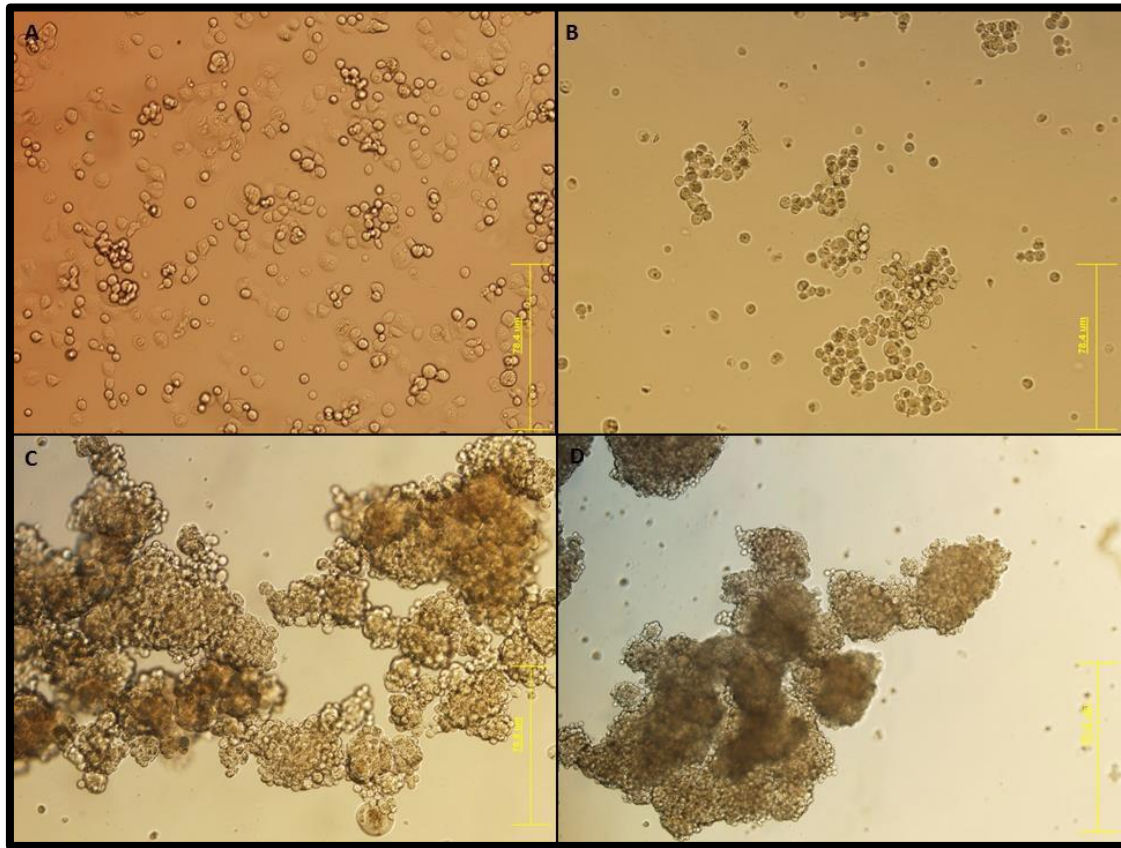


Figure 3.10 Morphological changes of PANC-1 cells

A) PANC-1 cells cultured in proliferation medium where they grow as flattened monolayers. B) PANC-1 cells cultured in serum-free medium for 1 day and C) 3 days that shows insulin-expressing cells. D) These islet-like cell aggregates became more compact after 4 days exposure to serum-free medium.

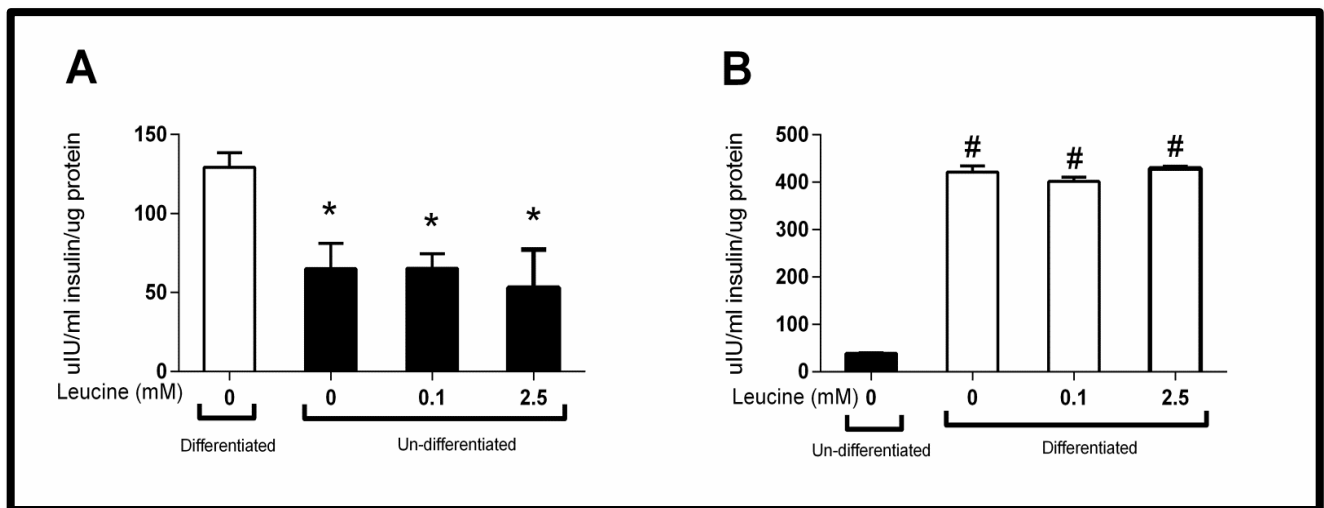


Figure 3.11 Insulin secretion in Panc-1 cells

A) Un-differentiated Panc-1 cells (black bars) were exposed to conditioned medium from HepG2 cells treated (or not) with 0.1 mM and 2.5 mM leu for 48 hours before measuring insulin levels.

B) Differentiated Panc-1 cells (white bars) were exposed to conditioned medium from HepG2 cells treated (or not) with 0.1 mM and 2.5 mM leu for 48 hours before measuring insulin levels. Values are presented as the mean \pm SEM. Statistical significance relative to untreated control, * $P \leq 0.05$, # $P \leq 0.01$ (n=3).

3.12.2 Glucose uptake in myotubes exposed to conditioned medium from leucine-treated hepatocytes

Glucose is the major fuel used for muscular cell contraction and skeletal muscle is the main target of glucose uptake and utilization in the body dependent or independent of insulin stimulation (306). The insulin-independent uptake of glucose by muscle requires activation of AMPK (307). After four days under a differentiation protocol, myotubes (Figure 3.12) were treated with conditioned medium from leucine stimulated or non-stimulated HepG2 cells, and subsequent intracellular glucose levels measured by the 2-DG uptake assay described elsewhere (See sections 2.2 and 2.18 for methods). Again, conditioned media from leu treated hepatic cells did not further potentiate glucose uptake by the myotubes (Figure 3.13),

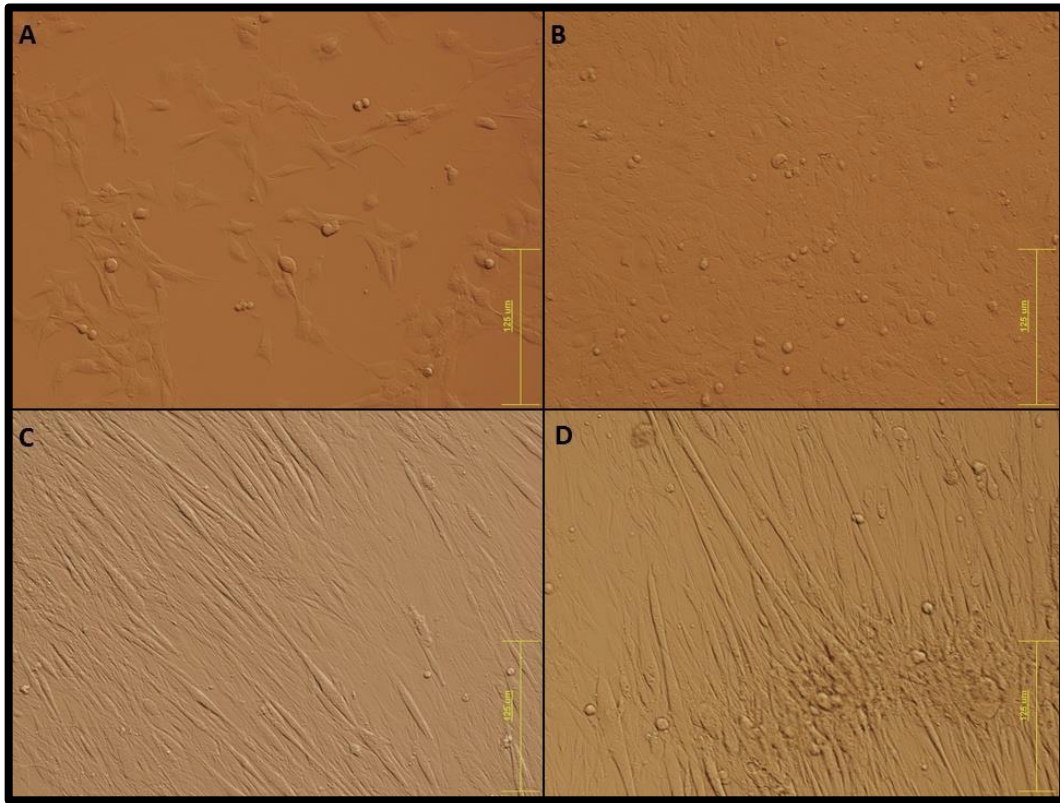


Figure 3.12 Morphological changes of C2C12 cells

A) C2C12 cells cultured with 20% confluence in proliferation medium. B) C2C12 with >100% confluence before the differentiation C) 3 days after myogenic differentiation. D) Completely differentiated myotubes.

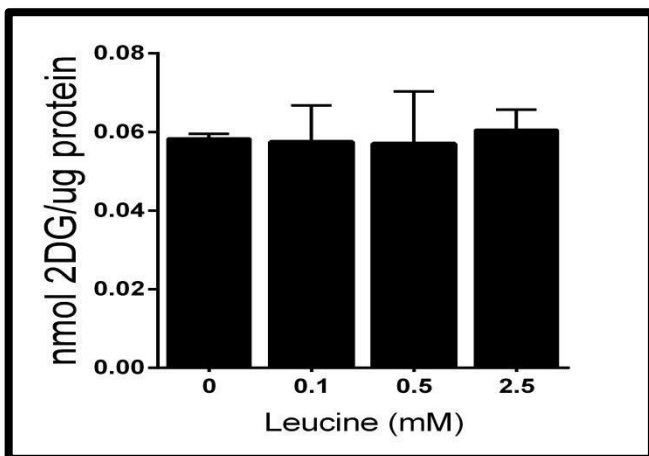


Figure 3.13 Glucose uptake in C2C12 cells

Differentiated C2C12 cells (myotubes) were exposed to the conditioned medium from HepG2 cells treated (or not) with 0.1 mM and 2.5 mM leu for 48 hours before measurement of glucose uptake by tritiated 2-DG. The glucose uptake result was normalized based on protein content of each sample. Values are presented as the mean \pm SEM (n=3).

3.12.2.1 General conclusion

These exploratory findings again do not seem to indicate that conditioned media generated from exposure of HepG2 cells *in vitro* at least, does not seem to exhibit any biological effect on glucose metabolism on peripheral tissue represented *ex vivo* here by a well characterized muscle cell line. Other than the obvious caveats described above, there are other possible reasons for the lack of biological effect in these experiments. Perhaps most significantly, as a singular cell-line HepG2 cells alone cannot recapitulate all aspects of liver tissue and it may be that the critical factors for which I am searching may in fact be induced (directly or indirectly) by cell types other than hepatocytes (eg immune cells) which are present in the heterogeneous environment which comprises the intact liver. If so, attempts to reduce some aspects of the complex biology of inter-tissue paracrine effects may not be addressable with simple *in vitro* based models. Additionally, it may be that the systemic consequences of micronutrients such as BCAA and FFAs arise mainly through direct influences on individual tissues, rather than through complex inter-tissue interactions. In this case, the hepatic secretion of factors such as hepatokines and miRNAs would likely serve as a barometer of metabolic status for tissues other than those primarily involved in maintaining homeostasis.

4 MICRO RNAS AS BIOMARKERS OF BARIATRIC SURGERY OUTCOME AND PUTATIVE REGULATORS OF HEPATOKINES SELECTIVELY AFTER GASTRIC BYPASS, BUT NOT SLEEVE GASTRECTOMY

4.1 Preface

The following chapter contains the published original research article “*Micro RNAs as biomarkers of bariatric surgery outcome and putative regulators of hepatokines selectively after gastric bypass, but not sleeve gastrectomy*”. The article was published in the journal of obesity and bariatrics in 2016. This journal is an open access, peer-reviewed journal that focuses on medical, clinical, surgical, nutritional and applied aspects of obesity and strives to investigate for the best possible remedies.

The rate of obesity and thus subsequently obesity-related co-morbidities such as non-alcoholic fatty liver (NAFLD), type 2 diabetes mellitus (T2DM) and cardiovascular diseases is increasing worldwide. Deregulation in adipose tissue metabolism is causative of hepatic defects leading to insulin resistance (IR) and eventually T2DM development. Therefore, body weight reduction might help to prevent or treat fatty liver which is the consequence of fat accumulation in the liver that can develop to cirrhosis. Bariatric surgery includes a variety of procedures on obese people to loss weight. Weight loss can be achieved by removal of a portion of stomach (sleeve gastrectomy, SG) resecting the small intestine to a small stomach pouch (gastric bypass surgery, GBP). Bariatric surgery is known as the more effective treatment of obesity than non-surgical treatments while precise recommendations for referring a patient to a specific type of bariatric surgery is not available. Moreover, the observed weight loss is comparable between GBP and SG after a long term however, the level of remission of T2DM and other long-term outcomes are not predictable yet due to lack of a biomarker. Therefore, in order to develop novel and valid therapeutic strategies, investigating the underpinned molecular mechanism to determine the metabolic shifts between surgeries is essential. Here, I hypothesized that miRNAs regulatory role on fetuin-A (FetA), that have recently been shown to reduce after GBP, may be functionally important for inducing remission induction.

Here, I have reported the change in miRNA expression following both GBP and SG bariatric surgeries where GBP introduced more distinctive miRNA clustering than SG (pre- vs. post-operative). Patients who underwent GBP yielded a significant degree of improvement in their BMI and blood glucose levels compared to SG. Regulation of hepatokine *FetA* and *Leukocyte cell-derived chemotaxin 2 (LECT2)* was regulated by MSTN. We showed the potential role of miRNA-335 in the regulation of hepatokine *FetA* as well as BMI post-GBP operation.

4.2 Abstract

The prevalence of obesity is increasing worldwide, resulting in more bariatric surgery interventions being performed. However, the success of surgical approaches in treating obesity and its comorbidities varies between types of surgery and is not readily explained by baseline clinical features. Better understanding is needed of the metabolic shifts, and their underpinning mechanisms, which result from different types of surgery. Such knowledge will help in the selection of surgery type based on individual's background.

We investigated effects of bariatric surgery on miRNA profile of nine obese patients with T2DM before and after either GBP or SG. Recent work (32) has identified early reduction in post-operative circulating levels of the hepatokine *FetA* after GBP but not SG, as a putative candidate to monitor the efficacy of intervention. Free fatty acid-induced HepG2 cells were used to study the underlying mechanism of *FetA* regulation by miRNAs.

A specific set of miRNAs including miR-27b, miR-29a, miR-192 and miR-335 whose post-surgery expression among GBP patients were identified that were correlated strongly with beneficial decreases in body mass index (BMI) and glycated hemoglobin (HbA1c) levels. Additionally, we reported that expression of both *FetA* and *LECT2* was dependent on intracellular signaling by metabolic regulator myostatin (MSTN). Finally, we linked miR-335 expression in particular to FFA-induced, MSTN-

dependent overexpression of *FetA*.

These data provide novel mechanistic insights into the metabolic stimulation of hepatokine *FetA* expression, and miRNA associated with greater weight loss and diabetes remission observed with GBP rather than SG.

4.3 Introduction

The rate of obesity is increasing worldwide, with at least 600 million people recently classified as clinically obese (309) which is associated with elevated morbidity, mortality and healthcare costs (310). Although bariatric surgery is a more effective intervention than other obesity treatment such as nutritional interventions and physical activity (310), overall leading to efficient weight loss, the different surgical procedures yield differing degrees of improvement in metabolic complications, particularly with regard to the remission of T2DM (311, 312) which is not readily explained by overall weight loss (310). The majority of prospective studies comparing the remission of T2DM following GBP and SG types of bariatric surgery suggest superior results with GBP than SG despite similar concurrent weight loss. While SG is considered a 'restrictive' type of surgery where the majority of the stomach is removed, GBP combines this restriction with limited malabsorption, whereby the stomach is reduced to a small pouch (<30mL) connected via a tight outlet to the jejunum just past the duodenum, while the jejunal stump is anastomosed to the lower jejunum in a Y conformation. While both procedures produce the rapid induction of negative calorie balance after surgery, the additional foregut bypass and more rapid nutrient delivery to the hindgut may underlie the superior T2DM remission following GBP (313, 314).

Currently, pre-operative clinical assessment is used to anticipate likely success and is the basis of strategies for individualizing post-operative risk, rather than any assessment of likely metabolic benefit based on objective predictive biomarkers or models (315, 316). While the observed weight loss is initially comparable between GBP and SG over the first 3 years, the remission of T2DM and longer-term outcomes are less predictable (317). However, the regain of substantial weight appears to be more

frequent following SG compared to GBP (318). Therefore, defining the underlying mechanisms that characterize post-surgery metabolic responses and differentiate the surgical approaches would improve understanding of the physiology linking obesity and T2DM and provide biomarkers with utility for predicting long-term metabolic response ahead of the standard clinical measures of metabolic syndrome. Lower HbA1c, higher C-peptide levels and a shorter duration of diabetes are associated with increased rate of T2DM remission (319, 320). The greater remission of T2DM observed after GBP rather than SG is thought to be due to the greater impact of GBP on gut hormones, bile acids and gut microbiota, however, the precise mechanisms underlying this are not well defined. We hypothesized that the epigenetically miRNA alteration of hepatokines such as *FetA* (also known as α 2-HS-glycoprotein) level that have recently been shown to decrease soon after GBP (32), may also be functionally important for driving remission.

Obesity is associated with the atypical secretion of liver-derived hepatokines (133, 146). *FetA* is expressed predominantly in the liver (321) and plays a major role in regulating insulin sensitivity, via the inhibition of insulin receptor tyrosine kinase mainly in liver, and peripherally in skeletal muscle (149). *FetA* mRNA abundance and circulating serum levels of FetA protein are increased in mice and humans with high liver-fat content (151, 322), suggesting this hepatokine may be key to understanding lipid-induced inflammation and metabolic syndrome disorders. In addition, leukocyte cell-derived chemotaxin 2 (*LECT2*), another secreted protein expressed mainly by the liver, is implicated in the homeostasis of hepatic natural killer cells and maybe represent a molecular link between obesity and insulin resistance (IR) in skeletal muscles (145). However, its importance in the context of over-nutrition induced hepatic fat accumulation has not yet been established.

Increasingly, the intracellular form of *MSTN*, a member of the transforming growth factor- β (TGF- β) superfamily typically associated with suppressing muscle growth, has been linked with the regulation of whole body metabolism. Elevated *MSTN* abundance is linked with metabolic disorders, such as obesity (323) and T2DM (324), while *MSTN*-null mice are resistant to high fat-induced IR and obesity

(200). In this study, we induced HepG2 cells with palmitic acid and the oleic acid as the most abundant saturated and unsaturated FAs, respectively in human diet and serum. We showed that MSTN regulates palmitate stimulated *FetA* expression in liver cells. Further, a pilot study of pre- and post-operative blood samples identifies miRNA species whose expression is strongly correlated with post-GBP levels of BMI and HbA1c. We then demonstrate FFA stimulation of these miRNA in liver cells, and that suppression of miR-355 in particular, inhibits the palmitate induced expression of both MSTN and *FetA*. Thus, obesity-dependent hepatokine production is likely to be a metabolic shift driven by the epigenetically dependent activation of MSTN signalling pathways.

4.4 Material and methods

4.4.1 Chemicals and antibodies

Low-glucose Dulbecco's modified eagle medium (DMEM) and fetal bovine serum (FBS) were purchased from Invitrogen (CA, USA). The rapamycin was from Calbiochem (Billerica, MA, USA). All other chemicals were from Sigma (St. Louis, MO, USA) unless otherwise stated. Antibodies for mTOR, pmTOR, AMPK and pAMPK were from Cell Signaling Technology (Boston, MA, USA) and B-actin antibody was from Santa Cruz Biotechnology (Santa Cruz, CA, USA). The predesigned miRNA primers/inhibitors and siRNAs were from Qiagen (Hilden, Germany).

4.4.2 Human clinical study

Nine obese subjects with T2DM participated in a prospective randomised bariatric surgery (four received GBP and five received SG) (The selection criteria have been shown in Table 4.1). Serum samples were obtained 3 days pre-operatively and 1 year post-operatively after either GBP or SG. All patients provided written informed consent and the experiments conformed to the principles set out in the [WMA Declaration of Helsinki](#) and the Department of Health and Human Services [Belmont Report](#). All experimental protocols were registered at clinicaltrials.gov (NCT01486680) and approved by our regional ethics committee (NZ93405) (See section 2.4 for more details on subjects).

Table 4.1 Selection criteria for bariatric surgery

<p style="text-align: center;">Inclusion Criteria</p>	<ul style="list-style-type: none"> ▪ T2DM for at least 6 months diagnosed by: <ul style="list-style-type: none"> 2 hours 75g oral glucose tolerance test > 11.1 mmol/l Or fasting glucose > 7mmol/l on at least 2 occasions And HbA1c > 48 mmol/mol ▪ Previous failed attempts at weight loss through dieting and exercise ▪ BMI \geq 35 kg/m² for at least 5 years ▪ Age between 20 and 55 years ▪ Suitable for either of the two surgical procedures ▪ Able to give informed consent and willing to commit to follow up
<p style="text-align: center;">Exclusion Criteria</p>	<ul style="list-style-type: none"> ▪ BMI > 65 ▪ Pregnancy ▪ T1DM ▪ Chronic pancreatitis ▪ Congestive heart failure ▪ Coronary artery bypass within 6 months ▪ Stroke within 6 months ▪ Chronic liver diseases other than fatty liver ▪ Chronic renal insufficiency ▪ Inflammatory bowel diseases ▪ Malabsorptive disorders ▪ Uncontrolled psychiatric disorders ▪ Blindness ▪ Current smoker

Abbreviations: T1/2 DM: type 1/2 diabetes mellitus

4.4.3 Cell culture and treatment

The human hepatoma HepG2 cell line (ATCC, Manassas, VA, USA) was cultured in DMEM supplemented with 10% FBS and incubated in a humidified atmosphere of 5% CO₂ at 37°C. Adherent cells were seeded at 10⁵ cells/cm² and after 36 hours, washed twice with serum-free medium followed by overnight incubation before treating (or not) with FFAs. Sodium palmitate and sodium oleate were conjugated to 2% fatty acid-free bovine serum albumin (BSA) dissolved in 50% ethanol in phosphate buffered saline (PBS). In all experiments, cells were treated with 0.25 mM of palmitate-BSA and oleate-BSA for 24 hours unless otherwise stated and 2% BSA was used as control. To inhibit mTORC1 phosphorylation in relevant experiments, cells were pre-incubated with rapamycin (10 nM in DMSO) for either 3 hours or 12 hours prior to the addition of sodium palmitate.

4.4.4 MiRNA microarray

Frozen plasma samples (See section 2.4 for samples details) thawed on ice at room temperature and were centrifuged to remove insoluble material. 200 µl of each supernatant was transferred to new tubes and 1ml of Qiazol was added. After incubation, 200 µl of chloroform and 1.5 vol of ethanol was added before adding the sample to a Qiagen miRNeasy serum/ plasma kit column (Qiagen, Hilden, Germany) and then processed according to the manufacturer's instruction. Reverse transcription was carried out using 155 ng of total RNA. The samples were sent to Adelaide microarray center to perform the array and preliminary data analysis. The, cRNA was conjugated with Biotin using Affymetrix Flash Tag Biotin HSR RNA Labeling kit. The fragmented-Biotin-labelled cRNA was then used in the array (Affymetrix GeneChip, miRNA 4.0). After removing unbounded RNA by washing, hybridization was evaluated by fluorescent staining (GeneChip Hybridization, Wash and Stain kit) before scanning with a GeneChip Scanner 3000 system (Affymetrix). Robust multi-array average (RMA) and quantile normalization also used to modify signals intensity (See section 2.13 for details).

4.4.5 RNA isolation and quantitative real-time PCR

Criteria for candidate miRNA selection for qPCR validation were: (1) at least a ranked ± 2 fold change in differential expression from the microarray analysis, (2) their putative function in the context of obesity and diabetes based on the existing literature, (3) *in silico* identification of predicted or validated miRNA targets using miRBase (<http://microrna.sanger.ac.uk/>) and miRWalk (<http://www.umm.uni-heidelberg.de/apps/zmf/mirwalk/>) databases. The Hierarchical clustering was performed using Pearson correlation to cluster the samples with more similarity in one group.

Total RNA including miRNAs was isolated from treated or not HepG2 cells with FFAs using PureLink RNA Mini Kit (Invitrogen, CA, USA). RNA was quantitated using a NanoDrop ND-1000 Spectrophotometer (NanoDrop Technologies, DE, USA). 2 μ g of total RNA was used for cDNA synthesis using Transcriptor First Strand Synthesis kit (Roche, Mannheim, Germany). Real-time polymerase chain reaction (qPCR) analysis was carried out in 10 μ l volumes containing Light Cycler 480 SYBR Green (Roche, Mannheim, Germany), 0.5 mM of reverse or forward PCR primers (Table 4.2) and 1 μ l of first-strand cDNA on a LightCycler-480 II (Roche, Switzerland). The mRNA expression levels were normalized against peptidyl-prolyl isomerase A (*PPIA*) and succinate dehydrogenase complex, subunit A (*SDHA*) as their threshold was constant across different conditions. The cDNA synthesis was carried out with 2 μ g total RNA using a miScript II RT Kit (Qiagen, Hilden, Germany) and expression of the miR-17, miR-27b, miR-29a, miR-99a, miR-148b, miR-192, miR-335 and miR-4532 (as miRNAs that met the criteria in section 4.4.5) was examined with miScript SYBR Green PCR kit and predesigned miScript primers (Qiagen, Hilden, Germany). Data was normalized to snoRNA SNORD72 and snRNA RNU6-2 expressions as their expression levels remained relatively constant across the samples.

Table 4.2 List of primers sequences used in real-time PCR (qPCR)

Gene name	Primers	Primer Sequence	Accession number
Acetyl-CoA carboxylase (<i>ACCI</i>)	Sense	5'-ATCCCG TACCTTCTTCTACTG-3'	NM_198836.2
	Antisense	5'-CCCAAACATAAGCCTTCACTG-3'	
Alpha-2-HS- glycoprotein (<i>Fetuin-A</i>)	Sense	5'-GCACGCCGCGAAAGC-3'	NM_001622.2
	Antisense	5'-TTCCTCCAGCTGAAAATTGGA-3'	
Glycerol-3- phosphate acyl transferase (<i>GPAT1</i>)	Sense	5'-AACCCAGTATCCCGTCTTT-3'	NM_001244949.1
	Antisense	5'-CAGTCACATTGGTGGCAAAC-3'	
Leukocyte cell derived chemotaxin 2 (<i>LECT2</i>)	Sense	5'-GGCAAGTCTTCCAATGA-3'	NM_002302.2
	Antisense	5'-CACATGCGATTGTATGC-3'	
Myostatin (<i>MSTN</i>)	Sense	5'-CGTCTGGAAACAGCTCCTAACA-3'	NM_005259.2
	Antisense	5'-GAAAATCAGACTCTGTAGGCATGGT-3'	
Peroxisome proliferator- activated receptor γ (<i>PPARγ</i>)	Sense	5'-CCACTATGGAGTTCATGCTTGTGAAGG-3'	NM_138711.3
	Antisense	5'-TGCAGCGGGGTGATGTGTTTGAAGT-3'	
Peptidyl-prolyl isomerase A (<i>PPIA</i>)	Sense	5'-TCTTGAGGGAAGCATATTGG-3'	NM_001300981.1
	Antisense	5'-CAGGGAGACTGACTGTAGCAC-3'	
Succinate dehydrogenase complex flavoprotein subunit A (<i>SDHA</i>)	Sense	5'-TGGGAACAAGAGGGCATCTG-3'	NM_001294332.1
	Antisense	5'-CCACCACTGCATCAAATTCATG-3'	
Sterol regulatory element binding transcription factor 1 <i>SREBP-1c</i>	Sense	5'-CCATGGATTGCACTTTCGAA-3'	NM_001321096.2
	Antisense	5'-CCAGCATAGGGTGGGTCAA-3'	

4.4.6 Western blotting

HepG2 cells were washed twice with ice-cold PBS and lysed with ice-cold lysis buffer containing 50 mM HEPES, 150 mM NaCl, 10 mM EDTA.Na₂ and 1% Triton X-100 with protease and phosphatase inhibitors. 20 µg of protein from whole cell lysates was then resolved by 10% SDS-PAGE gels and transferred to polyvinylidene fluoride membranes (Millipore, MA, USA). Primary and secondary antibodies were diluted in 3% BSA/PBS-0.1% Tween 20. Protein bands were visualised by using enhanced chemiluminescence using ECL reagent (ThermoScientific, Meridian, USA). Image J software (National Institutes of Health; <http://imagej.nih.gov/ij/>) was used for densitometric analysis of the protein bands.

4.4.7 Reverse transfection

Pre-designed MSTN siRNA (4392420-s5679, Invitrogen, CA, USA) or miScript miRNA inhibitors for miR-27b (MIN0000419, Qiagen, Hilden, Germany), miR-29a (MIN0000086, Qiagen, Hilden, Germany), miR-192 (MIN0000222, Qiagen, Hilden, Germany) and miR-335 (MIN0000765, Qiagen, Hilden, Germany) were used to inhibit MSTN and differentially expressed miRNAs (Qiagen, Hilden, Germany) following qPCR to assess their target genes expression. Inhibitors and negative control oligonucleotides (4390843/4464076, Invitrogen, CA, USA) were reverse transfected into HepG2 cells in 6-well plates using Lipofectamine RNAiMAX (Invitrogen, CA, USA). In brief, Lipofectamine and diluted inhibitors were incubated with Opti-MEM I Medium (Invitrogen, NY, USA) in the wells for 20 min at room temperature. Cells were then added at a density of 10⁵ cells/ml. Transfected cells were washed twice with serum-free medium followed by overnight incubation and exposed to FFA depends on the assays (See section 2.14 for details).

4.4.8 Statistical analysis

IBM SPSS statistical program (version 21, NY, USA) was used for data analysis. All results were presented as mean ± SEM from at least three independent experiments conducted in triplicates. Either one-way ANOVA with a LSD post-hoc test or independent samples *t*-test with SD was used to determine

differences between groups. Pearson correlation analysis with a two-tailed test of significance was performed. $P \leq 0.05$ was considered statistically significant.

4.5 Results

4.5.1 Clinical characteristics

For this study, subjects were chosen based on similarity of baseline characteristics with respect to pre-operative T2DM and morbid obesity (Table 4.3). One year post surgery, subjects averaged BMI of 29.05 ± 5.2 (post-GBP) and 28.62 ± 2.0 (post-SG) indicating significantly improved post-surgery BMI classification from Class II/III obesity to overweight. Waist circumference was significantly improved from 124.33 ± 7.2 pre-GBP to 96.75 ± 14.5 post-GBP ($P \leq 0.05$; Table 4.3). An improvement was also seen between pre- and post-SG albeit not significant. Glycated hemoglobin (HbA1c), as a proxy for blood glucose, was decreased by about 20 mmol/mol ($P \leq 0.05$) from about 65 mmol/mol pre-surgery to 45 mmol/mol post-surgery. Subjects 'homeostatic model assessment of insulin resistance' (HOMA-IR) decreased from >3 before surgery to about 2.1 after both surgery types, although not to statistically significant levels (Table 4.3). Blood pressure, triglyceride (TG) and high-density lipoprotein (HDL) were in the normal range either before or after surgery. The increased post-operative low-density lipoprotein (LDL) level could be also be accounted for discontinued medications and altered dietary behaviors (Table 4.3).

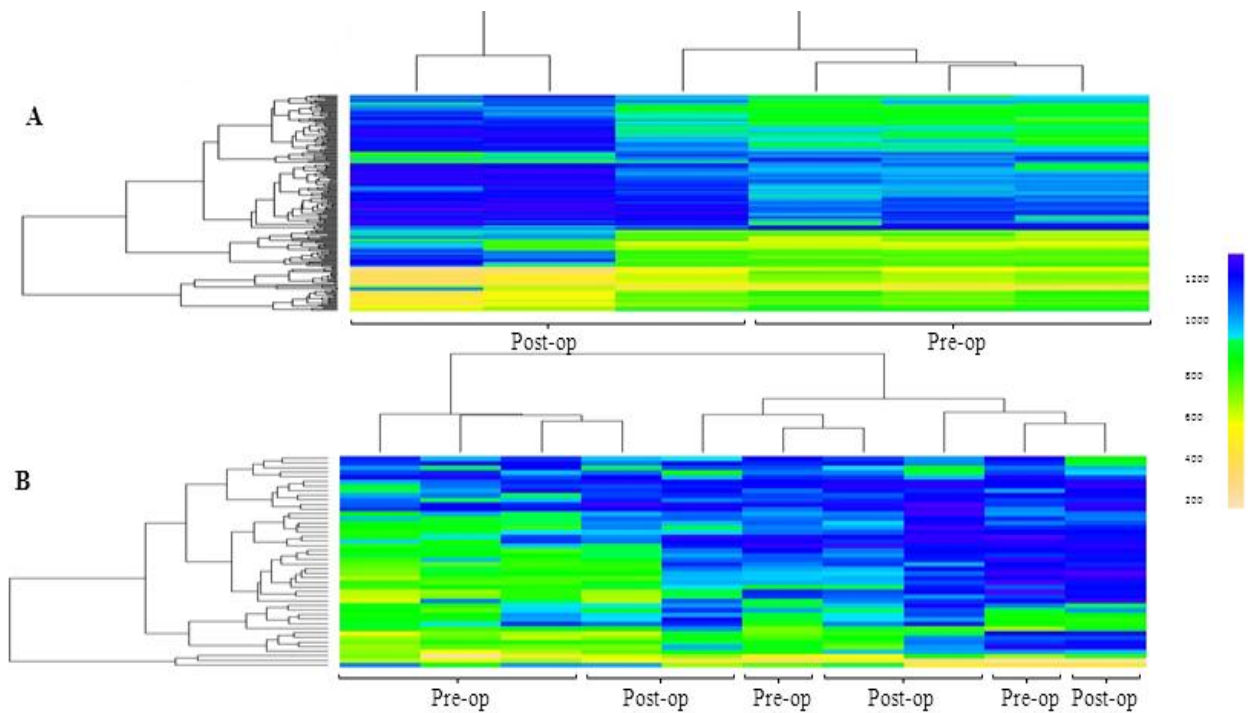
Table 4.3 Clinical characteristics of study subjects

	Pre-GBP	Post-GBP	<i>P</i> value	Pre-SG	Post-SG	<i>P</i> value
Age (years)	48.75 (6.7)	N/A	N/A	48.4 (5)	N/A	N/A
Gender (M:F)	2:2	N/A	N/A	3:2	N/A	N/A
Waist circumference (cm)	124.33 (7.2)	96.75 (14.5)	0.031	115.5 (17)	95.25 (9)	NS
Body wt (kg)	114.93 (16.3)	83.56 (19.5)	0.049	103.49 (24)	81.49 (13)	NS
BMI (kg/m ²)	40.07 (3.5)	29.05 (5.2)	0.013	35.98 (5)	28.62 (2)	0.031
Systolic blood pressure (mm Hg)	123 (10.8)	131.75 (13.6)	NS	133.4 (11)	123 (9)	NS
Diastolic blood pressure (mm Hg)	75.66 (6.1)	74.75 (11.8)	NS	86.6 (8)	79.2 (15)	NS
TG (mmol/L)	1.48 (0.3)	1.52 (0.9)	NS	1.21 (0.3)	1.26 (0.2)	NS
LDL (mmol/L)	2.77 (1)	5.28 (1.2)	0.023	1.95 (1)	3.77 (0.9)	0.035
HDL (mmol/L)	1.25 (0.3)	1.78 (0.2)	NS	1.21 (0.3)	1.88 (0.9)	NS
HbA1c (mmol/L)	66.5 (12.1)	46 (12.6)	0.01	62.8 (9.14)	43.8 (5.8)	0.028
HOMA-IR	4.69 (3.5)	2.32 (1.7)	NS	3.2 (1.64)	1.98 (1.03)	NS
Energy intake (kcal)	332 (323)	847.7 (33.5)	NS	687.25 (75.8)	951.8 (272)	NS

Clinical characteristics of obese subjects with T2DM before and after either GBP or SG surgery. Data presented after adjustment for age, BMI, ethnicity, medications and duration of T2DM. *P* values refer to overall difference across the groups as determined by independent samples *t*-test. Data are shown as mean (SD) and 95% confidence intervals; *p* values are calculated from independent samples *t*-test. Abbreviations: BMI: Body mass index; GBP: Gastric bypass surgery; HbA1c: Glycosylated haemoglobin level; HDL: High-density lipoprotein; HOMA-IR: homeostatic model assessment-insulin resistance; LDL: Low-density lipoprotein; NS: Non-significant for *p* values > 0.05; SG: sleeve gastrectomy; T2DM: type 2 diabetes mellitus; TG: Triglyceride.

4.5.2 MicroRNA expression profile between pre- and post-bariatric surgery

MiRNAs with at least ± 2 fold differential expression ($P \leq 0.05$) and relevant to metabolic syndrome features, were selected for further analysis. Among these, 71 and 12 miRNAs were up-regulated post GBP and SG respectively, while 209 and 60 miRNAs were down-regulated post GBP and SG respectively. Hierarchical clustering revealed distinct clustering of pre-GBP from post-GBP subjects (Figure 4.1A). However, the clustering of pre-SG from post-SG subjects was less distinct compared that of GBP surgery type (Figure 4.1B). A shortlist of 8 high-confidence candidate miRNAs for further evaluation in our HepG2 *in vitro* model, were identified. This functionally informed list of differentially expressed miRNAs is summarized in Figure 4.1 C (This table is summarised from the tables presented in Appendix III and IV).



C **Differentially expressed miRNAs between pre versus post operation**

miRNA ID	Fold-Change(post-GBP vs. pre-GBP)	Type of surgery	Functions	References
hsa-miR-27b-3p	-2.965	GBP	Adipogenesis & insulin secretion	(241)
hsa-miR-29a-3p	-5.912	GBP	Diabetes & insulin sensitivity	(244)
hsa-miR-17-3p	-4.035	GBP	Fasting plasma glucose & circulating adiponectin	(239)
hsa-miR-335-5p	-2.497	GBP	Adipogenesis	(235)
hsa-miR-192-5p	-4.801	GBP	Glucose-stimulated insulin secretion	(325)
hsa-miR-4532	6.198	GBP	—	—
hsa-miR-99a-5p	-3.005	GBP	Fatty acid metabolism, cholesterol biogenesis	(239)
hsa-miR-148b-3p	-4.555	GBP	Adipocytes differentiation	(237)

Figure 4.1 Hierarchical clustering heat map

Pre/post-operation miRNA expression level in (A) gastric bypass surgery (GBP) and (B) sleeve gastrectomy (SG) patients where blue indicates down-regulated, whereas yellow indicates up-regulated. C) List of differentially expressed miRNAs associated with the obesity-related disorders. MiR-4532 was chosen due to its highest overexpression after surgery.

4.5.3 Fatty acids induced hepatokines expression in HepG2 cells

Circulating FFAs from visceral fat stores can lead to hepatic fat accumulation which is associated with up-regulation of certain hepatokines including *FetA* which was also downregulated after GBP but not SG in subjects from similar cohort study (32). To investigate changes in expression of FFA-responsive hepatokines, we induced HepG2 cells with palmitate or oleate, and then assessed RNA level of candidate genes by real time qPCR. Peroxisome proliferator-activated receptor gamma (*PPAR* γ) is a nuclear receptor that is elevated in fatty liver and regulates hepatic TG homeostasis (326). We found that palmitate- and oleate-treated HepG2 increased *PPAR* γ expression by 3 fold ($P \leq 0.01$) and 5.7 fold ($P \leq 0.01$) respectively compared to untreated cells (control) (Figure 4.2A). In addition, palmitate and oleate stimulated the expression of acetyl-CoA carboxylase (*ACCI*) and glycerol-3-phosphate acyl transferase (*GPATI*) up to 2.1 fold ($P \leq 0.01$) and 1.8 fold ($P \leq 0.05$), respectively (Figure 4.2A). We also found that palmitate and oleate stimulated the expression of sterol regulatory element-binding protein 1c (*SREBP-1c*), by 2.6 fold ($P \leq 0.01$) compared to control (Figure 4.2A). *FetA* was overexpressed by about 2.6 fold ($P \leq 0.01$) in FFA-induced cells (Figure 4.2B) compared to controls. In contrast, *LECT2* was up-regulated by 2.9 fold ($P \leq 0.01$) after induction with palmitate, but not oleate (Figure 4.2B).

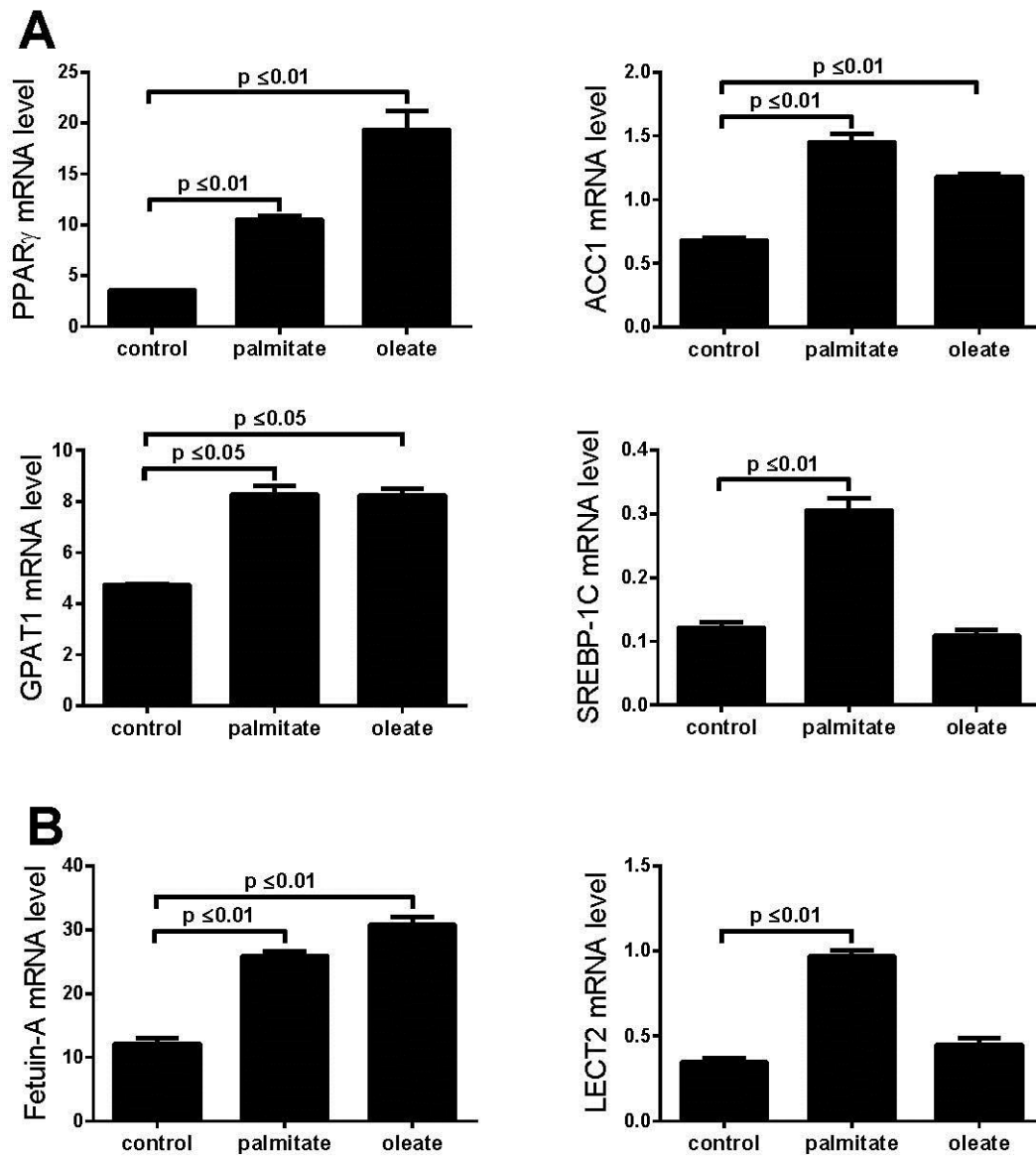


Figure 4.2 Fatty acids (FA) induction, regulated expression of lipogenesis enzymes and hepatokines

HepG2 cells were treated with either 250 μ M palmitate or oleate for 24 hours. A) Hepatic lipogenic enzymes and transcriptional factors were up-regulated after FAs supplementation. B) Hepatokines fetuin-A (*FetA*) and leukocyte cell-derived chemotaxin (*LECT2*) were overexpressed after FAs supplementation. After incubation, extracted RNA was applied for qPCR to determine mRNA expression. Values are presented as mean \pm SEM, (n=3).

4.5.4 Myostatin mediates the effects of free fatty acids on hepatokine Fetuin-A

Palmitate dramatically induced *MSTN* expression by 7.3 fold ($P \leq 0.05$) within 24 hours of treatment relative to controls (Figure 4.3A). Knockdown efficiency of 75% was achieved ($P \leq 0.01$) compared to control (Figure 4.3B). We found that *MSTN* knockdown reduced endogenous *FetA* expression by 2.9 fold ($P \leq 0.01$), and 5.5 fold ($P \leq 0.01$) in FFA-induced HepG2 cells (Figure 4.3C). In contrast, after *MSTN* knockdown, endogenous *LECT2*, *GPAT1* and *SREBP-1c* expression was decreased by 2.3, 1.7 and 2 fold, respectively ($P \leq 0.05$) while up-regulated following palmitate treatment (3.8 fold; $P \leq 0.01$) suggesting that feedback mechanisms may influence these genes expression. However, *MSTN* would appear to regulate only specific elements of FFA-dependent gene expression as there was no change in the level of either control or FFA-induced *ACCI* expression after *MSTN* knockdown (Figure 4.3C).

Following *MSTN* knockdown, phosphorylation of AMPK at Thr172 site (pAMPK) was reduced by 3.2 fold ($P \leq 0.05$) in control cells and pAMPK remained relatively unchanged in FFA-treated compared to control cells (Figure 4.3C). We also found that *MSTN* knockdown significantly reduced the phosphorylation of mTOR at Ser2448 site (pmTOR) by 2.2 fold ($P \leq 0.05$) in controls and similarly, by 2.6 fold ($P \leq 0.01$) in FFA-induced HepG2 cells (Figure 4.3C).

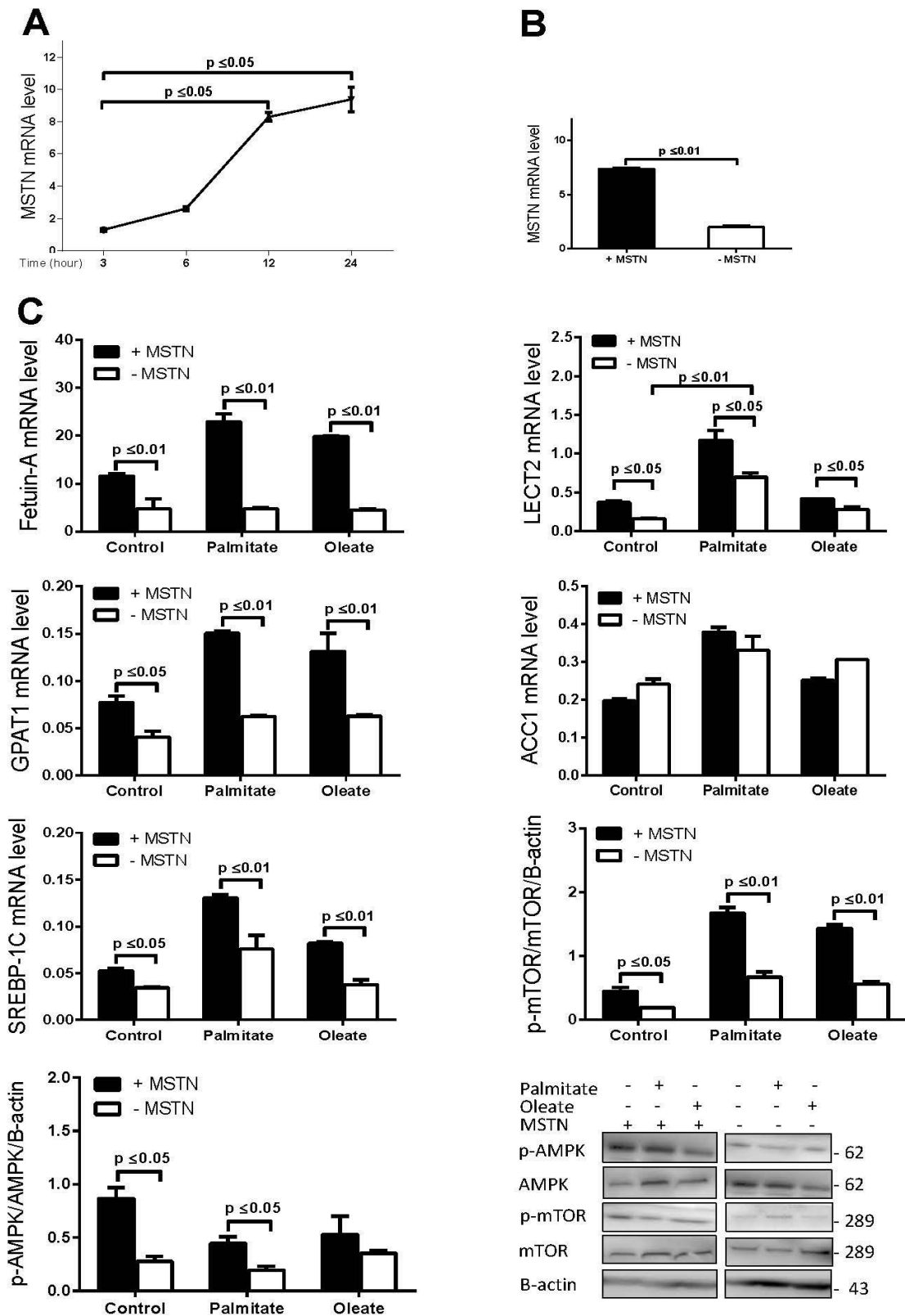


Figure 4.3 Myostatin (MSTN) regulated fatty acids-overexpressed genes

A) MSTN was up-regulated by palmitate. B) MSTN was knockdown in HepG2 cells using siRNA. C) The expression of fatty acids- induced genes was determined in the presence and absence of MSTN. Phosphorylation of mTORC1 and AMPK was measured after fatty acids induction in the presence and absence of MSTN. The samples derive from the same experiment and gels/blots were processed in parallel. Values are presented as mean \pm SEM, (n =3).

To confirm that *FetA* expression decreases in parallel with pAMPK reduction following MSTN knockdown, we further measured pAMPK, pmTOR and *FetA* expression after palmitate induction over a 24 hour time-course (Figure 4.4A). Whilst we found pAMPK levels remained relatively unchanged, pmTOR level increased by 1.9 fold ($P \leq 0.01$), to maximal levels by 6 hours of palmitate treatment relative to the 3-hour treatment (Figure 4.4A). Likewise, *FetA* expression increased by 2.1 fold ($P \leq 0.05$) by 6 hours, and 3 fold ($P \leq 0.05$) by 12 hours of palmitate treatment compared to the 3-hour treatment (Figure 4.4A). The similar temporal expression patterns suggested that activation of mTOR might be necessary for palmitate-induction of *FetA*. We used a pharmacological approach to test these further, treating cells with the selective inhibitor rapamycin prior to palmitate induction. We assayed the effect of different doses of rapamycin (0, 5, 10 and 25 nM) on mTOR phosphorylation and 10 nM of rapamycin for 12 hours was shown as an efficient dose to inhibit mTORC1 phosphorylation. We found no difference in pmTOR level following a 3-hour treatment of 10 nM rapamycin. However, pmTOR activity was decreased significantly and maximally by 1.5 fold ($P \leq 0.05$) following 12 hours of 10 nM rapamycin treatment (Figure 4.4B). After first suppression of MSTN by siRNA, we found that palmitate-induced *FetA* expression was decreased by 3 fold ($P \leq 0.01$), irrespective of pharmacological inhibition of pmTOR (Figure 4.4C). Notably, MSTN inhibition reduced pmTOR (2 fold; $P \leq 0.05$) (Figure 4.4C).

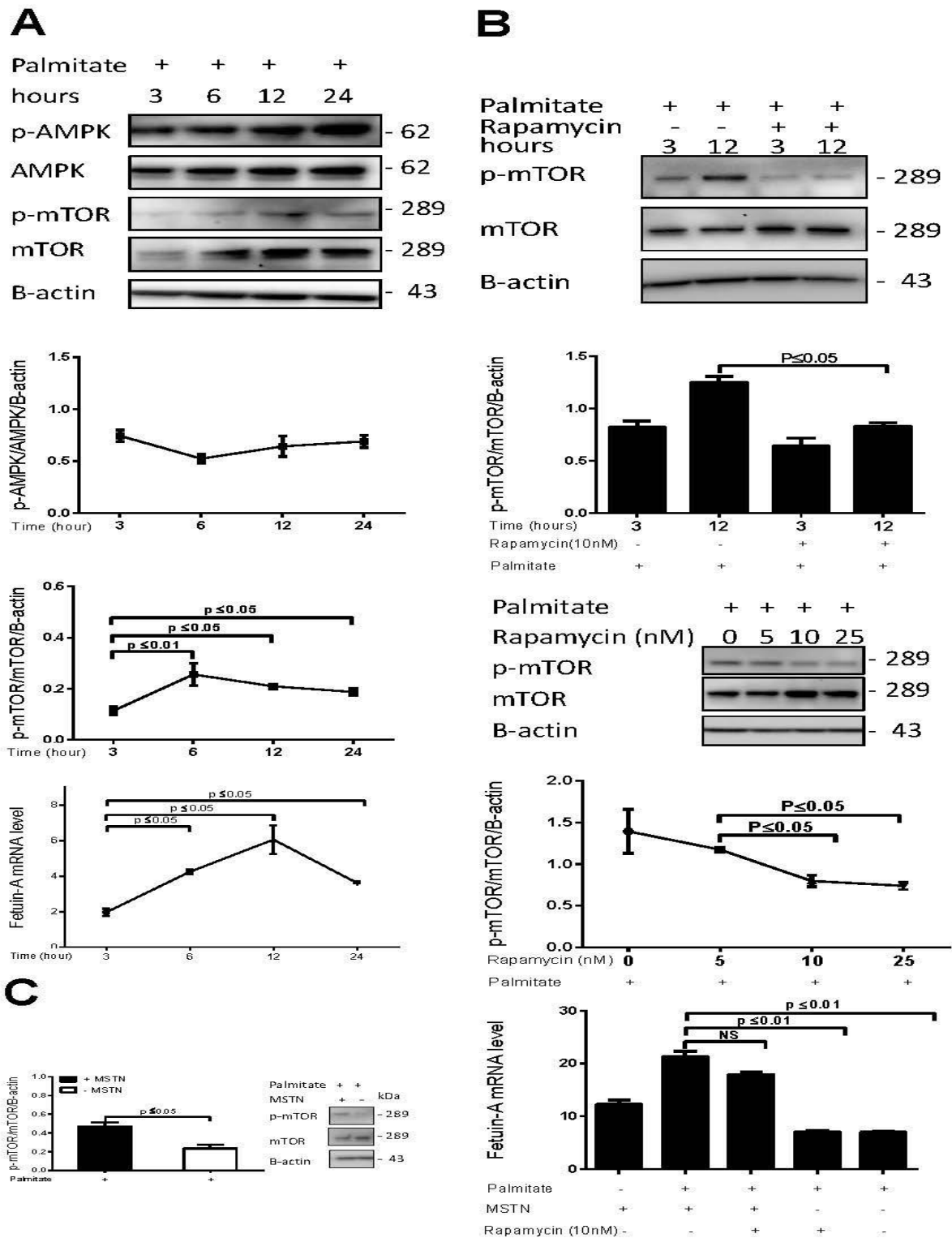


Figure 4.4 Mechanisms of fetuin-A (FetA) regulation by palmitate

A) Effect of palmitate on phosphorylation of AMP-kinase (AMPK), mammalian target of rapamycin (mTOR) and *FetA* expression. HepG2 cells were treated with 250 μ M palmitate over 24 hours. After incubation, the cell extracts were subject to Western blot analysis to determine AMPK and mTORC1 phosphorylation. B) Comparing effect of pmTOR with MSTN on *FetA* expression. HepG2 cells were treated or not with 250 μ M palmitate and 0, 5, 10 and 25 nM doses of rapamycin for 12 hours. C) MSTN expression, mTOR phosphorylation and *FetA* expression in mTOR/MSTN-inhibited HepG2 cells. After incubation, extracted RNA and cells were applied for qPCR and Western blot, respectively. The samples derived from the same experiment and gels/blots were processed in parallel. Values are presented as mean \pm SEM, (n =3).

4.5.5 MicroRNAs may play a role in the regulation of myostatin in the presence of palmitate

To determine the possible role of obesity-related miRNAs in regulating the hepatokines of interest, we first confirmed the expression of our 8 candidate plasma miRNAs after FFA exposure using our *in vitro* hepatic model. Expression of 4 miRNAs, miR-27b miR-29a, miR-192 and miR-335, was increased by 3 fold ($P \leq 0.05$) after palmitate treatment relative to untreated cells, but was unchanged after oleate treatment (Figure 4.5A). In contrast, expression of miR-99a was reduced by 3 fold ($P \leq 0.05$) after palmitate treatment relative to untreated cells, and a similar response was seen with oleate treatment (Figure 4.5A). MiR-4532 was increased by 1.7 fold ($P \leq 0.05$) after palmitate stimulation only relative to untreated controls. No change in the expression of either miR-17 or miR-148b was observed in HepG2 cells supplemented with FFAs palmitate and oleate. Our finding that miR-27b, miR-29a, miR-192 and miR-335 were inducible with palmitate is consistent with our results of these miRNAs reduced circulating levels in the post-GBP plasma.

We then investigated the effect of miR-27b, miR-29a, miR-192 and miR-335 suppression on *MSTN* and *FetA* mRNA abundance in the presence of palmitate, only. Among these, miR-335 exhibited the best alignment with *MSTN* and *FetA* following its inhibition in the presence of palmitate. We found that with suppression of miR-335 in our *in vitro* model, palmitate was not able to stimulate either *MSTN* or *FetA* expression (Figure 4.5B). This data are parsimonious with the finding that miR-335 is over expressed in obese subjects before GBP surgery and suggests that this miRNA enables to regulate *FetA* by palmitate.

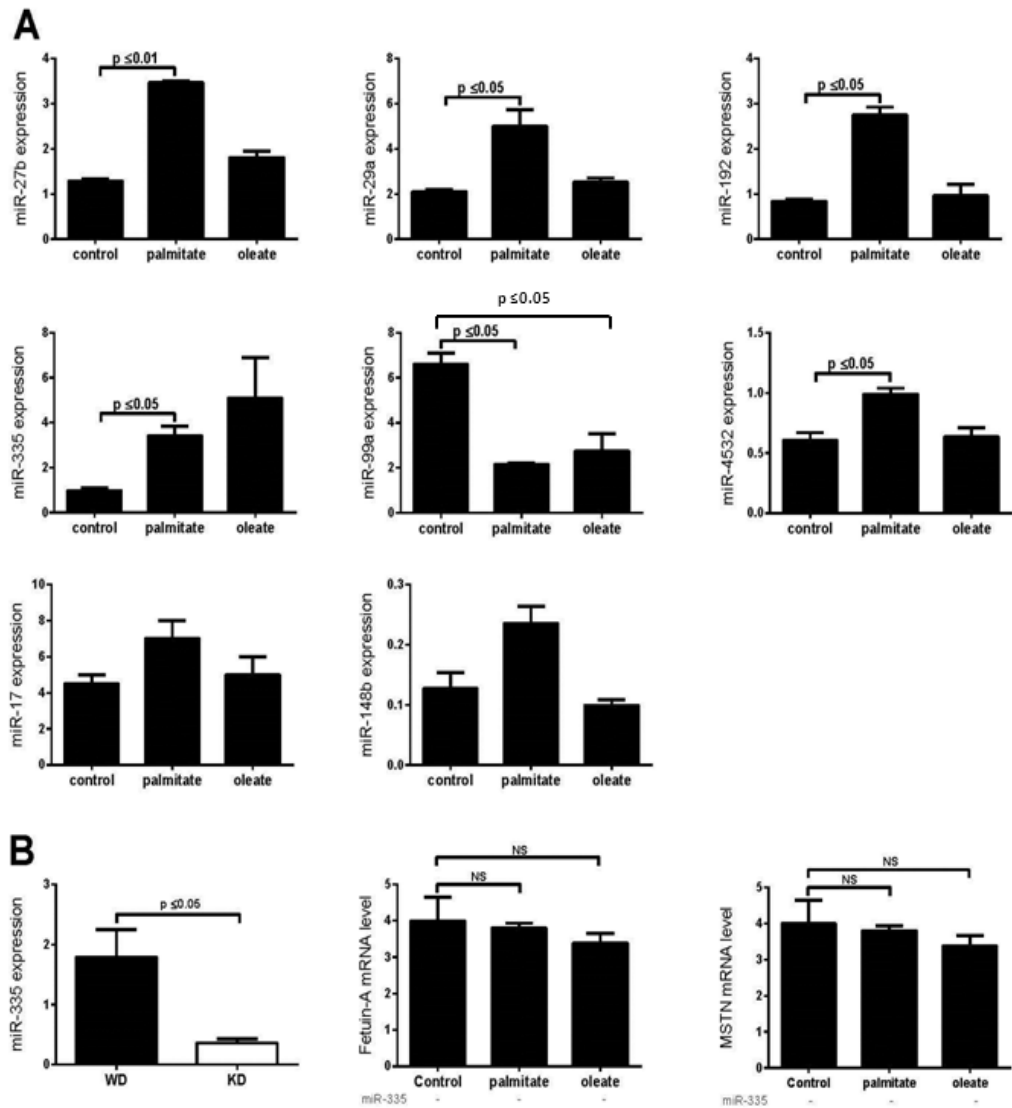


Figure 4.5 miRNA regulatory role on fatty acids (FA)-induced HepG2 cells

A) *In vitro* expression of candidate miRNAs after palmitate and oleate induction. HepG2 cells were treated with 250 μ M of either palmitate or oleate for 24 hours. After incubation, extracted RNA was used for qPCR to determine expression of the eight candidate miRNAs. B) Regulatory effect of miR-335 on myostatin (MSTN). HepG2 cells were treated with 250 μ M of palmitate for 24 hours. MiR-335 was inhibited using selective siRNAs. Values are presented as mean \pm SEM, (n =3). Abbreviation: WD: wild; KD: knockdown; NS: non-significant.

4.5.6 BMI and HbA1c were correlated with microRNAs expression

Since both BMI and HbA1c were significantly ($P \leq 0.05$) decreased after both types of surgery (Table 4.3), we looked for possible correlation with miRNAs that overexpressed in both plasma and FFA-induced hepatocytes (Table 4.4). Only after GBP surgery, expression of the miRNAs miR-335, miR-27 and miR-29 was well correlated with BMI ($P \leq 0.05$). Also post-GBP, both miR-29 and miR-192 were highly correlated with HbA1c concentration and expression of these miRNAs was also reduced ($P \leq 0.05$) in parallel with the decrease in HbA1c after surgery (Table 4.4). However, we found no correlation between either of these clinical measures and miRNAs expression, before or after SG surgery. Notably, in SG cases the pre-operative miRNA appears to have greater variance than the post-operative miRNA levels (Table 4.4).

In contrast, a Kolmogorov–Smirnov statistical test showed that the frequency distribution of miRNA expression in the pre-GBP surgery cases was significantly ($P \leq 0.05$) different to the frequency distribution post-GBP surgery. The frequency distributions we observed were clearly skewed and after a logarithmic transformation of the miRNA data, an analysis of variance of the miRNA levels pre and post-GBP showed that the mean miRNA level post-GBP was significantly ($P \leq 0.01$) less than the pre-GBP miRNA levels, but the residuals were not significantly different from normal, as assessed by a Shapiro–Wilk test.

Table 4.4 Correlation analysis between certain miRNA expression and BMI/HbA1c

	Pre-GBP	BMI	HbA1c	Post-GBP	BMI	HbA1c
hsa-miR-27b-3p	r	-0.503	0.035	r	0.986	0.920
	<i>P</i> value	0.497	0.965	<i>P</i> value	0.014*	0.080
hsa-miR-29a-3p	r	0.153	-0.748	r	0.952	0.992
	<i>P</i> value	0.847	0.252	<i>P</i> value	0.048*	0.008**
hsa-miR-335-5p	r	-0.475	-0.167	r	0.901*	0.905
	<i>P</i> value	0.525	0.833	<i>P</i> value	0.049	0.095
hsa-miR-192-5p	r	-0.07	-0.541	r	0.852	0.987
	<i>P</i> value	0.930	0.459	<i>P</i> value	0.148	0.013*
	Pre-SG			Post-SG		
hsa-miR-27b-3p	r	0.202	-0.722	r	0.208	0.107
	<i>P</i> value	0.744	0.169	<i>P</i> value	0.737	0.864
hsa-miR-29a-3p	r	0.259	-0.370	r	0.324	-0.156
	<i>P</i> value	0.673	0.539	<i>P</i> value	0.594	0.803
hsa-miR-335-5p	r	-0.135	-0.761	r	-0.527	0.665
	<i>P</i> value	0.829	0.135	<i>P</i> value	0.361	0.221
hsa-miR-192-5p	r	0.488	-0.204	r	0.863	-0.489
	<i>P</i> value	0.404	0.742	<i>P</i> value	0.060	0.403

Pearson correlation was performed with a two-tailed significance. r, correlation coefficient; * $P \leq 0.05$; ** $P \leq 0.01$. Abbreviations: BMI: body mass index; HbA1c: Glycolytic hemoglobin.

4.6 Discussion

The post-operative success in maintaining remission of obesity and T2DM varies significantly depending upon the type of bariatric surgery, suggesting different metabolic shifts may occur with each surgical strategy. Currently it is difficult to accurately assess the likely efficacy of different approaches to bariatric surgery, given the present knowledge of these shifts. In this context, one metabolic feature which may be of particular relevance is the secretion of hepatokines, which affect glucose metabolism and promote obesity induction (133, 146), and are reported to decrease significantly following GBP (32, 166). Pre-operative subjects with high serum levels of the hepatokine *FetA* have an increased risk of clinical outcomes such diabetes (169), stroke (327) and obesity related disorders such as NAFLD (328). *Fetuin-A* is known to inhibit insulin-stimulated phosphorylation of the insulin receptor and the insulin substrate-1 protein, in both liver and skeletal muscles (149). Further, it may serve as an adaptor protein for saturated FFAs enabling them to activate Toll-like receptor 4, leading to inflammatory signalling and IR (328). Similarly, serum levels of *LECT2* are also elevated in subjects with fatty liver and obesity (144), and again its secretion is believed to link obesity with IR in skeletal muscles (145). Our findings confirm the stimulation of hepatic *FetA* and *LECT2* expression by palmitate and oleate, the most abundant saturated and mono-unsaturated FAs respectively in human fat depots and diet (329).

Although long appreciated for its impact on whole body metabolism and in determination of muscle mass, *MSTN* has more recently been linked to glucose and lipid homeostasis (194, 330). However, its precise function remains somewhat enigmatic. While a loss-of-function *MSTN* mutation enhances glucose tolerance and protection against IR in mice maintained on a HFD (181), the restoration of its function with recombinant protein in *MSTN* mutant mice fed a HFD, paradoxically led to greater IR (209). Further, *MSTN* depletion with a ‘floxed’ *MSTN* gene construct caused hepatic steatosis and fat accumulation in muscles of HFD fed mice (215), yet inactivation of *MSTN* inhibitory genes leads to increasing *MSTN* activity, and greater hepatic steatosis and hypertension in mice (212).

AMPK is a central metabolic switch influenced by MSTN activity that regulates glucose and lipid metabolism in response to nutrients (181). A decrease in the AMP:ATP ratio leads to AMP binding to the γ subunit and thus increased phosphorylation and activation of pAMPK, which in turn directly phosphorylates tuberous sclerosis complex 2 (TSC2) to promote the conversion of Rheb-GTP to Rheb-GDP. In this way, catabolic pathways are directed towards ATP generation (331). A consequence of these shifts is the inhibition of phosphor-mTOR (332). The functionally related serine/threonine protein kinase mTOR belongs to the phosphoinositide-3-kinase-related kinase group and governs cellular homeostasis by synergizing anabolic and catabolic processes with nutrient and energy signalling (332). pmTOR acts as a scaffold to recruit a complex of downstream substrates, including ribosomal S6 kinase beta 1 (p70S6K1), which regulate mRNA translation and whose activity is acutely inhibited by the drug rapamycin (333). While FFAs such as palmitate have recently been shown to promote translation via recruiting mTOR onto the lysosomal surface (334, 335), it has also been suggested that pAMPK activation can suppress palmitate-induced hepatic *FetA* expression (332, 336). We found that while pmTOR and *FetA* were both induced by palmitate stimulation, pAMPK levels decreased and subsequently remained suppressed even as *FetA* continued to increase with time. Additional experiments with rapamycin confirmed that the palmitate induction of hepatic *FetA* is not a consequence of the FFA effect on translation, but rather is a result of MSTN activity acting to suppress AMPK function and to drive the process of transcription.

We have shown that distinct miRNAs present in serum pre-operatively in patients with morbid obesity and T2DM are associated with weight and glycemia achieved 1 year after GBP surgery. MiRNAs are known to regulate expression of genes at the post-transcriptional level, via either degradation of target mRNA or inhibitory translation (337, 338), and are suggested as putatively valuable biomarkers given their tissue specific expression and association with clinic-pathologic variables (339). The up-regulation of numerous miRNAs is associated with obesity in mice fed HFD (238) and hepatic lipid content in humans (340, 341). In this pilot study, we have observed differences in the expression of a particular set

of circulating miRNAs following surgery, although these were only significant with GBP. To further validate the potential relevance of these changes, we correlated expression of these miRNA species with clinically recognized measurements BMI and HbA1c. Although obesity is associated with an increase in impaired glucose tolerance (revealed by IGTT), dyslipidemia and diabetes (342), fasting blood glucose measures are often not diagnostically accurate, as many subjects with abnormal glucose tolerance often record normal range IGTT values (343, 344). An increasingly used alternative for assessment of pre-diabetic and T2DM status is measurement of serum HbA1c, the levels of which seem to more accurately reflect longer term glucose control and appear to be less biologically variable (342). Notably, expression of miR-29 showed a positive correlation with both BMI and HbA1c levels post-GBP, while miR-27 (for BMI), miR-335 (for BMI) and miR-192 (for HbA1c) were also strongly correlated after GBP surgery. We did not see any evidence of correlation between miRNA expression level and metabolic status either pre- or post-SG bariatric surgery. Moreover, we also found miR-335 to be a determinant of elevated MSTN and *FetA* expression suggesting that the pathological secretion of hepatokines is regulated in significant measure through miRNA and the major regulatory role of liver however we have no evidence of plasma miRNAs tissue of origin in this study. Consistent with this, the up-regulation of miR-335 has previously been linked with both increased hepatic TG content and adipose tissue lipid metabolism in genetically obese mice (235), and with human adipocyte differentiation (345). Most importantly, we found that miR-335 expression is critical for the ability of palmitate and oleate to stimulate hepatokine *FetA* expression (and its upstream regulator MSTN) arguing for an important role in underpinning the pathogenic changes associated with disease progression in metabolic syndrome.

In summary, we demonstrate a role for miR-335 in hepatokine *FetA* regulation (that was overexpressed through FFA induction in hepatocytes), which recent studies suggest is significantly reduced following GBP bariatric surgery in obese patients. Further, we suggest miR-335 activity may be a key to shifts in metabolic state, specifically affecting the MSTN-dependent regulation of physiologically significant targets such as *FetA*. Finally, we present pilot data suggesting that a distinct set of miRNAs

(including miR-335) are differentially expressed pre- and post-GBP surgery in serum of patients presenting with morbid obesity and T2DM, and are strongly correlated with BMI and HbA1c levels in these subjects.

MiRNA expressions were more sustained in GBP compared with SG also clustering before and after surgery were clearer only after GBP. In addition, specific miRNAs were positively correlated with patients body weight and blood glucose levels. Our data suggests that miRNAs can be used as biomarkers to track changes and efficacy of at least GBP surgery.

4.7 Acknowledgements

AZ is supported by a Univ. of Auckland Doctoral Scholarship and the Liggins institute Doctoral Scholarship Fund. The funders played no role in the conception or design of this study, data collection and analysis, decision to publish, or preparation of this manuscript. There are no potential conflicts of interest relevant to this article.

4.8 Conflict of interests

The authors declare that they have no conflict of interests.

4.9 Abstract for oral presentation based on this study

This study was presented in the “Annual Scientific Meeting of Australian & New Zealand Obesity Society, ANZOS” Melbourne, 15th- 17th October, 2015. The following is the abstract’s appearance in the handbook (<http://www.anzos2015.org/framework/main.php?url=/>).

Micro RNAs as biomarkers of bariatric surgery outcome and putative regulators of hepatokines selectively after gastric bypass, but not sleeve gastrectomy

Aida Zarfeshani¹, Sherry Ngo¹, Rinki Murphy², Allan Sheppard¹

1. Liggins Institute, Univ. of Auckland, Auckland, New Zealand

2. Department of Medicine, The University of Auckland, Auckland, New Zealand

Background: The prevalence of chronic obesity is increasing worldwide, resulting in more intervention with bariatric surgeries being performed each year. However, the variable success of surgical approaches in treating obesity and its co-morbidities varies between individuals and by the type of surgery, and is not readily explained by baseline clinical features. A better understanding is needed of the metabolic shifts, and their underpinning mechanisms, which result from different types of bariatric surgery. From this a better knowledge should emerge of biomarkers and causal pathways driving the development of obesity and its comorbidities.

Methods: We investigated the effects of bariatric surgery on miRNA profile before and after of either gastric bypass surgery (GBP) or sleeve gastrectomy (SG) in nine obese patients with T2DM. Recent work has identified an early reduction in post-operative circulating levels of the hepatokine fetuin-A (FetA) after GBP but not SG, as a putative candidate to monitor the efficacy of intervention. Therefore, we used FFA-induced HepG2 cells to indicate the underlying mechanism these miRNAs could lead to increased level of FetA.

Results: Here we extend these observations, and in plasma samples defined a specific set of miRNAs whose post-surgery expression among GBP patients correlated strongly with beneficial decreases in BMI and blood glucose (HbA1c) levels, demonstrated that particular miRNAs mediate signaling pathways that regulate *FetA* expression. Additionally, we reported that expression of both *FetA* and leukocyte cell-derived chemotaxin2 (*LECT2*; another major hepatokine) was dependent on intracellular signaling by metabolic regulator myostatin (MSTN). Finally, we linked the activity of a key miRNA in particular to FFA induced, MSTN-dependent regulation of *FetA*.

Conclusions: These data provide novel mechanistic insights into the metabolic stimulation of hepatokine expression, and the epigenetics role in mediating hepatocellular changes associated with greater weight loss and diabetes remission observed with GBP rather than SG.

5 GENERAL DISCUSSION AND CONCLUSION

The alarming upward trajectory in the incidence of obesity worldwide has been described as a non-communicable disease epidemic. The health costs are manifold as obesity underpins a raised BMI, a major risk factor for the development of IR, T2DM, cardiovascular diseases and some cancers. The path to obesity is somewhat insidious and often results from energy intake consistently surpassing energy expenditure over a persistent period. Attempts to identify singularly specific dietary components responsible for promoting the development of obesity have been inconclusive, although it is generally accepted that the collective dietary composition can influence body weight independently of total calorie intake. However, there is accumulating evidence that the excessive intake of particular classes of micronutrients, notably BCAAs and FFAs are associated with body weight gain and may contribute to metabolic syndrome as a consequence of disturbed metabolic homeostasis. Clinical studies of obese individuals indicate that increased plasma levels of BCAA promote the production of insulin by pancreatic β -cells, which would facilitate IR and metabolic syndrome. Elevated BCAAs may thus be sentinels of obesity risk driven by either protein-rich diets or obese phenotype microbiota signatures. Similarly, excess intake of FFAs is implicated as a strong driver of obesity, metabolic syndrome and sequela such as NAFLD, the emergence of which as the most common liver disease worldwide parallels the obesity epidemic. The prevalence of NAFLD is in part due to the increasing numbers of obese or overweight adults, but more critically because of increased pediatric presentation of metabolic syndrome and T2DM, which are known major risk factors for development of NAFLD. It is generally reported that NAFLD is strongly associated with IR in peripheral tissues, which in turn leads to increased FFAs in the circulation and further perpetuation and progression of the metabolic syndrome.

The work described herein is predicated on the assumption that liver tissue is the central mediator of systemic metabolism and critical for maintaining metabolic homeostasis. As such, it is assumed that changes in liver biology will be the key to understanding the systemic effects of excess and inappropriate dietary inputs. Much of what is presented is the result of exploration using the well

characterized human hepatic cell line HepG2 as an *in vitro* platform. HepG2 cells have been shown to faithfully recapitulate most of the cellular features of normal human hepatocytes, including the expression of liver-specific proteins (346), as well as normal TG, cholesterol and bile acids biosynthesis/transport systems (347). Although primary cell cultures would retain many of the parental *in vivo* characteristics, their use is very much restricted by their limited availability, short *ex vivo* lifespan and variations in donor genotype, strain, breed and age. An initial exploration of the potential clinical relevance for some of the findings arising from these *in vitro* studies is also reported here.

A considerable body of work links BCAAs, and leu in particular, with physiological and metabolic effects, although many of the reported findings appear somewhat contradictory. Notably, leu stimulates secretion of insulin from β -cells, not only as metabolic fuel but also as an allosteric activator of glutamate dehydrogenase, leading to closure of K_{ATP} channels and consequent β -cells dysfunction and IR (348, 349). Excessive levels of leu have been linked to the promotion of IR, in HFD obesity-induced rats for example (49). Yet, other studies suggest that leu supplementation in HFD obesity-induced mice leads to weight loss, through reduced adiposity and enhanced resting energy expenditure, while having no obvious metabolic effect in mice on normal chow (268). These beneficial effects are correlated with improved glucose tolerance and insulin signaling, and decreased hepatic steatosis (28). In the clinical setting circulating leu levels are again contra-indicative, with an excess correlating to the development of obesity-related IR (49) and the prediction of future T2DM after 12 years (350), while other findings suggest that BCAAs supplementation may be a useful therapeutic approach for reduction of IR that is associated with chronic liver disease (351). A major outcome of the current work is to propose a plausible resolution to these somewhat paradoxical observations. The empirical *in vitro* data presented herein, suggests that although leu may initially be 'beneficial' for metabolic homeostasis (as it promotes hepatic glucose uptake), if the leu stimulus is persistent it may have the unintended effect of driving storage of excessive glucose and consequential lipid accumulation in liver cells, chronic exposure to elevated

leu thus promoting intracellular fat deposition on longer time scales. In this notion is accurate, the metabolic response to excessive dietary intake of specific nutrients such as leu might be better understood in terms of an adaptive response to a nutritional challenge. Implicit within this conceptual framework is the notion of a deleterious ‘trade-off’, such that necessary shorter term beneficial outcomes are realized but at the expense of a longer-term deferred cost. Although the concept of adaptive responses is frequently applied when explaining observations in evolutionary and development biology, its potential relevance to understanding shifts in physiological function that contributor to disease progression is still relatively untested experimentally.

A further outcome of the current work is to focus greater attention on MSTN as a putative and central metabolic regulator and its potential role in the etiology of metabolic syndrome. Although a growing literature substantiates elevated MSTN with the progression of obesity and T2DM, for the mechanisms of MSTN dysregulation and the consequences thereof, remain to be defined. Firstly, the current work links excessive leu as a potential trigger of hepatic MSTN expression leading to AMPK activity, thus providing further context to reports that MSTN inhibition attenuates the expression of glucose/lipid sensing in hepatocytes, and that MSTN can regulate glucose metabolism in rodent skeletal muscle (211, 289). Secondly, MSTN is also shown to mediate the expression of the principal hepatokines *FetA* and *LECT2* in response to FFA supplementation. The observed recurrence of MSTN-dependent signaling, triggered by two of the major micronutrient components repeatedly associated with excessive intake in Western style diets, suggests that interventional targeting of this seemingly integrative downstream pathway would be valuable, even in the absence of precise detailed knowledge of dietary compositions in metabolic syndrome.

The current work also draws attention to the role of epigenetic mechanisms in the regulation of these micronutrient induced shifts in metabolic status, particularly for that of miRNAs. Changes in gene expression underlining environmental induced phenotypic alterations often occur on time scales which preclude direct modifications in DNA sequence as being causative in their realization.

Epigenetics offers an obvious alternative conceptual and mechanistic framework for defining the etiology of those disease processes for which a genetic-environment interaction is not evident. Of the recognized epigenetic mechanisms, the importance of miRNA regulatory pathways would seem most relevant to disease progression, both as useful biomarkers of change and as facilitators of systemic responses to the disease challenge. Evidence of miRNA regulation is reported here for both leu stimulated key glucose/lipid sensing genes (including MSTN), and FFA (palmitate) induced MSTN dependent hepatokine induction. The implication of these findings is that abrogation of metabolic syndrome and associated disorders, such as NAFLD, may be possible by attenuating the primary miRNA based signalling which initiates key effector pathways. The practicalities of such approaches are already being actively explored for applications in the treatment of cancers and neurological syndromes.

As an initial step to translating these experimental findings to a clinical setting, an exploratory study in the biologically relevant setting of chronic obesity treatment by bariatric surgery is also reported here. On the premise that epigenetic mechanism are indeed key, the initial aim of this study was to align a set of miRNAs whose expression was associated with the reversal of obesity and associated hepatokine expression, and improved metabolic status, following clinical intervention with those candidates arising from the prior *in vitro* studies. Indeed, a subset of miRNAs was identified which seem to ‘translate’ to this clinical setting. Notably, a strong positive correlation was seen between the expression of miR-335, miR-29a, miR-27b and miR-192 with significant reductions in BMI, HbA1c, or bot but only after bariatric surgery based on the GBP protocol. This group of candidate miRNAs includes those implicated in the experimentally induced effects of excessive dietary intake on hepatic metabolism described above, and in particular, illuminates miR-335 has a potentially pivotal species in the etiology of metabolic syndrome. The clinical measurement of changes in miR-355 expression in plasma samples (pre and post surgery) and the demonstration of functional importance in hepatic cells *in vitro*, and the likely mechanistic and functional commonalities in both scenarios, strongly implies that this species may be archetypal of a hepatic derived and exosomally transported regulator

of systemic change is response to disease challenge.

The very encouraging findings made with just this pilot clinical study strongly encourages a larger investigation, so that potential confounders can be assessed, and the value of miRNAs as pre-operative biomarkers of obesity (and associated risk) and the causality of miRNA function in disease can be further tested. An obvious confounder in the current pilot study was the drug treatment; metformin, which is common among diabetic patients and taken post-operatively by one-third of the current subjects assessed (subjects were using metformin post-op). A larger sample size should establish whether drug treatment and other possible covariables are in of themselves significantly altering epigenetic profiles. In addition, comparison to an appropriate healthy control group might be instructive for confirming that miRNA expression is indeed a pathologically driven change, although the clinically relevant features of such a comparative control group are not easily defined. Bariatric surgery is considered a last resort intervention for chronically obese subjects who have failed to respond to other therapeutics approaches, such as dietary, drug and lifestyle changes. As such, they constitute an 'extreme' group that would be seemingly difficult to match with 'healthy' controls was challenging in this study. My patients underwent a bariatric surgery and reached either overweight or class I obese BMI after surgery rather than normal. The subjects were selective as they were not responsive to other methods of weight loss such as diet and exercise.

In summary, the work presented here highlights the potential importance of MSTN dependent signaling and the importance of epigenetic regulation in the manifestation of metabolic syndrome (and associated clinical features) in response to 'sub-optimal nutrition', defined in the current studies as an excessive dietary intake of physiologically notable micronutrients. The initial success in extending the experimental findings to a clinical setting in a small pilot study only encourages the view that these pathways and regulatory mechanisms should be explored more fully, as potential biomarkers of risk assessment and as possible targets for intervention.

5.1 Future Directions

5.1.1 Does MSTN levels serve as a biomarker for the beginning of the NAFLD

As shown in Chapters 3 and 4, the preliminary results point out that hepatic MSTN expression is not only elevated but also is responsible for regulation of lipid sensing genes in poor nutrition conditions such as high protein/fat diet. In order to completely validate MSTN as a biomarker for NAFLD, we need to test large numbers of its circulating level in well phenotyped individuals recognised by fatty liver. For example, by using ELISA for MSTN, it would be possible to establish a positive correlation between MSTN levels and NAFLD.

5.1.2 Does MSTN/MSTN regulatory miRNAs drug targeting combat NAFLD

Myostatin plays major role in the development of obesity, IR and T2DM. Moreover, it is evident from my studies that MSTN inhibition could potentially protect against developing fatty liver and other metabolic risks consequently through hepatokines overexpression. Since MSTN regulates the whole body metabolic homeostasis, targeting MSTN is a sensible therapeutic strategy to prevent metabolic syndrome disorders. On the other hand, in my study I have particularly identified specific miRNA that targets MSTN. Taken together, developing MSTN inhibitors such as antibodies and propeptide also miRNA inhibitors to knockdown MSTN may offer new therapeutic strategy to combat different forms of NAFLD.

5.1.3 MiRNAs as diagnostic biomarkers for the efficiency of different types of bariatric surgery

In the second part of this thesis, I reported the difference in miRNAs profile and clustering following GBP and SG bariatric surgery whereby GBP offered more distinct miRNA clustering in pre-versus post-operation as well as yielding better degree of improvement in the attendant BMI and blood glucose level. Therefore, to be able to refer patients to a specific type of bariatric surgery based on individualised characteristics, profiling miRNA expressions in a large number of patients following

various types of this operation may lead to developing a standard guidance for candidate/procedure selection criteria.

5.1.4 Exosomes as leading biomarkers in miRNA studies

MiRNAs are packaged into exosomes or complexes with RNA-binding proteins. Circulating miRNAs are mediators of cell-cell communication and presumably targeted for export in one organ whereby recognized, imported and utilized by other tissues. It is now generally appreciated that exosomes and microvesicles are likely to be the primary source of circulating miRNAs and are released from a wide variety of cells and tissues as an indication of the functional/dysfunctional state of the originating organ. These properties lend themselves to the potential utility of circulating miRNAs as diagnostic and prognostic tools in NAFLD and other metabolic diseases.

5.1.5 Histone modification

Chromatin remodelling regulates gene expression through histones post-translational modifications that determines access of transcriptional regulators to the promoter region of target genes. It is proposed that under IR and diabetic conditions, the negative regulators such as histone methylation marks of repressed chromatin would be lost while positive regulators or activating histone marks including histone methylation and acetylation may be increased hence resulting to relaxation or opening of the chromatin structure around key pathological genes to enhance their transcription. However, the potential for BCAAs to enhance healthy outcomes via histone modifications has yet to be determined.

Appendices

Appendix I

1. MATERIALS

This section presents the relevant information on the basic materials used for this thesis.

1.1 Cell culture materials and reagents

Table 1 List of cell lines used in cell culture for this thesis

Chemical	Company
HepG2	ATCC, Manassas, VA -20108, USA.
C2C12 mouse myoblasts	ATCC, Manassas, VA -20108, USA.
PANC-1	ATCC, Manassas, VA -20108, USA.

Table 2 List of reagents used in cell culture for this thesis

Chemical	Catalogue Number	Company
Low-glucose Dulbecco's Modified Eagle Medium (DMEM)	11885-092	Invitrogen (Gibco) Carlsbad, USA
Glucose and phenol red-free DMEM	A 14430-01	Invitrogen (Gibco) Carlsbad, USA
DMEM/F-12	11320-033	Invitrogen (Gibco) Carlsbad, USA
High-glucose DMEM	11995-073	Invitrogen (Gibco) Carlsbad, USA
Fetal bovine serum	16000044	Life Technologies
Horse serum	16050122	Invitrogen (Gibco) Carlsbad, USA
0.25% Trypsin-Ethylenediaminetetraacetic acid (EDTA) (1X) 4Na, liquid	25200-056	Invitrogen (Gibco) Carlsbad, USA
0.05% Trypsin-EDTA (1X), phenol red	25300054	Invitrogen (Gibco) Carlsbad, USA

L-Glutamin	25030-081	Life Technologies
100X Insulin-Transferrin-Selenium (ITS -G)	41400-045	Invitrogen (Gibco) Carlsbad, USA

1.2 General chemical and reagents

Table 3 List of chemicals, reagents and kits used for this thesis

Chemical	Company
1 kb PLUS DNA ladder	Invitrogen, Carlsbad, NM, USA
2-[3H]-deoxy-D-glucose	PerkinElmer Life Sciences, Waltham, MA, USA.
2-Deoxy-D-glucose Grade III, $\geq 99\%$ (GC), crystalline	Sigma-Aldrich, St. Louis, MO, USA
2-propanol	Sigma-Aldrich, St. Louis, MO, USA
10X DPBS, no calcium, no magnesium	Invitrogen, Carlsbad, NM, USA
30% Acrylamide	Bio-Rad, CA, USA
Acetic acid	Sigma-Aldrich, St. Louis, MO, USA
Amplex® Red Glucose/Glucose Oxidase Assay Kit	Invitrogen, Carlsbad, NM, USA
Ammonium persulfate (APS)	Sigma-Aldrich, St. Louis, MO, USA
Beta-mercaptoethanol	Sigma-Aldrich, St. Louis, MO, USA
BLOCK-iT™ Alexa Fluor® Red Fluorescent Control	Invitrogen, Carlsbad, NM, USA
Bovine serum albumin (BSA)	Invitrogen, Carlsbad, NM, USA
Bromophenol blue	Sigma-Aldrich, St. Louis, MO, USA

BSA, Fatty acid free	Sigma-Aldrich, St. Louis, MO, USA
CaCl ₂	Scharlau, Barcelona, Spain
Chloroform	Sigma-Aldrich, St. Louis, MO, USA
Coomassie brilliant blue	Fluka, Buchs, Switzerland
CpGenome Universal Methylated DNA; (Human)	New England BioLabs, Germany
CpGenome Universal Unmethylated DNA; (Human)	New England BioLabs, Germany
Cytochalasin B 98% (HPLC), powder	Sigma-Aldrich, St. Louis, MO, USA
Dithiothreitol (DTT)	Sigma-Aldrich, St. Louis, MO, USA
DNA loading dye	Thermo Scientific, IL, USA
EDTA.Na ₂	Sigma-Aldrich, St. Louis, MO, USA
Enhanced chemiluminescence (ECL)	Thermo Fisher, MA, USA
Ethanol	Merck Chemicals, Darmstadt
EZ DNA methylation kit	Zymo Research, CA, USA
Glycogen assay kit	BioVision, CA, USA
HCl	Sigma-Aldrich, St. Louis, MO, USA
HEPES	Invitrogen, Carlsbad, NM, USA
HotStar Taq DNA Polymerase	Qiagen, Hilden, Germany
Insulin (Bovine)	Sigma-Aldrich, St. Louis, MO, USA
Insulin human enzyme-linked immunosorbent assay (ELISA) kit	Abcam, Cambridge, MA, USA
KCl	Sigma-Aldrich, St. Louis, MO, USA
King Fisher cell and tissue DNA kit	Thermo Fisher, MA, USA
Lipofectamine® RNAiMAX Transfection Reagent	Invitrogen, NY, USA
L-leucine (leu)	Sigma-Aldrich, St. Louis, MO, USA
MassCLEAVE T reagent kit	BioLab, GA, USA

Methanol	Merck Chemicals, Darmstadt
MgSO ₄	Sigma-Aldrich, St. Louis, MO, USA
miRNeasy serum/plasma kit	Qiagen, Hilden, Germany
miScript II RT Kit	Qiagen, Hilden, Germany
miScript SYBR Green polymerase chain reaction (PCR) kit	Qiagen, Hilden, Germany
NaCl	Sigma-Aldrich, St. Louis, MO, USA
Na ₂ HPO ₄	Sigma-Aldrich, St. Louis, MO, USA
NaF	Sigma-Aldrich, St. Louis, MO, USA
NaH ₂ PO ₄	Sigma-Aldrich, St. Louis, MO, USA
NaOH	Sigma-Aldrich, St. Louis, MO, USA
Na ₄ P ₂ O ₇	Sigma-Aldrich, St. Louis, MO, USA
Na ₃ VO ₄	Sigma-Aldrich, St. Louis, MO, USA
Opti-MEM® I Reduced Serum Medium	Invitrogen, NY, USA
Pierce BCA Protein Assay	ThermoScientific, IL, USA
polyvinylidene difluoride (PVDF)	Millipore, MA, USA
Precision Plus Protein™ Dual Xtra Standards	Bio-Rad, CA, USA
Protease Inhibitor Cocktail (PIC) for Mammalian Cell and Tissue Extracts, 1mL in DMSO	Sigma-Aldrich, St. Louis, MO, USA
PureLink® RNA Mini Kit	Life Technologies, Ambion, CA, USA
Rapamycin	Millipore, MA, USA
Shrimp alkaline phosphatase (SAP)	Sequenom, CA, USA
Skim milk powder	Pams, Auckland, New Zealand
Sodium dodecyl sulfate (SDS)	Scharlau, Barcelona, Spain
Sodium palmitate	Sigma-Aldrich, St. Louis, MO, USA
Sodium Pyruvate	Sigma-Aldrich, St. Louis, MO, USA

Sodium L-lactate	Sigma-Aldrich, St. Louis, MO, USA
Sodium Oleate	Sigma-Aldrich, St. Louis, MO, USA
SpectroCHIP II Array and Clean Resin Kit	Thermo Fisher, MA, USA
SYBR Safe DNA gel stain	Invitrogen, Carlsbad, USA
SYBR Green I Master	Roche, Mannheim, Germany
TEMED	Sigma-Aldrich, St. Louis, MO, USA
Tergitol Type NP-40	Sigma-Aldrich, St. Louis, MO, USA
Transcriptor First Strand cDNA synthesis kit	Invitrogen, Carlsbad, USA
Triglyceride quantification kit	BioVision, CA, USA
TRIS Base	SERVA, Heidelberg, Germany
Triton® X-100	Sigma-Aldrich, St. Louis, MO, USA
TRIZOL reagent	Invitrogen, Carlsbad, USA
TWEEN® 20	Sigma-Aldrich, St. Louis, MO, USA
Ultima Gold	PerkinElmer, MA, USA
Ultrapure agarose	Invitrogen, Carlsbad, USA
UltraPure™ DNA Typing Grade® 50X Tris-acetate-EDTA (TAE) Buffer	Invitrogen, Carlsbad, USA
UltraPure™ DNase/RNase-Free Distilled Water	Invitrogen, Carlsbad, USA
UltraPure™ Glycerol	Invitrogen, Carlsbad, USA
Vybrant MTT Cell Proliferation Assay Kit	Life Technologies, Molecular Probes, CA, USA
X-Ray films	AGFA, Mortsels, Belgium

1.3 Reverse transfections

Table 4 List of reagents used for reverse transcription

Chemical	Company
Opti-MEM® I Reduced Serum Medium	Life Technologies
Lipofectamine® RNAiMAX Transfection Reagent	Life Technologies
BLOCK-iT™ Alexa Fluor® Red Fluorescent Control	Life Technologies
Inhibitors/ siRNA	Qiagen/ Invitrogen

1.4 Antibodies

Table 5 List of used primary and secondary antibodies and their working dilution

Primary antibody	Catalogue Number	Company	Dilution	Diluent
AKT	9272	Cell Signaling	1:1000	2% skim-milk:PBST
AMPK α	2532	Cell Signaling	1:1000	3% BSA:PBST
β -actin	sc-69879	Santa Cruz	1:1000	1% skim-milk:PBST
mTOR (7C10)	2983	Cell Signaling	1:1000	3% skim-milk:PBST
p-AKT (Ser473)	9271	Cell Signaling	1:1000	2% skim-milk:PBST
p-AMPK α (Thr172)	2535	Cell Signaling	1:1000	3% BSA:PBST
p-mTOR (Ser2448)	5536	Cell Signaling	1:1000	3% skim-milk:PBST
p-p70S6 kinase (Thr389)	9234	Cell Signaling	1:1000	2% skim-milk:PBST
Secondary antibody	Catalogue Number	Company	Dilution	Diluent
Goat HRP conjugate	31460	Thermo Scientific	1:10000	2% skim-milk:PBST
Rabbit HRP conjugate	Ab6728	abcam	1:10000	2% skim-milk:PBST

Appendix II

Full list of human miRNAs expressed ± 2 fold after treatment with 2.5 mM leu compared to untreated controls using Affymetrix micro array.

Transcript ID	Fold-Change
hsa-miR-1231_st	2.93
hsa-miR-4758-5p_st	2.45
hsa-miR-3940-5p_st	2.57
hsa-miR-4486_st	2.61
hsa-miR-4741_st	2.74
hsa-miR-663b_st	2.38
hsa-miR-4665-5p_st	2.66
hp_hsa-mir-3656_st	2.37
hp_hsa-mir-4466_st	2.02
hsa-miR-4651_st	2.19
hsa-miR-4707-5p_st	2.13
hsa-miR-4532_st	2.39
hsa-miR-4687-3p_st	2.22
hsa-miR-4745-5p_st	2.53
hsa-miR-4763-3p_st	2.50
hsa-miR-4690-5p_st	2.05
hsa-miR-4695-5p_st	2.02
hsa-miR-346_st	3.83
hsa-miR-4734_st	2.55
hsa-miR-3188_st	5.05
hsa-miR-2861_st	2.19
hsa-miR-134_st	3.24
hsa-miR-3124-5p_st	2.63
hp_hsa-mir-4634_st	3.09
hsa-miR-943_st	2.80
hsa-miR-3937_st	2.23
hsa-miR-631_st	2.64
hsa-miR-92b-star_st	2.39
hsa-miR-3656_st	2.01
hsa-miR-1909_st	2.31
hsa-miR-4490_st	3.14

Transcript ID	Fold-Change
hp_hsa-mir-4679-1_st	2.15
hsa-miR-1244_st	-5.03
hsa-miR-181d_st	-2.46
hsa-miR-143_st	-1.99
hsa-miR-335_st	2.00

Appendix III

Full list of human miRNAs expressed ± 2 fold after SG bariatric surgery compared to before surgery using Affymetrix micro array.

Transcript ID	Fold-Change
hsa-miR-548ac	3.132
hsa-miR-6800-3p	2.475
hsa-miR-8084	2.467
hsa-miR-548a-3p	2.243
hsa-miR-1234-3p	2.110
hsa-miR-4668-5p	2.064
hsa-miR-4539	2.033
hsa-miR-10a-5p	-1.966
hsa-miR-152-3p	-1.969
hsa-miR-6741-5p	-1.982
hsa-miR-532-3p	-1.986
hsa-miR-484	-2.007
hsa-miR-6722-3p	-2.031
hsa-mir-711	-2.032
hsa-miR-487b-3p	-2.070
hsa-miR-154-5p	-2.090
hsa-miR-194-5p	-2.098
hsa-miR-342-5p	-2.119
hsa-miR-6798-5p	-2.120
hsa-miR-140-5p	-2.129
hsa-miR-128-3p	-2.131
hsa-miR-654-3p	-2.134
hsa-miR-328-5p	-2.135
hsa-mir-6089-1	-2.135
hsa-mir-6089-2	-2.135
hsa-miR-494-3p	-2.152
hsa-miR-4689	-2.153
hsa-miR-132-3p	-2.159
hsa-miR-6794-5p	-2.183
hsa-miR-339-3p	-2.186
hsa-let-7f-5p	-2.190
hsa-miR-4443	-2.231
hsa-miR-21-5p	-2.281
hsa-miR-151b	-2.307
hsa-miR-6068	-2.363
hsa-miR-574-3p	-2.467

Transcript ID	Fold-Change
hsa-miR-181b-5p	-2.487
hsa-miR-6782-5p	-2.492
hsa-miR-148b-3p	-2.578
hsa-miR-4433b-3p	-2.594
hsa-miR-3621	-2.682
hsa-miR-125b-5p	-2.684
hsa-miR-431-5p	-2.701
hsa-miR-30a-5p	-2.874
hsa-miR-146b-5p	-2.924
hsa-miR-30b-5p	-3.103
hsa-miR-192-5p	-3.124
hsa-miR-150-5p	-3.325
hsa-miR-29a-3p	-3.530

Appendix IV

Full list of human miRNAs expressed ± 2 fold after GBP bariatric surgery compare to before surgery using Affymetrix micro array.

Transcript ID	Fold-Change
hsa-miR-4532	6.198
hsa-miR-3613-3p	3.966
hsa-miR-8075	3.944
hsa-miR-6732-5p	3.875
hsa-miR-4668-5p	3.474
hsa-mir-6722	3.439
hsa-miR-4793-3p	3.295
hsa-miR-4440	3.236
hsa-mir-6776	3.034
hsa-miR-455-3p	3.023
hsa-miR-5787	2.722
hsa-miR-4516	2.649
hsa-miR-6089	2.601
hsa-miR-4484	2.581
hsa-miR-1237-5p	2.565
hsa-miR-6090	2.547
hsa-miR-1915-3p	2.544
hsa-miR-4466	2.526
hsa-miR-638	2.525
hsa-miR-6750-5p	2.524
hsa-miR-8069	2.515
hsa-miR-486-5p	2.472
hsa-miR-3665	2.451
hsa-miR-1469	2.450
hsa-miR-6805-3p	2.448
hsa-miR-6729-5p	2.424
hsa-miR-6869-5p	2.394
hsa-miR-8084	2.380
hsa-miR-6087	2.360
hsa-miR-548x-3p	2.335
hsa-mir-320e	2.323
hsa-miR-4488	2.320
hsa-miR-3201	2.306
hsa-miR-1281	2.285
hsa-miR-6727-5p	2.284
hsa-miR-6850-5p	2.267

Transcript ID	Fold-Change
hsa-mir-6836	2.255
hsa-miR-3178	2.253
hsa-miR-4787-5p	2.236
hsa-mir-4722	2.231
hsa-mir-8075	2.207
hsa-miR-1184	2.196
hsa-miR-3196	2.156
hsa-miR-1263	2.150
hsa-miR-6088	2.144
hsa-miR-4281	2.136
hsa-miR-6125	2.122
hsa-miR-6786-5p	2.084
hsa-miR-3960	2.074
hsa-miR-548ac	2.050
hsa-miR-6800-5p	2.039
hsa-miR-619-5p	2.035
hsa-miR-668-5p	2.007
hsa-miR-3921	1.991
hsa-miR-29b-3p	-1.999
hsa-miR-6790-5p	-2.000
hsa-miR-28-5p	-2.008
hsa-miR-1273h-5p	-2.011
hsa-miR-452-5p	-2.011
hsa-miR-28-3p	-2.019
hsa-miR-3197	-2.027
hsa-miR-21-3p	-2.034
hsa-miR-551b-3p	-2.049
hsa-miR-224-3p	-2.053
hsa-miR-1185-2-3p	-2.058
hsa-miR-3120-3p	-2.072
hsa-miR-491-5p	-2.073
hsa-miR-27b-5p	-2.079
hsa-miR-550a-5p	-2.085
hsa-miR-574-3p	-2.087
hsa-miR-629-5p	-2.091
hsa-miR-181d-5p	-2.117

Transcript ID	Fold-Change
hsa-miR-30b-3p	-2.122
hsa-miR-378f	-2.122
hsa-miR-3141	-2.134
hsa-miR-937-5p	-2.134
hsa-miR-501-3p	-2.148
hsa-miR-30c-5p	-2.179
hsa-miR-493-3p	-2.191
hsa-miR-329-3p	-2.192
hsa-miR-424-3p	-2.194
hsa-miR-330-3p	-2.194
hsa-miR-6782-5p	-2.203
hsa-miR-4284	-2.209
hsa-miR-3617-5p	-2.213
hsa-miR-7847-3p	-2.219
hsa-miR-19a-3p	-2.226
hsa-miR-127-3p	-2.227
hsa-miR-6852-5p	-2.229
hsa-miR-29b-2-5p	-2.231
hsa-miR-497-5p	-2.232
hsa-miR-210-3p	-2.233
hsa-miR-4443	-2.234
hsa-miR-1287-5p	-2.246
hsa-miR-7150	-2.272
hsa-miR-194-5p	-2.287
hsa-miR-15b-5p	-2.290
hsa-miR-6516-5p	-2.292
hsa-miR-181a-2-3p	-2.309
hsa-miR-671-5p	-2.315
hsa-miR-664a-5p	-2.340
hsa-miR-495-3p	-2.362
hsa-miR-30a-5p	-2.370
hsa-miR-182-5p	-2.392
hsa-miR-589-3p	-2.396
hsa-miR-29c-3p	-2.403
hsa-miR-5680	-2.404
hsa-miR-3648	-2.408
hsa-miR-4649-5p	-2.412
hsa-miR-151b	-2.418
hsa-miR-200c-3p	-2.420
hsa-miR-324-3p	-2.428
hsa-miR-421	-2.476
hsa-miR-224-5p	-2.479

Transcript ID	Fold-Change
hsa-miR-378d	-2.495
hsa-miR-335-5p	-2.497
hsa-miR-26b-5p	-2.503
hsa-miR-425-3p	-2.508
hsa-miR-378a-5p	-2.516
hsa-miR-1973	-2.524
hsa-miR-345-5p	-2.540
hsa-miR-7107-5p	-2.543
hsa-miR-6802-5p	-2.547
hsa-miR-487b-3p	-2.549
hsa-miR-381-3p	-2.556
hsa-miR-494-3p	-2.564
hsa-miR-1185-1-3p	-2.579
hsa-miR-27a-3p	-2.619
hsa-let-7g-5p	-2.655
hsa-miR-654-3p	-2.659
hsa-miR-99b-3p	-2.667
hsa-miR-21-5p	-2.684
hsa-miR-7641	-2.699
hsa-miR-543	-2.700
hsa-miR-326	-2.704
hsa-miR-532-5p	-2.778
hsa-miR-18a-3p	-2.791
hsa-miR-1271-5p	-2.810
hsa-miR-223-3p	-2.814
hsa-miR-370-3p	-2.824
hsa-miR-410-3p	-2.828
hsa-miR-378c	-2.870
hsa-miR-331-3p	-2.878
hsa-miR-181c-5p	-2.924
hsa-miR-324-5p	-2.927
hsa-miR-22-5p	-2.938
hsa-miR-30e-3p	-2.940
hsa-miR-628-3p	-2.958
hsa-miR-625-5p	-2.959
hsa-miR-378i	-2.960
hsa-miR-27b-3p	-2.965
hsa-miR-422a	-2.979
hsa-miR-362-5p	-2.983
hsa-miR-4459	-2.988
hsa-miR-99a-5p	-3.005
hsa-miR-154-5p	-3.030

Transcript ID	Fold-Change
hsa-miR-376a-3p	-3.032
hsa-miR-3651	-3.040
hsa-miR-500a-3p	-3.043
hsa-miR-185-3p	-3.119
hsa-miR-409-5p	-3.137
hsa-miR-195-5p	-3.147
hsa-miR-199a-5p	-3.199
hsa-miR-339-5p	-3.329
hsa-miR-431-5p	-3.337
hsa-miR-24-2-5p	-3.390
hsa-miR-4306	-3.411
hsa-miR-379-5p	-3.524
hsa-miR-502-3p	-3.559
hsa-miR-660-5p	-3.563
hsa-miR-140-5p	-3.579
hsa-miR-337-5p	-3.591
hsa-mir-711	-3.597
hsa-miR-487a-3p	-3.649
hsa-miR-199a-3p	-3.718
hsa-miR-199b-3p	-3.718
hsa-miR-301a-3p	-3.720
hsa-miR-152-3p	-3.780
hsa-miR-18b-5p	-3.825
hsa-miR-363-3p	-3.850
hsa-miR-376c-3p	-3.896
hsa-miR-3175	-4.019
hsa-miR-17-3p	-4.035
hsa-miR-342-5p	-4.069
hsa-miR-148a-3p	-4.119
hsa-miR-15a-5p	-4.269
hsa-miR-128-3p	-4.473
hsa-miR-148b-3p	-4.555
hsa-miR-146b-5p	-4.603
hsa-miR-192-5p	-4.801
hsa-let-7f-5p	-4.935
hsa-miR-30e-5p	-5.117
hsa-miR-30b-5p	-5.673
hsa-miR-29a-3p	-5.912

1 MICRORNA EXPRESSION RELATING TO THE DIETARY INDUCED LIVER STEATOSIS AND NASH

1.1 Preface

The following chapter contains an unaltered review article “*MicroRNA expression relating to the dietary induced liver steatosis and NASH*”. The review has been published in the Journal of Clinical Medicine in 2015. The Journal of Clinical Medicine is an open access, peer-reviewed journal that provides a publishing platform for advances clinical articles and reviews that are related to the disciplines within medicine.

NAFLD is the most common liver diseases in developed countries and ranges from simple steatosis to NASH which may progress to cirrhosis and hepatocellular carcinoma. MiRNAs are short noncoding single stranded RNAs that control mRNA activity at posttranscriptional levels. MiRNAs have been suggested as the ideal blood-based candidate biomarkers in many pathophysiological conditions. MiRNAs are dysregulated in liver diseases; therefore, their analysis in different tissues and circulation may offer prediction of NAFLD and monitoring its progression and response to treatment.

Here we have summarised a collection of papers related to the study of miRNAs expression in fatty liver diseases including recently discovered miRNAs in the development of NAFLD. We also have indicated the common miRNAs in circulation and their reported intracellular alteration in NAFLD paradigm. In addition, we addressed the very recent studies that present molecular mechanisms of miRNAs regulatory role in NAFLD models as well as their therapeutic observations.

1.2 Abstract

Health issues associated with excessive caloric intake and sedentary lifestyle are driving a

modern ‘epidemic’ of liver disease. Initially presenting in the clinic as excessive fat accumulation within hepatocyte cells (steatosis), ‘non-alcoholic fatty liver disease’ (NAFLD) is increasingly progressing to more severe ‘non-alcoholic steatohepatitis’ (NASH), in which liver damage and inflammation are overt features. Often developing as a sequela of obesity, NAFLD arises in almost one-third of people initially carrying excess hepatic fat and is likely the result of the liver’s limited capacity to cope with the modern day levels of dietary fatty acids circulating in the blood. While routine imaging can readily assess the presence and level of ‘extra-hepatic fat’, a proper diagnosis of disease progression to NASH is currently only possible by liver biopsy. A general reluctance to undergo such screening means that the prevalence of NASH is likely to be under reported and thus, risk assessment for future metabolic syndrome (MetS) markedly compromised. The seemingly inevitable progression to overt insulin resistance which characterizes MetS may in part be the consequence of the body’s attempt to cope with NAFLD by driving systemic insulin sensitivity and thus fatty acid breakdown. The significance of non- coding RNAs (especially miRNAs) in physiological homeostasis and pathogenesis is increasingly appreciated, and in the liver may contribute to the regulation of lipid pathways and NAFLD progression. As such they may have utility as molecular indicators for the accurate profiling of both initial risk and disease progression from simple steatosis to NASH, and further to fibrosis/cirrhosis.

1.3 Diet-induced fatty liver disease

A combination of dietary based caloric excess and a sedentary lifestyle (confounded by socioeconomic factors) has led to population-wide weight gain and subsequently, an increasing incidence of obesity-related comorbidities (e.g., NAFLD, T2DM and cardiovascular diseases) (352, 353). In addition to driving the uptake and ‘storage’ of excess circulating fatty acids (FAs) into peripheral tissues, this generalized metabolic syndrome is also characterized by elevated triglyceride (TG) synthesis, leading to yet further fat accumulation particularly in liver and adipose tissues (354) (Figure 1).

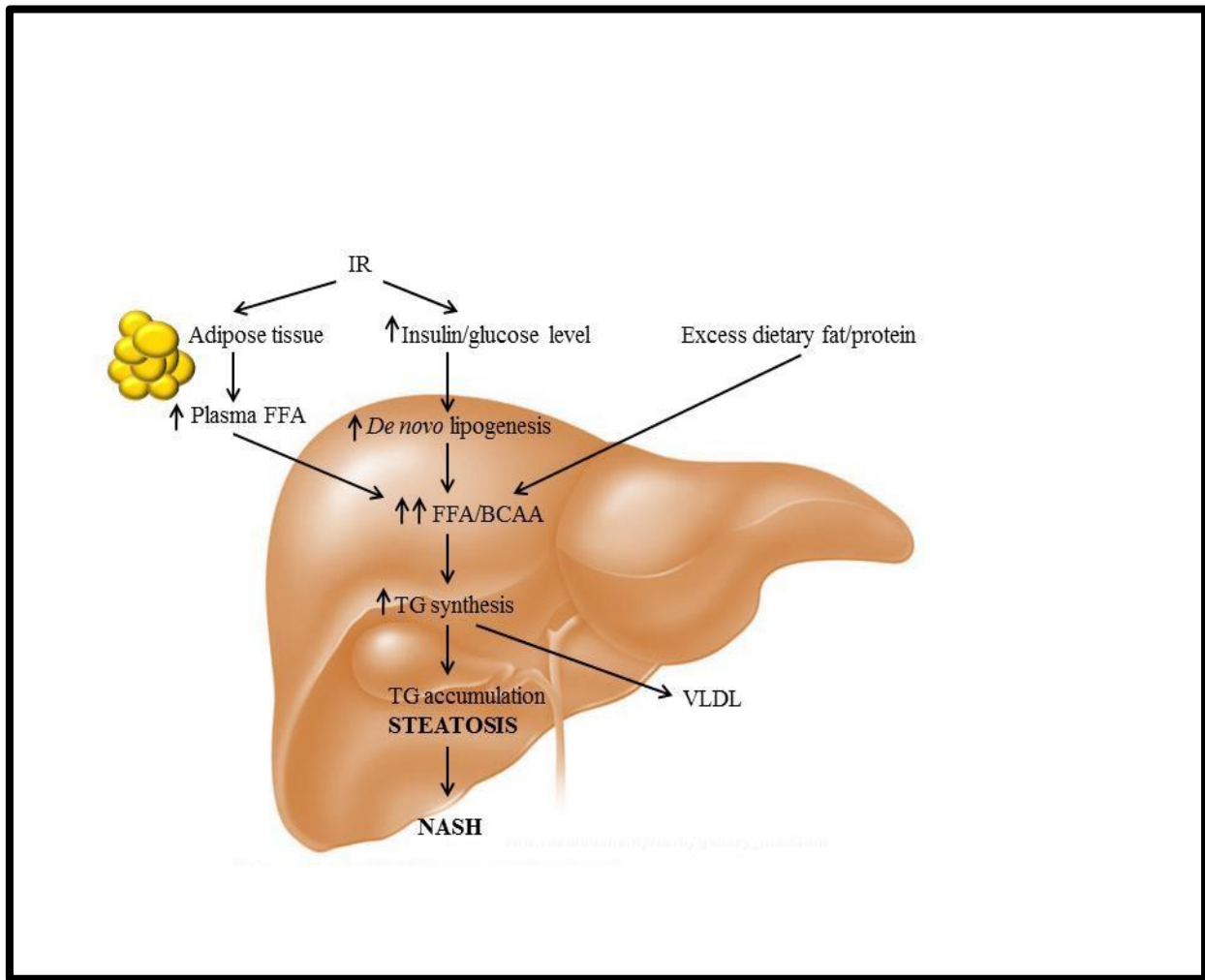


Figure 1. Hepatic TG accumulation

Free fatty acids are derived from the diet or synthesized *de novo* by hepatocytes. High levels of dietary protein intake (leading to increased circulating BCAA) can induce peripheral IR by inhibiting insulin signaling, resulting in increased uptake of glucose and TG storage in hepatocytes. Meanwhile, IR in adipose tissue reduces the inhibitory effect of insulin on lipoprotein lipase, resulting in increased lipolysis (i.e., breakdown of TG) and thus, to increased circulating FAs to be taken up by the liver. Hyperinsulinemia can also induce *de novo* synthesis of FFAs in hepatocytes leading to hepatic TG synthesis. These pathways drive hepatic TG accumulation and ultimately may contribute to the development of NASH. IR: insulin resistance, FFA: free fatty acid, BCAA: branched-chain amino acid, NASH: non-alcoholic steatohepatitis, VLDL: very-low-density lipoprotein.

The abnormal accumulation of fat in the liver (occurring in the absence of significant alcohol consumption) is a defining characteristic of NAFLD and begins with the intra-cytoplasmic accumulation of TG as liposomes around the hepatocyte nucleus. At more advanced stages these vesicles increase in size such that the nucleus is distorted and displaced to the periphery of the hepatocyte, a condition that is known as macrovesicular steatosis (76). The pathological spectrum of NAFLD progresses then to NASH which is defined by the additional degeneration of the hepatocytes and sinusoidal fibrosis (76, 355), and finally to end-stage cirrhosis, the main driver of liver transplant interventions (73, 74).

Lipids are not only important as structural components of cell membranes (in the form of cholesterol and phospholipids) and energy storage (in the form of TG) but also serve as signalling molecules. Although generally sourced through the diet, fatty acids are also synthesized *de novo* as a normal function of hepatocyte cells (341). However, abnormally elevated hepatic FA biosynthesis can precipitate glucose intolerance and insulin resistance (IR) as a consequence of the systemic attempt to restore homeostasis by promoting fat turnover (356). By driving lipolysis this adaptive mechanism unfortunately results in further increases in the circulating level of TG-derived free fatty acids (FFAs) (357). Furthermore, the pathogenesis of IR is commonly accompanied by inflammation (86, 169), which in turn stimulates secretion of hepatokines (131, 134, 169, 358). Consequently, the progression of liver disease often occurs in parallel with that of MetS.

1.4 MicroRNAs in metabolic syndrome and NAFLD

MicroRNAs (miRNAs) are a class of endogenous, short, non-protein coding, single-stranded gene products typically 20–22 nucleotides long (359). The majority of miRNAs are intracellular (360) and encoded in the introns of protein-coding genes (361). The primary miRNA is transcribed in the nucleus and subsequently integrated into the RNA-induced silencing complex in cytoplasm (362) to regulate the expression of target genes (363, 364). They are present in genomes across all eukaryotic organisms and are thought to modulate the expression of target genes post-

transcriptionally via interactions with specific mRNAs (233).

MicroRNA activity is known to impact a diverse range of biological processes, including cellular growth and development, cardiovascular and cerebrovascular function, protein secretion and glucose and fatty acid metabolism (244-246, 341, 359). Their potential importance for regulating metabolic homeostasis is also becoming clear. For example, the antisense targeting of just miR-122 in high-fat fed mice leads to a significant 30% decrease in circulating cholesterol levels (252, 365), hepatic cholesterol and fatty acids biosynthesis, and elevated fatty acid β -oxidation associated with a reduction in TG and hepatosteatosis (252). Further, miR-33a and miR-33b are co-transcribed with their respective human host genes SREBP2 and SREBP1 (341), the sterol regulatory element-binding protein (SREBP) family of transcription factors being key regulators of many genes involved in FA and cholesterol biosynthesis, as well as TG and phospholipids production. MiR-33a and miR-33b both target and act on the α -subunit of AMP-activated protein kinase (AMPK) (253, 341, 366). In response to low cellular energy levels, AMPK decreases energy-consuming processes (such as FA biogenesis) to promote ATP synthesis. AMPK inhibits the activity of SREBPs and by catalyzing phosphorylation activates their target substrates, such as acetyl-CoA carboxylase (ACC)-1. Therefore, inhibition of AMPK expression via miR-33 leads to the stimulation of SREBPs, (and their target genes) to increase intracellular levels of TG, cholesterol and FAs.

A number of miRNAs have been reported to be dysregulated in rodent models of NAFLD, obesity and T2DM, in some cases aligning to changes observed in obese human patients with NAFLD and NASH (256, 258, 367). Notably, miR-200a/b and miR-429, key members of the miR-200 family (miR-200a, miR-200b, miR-200c, miR-141 and miR-429), are all up-regulated with disease. In addition, miR-451, miR-27a and miR-122 are down-regulated in the liver of rats fed with a diet of high fat or high fructose, or their combination (264). Also reported as suppressed are miR-29c in diet-induced NASH (368), and miR-21, miR-29c and miR-451 in livers of *ob/ob* mice with fatty liver (369).

MiR-34a is yet another species that is particularly associated with hepatic metabolic diseases, being highly expressed in patients with steatosis and NASH (256), as well as T2DM subjects (258). In particular, miR-34a expression increases with the severity of NASH (370). Castro *et al.* have demonstrated that miR-34a expression, upon stimulation by ursodeoxycholic acid (UDCA) (a potent inhibitor of apoptosis), inhibits p53 via the miR34a/sirtuin (SIRT)-1/p53 pathway in primary hepatocytes. In turn, p53 modulates miR-34a expression through a positive feedback loop and highlights the important role of miR-34a in regulating hepatocyte apoptosis and NAFLD progression (370). The link with SIRT-1 is also clear evidence that miRNAs influence metabolism. SIRT-1 has recently been identified as a critical central metabolic regulator that is responsive to intracellular NAD^+ levels and by de-acetylating both histone and non-histone targets, alters the expression of genes involved in lipid and cholesterol synthesis and energy homeostasis, including proliferator-activated receptors (PPARs), proliferator-activated receptor gamma coactivator 1- α (PGC-1 α), forkhead box-protein 1 (FOXO1), p53 and SREBPs (259-261).

MiR-335 is also highly expressed in obese mice (235) and is encoded within an intronic region of the imprinted gene MEST (371), although the transcriptional control of miR-335 is independent of the host gene (235). While MEST has been reported to enhance the capacity for lipid storage in adipocytes (372), miR-335 is up-regulated in the liver and adipose tissue of diabetic *db/db* mice and promotes lipid accumulation during adipocyte differentiation in the murine 3T3-L1 cell model (235). It has also been linked with adipose tissue inflammation (345) and more recently shown to inhibit hepatic stellate cell activation and migration, suggesting a potentially positive role in reducing hepatic fibrosis (373). Given that liver fibrosis and increased TG (both in liver and in circulation) are characteristics of NAFLD, miR-335 presents a potentially valuable therapeutic candidate for the diagnosis and treatment of NAFLD. In our own studies, we have found that circulating miR-335 is significantly decreased after weight loss in obese patients with T2DM who underwent gastric bypass (GBP) bariatric surgery, and that this reduction in miR-335 level was strongly correlated with BMI (374). It has previously been reported that circulating levels of the hepatokine fetuin A (FetA), a glycoprotein

shown to promote lipid-induced insulin resistance (375), decrease after GBP surgery in obese subjects with T2DM (32). Using the approach of RNA interference-mediated knockdown in the liver cell line HepG2, we have demonstrated that miR-335 mediates the increase in *FetA* expression that results from incubation with the FFA palmitate (374).

In these same studies we also showed that the palmitate-induced increase in *FetA* expression is myostatin (MSTN)-dependent. A member of the transforming growth factor- β (TGF- β) superfamily, MSTN is classically known as a regulator of skeletal muscle growth. However, elevated MSTN expression (circulating and intracellular) is associated with metabolic disorders such as obesity (194) and type 1 diabetes mellitus (T1DM) (324). The secreted form of MSTN is strongly correlated with human obesity (194) and weight loss (196), suggesting an emergent and important role for MSTN in the regulation of energy metabolism. Further, murine models of loss-of-function MSTN mutations (376), gene knockout (330) or pro-peptide overexpression (200) are all resistant to high fat diet-induced IR and obesity. Indeed, MSTN depletion attenuates adipose formation and reduces hepatic steatosis in high fat diet-induced obese mice (330). In the context of NAFLD, the importance of miRNA in regulating MSTN function remains to be fully elucidated. However, we have shown miRNA dependent MSTN activity mediates both hepatic TG levels and biosynthesis in response to leucine, a branched-chain amino acid (BCAA) (15) which is known to be elevated in obese and IR patients and in subjects progressing from steatosis to NASH (377). Notably, miR-143 and miR-92b modulated the MSTN-dependent regulation of key metabolic genes involved in glucose uptake and TG accumulation in HepG2 cells supplemented with leu (15). Given that elevated TG and insulin resistance are common features of NAFLD, miR-143 and miR-92b present potential candidates for intervention in NAFLD, although how these miRNAs may be involved in the regulation of lipid homeostasis remains to be fully investigated.

1.5 The clinical relevance of exosomal signalling in NAFLD

While an initial diagnosis of NAFLD can be made with modern imaging technologies, a definitive diagnosis of NASH requires confirmation by liver biopsy (378). However, the invasive nature of this procedure often deters patient uptake, suggesting that the prevalence of NAFLD worldwide is likely to be understated. Furthermore, the inherent sampling variability associated with the biopsy process makes accurate histopathological diagnosis difficult and unreliable (378). Meanwhile, the metabolites currently used to assess metabolic disease (such as ALT and AST) by computed tomography (CT) are not sufficiently correlated to liver disease to be specifically useful for accurate monitoring of progression, nor to account for differences between patients in various stages of NAFLD (379).

Early indications suggest that miRNA profiles measured in readily sourced plasma and serum samples may however represent a new diagnostic approach for liver diseases (266). Several differentially expressed miRNA species have specifically been reported in plasma samples of NAFLD subjects. In particular, miR-16 is significantly overexpressed in both human and rats with steatosis/NASH compared to healthy subjects (256), while in patients with NAFLD, miR-21, miR-122, miR-192, miR-375, miR-19a, miR-19b and miR-146b are all significantly up-regulated (256, 265-267, 306, 380). Furthermore, the level of expression for particular miRNAs appears to correlate with the severity of clinical histopathology, notably miR-181a, miR-34a, miR-122, miR-200 and miR-192, while miR-34a exhibits the strongest correlation with a histopathology score in mice with fat induced-liver injury (267). Interestingly, increased miR-192, miR-375 and miR-122 distinguish more advanced NASH compared to simple steatosis, while miR-122 distinguishes liver fibrosis specifically (266).

In this review, we have described a number of miRNAs (summarized in Table 1) that are clearly associated with steatosis/NASH and have sought to highlight those which may underpin diagnostic profiles in 'soluble biopsy' samples. Since miRNAs generally show a great degree of stability in extracellular environments (including blood) which contain active ribonucleases, it is clear that secreted

Table 1 List of miRNAs involved in different biological processes of hepatic lipid homeostasis

Biological samples	miRNA(s)	Outcome	Target*	References
Plasma	miR-122	Inhibition of miR-122 reduced hepatic cholesterol and FA biosynthesis and elevated FA oxidation in humans	SREBP-1c, SREBP-2	(252, 256, 365)
Intracellular	miR-122, miR-451, miR-27a	Downregulated in the liver of high fat/fructose-fed rats	miR-451→NFκB miR-27a→PPARγ	(264, 381, 382)
Plasma/ Intracellular	miR-33a/b, miR-143, miR-92b	Inhibition of miR-33a/b increased HDL & lowers VLDL Overexpression of miR-33a/b increased HDL & reduces VLDL	SREBP-1, SREBP-2, AMPKα, IRS2, MSTN, FOXO1	(15, 253, 366)
Plasma/ Intracellular	miR-34a, miR-16, miR-21, miR-27b, miR-122, miR-192, miR-375, miR-19a/b, miR-146b, miR-181a, miR-200	Overexpressed in circulation of steatotic, NASH and T2DM humans/ rats	miR-34a→p53 miR-21→HMG-CoA miR-27b→PPARγ miR-146b→IL-6, TNF-α	(256-258, 265, 267, 383-385)
Intracellular	miR-200a/b, miR-429	Upregulated in the liver of high-fat/fructose-fed rats	—	(264)
Intracellular	miR-29c	Downregulated in the liver of <i>ob/ob</i> mice on a lipogenic diet	—	(368)
Plasma	miR-192, miR-375, miR-122	Increased particularly in NASH, suppression of glucose-induced insulin secretion	miR-375→HMG-CoA	(256, 267, 386)
Plasma	miR-155, miR-122	Upregulated in rats with ASH	miR-155→LXRα	(387, 388)

ASH: alcoholic steatohepatitis, FA(s): fatty acid(s), HMG-CoA: 3-hydroxy-3-methyl-glutaryl-CoA, NAFLD: non-alcoholic fatty liver, NASH: nonalcoholic steatohepatitis, SREBP: *Sterol regulatory element-binding protein*, p53: Tumor protein p53, T2DM: type 2 diabetes mellitus, TG: triglyceride.

*Genes are listed as human homologs.

miRNAs must be packaged to protect against degradation(360). Generally this involves incorporation into either exosomes (389) or RNA-binding protein complexes (390), and this enables their efficient recovery from biofluid clinical samples (391). Notably, up regulation of both miR-122 and miR-155 following inflammation, and the related pathology alcoholic liver disease (ASH), has been reported in exosome-rich biochemical fractions from serum (388). As components of exosomes, secreted miRNAs are intended to mediate inter-tissue communication, often following pathological challenges (392, 393), and specifically to co-ordinate systemic responses between the primary tissue which exports them and the cells at secondary sites (360). Critically, there is already evidence for some species (notably miR- 122, miR-34a and miR-200a) being similarly elevated with disease in both intra-hepatocytes tissue and serum/blood samples. This inter-tissue concordance encourages the view that liver specific miRNA profiles of disease can be accurately assessed by interrogation of exosome fractions derived from more easily obtained soluble biopsy.

We are unaware of any miRNA-based therapeutic candidate for NAFLD currently being tested by clinical trial. Although many miRNAs represent attractive potential therapeutic targets for intervening in disease progression, the efficient delivery of an effector molecule remains a significant challenge for RNA interference-based approaches to treatment. As delivery of miRNA mimics or antagomirs may lead to rapid degradation of the naked molecules, it is likely that they will need to be incorporated into stable vehicles such as nucleic acid lipid particles, or lipid bilayers coated with polyethylene glycol or conjugated to cholesterol, in order to be taken up by liver (394, 395). However, the injection of miR-122 antagomir in the form of a ‘locked nucleic acid’ (LNA)–modified oligonucleotide has been shown to suppress viremia in chronically hepatitis C viral-infected chimpanzees (396). Indeed, a miR-122 based therapeutic approach has successfully undergone Phase IIa human clinical trials for the treatment of hepatic viral infection (397), encouraging the view that the extension of miRNA based approaches to NAFLD related syndrome may be on the near horizon.

1.6 Conclusion

While the precise molecular mechanisms underlying progression of NAFLD remain unclear, the emerging regulatory roles of miRNA species' offers the potential for diagnostic tools and potential therapeutic approaches to emerge from an epigenetic perspective of these pathologies. Although no miRNA based trials are yet underway to address their utility for intervention, a growing body of literature suggests that miRNA profiles, measured in readily obtainable (least invasive) soluble biopsy specimens, offer considerable promise for assessing both risk and disease status along the NAFLD spectrum of pathologies. Critically, such tools would help to overcome current clinical limitations to the identification and accurate diagnostic assessment of 'at risk' individuals, the numbers of which appear to be increasing as the epidemic of metabolic syndrome continues.

1.7 Acknowledgments

A.Z. is supported by a Univ. of Auckland Doctoral Scholarship and the Liggins institute Doctoral Scholarship Fund. The funders played no role in the conception or design of this study, data collection and analysis, decision to publish, or preparation of this manuscript. There are no potential conflicts of interest relevant to this article.

1.8 Author Contributions

A.Z. wrote the preliminary draft of the manuscript, reviewed the manuscript, and edited the manuscript. S.N. and A.S reviewed and edited the manuscript. All authors read and approved the final manuscript.

1.9 Conflict of interest

The authors declare no conflict of interest.

LIST OF REFERENCES

1. Stover PJ, Caudill MA. Genetic and epigenetic contributions to human nutrition and health: managing genome-diet interactions. *Journal of the American Dietetic Association*. 2008;108(9):1480-7.
2. Waterland RA, Garza C. Potential mechanisms of metabolic imprinting that lead to chronic disease. *The American Journal of Clinical Nutrition*. 1999;69(2):179-97.
3. Hensrud DD, Klein S, editors. *Extreme obesity: a new medical crisis in the United States*. Mayo Clinic Proceedings; 2006: Elsevier.
4. Blair SN, Nichaman MZ, editors. *The public health problem of increasing prevalence rates of obesity and what should be done about it*. Mayo Clinic Proceedings; 2002: Elsevier.
5. Harnack LJ, Jeffery RW, Boutelle KN. Temporal trends in energy intake in the United States: an ecologic perspective. *The American journal of clinical nutrition*. 2000;71(6):1478-84.
6. Jequier E. Pathways to obesity. *International Journal of Obesity*. 2002.
7. Flatt J. Carbohydrate balance and body-weight regulation. *Proceedings of the Nutrition Society*. 1996;55(1B):449-65.
8. Astrup A, Grunwald G, Melanson E, Saris W, Hill J. The role of low-fat diets in body weight control: a meta-analysis of ad libitum dietary intervention studies. *International journal of obesity*. 2000;24(12):1545-52.
9. Roberts SB, McCrory MA, Saltzman E. The influence of dietary composition on energy intake and body weight. *Journal of the American College of Nutrition*. 2002;21(2):140S-5S.
10. Willett WC, Leibel RL. Dietary fat is not a major determinant of body fat. *The American journal of medicine*. 2002;113(9):47-59.
11. Jéquier E, Bray GA. Low-fat diets are preferred. *The American journal of medicine*. 2002;113(9):41-6.
12. Atkins RD. *Dr. Atkins' new diet revolution: Government Institutes*; 2002.
13. Felig P, Wahren J, Hendler R, Brundin T. Splanchnic glucose and amino acid metabolism in obesity. *Journal of Clinical Investigation*. 1974;53(2):582.
14. Felig P, Marliss E, Cahill Jr G. Hyperaminoacidemia: possible mechanism of hyperinsulinemia in obesity. *Clin Res*. 1969;17:382.
15. Zarfeshani A, Ngo S, Sheppard AM. Leucine alters hepatic glucose/lipid homeostasis via the myostatin-AMP-activated protein kinase pathway-potential implications for nonalcoholic fatty liver disease. *Clinical epigenetics*. 2014;6(1):27.
16. Kaidar-Person O, Rosenthal R. Malnutrition in morbidly obese patients: fact or fiction? *Minerva chirurgica*. 2009;64(3):297-302.
17. Flancbaum L, Belsley S, Drake V, Colarusso T, Tayler E. Preoperative nutritional status of patients undergoing Roux-en-Y gastric bypass for morbid obesity. *Journal of Gastrointestinal Surgery*. 2006;10(7):1033-7.
18. Schweiger C, Weiss R, Berry E, Keidar A. Nutritional deficiencies in bariatric surgery candidates. *Obesity surgery*. 2010;20(2):193-7.

19. Bäckhed F, Ding H, Wang T, Hooper LV, Koh GY, Nagy A, et al. The gut microbiota as an environmental factor that regulates fat storage. *Proceedings of the National Academy of Sciences of the United States of America*. 2004;101(44):15718-23.
20. Furet J-P, Kong L-C, Tap J, Poitou C, Basdevant A, Bouillot J-L, et al. Differential Adaptation of Human Gut Microbiota to Bariatric Surgery–Induced Weight Loss Links With Metabolic and Low-Grade Inflammation Markers. *Diabetes*. 2010;59(12):3049-57.
21. Turnbaugh PJ, Ridaura VK, Faith JJ, Rey FE, Knight R, Gordon JI. The effect of diet on the human gut microbiome: a metagenomic analysis in humanized gnotobiotic mice. *Science translational medicine*. 2009;1(6):6ra14-6ra.
22. Ley RE, Turnbaugh PJ, Klein S, Gordon JI. Microbial ecology: human gut microbes associated with obesity. *Nature*. 2006;444(7122):1022-3.
23. Choi SW, Friso S. Epigenetics: a new bridge between nutrition and health. *Advances in Nutrition: An International Review Journal*. 2010;1(1):8-16.
24. Waterland RA, Jirtle RL. Early nutrition, epigenetic changes at transposons and imprinted genes, and enhanced susceptibility to adult chronic diseases. *Nutrition-New York*. 2004;20(1):63-8.
25. Dennis C. Epigenetics and disease: Altered states. *Nature*. 2003;421(6924):686-8.
26. Zhang Y, Guo K, LeBlanc RE, Loh D, Schwartz GJ, Yu Y-H. Increasing dietary leucine intake reduces diet-induced obesity and improves glucose and cholesterol metabolism in mice via multimechanisms. *Diabetes*. 2007;56(6):1647-54.
27. Adams SH. Emerging perspectives on essential amino acid metabolism in obesity and the insulin-resistant state. *Advances in Nutrition: An International Review Journal*. 2011;2(6):445-56.
28. Macotela Y, Emanuelli B, Bang AM, Espinoza DO, Boucher J, Beebe K, et al. Dietary leucine—an environmental modifier of insulin resistance acting on multiple levels of metabolism. *PloS one*. 2011;6(6):e21187.
29. Etzel MR. Manufacture and use of dairy protein fractions. *The Journal of Nutrition*. 2004;134(4):996S-1002S.
30. Adeva MM, Calviño J, Souto G, Donapetry C. Insulin resistance and the metabolism of branched-chain amino acids in humans. *Amino acids*. 2012;43(1):171-81.
31. Lu J, Xie G, Jia W, Jia W. Insulin resistance and the metabolism of branched-chain amino acids. *Frontiers of medicine*. 2013;7(1):53-9.
32. Jüllig M, Yip S, Xu A, Smith G, Middleditch M, Booth M, et al. Lower fetuin-A, retinol binding protein 4 and several metabolites after gastric bypass compared to sleeve gastrectomy in patients with type 2 diabetes. *PloS one*. 2014;9(5):e96489.
33. Harper A, Miller R, Block K. Branched-chain amino acid metabolism. *Annual review of nutrition*. 1984;4(1):409-54.
34. Anthony JC, Yoshizawa F, Anthony TG, Vary TC, Jefferson LS, Kimball SR. Leucine stimulates translation initiation in skeletal muscle of postabsorptive rats via a rapamycin-sensitive pathway. *The Journal of nutrition*. 2000;130(10):2413-9.
35. Yin Y, Yao K, Liu Z, Gong M, Ruan Z, Deng D, et al. Supplementing L-leucine to a low-protein diet increases tissue protein synthesis in weanling pigs. *Amino acids*. 2010;39(5):1477-86.

36. Higuchi N, Kato M, Miyazaki M, Tanaka M, Kohjima M, Ito T, et al. Potential role of branched-chain amino acids in glucose metabolism through the accelerated induction of the glucose-sensing apparatus in the liver. *Journal of cellular biochemistry*. 2011;112(1):30-8.
37. Nordlie RC, Foster JD, Lange AJ. Regulation of glucose production by the liver. *Annual review of nutrition*. 1999;19(1):379-406.
38. Nagle CA, Klett EL, Coleman RA. Hepatic triacylglycerol accumulation and insulin resistance. *Journal of lipid research*. 2009;50(Supplement):S74-S9.
39. Cota D, Proulx K, Smith KAB, Kozma SC, Thomas G, Woods SC, et al. Hypothalamic mTOR signaling regulates food intake. *Science*. 2006;312(5775):927-30.
40. Yao K, Yin Y-L, Chu W, Liu Z, Deng D, Li T, et al. Dietary arginine supplementation increases mTOR signaling activity in skeletal muscle of neonatal pigs. *The Journal of nutrition*. 2008;138(5):867-72.
41. Polak P. Regulation of adipogenesis and adipose maintenance by the mammalian TOR complex 1: University_of_Basel; 2008.
42. Kimball SR, Jefferson LS. Signaling pathways and molecular mechanisms through which branched-chain amino acids mediate translational control of protein synthesis. *The Journal of nutrition*. 2006;136(1):227S-31S.
43. Patti M-E, Brambilla E, Luzi L, Landaker EJ, Kahn CR. Bidirectional modulation of insulin action by amino acids. *Journal of Clinical Investigation*. 1998;101(7):1519.
44. Tremblay F, Marette A. Amino acid and insulin signaling via the mTOR/p70 S6 kinase pathway A negative feedback mechanism leading to insulin resistance in skeletal muscle cells. *Journal of Biological Chemistry*. 2001;276(41):38052-60.
45. Tremblay F, Jacques H, Marette A. Modulation of insulin action by dietary proteins and amino acids: role of the mammalian target of rapamycin nutrient sensing pathway. *Current Opinion in Clinical Nutrition & Metabolic Care*. 2005;8(4):457-62.
46. Tremblay F, Lavigne C, Jacques H, Marette A. Role of dietary proteins and amino acids in the pathogenesis of insulin resistance. *Annu Rev Nutr*. 2007;27:293-310.
47. Krebs M, Roden M. Nutrient-induced insulin resistance in human skeletal muscle. *Current medicinal chemistry*. 2004;11(7):901-8.
48. Promintzer M, Krebs M. Effects of dietary protein on glucose homeostasis. *Current Opinion in Clinical Nutrition & Metabolic Care*. 2006;9(4):463-8.
49. Newgard CB, An J, Bain JR, Muehlbauer MJ, Stevens RD, Lien LF, et al. A branched-chain amino acid-related metabolic signature that differentiates obese and lean humans and contributes to insulin resistance. *Cell metabolism*. 2009;9(4):311-26.
50. Balage M, Dupont J, Mothe-Satney I, Tesseraud S, Mosoni L, Dardevet D. Leucine supplementation in rats induced a delay in muscle IR/PI3K signaling pathway associated with overall impaired glucose tolerance. *The Journal of nutritional biochemistry*. 2011;22(3):219-26.
51. Stipanuk MH. Leucine and protein synthesis: mTOR and beyond. *Nutrition reviews*. 2007;65(3):122-9.
52. Holz MK, Ballif BA, Gygi SP, Blenis J. mTOR and S6K1 mediate assembly of the translation preinitiation complex through dynamic protein interchange and ordered phosphorylation events. *Cell*. 2005;123(4):569-80.

53. Richter JD, Sonenberg N. Regulation of cap-dependent translation by eIF4E inhibitory proteins. *Nature*. 2005;433(7025):477-80.
54. Easton J, Houghton P. mTOR and cancer therapy. *Oncogene*. 2006;25(48):6436-46.
55. Inoki K, Ouyang H, Li Y, Guan K-L. Signaling by target of rapamycin proteins in cell growth control. *Microbiology and Molecular Biology Reviews*. 2005;69(1):79-100.
56. Shigemitsu K, Tsujishita Y, Miyake H, Hidayat S, Tanaka N, Hara K, et al. Structural requirement of leucine for activation of p70 S6 kinase. *FEBS letters*. 1999;447(2):303-6.
57. Kimball SR, Jefferson LS. Molecular mechanisms through which amino acids mediate signaling through the mammalian target of rapamycin. *Current Opinion in Clinical Nutrition & Metabolic Care*. 2004;7(1):39-44.
58. Dennis PB, Jaeschke A, Saitoh M, Fowler B, Kozma SC, Thomas G. Mammalian TOR: a homeostatic ATP sensor. *Science*. 2001;294(5544):1102-5.
59. Inoki K, Li Y, Zhu T, Wu J, Guan K-L. TSC2 is phosphorylated and inhibited by Akt and suppresses mTOR signalling. *Nature cell biology*. 2002;4(9):648-57.
60. Kim J-a, Wei Y, Sowers JR. Role of mitochondrial dysfunction in insulin resistance. *Circulation research*. 2008;102(4):401-14.
61. Schrauwen-Hinderling VB, Roden M, Kooi ME, Hesselink MK, Schrauwen P. Muscular mitochondrial dysfunction and type 2 diabetes mellitus. *Current Opinion in Clinical Nutrition & Metabolic Care*. 2007;10(6):698-703.
62. Sun X, Zemel MB. Leucine and calcium regulate fat metabolism and energy partitioning in murine adipocytes and muscle cells. *Lipids*. 2007;42(4):297-305.
63. Sun X, Zemel MB. Leucine modulation of mitochondrial mass and oxygen consumption in skeletal muscle cells and adipocytes. *Nutr Metab (Lond)*. 2009;6:26.
64. MacDonald MJ, Fahien LA, Brown LJ, Hasan NM, Buss JD, Kendrick MA. Perspective: emerging evidence for signaling roles of mitochondrial anaplerotic products in insulin secretion. *American Journal of Physiology-Endocrinology And Metabolism*. 2005;288(1):E1-E15.
65. Xu G, Kwon G, Cruz WS, Marshall CA, McDaniel ML. Metabolic regulation by leucine of translation initiation through the mTOR-signaling pathway by pancreatic β -cells. *Diabetes*. 2001;50(2):353-60.
66. Filiputti E, Rafacho A, Araújo EP, Silveira LR, Trevisan A, Batista TM, et al. Augmentation of insulin secretion by leucine supplementation in malnourished rats: possible involvement of the phosphatidylinositol 3-phosphate kinase/mammalian target protein of rapamycin pathway. *Metabolism*. 2010;59(5):635-44.
67. Fraenkel M, Ketzinel-Gilad M, Ariav Y, Pappo O, Karaca M, Castel J, et al. mTOR inhibition by rapamycin prevents β -cell adaptation to hyperglycemia and exacerbates the metabolic state in type 2 diabetes. *Diabetes*. 2008;57(4):945-57.
68. Li F, Yin Y, Tan B, Kong X, Wu G. Leucine nutrition in animals and humans: mTOR signaling and beyond. *Amino acids*. 2011;41(5):1185-93.
69. Hashimoto T, Cook WS, Qi C, Yeldandi AV, Reddy JK, Rao MS. Defect in peroxisome proliferator-activated receptor α -inducible fatty acid oxidation determines the severity of hepatic steatosis in response to fasting. *Journal of Biological Chemistry*. 2000;275(37):28918-28.

70. Reddy JK, Hashimoto T. Peroxisomal β -oxidation and peroxisome proliferator-activated receptor α : an adaptive metabolic system. *Annual review of nutrition*. 2001;21(1):193-230.
71. Cohen JC, Horton JD, Hobbs HH. Human fatty liver disease: old questions and new insights. *Science*. 2011;332(6037):1519-23.
72. Reddy JK, Rao MS. Lipid metabolism and liver inflammation. II. Fatty liver disease and fatty acid oxidation. *American Journal of Physiology-Gastrointestinal and Liver Physiology*. 2006;290(5):G852-G8.
73. Marrero JA, Fontana RJ, Su GL, Conjeevaram HS, Emick DM, Lok AS. NAFLD may be a common underlying liver disease in patients with hepatocellular carcinoma in the United States. *Hepatology*. 2002;36(6):1349-54.
74. Bullock RE, Zaitoun AM, Aithal GP, Ryder SD, Beckingham IJ, Lobo DN. Association of non-alcoholic steatohepatitis without significant fibrosis with hepatocellular carcinoma. *Journal of hepatology*. 2004;41(4):685-6.
75. Adams LA, Lymp JF, Sauver JS, Sanderson SO, Lindor KD, Feldstein A, et al. The natural history of nonalcoholic fatty liver disease: a population-based cohort study. *Gastroenterology*. 2005;129(1):113-21.
76. Goldman L, Ausiello D. Cecil textbook of medicine. Trans Arjomand M, Setudeniah AH, Qasemi Sh Tehran: Nasle Farda. 2003:11.
77. Crabb DW, Galli A, Fischer M, You M. Molecular mechanisms of alcoholic fatty liver: role of peroxisome proliferator-activated receptor alpha. *Alcohol*. 2004;34(1):35-8.
78. Schwimmer JB, Behling C, Newbury R, Deutsch R, Nievergelt C, Schork NJ, et al. Histopathology of pediatric nonalcoholic fatty liver disease. *Hepatology*. 2005;42(3):641-9.
79. Adiels M, Olofsson S-O, Taskinen M-R, Borén J. Diabetic dyslipidaemia. Current opinion in lipidology. 2006;17(3):238-46.
80. Roden M. Mechanisms of disease: hepatic steatosis in type 2 diabetes—pathogenesis and clinical relevance. *Nature Reviews Endocrinology*. 2006;2(6):335-48.
81. Saltiel AR, Kahn CR. Insulin signalling and the regulation of glucose and lipid metabolism. *Nature*. 2001;414(6865):799-806.
82. Glass CK, Olefsky JM. Inflammation and lipid signaling in the etiology of insulin resistance. *Cell metabolism*. 2012;15(5):635-45.
83. Takamura T, Misu H, Ota T, Kaneko S. Fatty liver as a consequence and cause of insulin resistance: lessons from type 2 diabetic liver. *Endocrine journal*. 2012;59(9):745-63.
84. Hsieh P-S, Hsieh Y-J. Impact of liver diseases on the development of type 2 diabetes mellitus. *World journal of gastroenterology: WJG*. 2011;17(48):5240.
85. Kotronen A, Seppälä-Lindroos A, Bergholm R, Yki-Järvinen H. Tissue specificity of insulin resistance in humans: fat in the liver rather than muscle is associated with features of the metabolic syndrome. *Diabetologia*. 2008;51(1):130-8.
86. Fabbrini E, Magkos F, Mohammed BS, Pietka T, Abumrad NA, Patterson BW, et al. Intrahepatic fat, not visceral fat, is linked with metabolic complications of obesity. *Proceedings of the National Academy of Sciences*. 2009;106(36):15430-5.
87. D'Adamo E, Cali AM, Weiss R, Santoro N, Pierpont B, Northrup V, et al. Central role of fatty liver in the pathogenesis of insulin resistance in obese adolescents. *Diabetes care*. 2010;33(8):1817-22.

88. Redgrave T. Formation of cholesteryl ester-rich particulate lipid during metabolism of chylomicrons. *Journal of Clinical Investigation*. 1970;49(3):465.
89. Li S, Brown MS, Goldstein JL. Bifurcation of insulin signaling pathway in rat liver: mTORC1 required for stimulation of lipogenesis, but not inhibition of gluconeogenesis. *Proceedings of the National Academy of Sciences*. 2010;107(8):3441-6.
90. Horton JD, Goldstein JL, Brown MS. SREBPs: activators of the complete program of cholesterol and fatty acid synthesis in the liver. *Journal of Clinical Investigation*. 2002;109(9):1125-32.
91. Bugianesi E, Leone N, Vanni E, Marchesini G, Brunello F, Carucci P, et al. Expanding the natural history of nonalcoholic steatohepatitis: from cryptogenic cirrhosis to hepatocellular carcinoma. *Gastroenterology*. 2002;123(1):134-40.
92. Evans RM, Barish GD, Wang Y-X. PPARs and the complex journey to obesity. *Nature medicine*. 2004;10(4):355-61.
93. Matsusue K, Haluzik M, Lambert G, Yim S-H, Gavrilova O, Ward JM, et al. Liver-specific disruption of PPAR γ in leptin-deficient mice improves fatty liver but aggravates diabetic phenotypes. *Journal of Clinical Investigation*. 2003;111(5):737.
94. Erickson SK. Nonalcoholic fatty liver disease. *Journal of lipid research*. 2009;50(Supplement):S412-S6.
95. Gaggini M, Morelli M, Buzzigoli E, DeFronzo RA, Bugianesi E, Gastaldelli A. Non-alcoholic fatty liver disease (NAFLD) and its connection with insulin resistance, dyslipidemia, atherosclerosis and coronary heart disease. *Nutrients*. 2013;5(5):1544-60.
96. Gastaldelli A, Cusi K, Pettiti M, Hardies J, Miyazaki Y, Berria R, et al. Relationship between hepatic/visceral fat and hepatic insulin resistance in nondiabetic and type 2 diabetic subjects. *Gastroenterology*. 2007;133(2):496-506.
97. Heni M, Machann J, Staiger H, Schwenzer NF, Peter A, Schick F, et al. Pancreatic fat is negatively associated with insulin secretion in individuals with impaired fasting glucose and/or impaired glucose tolerance: a nuclear magnetic resonance study. *Diabetes/metabolism research and reviews*. 2010;26(3):200-5.
98. Albu JB, Curi M, Shur M, Murphy L, Matthews DE, Pi-Sunyer FX. Systemic resistance to the antilipolytic effect of insulin in black and white women with visceral obesity. *American Journal of Physiology-Endocrinology and Metabolism*. 1999;277(3):E551-E60.
99. Wajchenberg BL. Subcutaneous and visceral adipose tissue: their relation to the metabolic syndrome. *Endocrine reviews*. 2000;21(6):697-738.
100. Jensen MD. Role of body fat distribution and the metabolic complications of obesity. *The Journal of Clinical Endocrinology & Metabolism*. 2008;93(11_supplement_1):s57-s63.
101. Moore MC, Connolly CC, Cherrington AD. Autoregulation of hepatic glucose production. *European Journal of Endocrinology*. 1998;138(3):240-8.
102. Schwarz J-M, Linfoot P, Dare D, Aghajanian K. Hepatic de novo lipogenesis in normoinsulinemic and hyperinsulinemic subjects consuming high-fat, low-carbohydrate and low-fat, high-carbohydrate isoenergetic diets. *The American Journal of Clinical Nutrition*. 2003;77(1):43-50.
103. Brown MS, Goldstein JL. Selective versus total insulin resistance: a pathogenic paradox. *Cell metabolism*. 2008;7(2):95-6.

104. Bugianesi E, Gastaldelli A, Vanni E, Gambino R, Cassader M, Baldi S, et al. Insulin resistance in non-diabetic patients with non-alcoholic fatty liver disease: sites and mechanisms. *Diabetologia*. 2005;48(4):634-42.
105. Gastaldelli A, Kozakova M, Højlund K, Flyvbjerg A, Favuzzi A, Mitrakou A, et al. Fatty liver is associated with insulin resistance, risk of coronary heart disease, and early atherosclerosis in a large European population. *Hepatology*. 2009;49(5):1537-44.
106. Thiele C, Spandl J. Cell biology of lipid droplets. *Current opinion in cell biology*. 2008;20(4):378-85.
107. Lam TK, Yoshii H, Haber CA, Bogdanovic E, Lam L, Fantus IG, et al. Free fatty acid-induced hepatic insulin resistance: a potential role for protein kinase C- δ . *American Journal of Physiology-Endocrinology And Metabolism*. 2002;283(4):E682-E91.
108. Park SH, Kim BI, Yun JW, Kim JW, Park DI, Cho YK, et al. Insulin resistance and C-reactive protein as independent risk factors for non-alcoholic fatty liver disease in non-obese Asian men. *Journal of gastroenterology and hepatology*. 2004;19(6):694-8.
109. Yasutake K, Nakamuta M, Shima Y, Ohyama A, Masuda K, Haruta N, et al. Nutritional investigation of non-obese patients with non-alcoholic fatty liver disease: the significance of dietary cholesterol. *Scandinavian journal of gastroenterology*. 2009;44(4):471-7.
110. Hebbard L, George J. Animal models of nonalcoholic fatty liver disease. *Nature Reviews Gastroenterology and Hepatology*. 2011;8(1):35-44.
111. Qatanani M, Lazar MA. Mechanisms of obesity-associated insulin resistance: many choices on the menu. *Genes & development*. 2007;21(12):1443-55.
112. Petersen KF, Shulman GI. Etiology of insulin resistance. *The American journal of medicine*. 2006;119(5):S10-S6.
113. Neyrinck AM, Cani PD, Dewulf EM, De Backer F, Bindels LB, Delzenne NM. Critical role of Kupffer cells in the management of diet-induced diabetes and obesity. *Biochemical and biophysical research communications*. 2009;385(3):351-6.
114. Odegaard JI, Ricardo-Gonzalez RR, Eagle AR, Vats D, Morel CR, Goforth MH, et al. Alternative M2 activation of Kupffer cells by PPAR δ ameliorates obesity-induced insulin resistance. *Cell metabolism*. 2008;7(6):496-507.
115. Lanthier N, Molendi-Coste O, Horsmans Y, van Rooijen N, Cani PD, Leclercq IA. Kupffer cell activation is a causal factor for hepatic insulin resistance. *American Journal of Physiology-Gastrointestinal and Liver Physiology*. 2010;298(1):G107-G16.
116. Coussens LM, Werb Z. Inflammation and cancer. *Nature*. 2002;420(6917):860-7.
117. Azad N, Rojanasakul Y, Vallyathan V. Inflammation and lung cancer: roles of reactive oxygen/nitrogen species. *Journal of Toxicology and Environmental Health, Part B*. 2008;11(1):1-15.
118. Constantinou C, Fentiman IS. Inflammation and breast cancer. *Breast Cancer Management*. 2013;2(4):311-25.
119. Koenig W, Sund M, Fröhlich M, Fischer H-G, Löwel H, Döring A, et al. C-reactive protein, a sensitive marker of inflammation, predicts future risk of coronary heart disease in initially healthy middle-aged men results from the MONICA (Monitoring Trends and Determinants in Cardiovascular Disease) Augsburg Cohort Study, 1984 to 1992. *Circulation*. 1999;99(2):237-42.

120. Libby P, Ridker PM, Maseri A. Inflammation and atherosclerosis. *Circulation*. 2002;105(9):1135-43.
121. Zafrani ES. Non-alcoholic fatty liver disease: an emerging pathological spectrum. *Virchows Archiv*. 2004;444(1):3-12.
122. Angulo P, Keach JC, Batts KP, Lindor KD. Independent predictors of liver fibrosis in patients with nonalcoholic steatohepatitis. *Hepatology*. 1999;30(6):1356-62.
123. Mofrad P, Contos MJ, Haque M, Sargeant C, Fisher RA, Luketic VA, et al. Clinical and histologic spectrum of nonalcoholic fatty liver disease associated with normal ALT values. *Hepatology*. 2003;37(6):1286-92.
124. Torres DM, Harrison SA. Diagnosis and therapy of nonalcoholic steatohepatitis. *Gastroenterology*. 2008;134(6):1682-98.
125. Rafiq N, Younossi ZM, editors. Effects of weight loss on nonalcoholic fatty liver disease. *Seminars in liver disease*; 2008.
126. Verna EC, Berk PD, editors. Role of fatty acids in the pathogenesis of obesity and fatty liver: impact of bariatric surgery. *Seminars in liver disease*; 2008.
127. Kopelman P, Grace C. New thoughts on managing obesity. *Gut*. 2004;53(7):1044-53.
128. Ayonrinde OT, Olynyk JK, Beilin LJ, Mori TA, Pennell CE, de Klerk N, et al. Gender-specific differences in adipose distribution and adipocytokines influence adolescent nonalcoholic fatty liver disease. *Hepatology*. 2011;53(3):800-9.
129. Stefan N, Kantartzis K, Machann J, Schick F, Thamer C, Rittig K, et al. Identification and characterization of metabolically benign obesity in humans. *Archives of internal medicine*. 2008;168(15):1609-16.
130. Stefan N, Kantartzis K, Häring H-U. Causes and metabolic consequences of fatty liver. *Endocrine reviews*. 2008;29(7):939-60.
131. Misu H, Takamura T, Takayama H, Hayashi H, Matsuzawa-Nagata N, Kurita S, et al. A liver-derived secretory protein, selenoprotein P, causes insulin resistance. *Cell metabolism*. 2010;12(5):483-95.
132. Misu H, Takamura T, Matsuzawa N, Shimizu A, Ota T, Sakurai M, et al. Genes involved in oxidative phosphorylation are coordinately upregulated with fasting hyperglycaemia in livers of patients with type 2 diabetes. *Diabetologia*. 2007;50(2):268-77.
133. Stefan N, Häring H-U. The metabolically benign and malignant fatty liver. *Diabetes*. 2011;60(8).
134. Yang S, Hwang S, Choi H, Yoo H, Seo J, Kim S, et al. Serum selenoprotein P levels in patients with type 2 diabetes and prediabetes: implications for insulin resistance, inflammation, and atherosclerosis. *The Journal of Clinical Endocrinology & Metabolism*. 2011;96(8):E1325-E9.
135. Oike Y, Akao M, Yasunaga K, Yamauchi T, Morisada T, Ito Y, et al. Angiopoietin-related growth factor antagonizes obesity and insulin resistance. *Nature medicine*. 2005;11(4):400-8.
136. Ebert T, Bachmann A, Lössner U, Kratzsch J, Blüher M, Stumvoll M, et al. Serum levels of angiopoietin-related growth factor in diabetes mellitus and chronic hemodialysis. *Metabolism*. 2009;58(4):547-51.
137. Fon Tacer K, Bookout AL, Ding X, Kurosu H, John GB, Wang L, et al. Research resource: comprehensive expression atlas of the fibroblast growth factor system in adult mouse. *Molecular endocrinology*. 2010;24(10):2050-64.

138. Kharitononkov A, Shiyanova TL, Koester A, Ford AM, Micanovic R, Galbreath EJ, et al. FGF-21 as a novel metabolic regulator. *Journal of Clinical Investigation*. 2005;115(6):1627.
139. Xu J, Lloyd DJ, Hale C, Stanislaus S, Chen M, Sivits G, et al. Fibroblast growth factor 21 reverses hepatic steatosis, increases energy expenditure, and improves insulin sensitivity in diet-induced obese mice. *Diabetes*. 2009;58(1):250-9.
140. Potthoff MJ, Kliewer SA, Mangelsdorf DJ. Endocrine fibroblast growth factors 15/19 and 21: from feast to famine. *Genes & development*. 2012;26(4):312-24.
141. Yamagoe S, Mizuno S, Suzuki K. Molecular cloning of human and bovine LECT2 having a neutrophil chemotactic activity and its specific expression in the liver. *Biochimica et Biophysica Acta (BBA)-Gene Structure and Expression*. 1998;1396(1):105-13.
142. Yamagoe S, Yamakawa Y, Matsuo Y, Minowada J, Mizuno S, Suzuki K. Purification and primary amino acid sequence of a novel neutrophil chemotactic factor LECT2. *Immunology letters*. 1996;52(1):9-13.
143. Saito T, Okumura A, Watanabe H, Asano M, Ishida-Okawara A, Sakagami J, et al. Increase in hepatic NKT cells in leukocyte cell-derived chemotaxin 2-deficient mice contributes to severe concanavalin A-induced hepatitis. *The Journal of Immunology*. 2004;173(1):579-85.
144. Okumura A, Unoki-Kubota H, Matsushita Y, Shiga T, Moriyoshi Y, Yamagoe S, et al. Increased serum leukocyte cell-derived chemotaxin 2 (LECT2) levels in obesity and fatty liver. *Bioscience trends*. 2013;7(6):276-83.
145. Lan F, Misu H, Chikamoto K, Takayama H, Kikuchi A, Mohri K, et al. LECT2 functions as a hepatokine that links obesity to skeletal muscle insulin resistance. *Diabetes*. 2014;63(5):1649-64.
146. Stefan N, Häring H-U. The role of hepatokines in metabolism. *Nature Reviews Endocrinology*. 2013;9(3):144-52.
147. Dziegielewska K, Møllgård K, Reynolds M, Saunders N. A fetuin-related glycoprotein (α 2HS) in human embryonic and fetal development. *Cell and tissue research*. 1987;248(1):33-41.
148. Denecke B, Gräber S, Schäfer C, Heiss A, Wöltje M, Jahnen-Dechent W. Tissue distribution and activity testing suggest a similar but not identical function of fetuin-B and fetuin-A. *Biochemical Journal*. 2003;376(1):135-45.
149. Auburger P, Falquerho L, Contreres JO, Pages G, Le Cam G, Rossi B, et al. Characterization of a natural inhibitor of the insulin receptor tyrosine kinase: cDNA cloning, purification, and anti-mitogenic activity. *Cell*. 1989;58(4):631-40.
150. Mathews ST, Singh GP, Ranalletta M, Cintron VJ, Qiang X, Goustin AS, et al. Improved insulin sensitivity and resistance to weight gain in mice null for the Ahsg gene. *Diabetes*. 2002;51(8):2450-8.
151. Stefan N, Hennige AM, Staiger H, Machann J, Schick F, Kröber SM, et al. α 2-Heremans-Schmid glycoprotein/fetuin-A is associated with insulin resistance and fat accumulation in the liver in humans. *Diabetes Care*. 2006;29(4):853-7.
152. Hu FB, Willett WC, Li T, Stampfer MJ, Colditz GA, Manson JE. Adiposity as compared with physical activity in predicting mortality among women. *New England Journal of Medicine*. 2004;351(26):2694-703.
153. Turer A, Scherer P. Adiponectin: mechanistic insights and clinical implications. *Diabetologia*. 2012;55(9):2319-26.

154. Kacerovsky-Bielesz G, Chmelik M, Ling C, Pokan R, Szendroedi J, Farukuoye M, et al. Short-term exercise training does not stimulate skeletal muscle ATP synthesis in relatives of humans with type 2 diabetes. *Diabetes*. 2009;58(6):1333-41.
155. Reinehr T, Roth CL. Fetuin-A and its relation to metabolic syndrome and fatty liver disease in obese children before and after weight loss. *The Journal of Clinical Endocrinology & Metabolism*. 2008;93(11):4479-85.
156. Bhattacharya S. NF- κ B mediates lipid-induced fetuin-A expression in hepatocytes that impairs adipocyte function effecting insulin resistance. 2010.
157. Hennige AM, Staiger H, Wicke C, Machicao F, Fritsche A, Häring H-U, et al. Fetuin-A induces cytokine expression and suppresses adiponectin production. *PLoS one*. 2008;3(3):e1765.
158. Srinivas P, Wagner AS, Reddy LV, Deutsch D, Leon MA, Goustin AS, et al. Serum alpha 2-HS-glycoprotein is an inhibitor of the human insulin receptor at the tyrosine kinase level. *Molecular Endocrinology*. 1993;7(11):1445-55.
159. Mathews ST, Chellam N, Srinivas PR, Cintron VJ, Leon MA, Goustin AS, et al. α 2-HSG, a specific inhibitor of insulin receptor autophosphorylation, interacts with the insulin receptor. *Molecular and cellular endocrinology*. 2000;164(1):87-98.
160. Dasgupta S, Bhattacharya S, Biswas A, Majumdar SS, Mukhopadhyay S, Ray S, et al. NF- κ B mediates lipid-induced fetuin-A expression in hepatocytes that impairs adipocyte function effecting insulin resistance. *Biochemical Journal*. 2010;429(3):451-62.
161. Lin X, Braymer H, Bray G, York D. Differential expression of insulin receptor tyrosine kinase inhibitor (fetuin) gene in a model of diet-induced obesity. *Life sciences*. 1998;63(2):145-53.
162. Stefan N, H. Alpha2-Heremans schmidglycoprotein/fetuin A is associated with insulin resistance and fat accumulation in the liver in humans. *Diabetescare*. 2006;29(4):853.
163. Mori K, Emoto M, Yokoyama H, Araki T, Teramura M, Koyama H, et al. Association of serum fetuin-A with insulin resistance in type 2 diabetic and nondiabetic subjects. *Diabetes Care*. 2006;29(2):468-.
164. Ishibashi A, Ikeda Y, Ohguro T, Kumon Y, Yamanaka S, Takata H, et al. Serum fetuin-A is an independent marker of insulin resistance in Japanese men. *Journal of atherosclerosis and thrombosis*. 2010;17(9):925-33.
165. Ix JH, Shlipak MG, Brandenburg VM, Ali S, Ketteler M, Whooley MA. Association between human fetuin-A and the metabolic syndrome data from the heart and soul study. *Circulation*. 2006;113(14):1760-7.
166. Brix JM, Stingl H, Höllerl F, Schernthaner GH, Kopp H-P, Schernthaner G. Elevated Fetuin-A concentrations in morbid obesity decrease after dramatic weight loss. *The Journal of Clinical Endocrinology & Metabolism*. 2010;95(11):4877-81.
167. Ix JH, Wassel CL, Chertow GM, Koster A, Johnson KC, Tylavsky FA, et al. Fetuin-A and change in body composition in older persons. *The Journal of Clinical Endocrinology & Metabolism*. 2009;94(11):4492-8.
168. Ix JH, Wassel CL, Kanaya AM, Vittinghoff E, Johnson KC, Koster A, et al. Fetuin-A and incident diabetes mellitus in older persons. *Jama*. 2008;300(2):182-8.
169. Stefan N, Fritsche A, Weikert C, Boeing H, Joost H-G, Häring H-U, et al. Plasma fetuin-A levels and the risk of type 2 diabetes. *Diabetes*. 2008;57(10):2762-7.

170. Jenkins NT, McKenzie JA, Hagberg JM, Witkowski S. Plasma fetuin-A concentrations in young and older high- and low-active men. *Metabolism*. 2011;60(2):265-71.
171. Mori K, Emoto M, Araki T, Yokoyama H, Lee E, Teramura M, et al. Effects of pioglitazone on serum fetuin-A levels in patients with type 2 diabetes mellitus. *Metabolism*. 2008;57(9):1248-52.
172. Belfort R, Harrison SA, Brown K, Darland C, Finch J, Hardies J, et al. A placebo-controlled trial of pioglitazone in subjects with nonalcoholic steatohepatitis. *New England Journal of Medicine*. 2006;355(22):2297-307.
173. Kaushik SV, Plaisance EP, Kim T, Huang EY, Mahurin AJ, Grandjean PW, et al. Extended-release niacin decreases serum fetuin-A concentrations in individuals with metabolic syndrome. *Diabetes/metabolism research and reviews*. 2009;25(5):427-34.
174. Shi H, Kokoeva MV, Inouye K, Tzameli I, Yin H, Flier JS. TLR4 links innate immunity and fatty acid-induced insulin resistance. *The Journal of clinical investigation*. 2006;116(11):3015-25.
175. Nguyen MA, Favelyukis S, Nguyen A-K, Reichart D, Scott PA, Jenn A, et al. A subpopulation of macrophages infiltrates hypertrophic adipose tissue and is activated by free fatty acids via Toll-like receptors 2 and 4 and JNK-dependent pathways. *Journal of Biological Chemistry*. 2007;282(48):35279-92.
176. Trepanowski J, Mey J, Varady K. Fetuin-A: a novel link between obesity and related complications. *International Journal of Obesity*. 2015;39(5):734-41.
177. Seo JA, Kim NH. Fibroblast growth factor 21: a novel metabolic regulator. *Diabetes & metabolism journal*. 2012;36(1):26-8.
178. Bakan I, Laplante M. Connecting mTORC1 signaling to SREBP-1 activation. *Current opinion in lipidology*. 2012;23(3):226-34.
179. Herbison AE, Neill J. Physiology of the gonadotropin-releasing hormone neuronal network. *Knobil and Neill's physiology of reproduction*. 2006;3:1415-82.
180. Huang Z, Chen X, Chen D. Myostatin: a novel insight into its role in metabolism, signal pathways, and expression regulation. *Cellular signalling*. 2011;23(9):1441-6.
181. Allen DL, Hittel DS, McPherron AC. Expression and function of myostatin in obesity, diabetes, and exercise adaptation. *Medicine and science in sports and exercise*. 2011;43(10):1828.
182. Wolfman NM, McPherron AC, Pappano WN, Davies MV, Song K, Tomkinson KN, et al. Activation of latent myostatin by the BMP-1/tolloid family of metalloproteinases. *Proceedings of the National Academy of Sciences*. 2003;100(26):15842-6.
183. Rebbapragada A, Benchabane H, Wrana J, Celeste A, Attisano L. Myostatin signals through a transforming growth factor β -like signaling pathway to block adipogenesis. *Molecular and cellular biology*. 2003;23(20):7230-42.
184. Rosendahl A, Checchin D, Fehniger TE, ten Dijke P, Heldin C-H, Sideras P. Activation of the TGF- β /activin-Smad2 pathway during allergic airway inflammation. *American journal of respiratory cell and molecular biology*. 2001;25(1):60-8.
185. Attisano L, Wrana JL. Smads as transcriptional co-modulators. *Current opinion in cell biology*. 2000;12(2):235-43.
186. Nakao A, Imamura T, Souchelnytskyi S, Kawabata M, Ishisaki A, Oeda E, et al. TGF- β receptor-mediated signalling through Smad2, Smad3 and Smad4. *The EMBO journal*. 1997;16(17):5353-62.

187. Feng XH, Lin X, Derynck R. Smad2, Smad3 and Smad4 cooperate with Sp1 to induce p15Ink4B transcription in response to TGF- β . *The EMBO journal*. 2000;19(19):5178-93.
188. Nakao A, Afrakhte M, Morn A, Nakayama T, Christian JL, Heuchel R, et al. Identification of Smad7, a TGF β -inducible antagonist of TGF- β signalling. *Nature*. 1997;389(6651):631-5.
189. Hayashi H, Abdollah S, Qiu Y, Cai J, Xu Y-Y, Grinnell BW, et al. The MAD-related protein Smad7 associates with the TGF β receptor and functions as an antagonist of TGF β signaling. *Cell*. 1997;89(7):1165-73.
190. Huang Z, Chen D, Zhang K, Yu B, Chen X, Meng J. Regulation of myostatin signaling by c-Jun N-terminal kinase in C2C12 cells. *Cellular signalling*. 2007;19(11):2286-95.
191. Philip B, Lu Z, Gao Y. Regulation of GDF-8 signaling by the p38 MAPK. *Cellular signalling*. 2005;17(3):365-75.
192. Jeong K-H, Choi CS. Myostatin as a Potential Therapeutic Target for Obesity and Insulin Resistance. *The Korean Journal of Obesity*. 2011;20(3):91-8.
193. Ríos Rn, Fernández-Nocelos S, Carneiro I, Arce VM, Devesa Js. Differential response to exogenous and endogenous myostatin in myoblasts suggests that myostatin acts as an autocrine factor in vivo. *Endocrinology*. 2004;145(6):2795-803.
194. Hittel DS, Berggren JR, Shearer J, Boyle K, Houmard JA. Increased secretion and expression of myostatin in skeletal muscle from extremely obese women. *Diabetes*. 2009;58(1):30-8.
195. Allen DL, Cleary AS, Speaker KJ, Lindsay SF, Uyenishi J, Reed JM, et al. Myostatin, activin receptor IIb, and follistatin-like-3 gene expression are altered in adipose tissue and skeletal muscle of obese mice. *American Journal of Physiology-Endocrinology and Metabolism*. 2008;294(5):E918-E27.
196. Milan G, Dalla Nora E, Pilon C, Pagano C, Granzotto M, Manco M, et al. Changes in muscle myostatin expression in obese subjects after weight loss. *The Journal of Clinical Endocrinology & Metabolism*. 2004;89(6):2724-7.
197. Park J-J, Berggren JR, Hulver MW, Houmard JA, Hoffman EP. GRB14, GPD1, and GDF8 as potential network collaborators in weight loss-induced improvements in insulin action in human skeletal muscle. *Physiological genomics*. 2006;27(2):114-21.
198. McPherron AC, Lee S-J. Suppression of body fat accumulation in myostatin-deficient mice. *The Journal of clinical investigation*. 2002;109(5):595-601.
199. Yang J, Zhao B. Postnatal expression of myostatin propeptide cDNA maintained high muscle growth and normal adipose tissue mass in transgenic mice fed a high-fat diet. *Molecular reproduction and development*. 2006;73(4):462-9.
200. Zhao B, Wall RJ, Yang J. Transgenic expression of myostatin propeptide prevents diet-induced obesity and insulin resistance. *Biochemical and biophysical research communications*. 2005;337(1):248-55.
201. Akpan I, Goncalves MD, Dhir R, Yin X, Pistilli E, Bogdanovich S, et al. The effects of a soluble activin type IIB receptor on obesity and insulin sensitivity. *International journal of obesity*. 2009;33(11):1265-73.
202. Kim H, Liang L, Dean R, Hausman D, Hartzell D, Baile C. Inhibition of preadipocyte differentiation by myostatin treatment in 3T3-L1 cultures. *Biochemical and biophysical research communications*. 2001;281(4):902-6.

203. Feldman BJ, Streeper RS, Farese RV, Yamamoto KR. Myostatin modulates adipogenesis to generate adipocytes with favorable metabolic effects. *Proceedings of the National Academy of Sciences*. 2006;103(42):15675-80.
204. Guo T, Jou W, Chanturiya T, Portas J, Gavrilova O, McPherron AC. Myostatin inhibition in muscle, but not adipose tissue, decreases fat mass and improves insulin sensitivity. *PloS one*. 2009;4(3):e4937.
205. Bernardo BL, Wachtmann TS, Cosgrove PG, Kuhn M, Opsahl AC, Judkins KM, et al. Postnatal PPAR δ activation and myostatin inhibition exert distinct yet complimentary effects on the metabolic profile of obese insulin-resistant mice. *PLoS one*. 2010;5(6):e11307.
206. Stolz L, Li D, Qadri A, Jalenak M, Klamann L, Tobin J. Administration of myostatin does not alter fat mass in adult mice. *Diabetes, Obesity and Metabolism*. 2008;10(2):135-42.
207. Palsgaard J, Brønns C, Friedrichsen M, Dominguez H, Jensen M, Storgaard H, et al. Gene expression in skeletal muscle biopsies from people with type 2 diabetes and relatives: differential regulation of insulin signaling pathways. *PLoS One*. 2009;4(8):e6575.
208. Hittel DS, Axelson M, Sarna N, Shearer J, Huffman KM, Kraus WE. Myostatin decreases with aerobic exercise and associates with insulin resistance. *Medicine and science in sports and exercise*. 2010;42(11):2023.
209. Wilkes JJ, Lloyd DJ, Gekakis N. Loss-of-function mutation in myostatin reduces tumor necrosis factor α production and protects liver against obesity-induced insulin resistance. *Diabetes*. 2009;58(5):1133-43.
210. Mitchell MD, Osepchuk CC, Leung K-C, McMahon CD, Bass JJ. Myostatin is a human placental product that regulates glucose uptake. *The Journal of Clinical Endocrinology & Metabolism*. 2006;91(4):1434-7.
211. Chen Y, Ye J, Cao L, Zhang Y, Xia W, Zhu D. Myostatin regulates glucose metabolism via the AMP-activated protein kinase pathway in skeletal muscle cells. *The international journal of biochemistry & cell biology*. 2010;42(12):2072-81.
212. Mukherjee A, Sidis Y, Mahan A, Raheer MJ, Xia Y, Rosen ED, et al. FSTL3 deletion reveals roles for TGF- β family ligands in glucose and fat homeostasis in adults. *Proceedings of the National Academy of Sciences*. 2007;104(4):1348-53.
213. Chen W, Woodruff TK, Mayo KE. Activin A-Induced HepG2 Liver Cell Apoptosis: involvement of activin receptors and smad proteins 1. *Endocrinology*. 2000;141(3):1263-72.
214. Woodruff TK, Krummen LA, Chen S, DeGuzman G, Lyon R, Baly DL, et al. Pharmacokinetic profile of recombinant human (rh) inhibin A and activin A in the immature rat. I. Serum profile of rh-inhibin A and rh-activin A in the immature female rat. *Endocrinology*. 1993;132(2):715-24.
215. Burgess K, Xu T, Brown R, Han B, Welle S. Effect of myostatin depletion on weight gain, hyperglycemia, and hepatic steatosis during five months of high-fat feeding in mice. *PloS one*. 2011;6(2):e17090.
216. Fafournoux P, Bruhat A, Jousse C. Amino acid regulation of gene expression. *Biochemical Journal*. 2000;351(1):1-12.
217. Qiu J. Epigenetics: unfinished symphony. *Nature*. 2006;441(7090):143-5.
218. Attwood J, Yung R, Richardson B. DNA methylation and the regulation of gene transcription. *Cellular and Molecular Life Sciences CMLS*. 2002;59(2):241-57.

219. Feinberg AP. Epigenetics at the epicenter of modern medicine. *Jama*. 2008;299(11):1345-50.
220. Dindot SV, Person R, Strivens M, Garcia R, Beaudet AL. Epigenetic profiling at mouse imprinted gene clusters reveals novel epigenetic and genetic features at differentially methylated regions. *Genome research*. 2009;19(8):1374-83.
221. Matouk CC, Marsden PA. Epigenetic regulation of vascular endothelial gene expression. *Circulation Research*. 2008;102(8):873-87.
222. Golding MC, Williamson GL, Stroud TK, Westhusin ME, Long CR. Examination of DNA methyltransferase expression in cloned embryos reveals an essential role for Dnmt1 in bovine development. *Molecular reproduction and development*. 2011;78(5):306-17.
223. Brown KS, Kalinowski SS, Megill JR, Durham SK, Mookhtiar KA. Glucokinase regulatory protein may interact with glucokinase in the hepatocyte nucleus. *Diabetes*. 1997;46(2):179-86.
224. Jin B, Seong JK, Ryu D-Y. Tissue-specific and de novo promoter methylation of the mouse glucose transporter 2. *Biological and Pharmaceutical Bulletin*. 2005;28(11):2054-7.
225. Jiang M, Zhang Y, Liu M, Lan MS, Fei J, Fan W, et al. Hypermethylation of hepatic glucokinase and L-type pyruvate kinase promoters in high-fat diet-induced obese rats. *Endocrinology*. 2011;152(4):1284-9.
226. Bartel DP. MicroRNAs: genomics, biogenesis, mechanism, and function. *cell*. 2004;116(2):281-97.
227. Lagos-Quintana M, Rauhut R, Lendeckel W, Tuschl T. Identification of novel genes coding for small expressed RNAs. *Science*. 2001;294(5543):853-8.
228. Fabian MR, Sonenberg N, Filipowicz W. Regulation of mRNA translation and stability by microRNAs. *Annual review of biochemistry*. 2010;79:351-79.
229. Heneghan H, Miller N, Kerin M. Role of microRNAs in obesity and the metabolic syndrome. *Obesity reviews*. 2010;11(5):354-61.
230. Chakrabarti SK, Francis J, Ziesmann SM, Garmey JC, Mirmira RG. Covalent histone modifications underlie the developmental regulation of insulin gene transcription in pancreatic β cells. *Journal of Biological Chemistry*. 2003;278(26):23617-23.
231. Vasudevan S, Steitz JA. AU-rich-element-mediated upregulation of translation by FXR1 and Argonaute 2. *Cell*. 2007;128(6):1105-18.
232. Vasudevan S, Tong Y, Steitz JA. Switching from repression to activation: microRNAs can up-regulate translation. *Science*. 2007;318(5858):1931-4.
233. Valinezhad Orang A, Safaralizadeh R, Kazemzadeh-Bavili M. Mechanisms of miRNA-mediated gene regulation from common downregulation to mRNA-specific upregulation. *International journal of genomics*. 2014;2014.
234. Manolis AS, Manolis TA. Micro RNAs: a revolutionary discovery in biology. *Hospital Chronicles*. 2012;7(1):4-8.
235. Nakanishi N, Nakagawa Y, Tokushige N, Aoki N, Matsuzaka T, Ishii K, et al. The up-regulation of microRNA-335 is associated with lipid metabolism in liver and white adipose tissue of genetically obese mice. *Biochemical and biophysical research communications*. 2009;385(4):492-6.

236. Zhao E, Keller MP, Rabaglia ME, Oler AT, Stapleton DS, Schueler KL, et al. Obesity and genetics regulate microRNAs in islets, liver, and adipose of diabetic mice. *Mammalian Genome*. 2009;20(8):476-85.
237. Xie H, Lim B, Lodish HF. MicroRNAs induced during adipogenesis that accelerate fat cell development are downregulated in obesity. *Diabetes*. 2009;58(5):1050-7.
238. Takanabe R, Ono K, Abe Y, Takaya T, Horie T, Wada H, et al. Up-regulated expression of microRNA-143 in association with obesity in adipose tissue of mice fed high-fat diet. *Biochemical and biophysical research communications*. 2008;376(4):728-32.
239. Klöting N, Berthold S, Kovacs P, Schön MR, Fasshauer M, Ruschke K, et al. MicroRNA expression in human omental and subcutaneous adipose tissue. *PloS one*. 2009;4(3):e4699.
240. Esau C, Kang X, Peralta E, Hanson E, Marcusson EG, Ravichandran LV, et al. MicroRNA-143 regulates adipocyte differentiation. *Journal of Biological Chemistry*. 2004;279(50):52361-5.
241. Karbiener M, Fischer C, Nowitsch S, Opriessnig P, Papak C, Ailhaud G, et al. microRNA miR-27b impairs human adipocyte differentiation and targets PPAR γ . *Biochemical and biophysical research communications*. 2009;390(2):247-51.
242. Lee EK, Lee MJ, Abdelmohsen K, Kim W, Kim MM, Srikantan S, et al. miR-130 suppresses adipogenesis by inhibiting peroxisome proliferator-activated receptor γ expression. *Molecular and cellular biology*. 2011;31(4):626-38.
243. Martinelli R, Nardelli C, Pilone V, Buonomo T, Liguori R, Castanò I, et al. miR-519d overexpression is associated with human obesity. *Obesity*. 2010;18(11):2170-6.
244. He A, Zhu L, Gupta N, Chang Y, Fang F. Overexpression of micro ribonucleic acid 29, highly up-regulated in diabetic rats, leads to insulin resistance in 3T3-L1 adipocytes. *Molecular endocrinology*. 2007;21(11):2785-94.
245. Gauthier B, Wollheim C. MicroRNAs:'ribo-regulators' of glucose homeostasis. *Nature medicine*. 2006;12(1):36-8.
246. Poy M, Spranger M, Stoffel M. microRNAs and the regulation of glucose and lipid metabolism. *Diabetes, Obesity and Metabolism*. 2007;9(s2):67-73.
247. Guay C, Roggli E, Nesca V, Jacovetti C, Regazzi R. Diabetes mellitus, a microRNA-related disease? *Translational Research*. 2011;157(4):253-64.
248. Tang X, Muniappan L, Tang G, Özcan S. Identification of glucose-regulated miRNAs from pancreatic β cells reveals a role for miR-30d in insulin transcription. *Rna*. 2009;15(2):287-93.
249. Poy MN, Eliasson L, Krutzfeldt J, Kuwajima S, Ma X, MacDonald PE, et al. A pancreatic islet-specific microRNA regulates insulin secretion. *Nature*. 2004;432(7014):226-30.
250. Ling HY, Ou HS, Feng SD, Zhang XY, Tuo QH, Chen LX, et al. CHANGES IN microRNA (miR) PROFILE AND EFFECTS OF miR-320 IN INSULIN-RESISTANT 3T3-L1 ADIPOCYTES. *Clinical and Experimental Pharmacology and Physiology*. 2009;36(9):e32-e9.
251. Xu J, Wong C. A computational screen for mouse signaling pathways targeted by microRNA clusters. *Rna*. 2008;14(7):1276-83.
252. Esau C, Davis S, Murray SF, Yu XX, Pandey SK, Pear M, et al. miR-122 regulation of lipid metabolism revealed by in vivo antisense targeting. *Cell metabolism*. 2006;3(2):87-98.

253. Dávalos A, Goedeke L, Smibert P, Ramírez CM, Warriar NP, Andreo U, et al. miR-33a/b contribute to the regulation of fatty acid metabolism and insulin signaling. *Proceedings of the National Academy of Sciences*. 2011;108(22):9232-7.
254. Rottiers V, Najafi-Shoushtari SH, Kristo F, Gurumurthy S, Zhong L, Li Y, et al., editors. *MicroRNAs in metabolism and metabolic diseases*. Cold Spring Harbor symposia on quantitative biology; 2011: Cold Spring Harbor Laboratory Press.
255. Kohjima M, Higuchi N, Kato M, Kotoh K, Yoshimoto T, Fujino T, et al. SREBP-1c, regulated by the insulin and AMPK signaling pathways, plays a role in nonalcoholic fatty liver disease. *International journal of molecular medicine*. 2008;21(4):507-11.
256. Cheung O, Puri P, Eicken C, Contos MJ, Mirshahi F, Maher JW, et al. Nonalcoholic steatohepatitis is associated with altered hepatic MicroRNA expression. *Hepatology*. 2008;48(6):1810-20.
257. Cermelli S, Ruggieri A, Marrero JA, Ioannou GN, Beretta L. Circulating microRNAs in patients with chronic hepatitis C and non-alcoholic fatty liver disease. *PloS one*. 2011;6(8):e23937.
258. Kong L, Zhu J, Han W, Jiang X, Xu M, Zhao Y, et al. Significance of serum microRNAs in pre-diabetes and newly diagnosed type 2 diabetes: a clinical study. *Acta diabetologica*. 2011;48(1):61-9.
259. Kemper JK, Xiao Z, Ponugoti B, Miao J, Fang S, Kanamaluru D, et al. FXR acetylation is normally dynamically regulated by p300 and SIRT1 but constitutively elevated in metabolic disease states. *Cell metabolism*. 2009;10(5):392-404.
260. Motta MC, Divecha N, Lemieux M, Kamel C, Chen D, Gu W, et al. Mammalian SIRT1 represses forkhead transcription factors. *Cell*. 2004;116(4):551-63.
261. Ponugoti B, Kim D-H, Xiao Z, Smith Z, Miao J, Zang M, et al. SIRT1 deacetylates and inhibits SREBP-1C activity in regulation of hepatic lipid metabolism. *Journal of Biological Chemistry*. 2010;285(44):33959-70.
262. Vaziri H, Dessain SK, Eaton EN, Imai S-I, Frye RA, Pandita TK, et al. hSIR2/SIRT1 functions as an NAD-dependent p53 deacetylase. *Cell*. 2001;107(2):149-59.
263. Lee J, Padhye A, Sharma A, Song G, Miao J, Mo Y-Y, et al. A pathway involving farnesoid X receptor and small heterodimer partner positively regulates hepatic sirtuin 1 levels via microRNA-34a inhibition. *Journal of Biological Chemistry*. 2010;285(17):12604-11.
264. Alisi A, Da Sacco L, Bruscalupi G, Piemonte F, Panera N, De Vito R, et al. Mirnome analysis reveals novel molecular determinants in the pathogenesis of diet-induced nonalcoholic fatty liver disease. *Laboratory investigation*. 2011;91(2):283-93.
265. Gori M, Arciello M, Balsano C. MicroRNAs in nonalcoholic fatty liver disease: novel biomarkers and prognostic tools during the transition from steatosis to hepatocarcinoma. *BioMed research international*. 2014;2014.
266. Pirola CJ, Gianotti TF, Castaño GO, Mallardi P, San Martino J, Ledesma MMGL, et al. Circulating microRNA signature in non-alcoholic fatty liver disease: from serum non-coding RNAs to liver histology and disease pathogenesis. *Gut*. 2014:gutjnl-2014-306996.
267. Tryndyak VP, Latendresse JR, Montgomery B, Ross SA, Beland FA, Rusyn I, et al. Plasma microRNAs are sensitive indicators of inter-strain differences in the severity of liver injury induced in mice by a choline-and folate-deficient diet. *Toxicology and applied pharmacology*. 2012;262(1):52-9.
268. Zhang Y, Guo K, LeBlanc RE, Loh D, Schwartz GJ, Yu YH. Increasing dietary leucine intake reduces diet-induced obesity and improves glucose and cholesterol metabolism in mice via multimechanisms. *Diabetes*. 2007;56(6):1647-54.

269. Layman DK, Walker DA. Potential importance of leucine in treatment of obesity and the metabolic syndrome. *The Journal of nutrition*. 2006;136(1):319S-23S.
270. Layman DK, Shiue H, Sather C, Erickson DJ, Baum J. Increased dietary protein modifies glucose and insulin homeostasis in adult women during weight loss. *The Journal of nutrition*. 2003;133(2):405.
271. Corkey BE. Banting Lecture 2011 Hyperinsulinemia: Cause or Consequence? *Diabetes*. 2012;61(1):4-13.
272. Nishitani S, Matsumura T, Fujitani S, Sonaka I, Miura Y, Yagasaki K. Leucine promotes glucose uptake in skeletal muscles of rats. *Biochemical and biophysical research communications*. 2002;299(5):693-6.
273. Oddy WH, Herbison CE, Jacoby P, Ambrosini GL, O'Sullivan TA, Ayonrinde OT, et al. The Western dietary pattern is prospectively associated with nonalcoholic fatty liver disease in adolescence. *The American journal of gastroenterology*. 2013;108(5):778-85.
274. Aiston S, Trinh KY, Lange AJ, Newgard CB, Agius L. Glucose-6-phosphatase Overexpression Lowers Glucose 6-Phosphate and Inhibits Glycogen Synthesis and Glycolysis in Hepatocytes without Affecting Glucokinase Translocation EVIDENCE AGAINST FEEDBACK INHIBITION OF GLUCOKINASE. *Journal of Biological Chemistry*. 1999;274(35):24559-66.
275. Im S-S, Kim J-W, Kim T-H, Song X-L, Kim S-Y, Kim HI, et al. Identification and characterization of peroxisome proliferator response element in the mouse GLUT2 promoter. *Exp Mol Med*. 2005;37(2):101-10.
276. Bae J-S, Kim T-H, Kim M-Y, Park J-M, Ahn Y-H. Transcriptional regulation of glucose sensors in pancreatic β -Cells and liver: an update. *Sensors*. 2010;10(5):5031-53.
277. Xu H, Wilcox D, Nguyen P, Voorbach M, Suhar T, Morgan SJ, et al. Hepatic knockdown of mitochondrial GPAT1 in *ob/ob* mice improves metabolic profile. *Biochemical and biophysical research communications*. 2006;349(1):439-48.
278. Abdel-Magid AF. Treatment of Obesity and Related Disorders with Acetyl-CoA Carboxylase Inhibitors. *ACS Medicinal Chemistry Letters*. 2012;4(1):16-7.
279. Puigserver P, Rhee J, Donovan J, Walkey CJ, Yoon JC, Oriente F, et al. Insulin-regulated hepatic gluconeogenesis through FOXO1–PGC-1 α interaction. *Nature*. 2003;423(6939):550-5.
280. Kamagate A, Qu S, Perdomo G, Su D, Kim DH, Slusher S, et al. FoxO1 mediates insulin-dependent regulation of hepatic VLDL production in mice. *The Journal of clinical investigation*. 2008;118(6):2347-64.
281. Laplante M, Sabatini DM. mTORC1 activates SREBP-1c and uncouples lipogenesis from gluconeogenesis. *Proceedings of the National Academy of Sciences*. 2010;107(8):3281-2.
282. Tzatsos A, Kandror KV. Nutrients suppress phosphatidylinositol 3-kinase/Akt signaling via raptor-dependent mTOR-mediated insulin receptor substrate 1 phosphorylation. *Molecular and cellular biology*. 2006;26(1):63-76.
283. Kovacic S, Soltys C-LM, Barr AJ, Shiojima I, Walsh K, Dyck JRB. Akt activity negatively regulates phosphorylation of AMP-activated protein kinase in the heart. *Journal of Biological Chemistry*. 2003;278(41):39422-7.
284. Fisher JS, Gao J, Han D-H, Holloszy JO, Nolte LA. Activation of AMP kinase enhances sensitivity of muscle glucose transport to insulin. *American Journal of Physiology-Endocrinology And Metabolism*. 2002;282(1):E18-E23.

285. Iglesias MA, Ye J-M, Frangioudakis G, Saha AK, Tomas E, Ruderman NB, et al. AICAR administration causes an apparent enhancement of muscle and liver insulin action in insulin-resistant high-fat-fed rats. *Diabetes*. 2002;51(10):2886-94.
286. Sanchez AMJ, Candau RB, Csibi A, Pagano AF, Raibon A, Bernardi H. The role of AMP-activated protein kinase in the coordination of skeletal muscle turnover and energy homeostasis. *American Journal of Physiology-Cell Physiology*. 2012;303(5):C475-C85.
287. Way JM, Harrington WW, Brown KK, Gottschalk WK, Sundseth SS, Mansfield TA, et al. Comprehensive messenger ribonucleic acid profiling reveals that peroxisome proliferator-activated receptor γ activation has coordinate effects on gene expression in multiple insulin-sensitive tissues. *Endocrinology*. 2001;142(3):1269-77.
288. Inoue M, Ohtake T, Motomura W, Takahashi N, Hosoki Y, Miyoshi S, et al. Increased expression of PPAR γ in high fat diet-induced liver steatosis in mice. *Biochemical and biophysical research communications*. 2005;336(1):215-22.
289. Zhang C, McFarlane C, Lokireddy S, Bonala S, Ge X, Masuda S, et al. Myostatin-deficient mice exhibit reduced insulin resistance through activating the AMP-activated protein kinase signalling pathway. *Diabetologia*. 2011;54(6):1491-501.
290. Goldberg IJ, Ginsberg HN. Ins and outs modulating hepatic triglyceride and development of nonalcoholic fatty liver disease. *Gastroenterology*. 2006;130(4):1343-6.
291. Attie AD, Scherer PE. Adipocyte metabolism and obesity. *Journal of lipid research*. 2009;50(Supplement):S395-S9.
292. Adiels M, Taskinen M-R, Borén J. Fatty liver, insulin resistance, and dyslipidemia. *Current diabetes reports*. 2008;8(1):60-4.
293. Plaisance V, Abderrahmani A, Perret-Menoud V, Jacquemin P, Lemaigre F, Regazzi R. MicroRNA-9 controls the expression of Granuphilin/Slp4 and the secretory response of insulin-producing cells. *Journal of biological chemistry*. 2006;281(37):26932-42.
294. Baroukh N, Ravier MA, Loder MK, Hill EV, Bounacer A, Scharfmann R, et al. MicroRNA-124a regulates Foxa2 expression and intracellular signaling in pancreatic β -cell lines. *Journal of Biological Chemistry*. 2007;282(27):19575-88.
295. Fernandez-Valverde SL, Taft RJ, Mattick JS. MicroRNAs in β -cell biology, insulin resistance, diabetes and its complications. *Diabetes*. 2011;60(7):1825-31.
296. Wang Q, Li YC, Wang J, Kong J, Qi Y, Quigg RJ, et al. miR-17-92 cluster accelerates adipocyte differentiation by negatively regulating tumor-suppressor Rb2/p130. *Proceedings of the National Academy of Sciences*. 2008;105(8):2889-94.
297. Zhu L, Chen L, Shi C-M, Xu G-F, Xu L-L, Zhu L-L, et al. MiR-335, an adipogenesis-related MicroRNA, is involved in adipose tissue inflammation. *Cell biochemistry and biophysics*. 2013:1-8.
298. Ha DT, Trung TN, Hien TT, Dao TT, Yim N, Ngoc TM, et al. Selected compounds derived from Moutan Cortex stimulated glucose uptake and glycogen synthesis via AMPK activation in human HepG2 cells. *Journal of ethnopharmacology*. 2010;131(2):417-24.
299. Cota D, Proulx K, Smith KAB, Kozma SC, Thomas G, Woods SC, et al. Hypothalamic mTOR signaling regulates food intake. *Science Signalling*. 2006;312(5775):927.
300. Kondo Y, Shen L, Suzuki S, Kurokawa T, Masuko K, Tanaka Y, et al. Alterations of DNA methylation and histone modifications contribute to gene silencing in hepatocellular carcinomas. *Hepatology Research*. 2007;37(11):974-83.

301. Sookoian S, Rosselli MS, Gemma C, Burgueño AL, Fernández Gianotti T, Castaño GO, et al. Epigenetic regulation of insulin resistance in nonalcoholic fatty liver disease: Impact of liver methylation of the peroxisome proliferator-activated receptor γ coactivator 1 α promoter. *Hepatology*. 2010;52(6):1992-2000.
302. McClelland M, Ivarie R. Asymmetrical distribution of CpG in an 'average' mammalian gene. *Nucleic acids research*. 1982;10(23):7865-77.
303. Cedar H, Bergman Y. Linking DNA methylation and histone modification: patterns and paradigms. *Nature Reviews Genetics*. 2009;10(5):295-304.
304. Davis CD, Uthus EO, Finley JW. Dietary selenium and arsenic affect DNA methylation in vitro in Caco-2 cells and in vivo in rat liver and colon. *The Journal of nutrition*. 2000;130(12):2903-9.
305. Lomba A, Milagro FI, García-Díaz DF, Marti A, Campión J, Martínez JA. Obesity induced by a pair-fed high fat sucrose diet: methylation and expression pattern of genes related to energy homeostasis. *Lipids in health and disease*. 2010;9(1):1.
306. McArdle MA, Finucane OM, Connaughton RM, McMorrow AM, Roche HM. Mechanisms of obesity-induced inflammation and insulin resistance: insights into the emerging role of nutritional strategies. *Front Endocrinol (Lausanne)*. 2013;4:52.
307. Fujii N, Jessen N, Goodyear LJ. AMP-activated protein kinase and the regulation of glucose transport. *American Journal of Physiology-Endocrinology and Metabolism*. 2006;291(5):E867-E77.
308. Maloney CA, Rees WD. Gene-nutrient interactions during fetal development. *Reproduction*. 2005;130(4):401-10.
309. World Health O. Information available at <http://www.who.int/mediacentre/factsheets/fs311/en/index.html>. Accessed November. 2008.
310. Neff KJ, Olbers T, le Roux CW. Bariatric surgery: the challenges with candidate selection, individualizing treatment and clinical outcomes. *BMC medicine*. 2013;11(1):8.
311. Reoch J, Mottillo S, Shimony A, Fillion KB, Christou NV, Joseph L, et al. Safety of laparoscopic vs open bariatric surgery: a systematic review and meta-analysis. *Archives of surgery*. 2011;146(11):1314-22.
312. Smith BR, Schauer P, Nguyen NT. Surgical approaches to the treatment of obesity: bariatric surgery. *Endocrinology and metabolism clinics of North America*. 2008;37(4):943-64.
313. Lee W-J, Chong K, Ser K-H, Lee Y-C, Chen S-C, Chen J-C, et al. Gastric bypass vs sleeve gastrectomy for type 2 diabetes mellitus: a randomized controlled trial. *Archives of surgery*. 2011;146(2):143-8.
314. Schauer PR, Kashyap SR, Wolski K, Brethauer SA, Kirwan JP, Pothier CE, et al. Bariatric surgery versus intensive medical therapy in obese patients with diabetes. *New England Journal of Medicine*. 2012;366(17):1567-76.
315. Ogden J, Avenell S, Ellis G. Negotiating control: patients' experiences of unsuccessful weight-loss surgery. *Psychology & health*. 2011;26(7):949-64.
316. Saltzman E, Anderson W, Apovian CM, Boulton H, Chamberlain A, Cullum-Dugan D, et al. Criteria for patient selection and multidisciplinary evaluation and treatment of the weight loss surgery patient. *Obesity research*. 2005;13(2):234-43.

317. Kehagias I, Karamanakos SN, Argentou M, Kalfarentzos F. Randomized clinical trial of laparoscopic Roux-en-Y gastric bypass versus laparoscopic sleeve gastrectomy for the management of patients with BMI < 50 kg/m². *Obesity surgery*. 2011;21(11):1650-6.
318. Himpens J, Dobbeleir J, Peeters G. Long-term results of laparoscopic sleeve gastrectomy for obesity. *Annals of surgery*. 2010;252(2):319-24.
319. Hayes MT, Hunt LA, Foo J, Tychinskaya Y, Stubbs RS. A model for predicting the resolution of type 2 diabetes in severely obese subjects following Roux-en Y gastric bypass surgery. *Obesity surgery*. 2011;21(7):910-6.
320. Lee W-J, Chong K, Ser K-H, Chen J-C, Lee Y-C, Chen S-C, et al. C-peptide predicts the remission of type 2 diabetes after bariatric surgery. *Obesity surgery*. 2012;22(2):293-8.
321. Denecke B, Graber S, Schafer C, Heiss A, Woltje M, Jahnen-Dechent W. Tissue distribution and activity testing suggest a similar but not identical function of fetuin-B and fetuin-A. *Biochem J*. 2003;376:135-45.
322. Haukeland JW, Dahl TB, Yndestad A, Gladhaug IP, Løberg EM, Haaland T, et al. Fetuin A in nonalcoholic fatty liver disease: in vivo and in vitro studies. *European Journal of Endocrinology*. 2012;166(3):503-10.
323. Hittel DS, Berggren JR, Shearer J, Boyle K, Houmard JA. Increased secretion and expression of myostatin in skeletal muscle from extremely obese women. *Diabetes*. 2009;58(1):30-8.
324. Chen Y, Cao L, Ye J, Zhu D. Upregulation of myostatin gene expression in streptozotocin-induced type 1 diabetes mice is attenuated by insulin. *Biochemical and biophysical research communications*. 2009;388(1):112-6.
325. Hennessy E, Clynes M, Jeppesen PB, O'Driscoll L. Identification of microRNAs with a role in glucose stimulated insulin secretion by expression profiling of MIN6 cells. *Biochemical and biophysical research communications*. 2010;396(2):457-62.
326. Gavrilova O, Haluzik M, Matsusue K, Cutson JJ, Johnson L, Dietz KR, et al. Liver peroxisome proliferator-activated receptor γ contributes to hepatic steatosis, triglyceride clearance, and regulation of body fat mass. *Journal of Biological Chemistry*. 2003;278(36):34268-76.
327. Tuttolomondo A, Di Raimondo D, Di Sciacca R, Casuccio A, Bivona G, Bellia C, et al. Fetuin-A and CD40 L plasma levels in acute ischemic stroke: differences in relation to TOAST subtype and correlation with clinical and laboratory variables. *Atherosclerosis*. 2010;208(1):290-6.
328. Trepanowski JF, Mey J, Varady KA. Fetuin-A: a novel link between obesity and related complications. *International Journal of Obesity*. 2014.
329. Kingsbury KJ, Paul S, Crossley A, Morgan DM. The fatty acid composition of human depot fat. *Biochemical Journal*. 1961;78(3):541.
330. Zhang C, McFarlane C, Lokireddy S, Masuda S, Ge X, Gluckman PD, et al. Inhibition of myostatin protects against diet-induced obesity by enhancing fatty acid oxidation and promoting a brown adipose phenotype in mice. *Diabetologia*. 2012;55(1):183-93.
331. Hardie DG. New roles for the LKB1 \rightarrow AMPK pathway. *Current opinion in cell biology*. 2005;17(2):167-73.
332. Sengupta S, Peterson TR, Sabatini DM. Regulation of the mTOR complex 1 pathway by nutrients, growth factors, and stress. *Molecular cell*. 2010;40(2):310-22.

333. Kambadur R, Sharma M, Smith TPL, Bass JJ. Mutations in myostatin (GDF8) in double-muscled Belgian Blue and Piedmontese cattle. *Genome research*. 1997;7(9):910-5.
334. Hatanaka M, Maier B, Sims EK, Templin AT, Kulkarni RN, Evans-Molina C, et al. Palmitate Induces mRNA Translation and Increases ER Protein Load in Islet β -Cells via Activation of the Mammalian Target of Rapamycin Pathway. *Diabetes*. 2014;63(10):3404-15.
335. Yasuda M, Tanaka Y, Kume S, Morita Y, Chin-Kanasaki M, Araki H, et al. Fatty acids are novel nutrient factors to regulate mTORC1 lysosomal localization and apoptosis in podocytes. *Biochimica et Biophysica Acta (BBA)-Molecular Basis of Disease*. 2014;1842(7):1097-108.
336. Jung TW, Youn B-S, Choi HY, Lee SY, Hong HC, Yang SJ, et al. Salsalate and adiponectin ameliorate hepatic steatosis by inhibition of the hepatokine fetuin-A. *Biochemical pharmacology*. 2013;86(7):960-9.
337. Ying S-Y, Chang DC, Miller JD, Lin S-L. The microRNA: overview of the RNA gene that modulates gene functions. *MicroRNA Protocols: Springer*; 2006. p. 1-18.
338. Tanzer A, Stadler PF. Evolution of microRNAs. *MicroRNA Protocols: Springer*; 2006. p. 335-50.
339. Heneghan HM, Miller N, Kerin MJ. Role of microRNAs in obesity and the metabolic syndrome. *Obesity reviews*. 2010;11(5):354-61.
340. Whittaker R, Loy PA, Sisman E, Suyama E, Aza-Blanc P, Ingermanson RS, et al. Identification of MicroRNAs that control lipid droplet formation and growth in hepatocytes via high-content screening. *Journal of biomolecular screening*. 2010;15(7):798-805.
341. Rottiers V, Näär AM. MicroRNAs in metabolism and metabolic disorders. *Nature reviews Molecular cell biology*. 2012;13(4):239-50.
342. Lee HS, Park HK, Hwang JS. HbA1c and glucose intolerance in obese children and adolescents. *Diabetic Medicine*. 2012;29(7):e102-e5.
343. Law LSC, Tso AWK, Tam S, Wat NMS, Cheung BMY, Lam KSL. Haemoglobin A1c is superior to fasting glucose in predicting the incidence of diabetes over 8 years among Chinese. *Diabetes research and clinical practice*. 2011;91(2):e53-e6.
344. Wiegand S, Maikowski U, Blankenstein O, Biebermann H, Tarnow P, Gruters A. Type 2 diabetes and impaired glucose tolerance in European children and adolescents with obesity--a problem that is no longer restricted to minority groups. *European Journal of Endocrinology*. 2004;151(2):199-206.
345. Zhu L, Chen L, Shi C-M, Xu G-F, Xu L-L, Zhu L-L, et al. MiR-335, an adipogenesis-related microRNA, is involved in adipose tissue inflammation. *Cell biochemistry and biophysics*. 2014;68(2):283-90.
346. Bouma M-E, Rogier E, Verthier N, Labarre C, Feldmann G. Further cellular investigation of the human hepatoblastoma-derived cell line HepG2: morphology and immunocytochemical studies of hepatic-secreted proteins. *In vitro cellular & developmental biology*. 1989;25(3):267-75.
347. Javitt NB. Hep G2 cells as a resource for metabolic studies: lipoprotein, cholesterol, and bile acids. *The FASEB Journal*. 1990;4(2):161-8.
348. Sener A, Malaisse WJ. L-leucine and a nonmetabolized analogue activate pancreatic islet glutamate dehydrogenase. 1980.
349. Liu Y-J, Cheng H, Drought H, MacDonald MJ, Sharp GW, Straub SG. Activation of the KATP channel-independent signaling pathway by the nonhydrolyzable analog of leucine, BCH. *American Journal of Physiology-Endocrinology and Metabolism*. 2003;285(2):E380-E9.

350. Wang TJ, Larson MG, Vasani RS, Cheng S, Rhee EP, McCabe E, et al. Metabolite profiles and the risk of developing diabetes. *Nature medicine*. 2011;17(4):448-53.
351. Kawaguchi T, Nagao Y, Matsuoka H, Ide T, Sata M. Branched-chain amino acid-enriched supplementation improves insulin resistance in patients with chronic liver disease. *International journal of molecular medicine*. 2008;22(1):105.
352. Kopelman PG. Obesity as a medical problem. *Nature*. 2000;404(6778):635-43.
353. Mokdad AH, Ford ES, Bowman BA, Dietz WH, Vinicor F, Bales VS, et al. Prevalence of obesity, diabetes, and obesity-related health risk factors, 2001. *Jama*. 2003;289(1):76-9.
354. Spiegelman BM, Flier JS. Obesity and the regulation of energy balance. *Cell*. 2001;104(4):531-43.
355. Lara-Castro C, Garvey WT. Intracellular lipid accumulation in liver and muscle and the insulin resistance syndrome. *Endocrinology and metabolism clinics of North America*. 2008;37(4):841-56.
356. Yahagi N, Shimano H, Matsuzaka T, Sekiya M, Najima Y, Okazaki S, et al. p53 involvement in the pathogenesis of fatty liver disease. *Journal of Biological Chemistry*. 2004;279(20):20571-5.
357. Sethi JK, Vidal-Puig AJ. Thematic review series: adipocyte biology. Adipose tissue function and plasticity orchestrate nutritional adaptation. *Journal of lipid research*. 2007;48(6):1253-62.
358. Misu H, Ishikura K, Kurita S, Takeshita Y, Ota T, Saito Y, et al. Inverse correlation between serum levels of selenoprotein P and adiponectin in patients with type 2 diabetes. *PLoS One*. 2012;7(4):e34952.
359. Williams MD, Mitchell GM. MicroRNAs in insulin resistance and obesity. *Experimental diabetes research*. 2012;2012.
360. Etheridge A, Lee I, Hood L, Galas D, Wang K. Extracellular microRNA: a new source of biomarkers. *Mutation Research/Fundamental and Molecular Mechanisms of Mutagenesis*. 2011;717(1):85-90.
361. Aravin AA, Lagos-Quintana M, Yalcin A, Zavolan M, Marks D, Snyder B, et al. The small RNA profile during *Drosophila melanogaster* development. *Developmental cell*. 2003;5(2):337-50.
362. Ketting RF. *microRNA Biogenesis and Function. Regulation of microRNAs*: Springer; 2010. p. 1-14.
363. Lim LP, Lau NC, Garrett-Engle P, Grimson A, Schelter JM, Castle J, et al. Microarray analysis shows that some microRNAs downregulate large numbers of target mRNAs. *Nature*. 2005;433(7027):769-73.
364. Pillai RS, Bhattacharyya SN, Artus CG, Zoller T, Cougot N, Basyuk E, et al. Inhibition of translational initiation by Let-7 MicroRNA in human cells. *Science*. 2005;309(5740):1573-6.
365. Krützfeldt J, Rajewsky N, Braich R, Rajeev KG, Tuschl T, Manoharan M, et al. Silencing of microRNAs in vivo with 'antagomirs'. *Nature*. 2005;438(7068):685-9.
366. Rayner KJ, Esau CC, Hussain FN, McDaniel AL, Marshall SM, van Gils JM, et al. Inhibition of miR-33a/b in non-human primates raises plasma HDL and lowers VLDL triglycerides. *Nature*. 2011;478(7369):404-7.
367. Trajkovski M, Hausser J, Soutschek J, Bhat B, Akin A, Zavolan M, et al. MicroRNAs 103 and 107 regulate insulin sensitivity. *Nature*. 2011;474(7353):649-53.
368. Pogribny IP, Starlard-Davenport A, Tryndyak VP, Han T, Ross SA, Rusyn I, et al. Difference in expression of hepatic microRNAs miR-29c, miR-34a, miR-155, and miR-200b is associated with strain-

- specific susceptibility to dietary nonalcoholic steatohepatitis in mice. *Laboratory investigation*. 2010;90(10):1437-46.
369. Li S, Chen X, Zhang H, Liang X, Xiang Y, Yu C, et al. Differential expression of microRNAs in mouse liver under aberrant energy metabolic status. *Journal of lipid research*. 2009;50(9):1756-65.
370. Castro RE, Ferreira DM, Afonso MB, Borralho PM, Machado MV, Cortez-Pinto H, et al. miR-34a/SIRT1/p53 is suppressed by ursodeoxycholic acid in the rat liver and activated by disease severity in human non-alcoholic fatty liver disease. *Journal of hepatology*. 2013;58(1):119-25.
371. Dohi O, Yasui K, Gen Y, Takada H, Endo M, Tsuji K, et al. Epigenetic silencing of miR-335 and its host gene MEST in hepatocellular carcinoma. *International journal of oncology*. 2013;42(2):411-8.
372. Takahashi M, Kamei Y, Ezaki O. Mest/Peg1 imprinted gene enlarges adipocytes and is a marker of adipocyte size. *American Journal of Physiology-Endocrinology and Metabolism*. 2005;288(1):E117-E24.
373. Chen C, Wu C-Q, Zhang Z-Q, Yao D-K, Zhu L. Loss of expression of miR-335 is implicated in hepatic stellate cell migration and activation. *Experimental cell research*. 2011;317(12):1714-25.
374. Zarfeshani A, Ngo S, Murphy R, Sheppard, A. Micro RNAs as Biomarkers of Bariatric Surgery Outcome and Putative Regulators of Hepatokines Selectively after Gastric Bypass, but not Sleeve Gastrectomy. *Journal of Obesity and Bariatrics*. 2016;3(1): 12.
375. Pal D, Dasgupta S, Kundu R, Maitra S, Das G, Mukhopadhyay S, et al. Fetuin-A acts as an endogenous ligand of TLR4 to promote lipid-induced insulin resistance. *Nature medicine*. 2012;18(8):1279-85.
376. Schuelke M, Wagner KR, Stolz LE, Hübner C, Riebel T, Kömen W, et al. Myostatin mutation associated with gross muscle hypertrophy in a child. *New England Journal of Medicine*. 2004;350(26):2682-8.
377. Lake AD, Novak P, Shipkova P, Aranibar N, Robertson DG, Reily MD, et al. Branched chain amino acid metabolism profiles in progressive human nonalcoholic fatty liver disease. *Amino acids*. 2015;47(3):603-15.
378. Castera L, Vilgrain V, Angulo P. Noninvasive evaluation of NAFLD. *Nature Reviews Gastroenterology and Hepatology*. 2013;10(11):666-75.
379. Lee S-K. Exosomes and Microvesicles as Biomarkers in Metabolic Diseases. *The Korean Journal of Obesity*. 2014;23(3):150-5.
380. Celikbilek M, Baskol M, Taheri S, Deniz K, Dogan S, Zararsiz G, et al. Circulating microRNAs in patients with non-alcoholic fatty liver disease. *World J Hepatol*. 2014;6(8):613-20.
381. Hur W, Lee JH, Kim SW, Kim J-H, Bae SH, Kim M, et al. Downregulation of microRNA-451 in non-alcoholic steatohepatitis inhibits fatty acid-induced proinflammatory cytokine production through the AMPK/AKT pathway. *The international journal of biochemistry & cell biology*. 2015;64:265-76.
382. Lin Q, Gao Z, Alarcon RM, Ye J, Yun Z. A role of miR-27 in the regulation of adipogenesis. *Febs Journal*. 2009;276(8):2348-58.
383. Raver-Shapira N, Marciano E, Meiri E, Spector Y, Rosenfeld N, Moskovits N, et al. Transcriptional activation of miR-34a contributes to p53-mediated apoptosis. *Molecular cell*. 2007;26(5):731-43.
384. Montanini L, Lazzeroni P, Sartori C, Nobili V, Crafa P, Bernasconi S, et al. Mir-146a and-155 are Involved in FOXO1 Regulation and Non Alcoholic Fatty Liver Disease in Childhood Obesity. 2014.

385. Jiang W, Liu J, Dai Y, Zhou N, Ji C, Li X. MiR-146b attenuates high-fat diet-induced non-alcoholic steatohepatitis in mice. *Journal of gastroenterology and hepatology*. 2015;30(5):933-43.
386. Cheung O, J Sanyal A. Role of microRNAs in non-alcoholic steatohepatitis. *Current pharmaceutical design*. 2010;16(17):1952-7.
387. Miller AM, Gilchrist DS, Nijjar J, Araldi E, Ramirez CM, Lavery CA, et al. MiR-155 has a protective role in the development of non-alcoholic hepatosteatosis in mice. *PLoS One*. 2013;8(8):e72324.
388. Chen Yp, Jin X, Xiang Z, Chen Sh, Li Ym. Circulating MicroRNAs as potential biomarkers for alcoholic steatohepatitis. *Liver International*. 2013;33(8):1257-65.
389. Gallo A, Tandon M, Alevizos I, Illei GG. The majority of microRNAs detectable in serum and saliva is concentrated in exosomes. *PloS one*. 2012;7(3):e30679.
390. Arroyo JD, Chevillet JR, Kroh EM, Ruf IK, Pritchard CC, Gibson DF, et al. Argonaute2 complexes carry a population of circulating microRNAs independent of vesicles in human plasma. *Proceedings of the National Academy of Sciences*. 2011;108(12):5003-8.
391. Berger F, Reiser MF. Micro-RNAs as potential new molecular biomarkers in oncology: have they reached relevance for the clinical imaging sciences? *Theranostics*. 2013;3(12):943.
392. Boeri M, Verri C, Conte D, Roz L, Modena P, Facchinetti F, et al. MicroRNA signatures in tissues and plasma predict development and prognosis of computed tomography detected lung cancer. *Proceedings of the National Academy of Sciences*. 2011;108(9):3713-8.
393. Lu Z, Liu M, Stribinskis V, Klinge C, Ramos K, Colburn N, et al. MicroRNA-21 promotes cell transformation by targeting the programmed cell death 4 gene. *Oncogene*. 2008;27(31):4373-9.
394. Morrissey DV, Lockridge JA, Shaw L, Blanchard K, Jensen K, Breen W, et al. Potent and persistent in vivo anti-HBV activity of chemically modified siRNAs. *Nature biotechnology*. 2005;23(8):1002-7.
395. Wolfrum C, Shi S, Jayaprakash KN, Jayaraman M, Wang G, Pandey RK, et al. Mechanisms and optimization of in vivo delivery of lipophilic siRNAs. *Nature biotechnology*. 2007;25(10):1149-57.
396. Lanford RE, Hildebrandt-Eriksen ES, Petri A, Persson R, Lindow M, Munk ME, et al. Therapeutic silencing of microRNA-122 in primates with chronic hepatitis C virus infection. *Science*. 2010;327(5962):198-201.
397. Janssen HL, Reesink HW, Lawitz EJ, Zeuzem S, Rodriguez-Torres M, Patel K, et al. Treatment of HCV infection by targeting microRNA. *New England Journal of Medicine*. 2013;368(18):1685-94.